UNIVERSITÀ
DEGLI STUDI
DI PADOVA

Head Office: Università degli Studi di Padova

Department of Geosciences

Ph.D. COURSE IN GEOSCIENCES
SERIES XXXV

SOIL ORGANIC MATTER AND CARBON DYNAMICS IN VENICE LAGOON SALT MARSHES UNDER NATURAL AND ANTHROPOGENIC FORCING

Thesis written with the financial contribution of the Research Programme Venezia2021, with contributions from the Provveditorato for the Public Works of Veneto, Trentino Alto Adige and Friuli Venezia Giulia, provided through the concessionary of State Consorzio Venezia Nuova and coordinated by CORILA

Coordinator: Prof. Claudia Agnini
Supervisor: Prof. Andrea D’Alpaos
Co-Supervisor: Prof. Marco Marani

Ph.D. student : Alice Puppin

University of Padova

Department of Geosciences

Ph.D. Course in Geosciences

Soil Organic Matter and Carbon dynamics in Venice Lagoon salt marshes under natural and anthropogenic forcing

Ph.D. Candidate: Alice Puppin

XXXV series

Thesis supervisor: Prof. Andrea D’Alpaos

Thesis co-supervisor: Prof. Marco Marani

November 2022

ABSTRACT

Salt marshes are critical intertidal coastal ecosystems characterized by the presence of salt-tolerant grasslands on periodically flooded sedimentary platforms. Being widely developed worldwide along temperate coastlines, salt marshes provide a wide range of ecological functions and ecosystem services, though they are in rapid and global decline. Thus, salt-marsh conservation and restoration has been recognized as a fundamental action in climate mitigation and adaptation strategies. It is becoming clear that the accumulation of organic matter in salt-marsh soils may play an important part in maintaining marsh surface elevation and blue carbon sequestration and storage potential, raising interest toward organic dynamics in salt-marsh landscapes.

To improve the current understanding of organic matter influencing coastal wetland resilience and carbon sink potential, the present work investigates Soil Organic Matter and Carbon dynamics in the microtidal salt marshes of the Venice Lagoon and explores the effects of natural and anthropogenic forcing. A multidisciplinary approach has been used, combining geomorphological, ecological, and sedimentological evaluations through field observations, field experiments, laboratory analyses, and statistical investigations. Decomposition processes affecting organic matter preservation were analysed through the Tea Bag Index protocol. Spatial and vertical patterns of soil organic matter were investigated combining analyses on sediment features, geomorphological setting, and vegetation characteristics. Lastly, carbon sequestration and storage potential of Venice Lagoon salt marshes were assessed. This work may provide important information for management and conservation strategies for optimizing wetland protection and restoration efforts.

SOMMARIO

Le barene sono ecosistemi costieri intertidali, ambienti sedimentari colonizzati da vegetazione erbacea periodicamente sommersa dalla marea. Diffuse lungo le coste temperate, le barene forniscono importanti funzioni ecologiche e servizi ecosistemici. Tuttavia, sono soggette ad un rapido e globale declino, e la loro conservazione ha un ruolo importante nelle strategie di mitigazione ed adattamento ai cambiamenti climatici. Vi è un crescente interesse nei confronti dell'accumulo di materia organica nei suoli di barena alla luce del suo ruolo nel favorirne l'accrescimento e la capacità di sequestrare e stoccare carbonio. Con lo scopo di implementare la comprensione dei processi organici capaci di influenzare la resilienza delle barene ed il loro ruolo nel ciclo del carbonio, il presente lavoro indaga le dinamiche della materia organica e del carbonio nei suoli di barena della Laguna di Venezia e ne esplora le forzanti naturali ed antropiche, attraverso un approccio multidisciplinare che ha integrato valutazioni sedimentologiche ed ecologiche, indagini in campo, attività di laboratorio ed analisi statistiche. I processi di decomposizione che influenzano la permanenza della materia organica nel suolo sono stati analizzati per mezzo di un protocollo sperimentale standardizzato, mentre la distribuzione della materia organica nel suolo, in senso orizzontale e verticale, è stata studiata esaminando le proprietà dei sedimenti, il contesto geomorfologico e la vegetazione. Infine è stato valutato il potenziale sequestro e stoccaggio di carbonio da parte delle barene della Laguna di Venezia. I risultati di questo lavoro forniscono informazioni importanti per ottimizzare gli sforzi di protezione e ripristino delle aree umide nell'ambito delle strategie di gestione costiera.

ACKNOWLEDGEMENT

This scientific activity was performed as part of the Research Programme Venezia2021, with contributions from the Provveditorato for the Public Works of Veneto, Trentino Alto Adige and Friuli Venezia Giulia, provided through the concessionary of State Consorzio Venezia Nuova and coordinated by CORILA, Research Line 3.2 (PI A.D.). The University of Padova SID2021 project, “Unraveling Carbon Sequestration Potential by Salt-Marsh Ecosystems” is also acknowledged (P.I. A. D.).

I would like to express my sincere gratitude to my supervisors, Prof. Andrea D’Alpaos and Prof. Marco Marani, for their support and guidance.

I would also like to thank the reviewers of this thesis, Dr. Sonia Silvestri and Dr. Simon Mudd, for all useful and helpful comments.

I must thank all my co-authors for their precious contributions and my collegues and technical staff of the Department of Biology, the Department of Pharmaceutical and Pharmacological Sciences and the Department of Geosciences, University of Padova, for fieldwork and laboratory analysis support.

Thanks of course to my collegues, friends and family for their support and encouragement during this journey.

ABBREVIATIONS

Abbreviations in alphabetical order	
C	Carbon
DBD	Dry Bulk Density
GHG	Greenhouse Gases
LOI	Loss On Ignition
MSL	Mean Sea Level
OC	Organic Carbon
OM	Organic Matter
OMD	Organic Matter Density
RSLR	Relative Sea Level Rise
SCD	Soil Carbon Density
SOC	Soil Organic Carbon
SOM	Soil Organic Matter
TBI	Tea Bag Index

CONTENTS

LIST OF FIGURES

LIST OF TABLES

1

INTRODUCTION

1.1 Salt marshes in intertidal ecosystems

Salt marshes are intertidal coastal ecosystems characterized by the presence of halophytic (salt-tolerant) grasslands or dwarf brushwoods on periodically flooded sedimentary platforms bordering saline tidal water bodies (Beeftink, 1977; FitzGerald and Hughes, 2021; Silvestri and Marani, 2004). They are found within the upper part of the intertidal zone in a variety of estuarine and coastal geomorphological contexts, being associated with barrier islands, spits, embayments and open shores exposed to low wave energy (Allen, 2000), as well as coastal lagoons (Adam, 2002; Perillo et al., 2009).

From a global perspective, salt marshes are widely distributed in middle and high latitudes along sheltered soft shores throughout the world (Chapman, 1977). In the tropics and subtropics, they are largely replaced by mangroves, but they can be found coexisting scattered in the mangrove belt (Adam, 2002; Mcowen et al., 2017). Recent compilations estimate global salt-marsh area at about 55,000 km^2 (Mcowen et al. (2017) presenting the first detailed global map of salt marshes) (Fig. 1.1). The largest concentrations of tidal marshes are found along the South Atlantic and Gulf coasts of North America, followed by China (Greenberg et al., 2006). The area of salt marshes in Canada and the United States alone is about

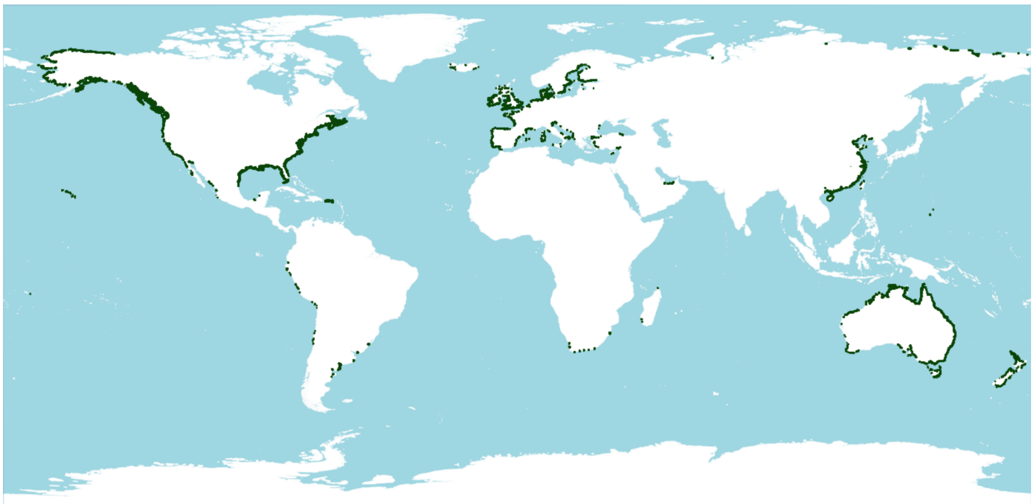

Figure 1.1: **Global distribution of salt marshes**. Mcowen et al. (2017) provide the first detailed global map of salt marshes, which are widely distributed in middle and high latitudes and can be found scattered in the mangrove belt in the tropics and subtropics (Mcowen et al., 2017).

20,000 km^2 according to Chmura et al. (2003) and Mcowen et al. (2017). Large areas of salt marshes might also exist in northern Russia and Australia (Mcowen et al., 2017).

As part of the complex intertidal system, including intertidal platforms and tidal channel networks cutting through them (Fig. 1.2), salt marshes are intrinsically dynamic environments, constantly experiencing varying boundary conditions, driven by tide periodic fluctuations. Tidal channels are the preferential pathway by which the system is regularly flooded and drained and, thus, they control the exchange of water, sediment, nutrients and biota (Geng et al., 2021). Lower elevation intertidal platforms are constituted by tidal flats, gentle sloping surfaces, that can be permanently submerged or exposed during low tide, depending on their relative elevation and local tidal range (Perillo et al., 2009). Due to sediment deposition, a tidal flat may arise above some critical elevation at which flow conditions become suitable for the settlement of pioneer vegetation seeds (Geng et al., 2021; Silvestri et al., 2005). As a result, the bare surface is progressively encroached by vegetation patches, triggering the formation of a salt marsh (e.g., D'Alpaos et al., 2007; Marani et al., 2006a, 2013; Mudd et al., 2009).

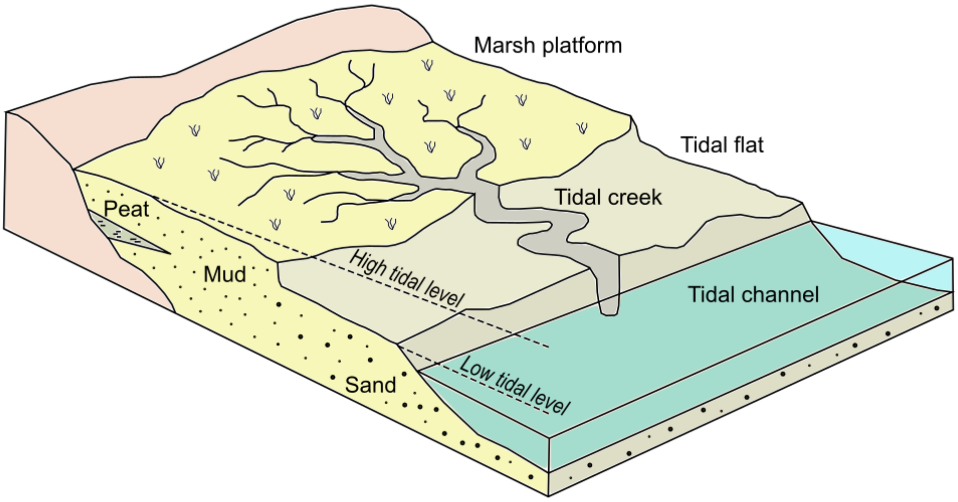

Figure 1.2: **Salt marshes within the intertidal environment**. Sketch of the intertidal system showing intertidal platforms and tidal channel and creeks. (Modified from Woodroffe, 2003).

1.2 Ecomorphodynamic processes driving salt-marsh evolution

The sedimentation process governing salt-marsh development relies mainly on the inflow of fine sediments transported through the system as well as organic production, in variable proportions. Salt-marsh evolution depends on mutual interactions and adjustments among hydrodynamic, morphological, and biological processes, as schematically represented in Fig. 1.3, being a fascinating example of ecomorphodynamics (Perillo et al., 2009). Water flow over intertidal surfaces drives sediment dynamics, shaping marsh morphology, which in turn importantly influences hydrodynamics.

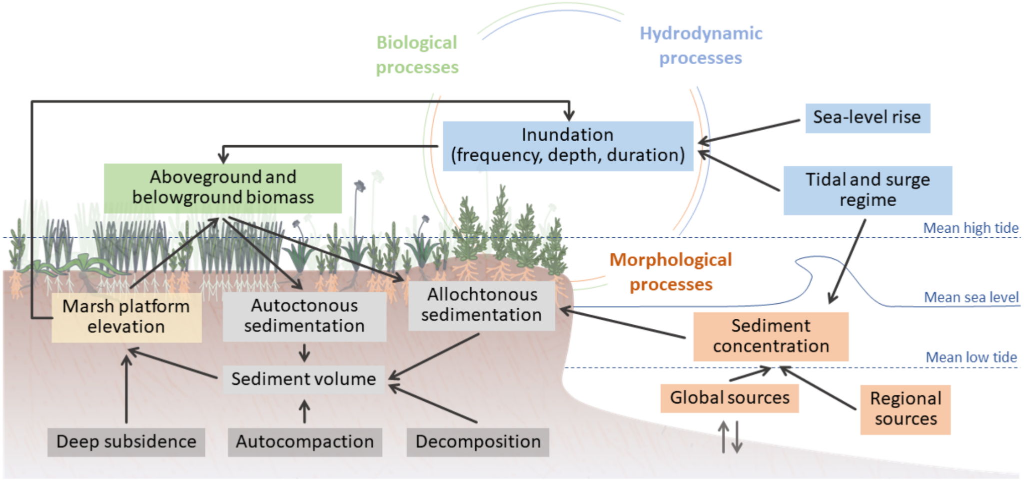

Figure 1.3: **Salt-marsh ecomorphodynamics**. Schematic representation of the intertwined hydrodynamic, morphological, and biological processes driving marsh evolution (Modified from French, 2006).

Furthermore, halophytic plants, spatially organized in characteristic patches (Bertness and Ellison, 1987; Pennings and Callaway, 1992; Silvestri et al., 2005) related to soil elevation and hydroperiod (i.e. the combination of flood frequency and duration (French and Spencer, 1993)), have a key role in marsh evolution, influencing the water flow, enhancing sediment settling and stabilization (e.g., Leonard and Luther, 1995; Mudd et al., 2010), and producing biomass that contributes to soil formation (Marani et al., 2006a; Mudd et al., 2009; Neubauer, 2008; Nyman et al., 2006). Hydrodynamic, morphological and biological controls are considered in turn below.

1.2.1 Hydromorphodynamic and morphological processes

The hydrodynamic processes, such as tidal currents, wind waves and storm surges, are the main mechanism for sediment transport, deposition or mobilisation on the intertidal platforms. Whether sediments are eroded, transported or deposited depends on flow velocity, turbulent energy, shear stress and particle size (Christiansen et al., 2000; Mudd et al., 2010) (Fig. 1.4).

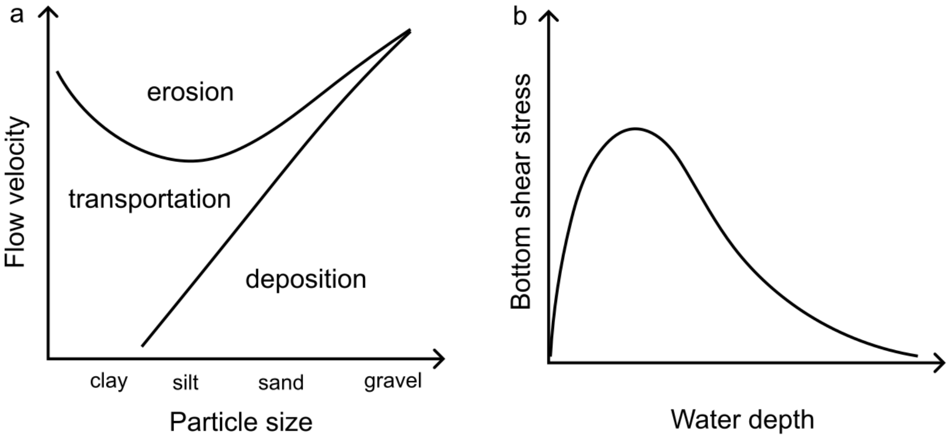

Figure 1.4: **Sediment transport dynamics**. Relationship between particle size and the tendency to be eroded, transported, or deposited at different current velocities (a) (from Hjulstrom, 1939), and dependence of the bottom shear stress on water depth (b) (Adapted from Marani et al., 2010).

Sediment dynamics in turn shape the morphology of salt-marsh landscapes, characterized by a complex geomorphic structure with broad platforms, with decimeter scale reliefs and highly variable drainage density, crossed by expansive tidal creek networks (Allen, 2000; Chen et al., 2016; D'Alpaos et al., 2005; Temmerman et al., 2007). The topographic structure of the salt marsh, in a feedback process, influences hydrodynamic, affecting spatial and temporal variability of over-marsh currents and consequently sediment dynamics (Marani et al., 2006a; Torres and Styles, 2007). In most marshes, sediment import takes place both from the seaward side through the tidal flow as well as through rivers or the catchment area (Sarika and Zikos, 2021). In addition, sediments from inside the system can be reworked and redistributed by tidal currents, wind waves and storm surges (Adam, 2002; Marani et al., 2007; Tognin et al., 2021; Leonardi et al., 2018).

Tidal currents transport suspended sediments along the channel network bringing them onto the marsh platform during flooding. As the water flow overspills on the marsh platform, it is strongly affected by friction effects (Friedrichs and Madsen, 1992) due to shallow water conditions and vegetation resistance. Water velocity and its transport capacity decrease, naturally promoting sediment deposition (Christiansen et al., 2000; D'Alpaos et al., 2007; Mudd et al., 2004).

Consequently, in accordance with field observations and modeling, sediment deposition decreases with increasing distance from sediment sources (i.e. tidal channels, seaward marsh edge) (e.g., D'Alpaos et al., 2007; Leonard, 1997; Temmerman et al., 2003), leading to the development of levees paralleling channel banks (e.g., D'Alpaos et al., 2007; Mudd et al., 2004; Silvestri et al., 2005; Temmerman et al., 2005). Relative elevation to the local mean sea level importantly influences sediment supply, as it determines frequency and duration of flooding. In fact, sedimentation rates were observed to decrease with increasing platform elevation (e.g., Cahoon and Reed, 1995; French and Spencer, 1993; Marani et al., 2007), as lower portions of the marsh platform are flooded more frequently, higher and longer, so that more sediment is supplied and deposited (Fagherazzi et al., 2012). Tidal asymmetry is also crucial for sediment delivery in the marsh, with deposition occurring mostly during slack phases (i.e. the period between flood and ebb phases), when current velocity is at its lowest (Allen, 2000; Sarika and Zikos, 2021). In addition, wind-driven waves were observed to be important drivers of sediment and morphological dynamics across bay-fronted marshes. During marsh flooding, the presence of waves alters the above described sediment deposition pattern, displacing maximum deposition inland and subjecting marsh fringe to possible erosional conditions (Duvall et al., 2019; Schuerch et al., 2019; Tognin et al., 2022). Wave-induced lateral erosion critically affects salt-marsh horizontal evolution (Leonardi et al., 2016, 2018; Mariotti and Fagherazzi, 2013), being counterbalanced by lateral progradation only if enough external sediment supply is available (Finotello et al., 2022; Goodwin and Mudd, 2020; Roner et al., 2021).

1.2.2 Vegetation role and zonation

Halophytic vegetation covering the marsh surface plays a key role in platform dynamics as it exerts significant friction on the flowing water (Fig. 1.5), decreasing tidal current velocity and turbulence and dissipating waves (Bouma et al., 2005; Leonard and Luther, 1995; Mudd et al., 2004; Leonardi et al., 2018), thereby favouring suspended sediment deposition and reducing erosion (Fig. 1.3). Some field studies have further highlighted the role of vegetation in trapping organic and inorganic particles directly on aboveground plant structures (Mudd et al., 2010), whereas plant roots strongly increase the shear resistance of the sediment bed

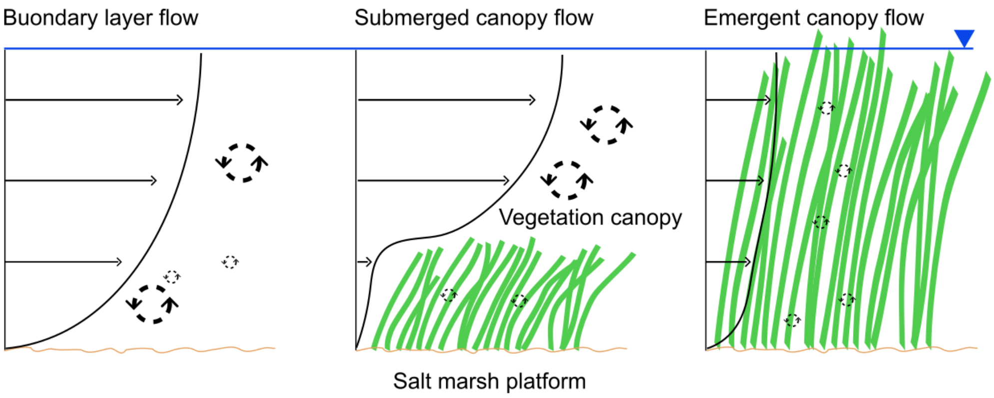

Figure 1.5: **Vegetation influence on water flow**. Sketch of three different flow regimes on a bare platform and in presence of vegetation of different height. Dashed circles are used to represent turbulence (Adapted from Beudin et al., 2017).

(Brooks et al., 2021; Howes et al., 2010). As a result, sedimentation is considered the dominant process on the marsh vegetated platform, while surface erosion is considered to be negligible (e.g., D'Alpaos et al., 2007; Temmerman et al., 2005).

Salt-marsh biomass, furthermore, contributes to vertical accretion with direct inputs of aboveground and belowground organic material, which blends with inorganic sediments within salt-marsh soils, as it will be dealt with in detail later in this chapter (e.g., Neubauer, 2008; Nyman et al., 2006; Turner et al., 2002). The trapping capacity of a plant and its contribution to soil formation are related to vegetation properties including plant morphology, density and biomass, which largely depend on vegetation type (e.g., Li et al., 2012; Morris et al., 2002). Salt-marsh vegetation is mostly constituted by halophytic grasses, herbs, and low shrubs adapted to inundation and saline conditions. However, various combinations of salt-marsh plant assemblages and vegetation types occur along a wide range of spatial scales from the global patterns to the individual sites (Adam, 2002; Chapman, 1976). At global scale, salt-marsh vegetation variations arise driven by climatic differences reflecting rainfall amount and seasonality, along with the biogeographic distribution of species (Perillo et al., 2009). As an example, vegetation of European salt marshes grows within the upper intertidal zone, with pioneer species forming short prairie (Beeftink, 1977; Lefeuvre et al., 2000). In contrast, in eastern North American coastal marshes vegetation extends almost to the mean low tide, with dense tall stands of *Spartina alterniflora* (McKee and Patrick, 1988). Furthermore, in general, species richness in salt marshes displays a latitudinal variation, with a low number of species in the tropics and maximal richness at high temperate latitudes (Adam, 1990). At the local scale, salt-marsh vegetation commonly exhibits clear patterns of zonation (Fig. 1.6) driven by their physiological response to the gradient of environmental factors as well as their competitive ability (Adam, 2002; Sarika and Zikos, 2021; Silvestri et al., 2005; Silvestri and Marani, 2004). Observations and model results show that salt-marsh zonation is the product of coupled geomorphological–biological dynamics in which vegetation engineers the landscape by tuning soil elevation within preferential ranges of optimal adaptation (Marani et al., 2013).

Figure 1.6: **Vegetation zonation**. *Aster tripolium* with its white pappus growing on the levees of a tidal creek surrounded by *Suaeda maritima* (redish leaves) and *Sarcocornia fruticosa* in a salt marsh of the southern Venice Lagoon (a). *Salicornia veneta* colonizing an infilling tidal creek in a salt marsh of the central Venice Lagoon. Photos: Alice Puppin.

Plant responses to environmental factors depend on individual species physiological needs, in terms of energy and vital substances (e.g. light, water, oxygen, salt ions like Na^+ and Cl^-, macro-nutrients like N, P, K, S, Ca, Mg and micronutrients like Cu, Zn, B, Cl, Mo, Mn, Fe) and tolerance to physical stress (e.g.

toxic substances build-up in soils, lack of oxygen in soils) (Silvestri and Marani, 2004). Abiotic factors most importantly linked to salt-marsh ecological zonation include salinity and oxygen availability, together with redox state, pH, nutrient limitation (Moffett et al., 2012; Silvestri et al., 2005; Silvestri and Marani, 2004), all of which are commonly correlated with elevation and hydroperiod across the salt marsh (Perillo et al., 2009). Salt accumulation in the soil is determined by the interaction between water salinity, flooding, and evaporation and a general positive correlation between elevation and salinity has long been proven (Adam, 2002; Sarika and Zikos, 2021). Oxygen availability, impacting root aerobic respiration, germination and early seedling growth (requiring moist but aerated conditions), is strongly linked to soil saturation, thus is determined by the frequency and duration of salt-marsh flooding and further affected by soil hydraulic conductivity, topography and drainage pattern (Marani et al., 2006b; Silvestri and Marani, 2004; Xin et al., 2017). Flooding and reduced oxygen availability change soil chemistry and lower soil redox potential, resulting in an accumulation of metabolic products potentially toxic for plants in porewater (e.g. sulfide) (Adam, 1990; Silvestri and Marani, 2004). Nutrient availability, affecting plant biomass production, may be influenced by flooding frequency as a nutrient input (Mueller et al., 2018). Furthermore, nutrient uptake from the soil is limited by several environmental factors, including hypersaline conditions, reducing environments, low soil-water potential, and sulphide accumulation (Silvestri and Marani, 2004).

Given the above, elevation within the tidal range is a primary determinant of plant zonation in salt marshes (Sarika and Zikos, 2021; Silvestri et al., 2005). At low elevation, salinity is comparatively low because of regular tidal flushing that prevents the accumulation of salt, and substrate stability, oxygenation, and sulfide toxicity are key factors controlling pioneer plant establishment on emerging salt marshes (Adam, 2002). At higher elevations, where tidal inundation becomes less frequent, anoxic stress decreases, while more intense evaporation causes challenging saline conditions (e.g., Adam, 2002). Despite these general patterns, salinity can be highly variable, depending on rainfall seasonality, interannual variations, or freshwater inputs from river discharge or high groundwater level. In presence of sufficient freshwater inputs, halophytic communities of the salt marsh are replaced by assemblages more typical of brackish or freshwater marshes, such as reeds (Perillo et al., 2009; Sarika and Zikos, 2021).

1.3 Ecosystem services of a Blue Carbon environment

Situated at the interface between terrestrial and marine ecosystems, salt-marsh environments often lie in some of the world's most densely populated areas, providing important ecological functions and delivering a wide range of ecosystem services that contribute to human well-being. Ecosystem services represent the benefits human populations derive, directly or indirectly, from natural ecosystem functions, including the production of goods (such as seafood and timber), life support processes (such as pollination and water purification), and life-fulfilling conditions (such as beauty and serenity) (Costanza et al., 1997; Perillo et al., 2009).

Salt-marsh ecosystems exhibit one of the highest rates of primary production in the world (Perillo et al., 2009) and provide critical habitat for ecologically important species (Perillo et al., 2009; Teixeira et al., 2014). As an example, submerged halophytic vegetation on salt-marsh platforms provides nursery habitat supplying protection and shelter for young fishes, shrimp, and shellfish (Boesch and Turner, 1984). This function serves, in addition, to maintain fisheries by boosting the production of economically important fishery species (Boesch and Turner, 1984; MacKenzie and Dionne, 2008). In the past, salt marshes were an important source of raw materials and food (Davy et al., 2009), and locally they still are (Barbier et al., 2011). For thousands of years, salt marshes have provided coastal protection from waves and storm surges, as well as from coastal erosion (Barbier et al., 2011; Leonardi et al., 2018) by buffering and attenuating flood and wave action (Möller et al., 2014; Temmerman et al., 2013) and acting as sediment trapping zones (Allen, 2000; Mudd et al., 2010). Salt-marsh vegetation and soil then act as natural filters that improve water quality (Barbier et al., 2011; Mitsch and Gosselink, 2000) enhancing sediment settling and nutrient uptake. Salt-marsh environments are ultimately an important stage for tourism, recreation, education, and research (Barbier et al., 2011; Perillo et al., 2009).

In addition, salt marshes, together with other vegetated coastal ecosystems (i.e. mangrove forests and seagrass meadows) have been increasingly recognised for their carbon (C) sequestration and storage potential, earning them the inclusion among "Blue Carbon ecosystems" (Chmura et al., 2003; Duarte et al., 2005; Macreadie et al., 2019; McLeod et al., 2011; Nellemann et al., 2009). The term

"Blue Carbon" was coined by (Nellemann et al., 2009) to indicate the biological C captured by marine living organisms, as a counterpart of the iconic terrestrial forests called green C, in order to emphasize the fact that over half (55%) of the global C sequestration is attributable to marine and coastal ecosystems (Nellemann et al., 2009). Global interest in blue C is rooted in its potential to mitigate climate change while achieving co-benefits (i.e. numerous other ecosystem services) (Macreadie et al., 2019) and importantly draws attention to the degradation of and the need to conserve and restore coastal ecosystems (Lovelock and Duarte, 2019).

Salt-marsh high potential for C sequestration derives from the peculiar "land-building" capabilities of these tidal vegetated environments. Salt-marsh vegetation captures the atmospheric C through photosynthesis and stores it within aboveground plant tissues and belowground root tissues inserted into the sediment (Craft et al., 1993; Day et al., 1999). Autochthonous organic litter and allochthonous organic debris transported by tides and storms are deposited and trapped on marsh surface (Howard et al., 2017; Perillo et al., 2009). Thanks to the vertical build-up characterizing tidal marshes, driven by the deposition of both organic matter itself and mineral sediments, plant tissues and organic litter are buried in the soil, where up to 90% of marsh C stocks are found (Pendleton et al., 2012; Serrano et al., 2019). Owing to these dynamics and to the anoxic nature of marsh soils, which inhibits microbial aerobic activity and slows decomposition (Keuskamp et al., 2013; Kirwan et al., 2014; Morris et al., 2016; Mueller et al., 2018), the C captured through plant photosynthesis is buried and preserved as Soil Organic Carbon (SOC) over centennial to millennial time scales (Duarte et al., 2005; Perillo et al., 2009).

Estimates showed that the C burial rate per unit area in vegetated coastal ecosystems may be exceptionally high, exceeding that of terrestrial forests by 1–2 orders of magnitude (Chmura et al., 2003; Duarte et al., 2005; Macreadie et al., 2019; McLeod et al., 2011). In light of this, tidal wetlands may boast a significant contribution to global long-term C sequestration, despite a smaller areal extension (Chmura et al., 2003; Duarte et al., 2005; Macreadie et al., 2019; McLeod et al., 2011), making them a key player in global strategies aimed at mitigating climate changes through CO_2 reduction programmes (Macreadie et al., 2019; McLeod et al., 2011).

However, the dimensions of the role of coastal vegetated habitats in the global C cycle and of their contribution to CO_2 emission offset are still unclear, due to high uncertainty of existing estimates of C storage in these environments and of their extent (Sifleet et al., 2011; Mcowen et al., 2017) (Fig. 1.7). OC storage measurements include OC stock, i.e. the quantity of OC contained in a reference soil interval (often 1-m top soil), and OC accumulation rate, i.e. the quantity of OC added to the soil in a reference time, both relying on C density of the soil. To measure the total amount of C stored in soils, knowledge on the C density of the soil and the depth of the organic-rich soil layer are needed. Reference soil interval in C assessment often correspond to 1 m, although the depth of the organic-rich soil layer in coastal wetlands may be highly variable. OC accumulation rates in salt-marsh soils are usually measured on an annual basis and are calculated as the product of sediment accretion rate and average C density of the soil, obtained by multiplying C content and bulk density of the soil.

Duarte et al. (2013) report a mean global estimate of salt-marsh SOC stock of 162 Mg C ha^{-1} within the top 1 m of soil, however a review by Sifleet et al. (2011) reveal SOC stock data ranging between 47.5 to 1900 Mg C ha^{-1}. The global OC accumulation rate in salt marshes is estimated at $151\,\mathrm{ton\,C\,km^{-2}\,yr^{-1}}$ by Nellemann et al. (2009) and $218 \pm 24\,\mathrm{ton\,C\,km^{-2}\,yr^{-1}}$ by Chmura et al. (2003), with the wide distribution reviewed by Sifleet et al. (2011) primarily clustered in the range of 27 to $273\,\mathrm{ton\,C\,km^{-2}\,yr^{-1}}$.

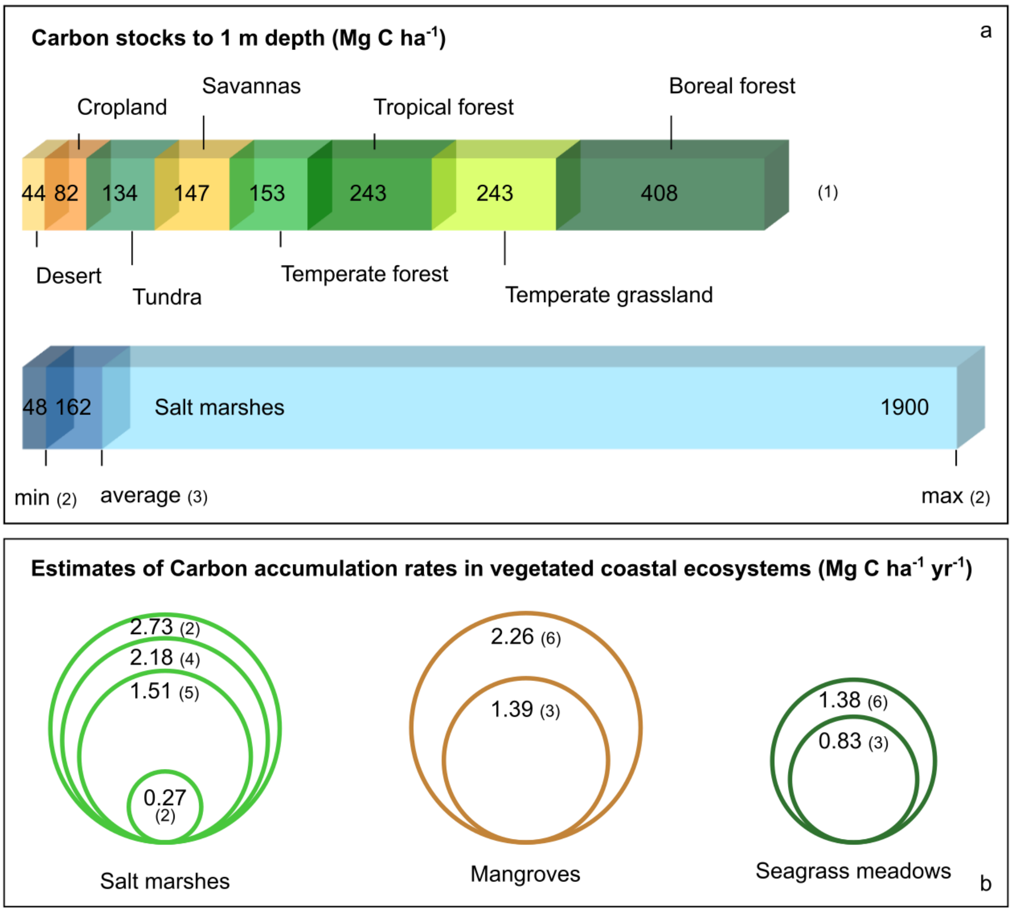

Figure 1.7: **Carbon sequestration and storage potential of salt-marsh environments**. Representation of the amount of organic carbon stored in top 1 m soil of major terrestrial biomes and in salt marshes (a), estimates of C accumulation rate in coastal vegetated ecosystems, including salt marshes, mangroves and seagrass meadows. Wide variability among global compilations derives from methodological differences, other than inherent diversity in SOC density and accretion rates between sites. Sources: 1 - Watson et al., 2000, 2 - Sifleet et al., 2011, 3 - Duarte et al., 2005, 4 - Chmura et al., 2003, 5 – Nellemann et al., 2009, 6 - McLeod et al., 2011.

The wide variability among global compilations derives from methodological differences (e.g. C content measurement approaches, accretion rate estimation methods, reference soil intervals), other than inherent diversity in SOC density and accretion rates between sites (e.g., Chmura et al., 2003; Sifleet et al., 2011).

Chmura et al. (2003) presented data on C storage in salt marshes from 26 published studies as well as some unpublished data at a total of 154 sites from the western and eastern Atlantic and Pacific coasts, the Indian Ocean, Mediterranean and Gulf of Mexico, summarizing information about organic carbon (OC) density and C accumulation rates. The average soil C density of salt marshes is $0.039 \pm 0.003\,\mathrm{g\,cm^{-3}}$, with highest values, reaching $0.19\,\mathrm{g\,cm^{-3}}$, found in the Mississippi Delta (Bryant and Chabreck, 1998).

SOC density directly derives from SOM content, whose variability in salt-marsh soils may be affected by organic inputs, sediment supply and preservation conditions, which are in turn driven by both physical (e.g. temperature, precipitation, hydroperiod, salinity, pH, nutrients, sediment type) and biological (e.g. primary productivity, species composition, bioturbation, microbial community) variables (McLeod et al., 2011), as explained below. In addition, the variability in accretion rates (ranging from a few mm/yr to cm/yr (Bryant and Chabreck, 1998; Chmura et al., 2001; Chmura and Hung, 2004; Craft et al., 1993; Oenema and DeLaune, 1988; Pethick, 1981)) strongly affects estimates of C accumulation rates. For instance, some of the highest values of C accumulation rate showed by Chmura et al. (2003) were reported for the Eastern Scheldt, South-west Netherlands, where observed mean accretion rates were up to $1.0 - 1.5\,\mathrm{cm\,yr^{-1}}$ (Oenema and DeLaune, 1988). The rate of increase of salt-marsh elevations is primarily affected by organic matter contributions, sediment supply, subsurface processes, and vertical accommodation space determined by tidal range and RSLR (Chmura and Hung, 2004; Reed, 1990; Stevenson et al., 1986).

1.4 The future of salt-marsh environments: controls and threats to salt-marsh maintenance

Accommodation space within which inorganic and organic deposition can occur (Allen, 2000) is a first-order control on ecomorphodynamic processes determining the occurrence and persistence of tidal salt marshes, and consequently of the related ecosystem services.

Tidal range, commonly classified in micro- (mean tidal range < 2 m), meso- (2 m $<$ mean tidal range < 4 m), and macrotidal (mean tidal range > 4 m), defines the width of the intertidal zone (Perillo et al., 2009). Exchanges of water and materials with adjacent systems can be highly energetic in macrotidal salt marshes (Perillo et al., 2009) and field observations suggest a correlation between tidal range and the potential for sediment transport (French, 2006). In microtidal systems, instead, nontidal storm inundation events are often of greater relative importance (French, 2006; Tognin et al., 2021).

Ecosystem response to sea level changes is in turn a dominant process in coastal wetland evolution, with sea level rise creating new accommodation space for the accumulation of intertidal sediments (Allen, 2000). Global sea levels have been rising since the last glacial maximum, at rates of around $1\,\mathrm{mm\,yr^{-1}}$ during late Holocene (Kemp et al., 2011). In response to melting of the glaciers, starting from 20 000 years ago, absolute sea level rose rapidly until about 6000-7000 years ago (Mudd, 2011) and then continued to rise slowly, for most of the world's oceans, until the mid-1800s (Perillo et al., 2009). Relative water level is not only affected by the sea surface height but also by changes in land elevation, occurring at different scales due to natural processes (e.g. tectonic activity, compression of the land by the weight of glaciers, post-glacial rebound, and natural subsidence) or human interferences (e.g. man-induced subsidence due to the extraction of water, oil and gas) (Perillo et al., 2009). Stratigraphic studies have shown that the latter period of relatively stabilized relative sea-level rise (RSLR) favoured the widespread development of salt marshes (Mudd, 2011). However, worldwide, the rate of RSLR has doubled or tripled since the late 19th century and it is predicted to accelerate throughout the 21st century (Cahoon and Guntenspergen, 2010), with IPCC projecting a global mean sea-level rise associated with climate change ranging between 0.29-1.1 m by 2100 (above the 1986–2005 baseline - 2022 Intergovernmental Panel on Climate Change (IPCC) Sixth Assessment Report). Therefore, a strong concern exists over salt-marsh ability to survive increasing rates of SLR (Kirwan et al., 2010).

The ephemeral and transitional nature of salt marshes particularly exposes them to the effects of climate change and anthropogenic disturbances, jeopardizing their survival together with their ability to provide key ecosystem services. Climate change and human pressure may, in fact, severely affect ecogeomorphic feedbacks building soil elevation, through alteration of climate, sediment dynamics, subsidence rates, nutrient inputs (Kirwan et al., 2010; Kirwan and Megonigal, 2013; Valiela et al., 2018).

Changing sea level is only one of the consequences of climate change which could impact on salt-marsh evolution. Increase in atmospheric CO_2 and global warming have the potential to strongly affect primary productivity, species distribution and decomposition processes (Osland et al., 2018; Perillo et al., 2009; Kirwan and Mudd, 2012), thereby altering the structure and function of coastal wetlands. Increased atmospheric CO_2 concentrations could increase net primary production and C sequestration if nutrients, precipitation, and other factors were not limiting to plant growth (Nguyen et al., 2015; Ratliff et al., 2015). However, warming temperature are indicated to accelerate decomposition (Keuskamp et al., 2013; Kirwan et al., 2014; Mueller et al., 2018). Thus, the effects of climate change may alter C cycle in wetland environments in ways that are still unclear.

Moreover, situated at the interface between terrestrial and marine ecosystems, on coastal regions which have constituted strategic points of human settlement through history, salt marshes are exposed to long-time anthropogenic pressures. Extensive salt-marsh areas have been directly transformed through land reclamation for agriculture (Netherlands and France by the 11th century and probably earlier in China) and urbanization (e.g. large coastal cities such as Boston, San Francisco, Amsterdam, Rotterdam, Venice, and Tokyo expanded on former coastal wetlands) by building dikes for flood protection (Perillo et al., 2009). Rigid infrastructures and hard engineering structures occurring at the inland boundary of salt marshes, moreover, preclude the landward migration of coastal wetlands in response to rising sea levels (Christiansen et al., 2000), so that coastal wetlands might disappear over time through a process known as coastal squeeze (Doody, 2004; Perillo et al., 2009).

Furthermore, sediment supply feeding salt-marsh elevation has been strongly affected by anthropogenic interferences in various ways. Humans have altered fluvial transport of sediments to the coast, mainly through soil erosion enhanced by deforestation and agriculture, which in turn increases sediment loads in rivers, and, on the other hand, through the widespread construction of dams, dikes and canals, together with dredging for mining, which reduce the amount of sediments being exported to the coastal zone (Perillo et al., 2009). In addition, other human interventions, such as river diversions, dredging and deepening of navigation channels and the construction of jetties may seriously modify local hydrodynamics, sediment transport and morphological settings of tidal environments (Brambati et al., 2003; Carniello et al., 2012; Tognin et al., 2022).

When the marsh accretion rate is lower than the rate of RSLR, the marsh platform progressively drowns and a salt marsh can experience a transition into a tidal flat (D'Alpaos et al., 2011; Kirwan et al., 2010; Marani et al., 2007). Salt marshes can also undergo a transition into tidal flats through lateral erosion and retreat of their margins (Fig. 1.8) (e.g., Fagherazzi et al., 2013; Geng et al., 2021; Leonardi et al., 2016; Marani et al., 2011). Deeper and wider tidal flats further favour the development of stronger wind waves (Fagherazzi et al., 2013; Tommasini et al., 2019; Leonardi et al., 2018), thereby enhancing wave-induced erosion of the salt-marsh border through a positive feedback process which leads to salt-marsh erosion and retreat.

Figure 1.8: **Salt-marsh erosion**. A collapsed margin facing the San Felice channel in the northern Venice Lagoon. Photo: Alice Puppin.

In addition, with global population under flooding threat dramatically growing (Neumann et al., 2015), the increasingly common construction of tidal barrages reducing tidal range further threatens salt-marsh preservation. For instance, de Jong et al. (1994) document loss and degradation of salt marsh following completion of the Oosterschelde (the Netherlands) storm surge barrier in 1987 and Tognin et al. (2021) proved that storm-surge barriers recently came into operation to prevent flooding of the city of Venice (Italy), strongly affect sediment accumulation and vertical accretion rate in salt marshes.

Consequently, salt-marsh ecosystems are experiencing a steep global decline at rates four times faster than rain forests (Duarte, 2009). Though quantifications can be problematic, it has been estimated that between 25% and 50% of global salt-marsh extent has been lost with respect to their historical coverage (Barbier et al., 2011; Bridgham et al., 2006; Crooks et al., 2011; Duarte et al., 2008; McLeod et al., 2011; Mcowen et al., 2017), with a minimum annual rate of loss of 1-2% of their current area (Duarte, 2009). For instance, salt-marsh area decreased by 85% since 1850 in the San Francisco Bay (Watson, 2004), about a quarter of wetlands were lost from 1930 to 2010 in the Mississippi Delta (Day et al., 2000; Perillo et al., 2009), in the estuaries of south-east England about 90% of salt marshes have been lost over the past few centuries (Hughes and Paramor, 2004), salt-marsh systems of the Venice lagoon (Italy) have experienced a 70% surface reduction in the last century (D'Alpaos, 2010; Tommasini et al., 2019), China experienced a 59% overall loss of salt-marsh extent from the 1980s to the 2010s (Gu et al., 2018).

Nevertheless, great interest exists in the preservation and restoration of salt marshes, due to their high ecological and economical value. Coastal wetland protection, however, is a difficult task as salt-marsh deterioration is motivated by multifaceted alteration of the complex feedbacks between hydrodynamics, geomorphology and vegetation controls driving their evolution. Maintenance of salt-marsh environments importantly depends on their ability to keep up with relative sea level rise through vertical and lateral accretion. Several models have been developed to reproduce the physical and ecological processes driving marsh evolution, using different levels of approximation and complexity, over different spatial scales (e.g., Mudd et al., 2004; D'Alpaos et al., 2007; Kirwan and Murray, 2007; Marani et al., 2007, 2013; Mudd et al., 2009). However, conflicting predictions exist about salt-marsh survival to increasing SLR and biomass accumulation and sediment supply are considered to be critical determinants for the marsh drowning rate (Best et al., 2018; Fagherazzi et al., 2020; Kirwan et al., 2016; Kirwan and Megonigal, 2013). As to salt-marsh vertical evolution, the elevation (referenced to Mean Sea Level) at a given site and time, is ultimately governed by the sediment continuity equation (where erosion is neglected due to the stabilizing presence of vegetation):

$$\frac{\partial z(x,t)}{\partial t} = Q_i(x,t) + Q_o(x,t) \tag{1.1}$$

where $Q_i(x,t)$ and $Q_o(x,t)$ are the local rates of inorganic and organic deposition, respectively. So, to maintain their elevation above mean sea level, the sum of inorganic and organic deposition needs to balance RSLR. The relative contribution of organic and inorganic constituents to vertical accretion rates may vary in space and time across the range of tidal wetland types and within individual wetlands depending on different conditions such as sediment supply and primary production (Kolker et al., 2009; Morris et al., 2016; Nyman et al., 2006; Turner et al., 2002). The organic component tends to be of greater relative importance in microtidal regimes, where the effective supply of inorganic sediment is limited by generally lower background suspended sediment concentrations and by less energetic tidal exchanges (Friedrichs and Perry, 2001; Morris et al., 2002, 2016; Perillo et al., 2009).

1.5 Soil Organic Matter in salt marshes

The organic component of the soil, consisting of plant or animal tissues in various stages of breakdown, is defined as soil organic matter (SOM) (Baldock and Nelson, 2000). SOM represents the largest C stock in the terrestrial biosphere and constitutes a fundamental component of the global C cycle (Jackson et al., 2017; Schlesinger, 1990). SOM has a key role within salt-marsh environment, since, as previously stated, on one hand it contributes to the building-up of marsh elevation, and on the other it supports the C sink potential of wetlands, attracting great scientific interest. Although OM content is strongly variable in space, in some conditions SOM, owing to its high porosity and low density, may contributes up to 1.5–3 times more toward vertical accretion than inorganic matter (Allen et al., 2021), having a key role in the persistence of coastal wetlands with low mineral sediment supply (Friedrichs and Perry, 2001; Morris et al., 2002, 2016; Perillo et al., 2009). SOM in salt marshes is constituted by a combination of in-situ production of belowground biomass (root, rhizome and tuber tissues) inserted into the sediments (Craft et al., 1993; Nyman et al., 2006) and autochthonous or allochthonous organic materials that are deposited over the salt marsh (Ewers Lewis et al., 2019; Mudd et al., 2009; Mueller et al., 2019) (Fig. 1.9).

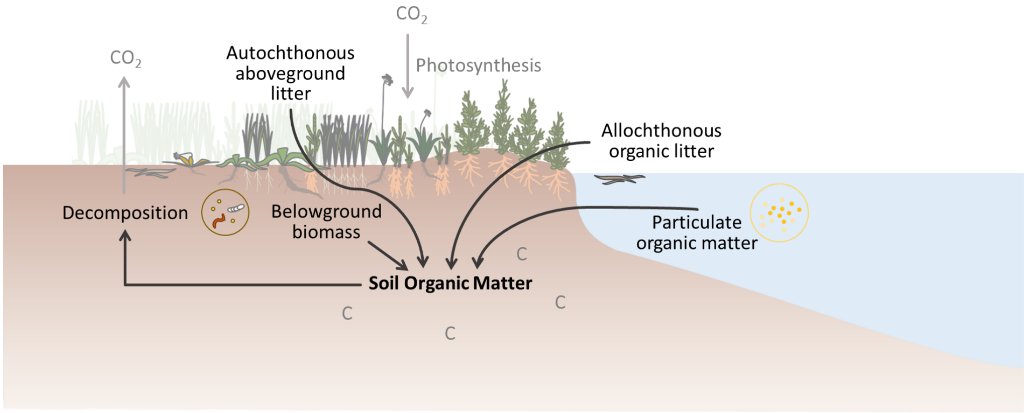

Figure 1.9: **Soil Organic Matter in tidal environments**. Schematic representation of the processes driving the formation of SOM in salt marshes.

Surface litter produced during the annual cycles of plant growth and decay settles on the ground and is trapped within the inorganic sediments deposited. A variable proportion of the salt-marsh SOM (Drexler et al., 2020; Middelburg et al., 1997; Mueller et al., 2019) has an allochthonous source, deriving from suspended particulate organic matter, often adsorbed on mineral matter, as well as estuarine and marine phytoplankton, microphytobenthos and non-local macrophytes litter carried to the marsh surface by waves and tides.

The fate of SOM, then, strongly depends on decomposition (Kirwan et al., 2013; Mudd et al., 2009; Rybczyk and Cahoon, 2002), i.e. the process of dead OM (litter) decay when OM is broken into simple compounds. Decomposition consists of concurrent processes operated by physical and biological agents, including fragmentation, leaching of water-soluble compounds, and microbial catabolism (Sanderman and Amundson, 2013), resulting in the release of CO_2 and other organic trace gases, water, mineral nutrients, and energy, playing a fundamental role in biogeochemical cycles (Pavao-Zuckerman, 2008). Decomposition is controlled by the interactions between the community of decomposer organisms, the quality of the substrate and the physical environment. Studies of litter decay have often emphasized the importance of climate on decomposition processes (Sanderman and Amundson, 2013), and temperature has long been thought to be an important control of decay rates in wetlands (Montagna and Ruber, 1980; White et al., 1978), with decomposition rates increasing with warming temperatures (Keuskamp et al., 2013; Kirwan et al., 2014; Mueller et al., 2018). Nevertheless, large variations in litter mass loss were observed within biomes, across marshes and across different sites (e.g, Kirwan et al., 2014; Morris et al., 2002; Mueller et al., 2018; Reents et al., 2021, suggesting that local-scale factors, such as e.g. soil aeration and drainage, have strong controls on decomposition dynamics (Cornwell et al., 2008; Djukic et al., 2018). As to elevation and hydroperiod, being key drivers of soil aeration, several studies investigated the influence of topography and flooding frequency and duration on decomposition rates in salt-marsh environments, revealing highly variable relationships (Halupa and Howes, 1995; Kirwan et al., 2013; Mueller et al., 2018; Yousefi Lalimi et al., 2018). Furthermore, the quality of the organic matter itself in terms of its chemical and structural composition, determining labile or recalcitrant compounds, is also known to strongly influence decomposition processes (Freschet et al., 2012; Lang et al., 2009; Wang et al., 2017). Lastly, SOM can be physically protected from decomposition through micro-aggregation or association with silt and clay particles, which limit its accessibility to microorganisms (Six et al., 2002).

SOM content ultimately depends on organic inputs and their preservation. However, drivers of SOM variability in salt marshes are innately difficult to identify as such a variability is the result of many complex processes acting simultaneously and occurring over a wide range of spatial scales (Ewers Lewis et al., 2020; Marani et al., 2006a). While at the global scale, climatic parameters appear to be important drivers for C sequestration and storage (Chmura et al., 2003), at the catchment scale, the geomorphological setting is a key predictor of SOM content, with physical and biological factors changing within the gradient generated by marine and fluvial influence (e.g. salinity, sediment inputs, stable allochthonous OM supply, vegetation type (van Ardenne et al., 2018a; Van De Broek et al., 2016; Kelleway et al., 2016; Macreadie et al., 2017)). Fluvially-influenced sites were observed to contain twice the soil organic C (SOC) stock of seaward sites by Kelleway et al. (2016) and Macreadie et al. (2017). In contrast, Gorham et al. (2021) observed no significant differences between SOC accumulation inventories between marine and fluvial settings suggesting this to be the consequence of the high heterogeneity among and within study sites. Of course, considerable variability in sediment organic content has been observed across vegetation types (Ewers Lewis et al., 2020; Saintilan et al., 2013), which determine above and belowground biomass production both quantitatively and qualitatively, in terms of decay resistance (Scarton et al., 2002; Stagg et al., 2018). SOM is influenced also by sediment type, associated to different concentrations of suspended particulate organic matter, and a negative relationship between SOM content and sediment grain size has been observed, which may be explained by multiple mechanisms (Van De Broek et al., 2016; Kelleway et al., 2016; Saintilan et al., 2013). First, fine sediments have been recognised to have a greater potential for C protection through organo-mineral interactions and micro- or macro-aggregates due to their greater specific surface area than coarser sediments and cation exchange capacity of fine-grained minerals (Bader et al., 1960; Baldock and Skjemstad, 2000; De Gryze et al., 2006). Furthermore, enhanced C preservation would be expected in fine sediments through a reduced oxygen exchange, due to lower porosity and drainage capacity, promoting anoxic conditions and consequently lower decomposition rates (Arnarson and Keil, 2007; Hartnett et al., 1998). At the marsh scale, elevation and hydroperiod may importantly influence SOM variability, affecting vegetation characteristics, organic-matter supply and sediment deposition (Chmura et al., 2003), other than microbial community and organic-matter preservation conditions (Kirwan et al., 2013; Marani et al., 2006a; Mudd et al., 2009; Yousefi Lalimi et al., 2018).

In addition, when addressing SOM distribution with depth in salt marshes, it is important to consider that depositional conditions and environmental variables differ at decadal to millennial time scales, therefore marsh history is an additional driver of SOM distribution and possible heterogeneity (Gorham et al., 2021; Miller et al., 2022). All the above considered, despite research advances in describing SOM dynamics in salt-marsh environments, large knowledge gaps and uncertainties remain, particularly in accounting for SOM variability at different temporal and spatial scales and identifying causal relationships driving the complex process of SOM accumulation.

1.6 Thesis aims and outline

Salt marshes are critical transitional zones between terrestrial and marine ecosystems, being widely developed along world's temperate coastlines, and providing a wide range of ecosystem services, though they are in rapid and global decline. Salt-marsh conservation and restoration have been recognized as a fundamental actions in mitigation and adaptation strategies, aiming at facing the increasing socio-economic impacts of climate change.

It is becoming clear that SOM accumulation may play an important part in maintaining marsh surface elevations, and the strategic importance of Blue Carbon sequestered and stored by coastal wetlands has been increasingly recognised, raising interest toward OM dynamics in salt-marsh environments.

Towards the goal of improving our current understanding of OM dynamics influencing coastal wetlands resilience and their carbon sink potential, the present work investigates soil organic matter and carbon dynamics in microtidal salt marshes under natural and anthropogenic forcing. A multidisciplinary approach has been used, combining ecological and sedimentological evaluations through field observations, laboratory analyses, and statistical investigations.

The selected study site is the Venice Lagoon, in the north-western Adriatic Sea (Italy), a microtidal back-barrier system being the largest lagoon in the Mediterranean. Here coastal populations and the tidal environment have been intertwined for centuries, thus the Venice Lagoon is a paradigmatic case for comprehending anthropogenic and natural forcing interactions.

In view of this, focuses and research questions of the present study can be listed as follows:

1. How does decomposition affect the amount of Organic Matter effectively contributing to soil formation and carbon burial in tidal marshes and which are the physical and biological factors that most decisively influence it?

2. Which are the spatial patterns of soil organic matter in surface salt-marsh soil and which physical and biological factors drive Organic Matter distribution?

3. How Organic Matter distribution with depth in salt-marsh soils can be de-

scribed and which is its relationship with different depositional environments?

4. What are the dimensions of carbon stock and carbon accumulation rates in the salt marshes of the Venice Lagoon (Italy) and how do storm-surge barriers affect carbon sequestration potential in coastal wetlands?

The introductory chapter is followed by a synthetic overview on the data and methods used and then by four main chapters, addressing the above-mentioned research questions.

Chapter 3 contributes to answer the first research question and it analyses empirically derived rates of organic matter decomposition and stabilization following the Tea Bag Index protocol. The data from a wide, standard litter decomposition experiment were used to inspect the influence of climatic and hydromorphological variables on decomposition metrics.

Chapter 4 focuses on the spatial variability of soil organic matter in salt-marsh surface sediments. Combining analyses on sediment characteristics, geomorphological and vegetation components, factors driving SOM variability and distribution are investigated.

Chapter 5 deals with patterns of OM content with depth (to the depth of 1 m) and with their spatial distribution in salt-marsh soils. On the basis of a large number of sediment samples, stratigraphic analyses are used to investigate the influence of depositional environments on SOM distribution. Then, the relationships between physical characteristics of the soil and SOM content are evaluated. In addition, an exponential decay model with depth is tested to describe SOM vertical distribution in a predictive manner.

Chapter 6 focuses on the assessment of Blue Carbon dimensions and variability in the salt marshes of the Venice Lagoon. Synthetizing the results of SOM spatial and vertical distribution, carbon stock and carbon accretion rates are estimated in different areas of the study site and the effects of management actions on carbon sink potential of the Venice Lagoon are evaluated.

In conclusion, a summary of the main results obtained from this thesis is traced in Chapter 7.

2

METHODS

2.1 Study site

We focused our analyses on the Venice Lagoon, a north-east-southwest oriented, 50-km long, 10-km wide water body located in the north-western Adriatic Sea (Italy), being the largest brackish tidal basin of the Mediterranean Sea (Fig. 2.1a and Fig. 2.1b). This back-barrier system, connected to the sea by three inlets (i.e. Lido, Malamocco, and Chioggia) is a shallow microtidal basin, characterized by a semidiurnal tidal regime with an average tidal range of 1.0 m and a mean water depth over tidal flats of about 1.5 m. Prevailing winds in the Venice Lagoon are the Bora wind, blowing from the northeast at speeds that can exceed 20 m/s, and the Sirocco wind, blowing from the southwest at speeds rarely exceeding 10 m/s (Tommasini et al., 2019) (Fig. 2.1c).

The present-day morphology of the Venice Lagoon, which formed during the Holocene transgression (Zecchin et al., 2009), is the result of a combination of natural forcings and human interventions. Since the 15th century, in order to prevent the ongoing infill of the lagoon and preserve channel and port functions, several hydraulic works have been carried out, which strongly modified sediment supply, local hydrodynamics and the morphological setting, favouring sediment starvation and the deepening of the lagoon (Brambati et al., 2003; D'Alpaos, 2010; Silvestri et al., 2018; Zecchin et al., 2009). Between the fifteenth and seventeenth centuries, major tributaries were diverted outside of the lagoon, dramatically decreasing the fluvial sediment input in the tidal system, and since the nineteenth century, inlet modifications and new deep canal dredging exacerbated sediment export toward the sea (Brambati et al., 2003; D'Alpaos, 2010; Finotello et al., 2022). Furthermore, large intertidal areas at the landward border of the lagoon were reclaimed to provide industrial and urban space and between 1930 and 1970 intense groundwater exploitation for industrial purposes enhanced local subsidence (Brambati et al., 2003; Carbognin et al., 2004; Teatini et al., 1995).

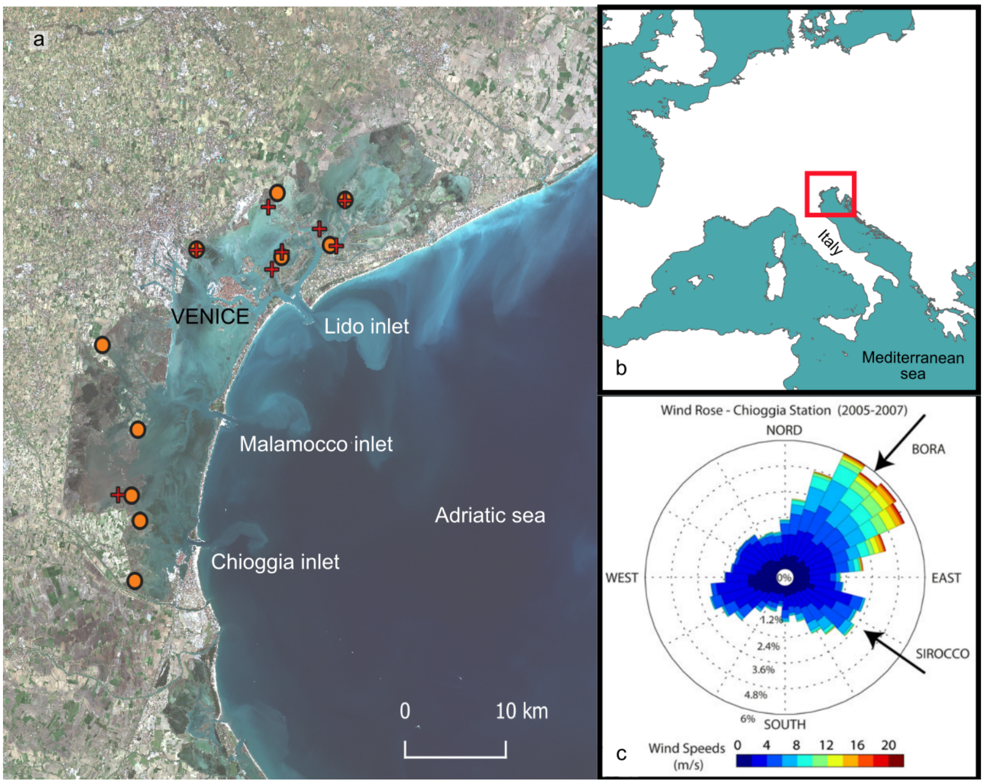

Figure 2.1: **Study area: the Venice Lagoon**. The Venice Lagoon, located in the north-western Adriatic Sea (Italy)(b), with study sites for the decomposition experiment (red plus symbols) and SOM and C content (orange circles) (a), and the wind rose from Tommasini et al. (2019) (c).

As a consequence, salt-marsh extension of the Venice lagoon decreased from about 180 km^2 in 1811 to about 43 km^2 in 2002 (Carniello et al., 2009; D'Alpaos, 2010; Tommasini et al., 2019). In addition, recent activation of storm-surge barriers, designed to prevent flooding of the city of Venice, was proved to further alter the lagoon hydrodynamics (Mel et al., 2021) contributing to the deepening of the tidal flats and reducing salt-marsh sedimentation (Tognin et al., 2021).

The landscape of the Venice Lagoon is characterised by the presence of deep channels departing from the inlets and cutting through the tidal flat surfaces together with shallower tidal channels which incise vegetated intertidal salt marshes (Carniello et al., 2009; Finotello et al., 2022). Salt marshes are dissected by intricate networks of branching and meandering tidal channels (D'Alpaos et al., 2005; Finotello et al., 2022; Marani et al., 2003) and are colonized by different halophytes organized in characteristic patches mostly depending on topographic elevation. For instance, the annual succulent *Salicornia veneta* and the perennial cord grass *Spartina maritima* grow on the most depressed soils (Silvestri et al., 2005; Silvestri and Marani, 2004), whereas the rosette-forming *Limonium narbonense* and grasses like *Puccinellia palustris* are found at periodically inundated platform areas (Ivajnšič et al., 2018; Silvestri et al., 2005). The perennial succulent dwarf shrub *Sarcocornia fruticosa* is found at slightly higher areas, while other species (e.g. *Aster tripolium*, *Inula crithmoides* and *Suaeda maritima*) grow preferentially along the edges of creeks and channels (Silvestri and Marani, 2004). In contrast, the perennial saline rush *Juncus maritimus* presents a weak dependence on soil elevation (Silvestri and Marani, 2004). At sites influenced by freshwater inputs, from river discharge or emerging groundwater, brackish swamp reed *Phragmites australis* is observed.

The northern lagoon is the most naturally preserved portion of the Venice Lagoon (Silvestri et al., 2018), whereas the central part is importantly affected by the excavation of a deep navigation channel, the Malamocco Marghera channel, responsible for morphology flattening and deepening. Southern lagoon presents a high naturalness that is, however, no longer an expression of the original environment, since river diversions radically altered the relationships between fluvial and marine waters, with the transformation of extensive reed beds in salt marshes (Bonometto, 2005). In addition, the southern lagoon is also the portion of the lagoon which is most affected by erosion processes both in the vertical and horizontal plane (D'Alpaos et al., 2013) due to the intertwined effects of natural and anthropogenic induced processes (Carniello et al., 2009; D'Alpaos, 2010).

2.2 Experimental design

The investigations on organic matter dynamics in salt-marsh soils are carried out through field observations of decomposition processes and SOM and C content in soil samples, coupled with the analysis of the environmental variables possibly affecting their variability. A stratified sampling method based on two scales was followed in order to account for different variation drivers. Stratified sampling is a probability sampling technique in which the total population is divided into homogenous groups (strata) formed based on shared attributes or characteristics (Howard et al., 2014). Literature information, satellite imagery and local knowledge were used to determine stratification criteria. The strata size and number are the result of a balance between accuracy desired, time required, and resources available. At the lagoon scale, sampling sites (7 for the decomposition experiment and 10 for SOM and C content analyses, see Fig. 2.1a) were located in different salt marshes in northern, central and southern lagoon in order to account for variations mainly driven by the gradient generated by marine and mainland influence. For SOM and C content analysis, in particular, a salt-marsh classification based on origins and functions was also considered. In fact, lagoon canal salt marshes, bordering main tidal channels and nourished by marine sediment input, as well as salt marshes along the lagoon boundary and at the borders of fluvial water entering the lagoon, and salt marshes originated on salinized pre-existing brackish environments (Bonometto, 2005) were included among sampling sites. At the marsh scale, given the influence of tidal channels as preferential pathway for the exchange of water, sediment, nutrients and biota (D'Alpaos et al., 2005; Fagherazzi et al., 1999; Geng et al., 2021), and considering the morphological structure and plant zonation characterizing salt-marsh environments, transect sampling was chosen to account for the variation of the variables analysed in this study. Sampling points were located on linear transects from the marsh main edge to the inner area, 30-40 m away from the edge. Detailed descriptions of sampling sites are found in Chapter 3, for the decomposition experiments, and Chapter 4 and 5 for SOM and C content analysis. Here a short description of the method used is reported for the sake of completeness.

2.3 Decomposition process study: the Tea Bag Index

To analyse decomposition processes of the organic matter in salt-marsh soils, the Tea Bag Index (TBI) protocol proposed by Keuskamp et al. (2013) was adopted. The protocol consists of a simplified litter-bag experiment carried out burying standard litter, which in this case are commercially available tea bags (Lipton, Uniliver), in salt-marsh soils for an incubation period of about 90 days and measuring the remaining mass after retrieval.

The TBI comprises two parameters: the decomposition rate (k), describing how fast the decomposition proceeds, and the litter stabilisation factor (S), which describes the fraction of labile material that becomes stabilized during deployment (Keuskamp et al., 2013). Two tea types with different decomposition rates (i.e. green tea and rooibos tea) were used in order to obtain the two parameters during one single incubation period. Green tea decomposition is faster, and all the labile material is assumed to be consumed during the incubation, whereas rooibos tea decay is slower (Keuskamp et al., 2013).

Using standard litter instead of site-specific litter Tea Bag Index intends to focus on climate and environmental effects on decomposition processes, allowing comparisons between different sites characterized by different local plant communities with different characteristics.

Green and rooibos tea bags were buried pairwise in salt-marsh soils along linear transects and placed at different depths, corresponding to 0, 16, 24, and 40 cm relative to the marsh surface, to analyse the effects of burial depths on decomposition dynamics. Decomposition data used in this work were previously collected between April and October in 2015, 2016, and 2017. The TBI litter-bag experiment and its results are described in detail in Chapter 3.

2.4 Soil sampling

SOM and C content investigation was based on the analysis of 720 soil samples from 60 sediment cores collected along linear transects from the marsh edge to the inner marsh, in 10 different areas of the Venice Lagoon (Fig. 2.1a).

In order to obtain relatively undisturbed soil samples that have undergone minimal compaction, an Eijkelkamp gouge auger was used to collect sediment cores (Fig. 2.2). It consists of a 1-m-long semi-cylindrical chamber that is pushed into the soil, twisted, and then pulled out. Extensions can be added so that longer cores (3–5m) can be recovered. The Eijkelkamp auger has an open bottom, and soils can be lost out the bottom if they are wet or if they lack cohesiveness, such as unconsolidated sands. For this work, cores were collected to the depth of 1 m, a core depth that is generally agreed to provide an effective estimate of coastal soil C stock in temperate regions (Howard et al., 2014).

Cores were split lengthwise in the laboratory, photographed, and sectioned to collect the samples. For each core, soil samples were taken at 12 depths, 0, 5, 10, 15, 20, 25, 30, 35, 40, 45, 50, 75 cm from the surface, as variations in organic content are considered most significant in the upper 20 to 50 cm of soil (see Howard et al. (2014)). Samples were weighted, oven-dried at 60°C until a constant weight was achieved and subsamples were prepared for different analyses, including soil density, organic matter and C content.

Figure 2.2: **Soil sampling**. Core collection with the Eijkelkamp gouge auger (a), and core transfer in a PVC liner to be packed and transported to the laboratory (b). Photos: Alice Puppin

2.5 Determination of the organic matter content

Organic matter content was determined through loss-on-ignition (LOI), a relatively cheap and rapid method, widely used to measure organic matter content in sediments, providing a wider context for direct comparisons (e.g., Craft et al., 1991; Howard et al., 2014; Ouyang and Lee, 2020). This method estimates SOM based on gravimetric weight change associated with high temperature combustion of organic matter in a muffle furnace (Fig. 2.3a).

However, it should be emphasized that an accepted standardized LOI procedure is still lacking (Hoogsteen et al., 2015; Roner et al., 2016) and caution is needed when comparing the results from different procedures, which may underestimate or overestimate the actual OM content depending on the specific sample type. Procedural differences in the LOI approach include, in particular, the ignition temperatures, exposure times, sample sizes, and position of samples in the furnace (Heiri et al., 2001; Barillé-Boyer et al., 2003; Fan and Brown, 2001). Many estimates of OM contents in sediments found in the literature derive from LOI at 550 °C. However, in the range of temperatures between 450 °C and 600 °C, samples may lose structural water during combustion (Ball, 1964; Howard and Howard, 1990) in sediments characterized by high clay content, thereby significantly affecting soil OM estimates (Mook and Hoskin, 1982; Dankers and Laane, 1983; Barillé-Boyer et al., 2003). Moreover, between 425 °C and 520 °C a potential loss of CO_2 can occur in sediments containing inorganic carbon (e.g. siderite ($FeCO_3$), magnesite ($MgCO_3$), rhodocrosite ($MnCO_3$) and dolomite ($CaMg(CO_3)_2$); (Weliky et al., 1983; Howard and Howard, 1990; Sutherland, 1998; Santisteban Navarro et al., 2004). Overall, a LOI test at 550 °C may lead to a large overestimation of the loss of organic matter mass (Frangipane et al., 2009). Consequently, we choose to perform LOI at low temperature.

About 2 grams of sediment for each sample were crumbled in a ceramic mortar and placed into a dry ceramic crucible (Fig. 2.3b). The LOI process started with a temperature increase of 5 °C/min until reaching 375 °C, and continued at a constant temperature for 16 h. The difference in weight, before and after the process, was used to estimate the amount of organic matter which was combusted. Chosen temperature-heating time combination allows one to limit organic content overestimation due to the removal of structural water from clay minerals and decomposition of soil carbonates, although it is likely to underestimate the amount of organic matter due to incomplete combustion (Ball, 1964; Frangipane et al., 2009; Roner et al., 2016).

Figure 2.3: **Loss-on-ignition samples**. Ceramic crucible with ground samples (b) in the muffle furnace (a), where they are combusted at 375 °C for 16 h. The difference in weight, before and after the LOI process, is used to estimate the amount of organic matter, which was combusted, in each sample. Photos: Alice Puppin

2.6 Determination of the organic carbon content

Measurements of OC content are needed to accurately determine the soil C stock and fluxes in salt-marsh soils. Moreover, OC is one of the main components of organic matter compounds along with hydrogen, oxygen, nitrogen, phosphorus, and sulphur. Thus, numerous empirical relationships between organic matter content determined through LOI and OC have been proposed for different wetland systems worldwide (Craft et al., 1991; Holmquist et al., 2018; Howard et al., 2014; Ouyang and Lee, 2020). Nevertheless, caution should be used in the application of these relationships to systems different from those for which they were calibrated, and site-specific relationships might provide a more accurate estimate of OC content. For this reason, a subset of 102 representative samples was selected to directly determine C content using an elemental analyser. The elemental analysis was performed by varioMicro Cube V4.0.10 Elementar Analysensysteme GmbH (CHNS) at the Department of Pharmaceutical and Pharmacological Sciences, University of Padova (Italy). Original samples and ashed subsamples (previously obtained from the LOI procedure) were analysed pairwise, in order to determine the total C content and the remaining inorganic C, respectively. Inorganic C content was subtracted from the total C measurements to estimate the OC content. Directly determined C content data (from elemental analysis) were used to fit a regression equation between organic matter and OC following Craft et al. (1991). The interpolated quadratic relationship (shown in Chapter 6) was used to determine the OC content of each soil sample.

2.7 Determination of the sediment Dry Bulk Density

Two methodologies were used to determine the sediment Dry Bulk Density (DBD) ($\mathrm{g\,m^{-3}}$). Firstly, DBD was determined as the ratio between sample dry weight and estimated wet volume using the depth interval of the section and the diameter of the core barrel.

In addition, DBD was calculated from the water content and organic and inorganic fractions as follows, according to Kolker et al. (2009):

$$\rho = \frac{1 - W}{\frac{W}{\rho_W} + \frac{1-W}{\rho_S}}, \tag{2.1}$$

where W is water content, estimated from the difference in weight between wet and dry samples, ρ_W is water density ($1.02\,\mathrm{g\,m^{-3}}$), and ρ_S is sediment density calculated as $(1 - LOI \times 2.6) + (LOI \times 1.2)$, where $2.6\,\mathrm{g\,m^{-3}}$ and $1.2\,\mathrm{g\,m^{-3}}$ are assumed as the densities of mineral and organic matter, respectively (Kolker et al., 2009).

2.8 Carbon stock and carbon accumulation rate

As reported in in Chapter 6, soil C stocks within 1 m soil depths were calculated based on Howard et al. (2014) summing the C content in each soil interval along the core:

$$C_{\text{stock}} = \sum SCD_i \times l_i \tag{2.2}$$

$$SCD = OC_i \times DBD_i \tag{2.3}$$

where SCD_i is Soil Carbon Density, l_i is the soil thickness, OC_i is the organic carbon content and DBD_i is Dry Bulk Density of the i-th interval.

Carbon accumulation rates were estimated by multiplying the average soil carbon density in a reference interval of 5 cm by salt-marsh accretion rates derived from measurements based on marker horizons over a 2-20 yr period (Day et al., 1999; Roner et al., 2017; Saintilan et al., 2022; Tognin et al., 2021).

The reference interval was chosen on the basis of the available marker horizon measurements of the accretion rates, which represent a robust, although short-term, estimate.

2.9 Inorganic sediment grain size analysis

Particle-size distribution is a fundamental physical property of a soil, defining many physical and chemical soil features. Inorganic particle size distribution analyses were performed using laser granulometry by Mastersizer 2000 - Version 5.40, MALVERN INSTRUMENTS at the Department of Pharmaceutical and Pharmacological Sciences, University of Padova (Italy). As removal of SOM is recommended before particle size analysis to ensure effective dispersion of micro-aggregates (Jensen et al., 2017), a pre-treatment with 35% hydrogen peroxide (H_2O_2) for 36 h was performed to oxidize organic content.

Laser diffraction is a widely used particle sizing technique for materials ranging from hundreds of nanometers up to several millimeters in size, being a rapid, well established and high-resolution method. Laser diffraction determines distributions by measuring the angular variation in the intensity of light scattered as a laser beam passes through a dispersed particulate sample. The angle of diffraction is inversely proportional to particle size, and the intensity of the diffracted beam at any angle is a measure of the number of particles with a specific cross-sectional area in the beam's path (Eshel et al., 2004). Laser diffraction uses Mie theory describing the propagation of the electromagnetic wave of light in space to calculate the particle size distribution, assuming a volume equivalent sphere model

(Eshel et al., 2004). Mie theory requires knowledge of both the dispersant, known from published data, and the sample optical properties. The latter can either be measured or estimated.

2.10 Sedimentological analysis

As reported in Chapter 5, sedimentological analyses were carried out on the study cores through the principles of modern facies analysis in order to link core characteristics with the corresponding sedimentary processes and depositional environments (Roner et al., 2017). Different types of deposits were differentiated on the basis of their distinctive features through the observation of their colour, grain size, texture, sedimentary structures and macroscopical biogenic content (e.g. shells, plant debris and vegetal remains).

2.11 Environmental parameters

In order to unravel major drivers of organic matter dynamics, a number of environmental parameters were determined at each study site, as described in detail in Chapter 3, 4 and 5. Elevation above Mean Sea Level (MSL) and geographic location were measured using two TOPCON GR-3 GPS receivers (dual frequency - L1/L2 - and dual constellation - NavStar/Glonass - with integrated Tx/Rx UHF radio) for the decomposition experiment and a GPS in RTK mode (Leica GS16) at core collection sites (Fig. 2.4a). Vegetation characteristics were surveyed within a 1×1 m quadrat (Fig. 2.4b) by the Braun-Blanquet method (Braun-Blanquet, 1964) and registering species cover percentages.

2.12 Statistical analyses

Statistical analyses were performed using MATLAB R2021a in order to investigate patterns, trends, and relationships among the data collected (i.e. decomposition parameters, soil characteristics, environmental variables). Analyses included the use of the Kendall test, Wilcoxon signed-rank test, Kruskal-Wallis H test, and post hoc median comparisons. Non-parametric tests were chosen as distribution-free tests, because our data did not always satisfy normal distribution

Figure 2.4: **GPS and vegetation survey**. A GPS survey (a) allowed to measure elevation above Mean Sea Level (MSL) and geographic location at each study site. Species cover percentages were surveyed within 1 x 1 m quadrat (b) by the Braun-Blanquet method. Photos: Alice Puppin

or homogeneous variance assumptions, as usual in environmental studies (Daniel, 1978; Yue et al., 2002; Montgomery, 2012; Mumby, 2002; Sheskin, 2011; Riaz et al., 2016). The Kendall test is a non-parametric, rank-based method, aimed to determining whether there exists a monotonic relationship between two variables of interest. The value of the coefficient ranges from $+1$ to -1, indicating a positive or a negative association, respectively. When large number of ties occurred, a modified equation that considers the number of ties was used (Soliani, 2019; Sprent and Smeeton, 2000). Wilcoxon signed-rank test is a non-parametric statistical hypothesis test used to compare two populations when the observations are paired, and it is appropriate for a repeated measure design where the same variables are evaluated under two different conditions. The Kruskal-Wallis test is a non-parametric version of classical one-way ANOVA using ranks of the data to compute the chi-square statistics and compare the medians of the groups of data to determine if the samples come from the same population. When Kruskal-Wallis test showed a significant difference between groups, a multiple comparison test was used to determine which pairs of means were significantly different.

3

DECOMPOSITION PROCESSES IN SALT MARSHES

This chapter is a manuscript ready to be submitted to JGR Biogeosciences under the title "Analysis of Organic Matter Decomposition in the Salt Marshes of the Venice Lagoon (Italy) Using Standard Litter Bags". A.D., M.M., and M.R. designed the study. M.R., A.D., M.G. and M.M. developed the methodology. M.R., L.T. and A.F. collected the data. A.P. and M.R. were responsible for data analysis and interpretation with the supervision of A.D., M.M. and A.F. All the authors discussed the data and agreed on their interpretation. A.P., A.D. and A.F. wrote the original draft. M.R. and M.M. provided comments and suggestions to improve the original draft. All the co-authors contributed to the final polishing of the manuscript.

Analysis of Organic Matter Decomposition in the Salt Marshes of the Venice Lagoon (Italy) Using Standard Litter Bags

A. Puppin[1], M. Roner[1], A. Finotello[1], M. Ghinassi[1], L. Tommasini[1], M. Marani[2] and A. D'Alpaos[1].
[1]Department of Geosciences, University of Padua, Padua, Italy
[2]Department of Civil, Environmental and Architectural Engineering, University of Padua, Padua, Italy

3.1 Key Points

- Decomposition rates in Venice marshes display a mean value of $0.012 \pm 0.003\,\mathrm{d}^{-1}$, confirming salt marshes as some of the biomes with slowest decomposition rates.
- Temperature critically controls the fate of organic matter in tidal marshes, leading to a 8% increase per °C in decomposition rates.
- Initial litter quality exerts a primary control on the amount of preserved organic matter contributing to carbon sequestration and marsh accretion.

3.2 Abstract

Tidal salt marshes are widespread along the World's coasts, and are ecologically and economically important as they provide several valuable ecosystem services. In particular, their significant primary production, coupled with sustained vertical accretion rates, enables marshes to sequester and store large amounts of organic carbon and makes them one of the most carbon-rich ecosystems on Earth. Organic carbon accumulation results from the balance between inputs, i.e. organic matter produced by local plants or imported, and outputs through decomposition and erosion. Besides, organic matter deposition actively contributes to marsh vertical accretion, thus critically affecting the resilience of marsh ecosystems against rising relative sea levels. A better understanding of organic-matter dynamics in salt marshes is key to address salt-marsh conservation issues and to elucidate marsh importance within the global carbon cycle. Toward this goal, we empirically derived rates of organic matter decomposition by burying 712 commercially available tea bags at different marshes in the microtidal Venice Lagoon (Italy), and analyzing them following the Tea Bag Index protocol. Our results reveal values of the decomposition rate (k) and stabilization factor (S) equal to $0.012 \pm 0.003\,\mathrm{d}^{-1}$ and 0.15 ± 0.063, respectively. Water temperature critically affects organic matter decomposition, enhancing decomposition rates by 8% per °C on average. We argue that, at least in the short term, the amount of undecomposed organic matter that actively contributes to carbon sequestration and marsh vertical accretion strongly depends on the initial organic matter quality, which is likely to vary as a function of marsh and vegetation characteristics.

3.3 Introduction

Salt marshes are transitional ecosystems found between permanently submerged and emerged coastal environments. They are the prevailing landscape in the intertidal zone of many low-energy temperate coasts (Adam, 1990; Allen and Pye, 1992; Mcowen et al., 2017), with vegetation dominated mostly by herbaceous halophytes adapted to regular inundation by saltwater (Perillo et al., 2009). Salt marshes are crucial ecomorphodynamic structures in tidal environments as they offer valuable ecosystem services (Barbier et al., 2011) by attenuating waves (Möller et al., 2014; Temmerman et al., 2013), acting as sediment trapping zones (Allen, 2000; Mudd et al., 2009), boosting the production of economically and ecologically important fishery species (Boesch and Turner, 1984; MacKenzie and Dionne, 2008), and filtering both nutrients and pollutants (Costanza et al., 1997).

In addition, marshes serve as highly efficient sinks for blue carbon, i.e., the organic Carbon (C) captured and stored by coastal ecosystems and oceans (Chmura et al., 2003; Duarte et al., 2005; Macreadie et al., 2019; McLeod et al., 2011). Such a potential for carbon sequestration derives from the high rates characterizing marsh primary production, coupled with sustained accretion rates in the vertical direction driven by the the deposition of both Organic Matter (OM) and mineral sediments (e.g., D'Alpaos et al., 2007; Kirwan and Murray, 2007; Marani et al., 2007; Morris et al., 2002; Mudd et al., 2009), as well as from the fact that carbon storage occurs predominantly in belowground biomass and soil is typically in anaerobic conditions (McLeod et al., 2011; Roner et al., 2016; Rogers et al., 2019; Wang et al., 2019; Ouyang and Lee, 2020). This allows marshes to sustain some of the highest rates of carbon sequestration per unit area of all ecosystems, making them a key player in global strategies aimed at mitigating climate changes through CO_2 reduction programmes (Macreadie et al., 2019; McLeod et al., 2011).

Despite their importance, coastal ecosystems are some of the most heavily used and threatened natural systems globally, experiencing widespread loss or degradation (Barbier et al., 2011; Duarte et al., 2005; Valiela et al., 2001). Marsh ecosystems are seriously exposed to the effects of climate changes and human interferences, sea level rise and lack of available sediments being the key factors in determining salt-marsh drowning and disappearance (D'Alpaos et al., 2011; Kirwan et al., 2010; Marani et al., 2007; Morris et al., 2002; Mudd, 2011).

Therefore, understanding of the processes regulating OM accumulation and C sequestration in salt marshes is critical to better estimate their resilience to climate change, as well as their contribution to the global carbon cycle, providing valuable information to improve management and conservation strategies (Cahoon and Guntenspergen, 2010; Couvillion et al., 2013; D'Alpaos and D'Alpaos, 2021; McLeod et al., 2011; Morris et al., 2016; Mueller et al., 2019; Nyman et al., 2006; Pendleton et al., 2012; Turner et al., 2002). However, the exact dimensions of the salt-marsh role on the global carbon cycle and of their contribution to offset CO_2 emissions, are still uncertain, also because of our current limited knowledge on the decomposition of organic matter in marsh soil and on how decomposition rates can be affected by climate changes and human disturbances (Djukic et al., 2018; Macreadie et al., 2019; Sifleet et al., 2011). This work deals with this important issue.

In particular, salt-marsh blue carbon is sequestered over the short term in living biomass aboveground (leaves, stems, branches) and belowground (roots) and over longer time scales within Soil Organic Matter (SOM) in sediments (McLeod et al., 2011). Local plant biomass and the OM imported by tidal currents and waves (Tognin et al., 2021) are the main sources of the SOM in marshes (Morris et al., 2016; Yousefi Lalimi et al., 2018). Organic inputs, together with inorganic sediments deposited over the marsh platform by tidal flooding and waves and captured by vegetation, are the main processes contributing to marsh accretion and forming marsh soil where carbon is stored (e.g., Kirwan et al., 2013; Mudd et al., 2009; Roner et al., 2016).

Accumulation of SOM is strongly influenced by decomposition processes, which determine the fraction of the OM produced or imported that effectively contributes to soil formation and carbon burial (Kirwan et al., 2013; Mudd et al., 2009; Rybczyk and Cahoon, 2002).

Decomposition is the process of decaying dead OM (litter) which is broken into simple compounds. Specifically, decomposition consists of three concurrent processes, namely, communition (or fragmentation), leaching of water-soluble compounds, and microbial catabolism (Sanderman and Amundson, 2013). Decomposition results in the release of CO_2 and other organic trace gases, water, mineral nutrients, and energy, playing a fundamental role in biogeochemical cycles (Pavao-Zuckerman, 2008).

Decomposition is controlled by the interactions between the physical environment, the quality of the substrate, and the community of decomposer organisms, and it is therefore characterized by different rates and different extents. Given enough time and the proper environmental conditions, most naturally occurring compounds can completely be mineralized to inorganic forms but a fraction of the organic residues is transformed into stable SOM (i.e., stabilization; Sanderman and Amundson, 2013).

Studies on litter decay have often emphasized the importance of climate on decomposition processes (Sanderman and Amundson, 2013), and temperature has long been thought to be an important control of decay rates in wetlands (Montagna and Ruber, 1980; White et al., 1978). Recent experimental results on a global scale suggest that the decomposition rate and the stabilisation factor are sensitive to temperature, with the first increasing and the second decreasing with warming (Keuskamp et al., 2013; Mueller et al., 2018). The results of a short cellulose decay experiment, conducted along the East Coast of the United States, showed a significant relationship between mean daily temperature and decay rate equivalent to a 19% increase in mass loss for each degree warming (Kirwan et al., 2014). Nevertheless, large variations in litter mass loss were observed within biomes, across marshes and across different sites (e.g, Kirwan et al., 2014; Morris et al., 2002; Mueller et al., 2018; Reents et al., 2021), suggesting that local-scale factors other than climate had strong controls on decomposition dynamics (Cornwell et al., 2008; Djukic et al., 2018).

Soil characteristics, in terms e.g. of aeration and drainage, and flooding conditions (hydroperiod), which are influenced by local topography and tidal levels, affect both biomass production and decomposition rates (Kirwan et al., 2013; Marani et al., 2006a; Mudd et al., 2009; Yousefi Lalimi et al., 2018). Several studies suggest that the relationship between the decomposition rate and elevation can be highly variable (Yousefi Lalimi et al., 2018). Halupa and Howes (1995), for instance, found that the rates of carbon loss measured in a New Jersey salt marsh through litterbag experiments and laboratory incubation were related to flooding frequency and duration. However, Kirwan et al. (2013) found an uncertain and weak relationship between decomposition rates and flooding duration in the Chesapeake Bay brackish tidal marshes. Mueller et al. (2018), who examined the results of standardized litterbag experiments on 30 tidal-wetland sites worldwide, found no relation between decomposition rates and elevation, but showed that the stabilisation factor was reduced in low-elevation and more frequently flooded zones compared to high-elevation zones. Yousefi Lalimi et al. (2018) found no clear trends of decomposition rates and stabilisation factors related to elevation and flooding along three transects on coastal marshes located in North Carolina (USA).

Furthermore, the characteristics of the organic matter itself are also known to strongly influence decomposition processes, and some authors indicate chemical and structural composition of the plant material as the main driver for decomposition rates (Freschet et al., 2012; Lang et al., 2009; Wang et al., 2017). These uncertainties in unravelling the governing processes for OM decomposition call for further analyses.

Here we aim at providing new insights on OM fate in salt-marsh soils, clarifying which are the physical and biological factors that most decisively influence OM decomposition, and how decomposition affects the amount of OM effectively contributing to soil formation and carbon burial in tidal marshes.

Toward these goals, we utilized the Tea Bags Index (TBI) approach (Keuskamp et al., 2013) to estimate the rates of OM decomposition and stabilization in salt-marsh soils within the microtidal Venice Lagoon (Italy), relating them to different environmental conditions measured directly in the field. By contributing to a better understanding of OM fate in tidal marshes, our study has the potential for informing models which aim to describe marsh ecosystem functioning and evolution (e.g., Mudd et al., 2009; Marani et al., 2010; Fagherazzi et al., 2012; D'Alpaos and Marani, 2016). Improved representation of soil organic matter dynamics in biomorphodynamic models may be fundamental in evaluating marsh resilience in the face of climate changes and anthropogenic disturbances. In addition, the description of soil organic matter decomposition is a key element for assessing carbon sequestration potential of salt-marsh environments.

3.4 Material and Methods

3.4.1 Study site

The litterbag experiments were conducted in the Venice Lagoon (Fig. 3.1), in the north-western Adriatic Sea (Italy). With an area of about 550 km^2 and an average water depth of 1.5 m, the Venice Lagoon is the largest lagoon in the Mediterranean and is characterised by a semidiurnal tidal regime with a mean tidal range of about 1.0 m. The lagoon is separated from the sea by two barrier islands and is connected to it by three inlets: Lido, Malamocco, and Chioggia.

Tea bags were deployed at 7 different marsh sites within the lagoon (Fig. 3.1). Most of the studied marshes - namely S. Felice, Saline, Scanello, S. Erasmo, Lazzaretto Nuovo, Pagliaga and Campalto (see Fig. 3.1) are located in the northern and most naturally-preserved part of the lagoon, and are found at variable distances from the Lido inlet, wheras the Fossei salt marsh is located in the southern lagoon (Fig. 3.1).

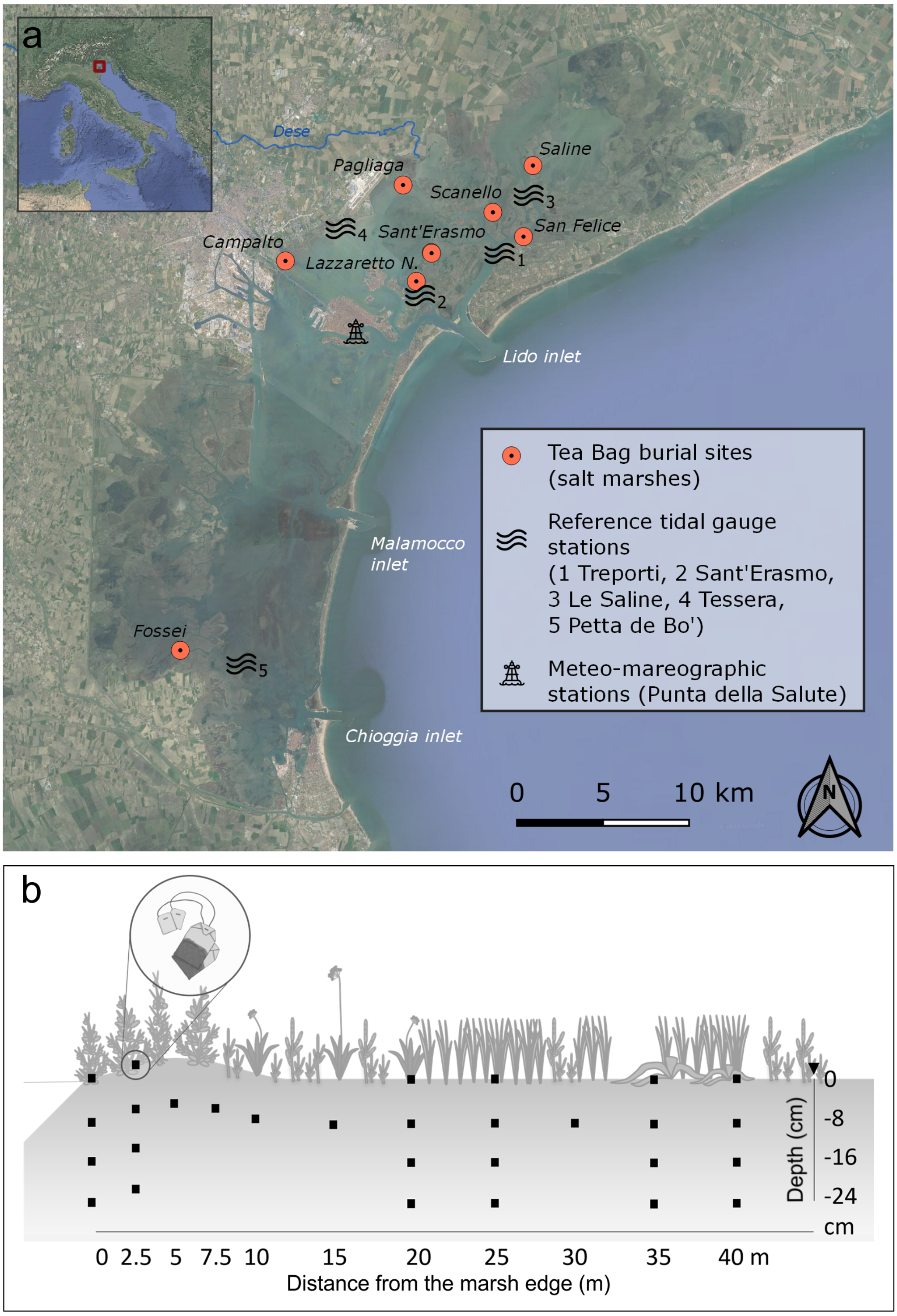

Figure 3.1: **Study area and configuration of the burial experiment.** Location of the study sites in the Venice lagoon, Italy (a), and a sketch of the scheme used for the burial experiments conducted along one of the analyzed marsh transects (b).

The salt marshes in S. Felice, Saline, Scanello, S. Erasmo, and Lazzaretto Nuovo are adjacent to large tidal channels departing from the Lido inlet, and their origin has been ascribed to marine sediment inputs transported by flood tides (Bonometto, 2005; Silvestri et al., 2005). These marshes show typically concave-up profiles, with raised edges and lower elevations toward the inner portion of the marsh (Bonometto, 2005), and host exclusively halophytic vegetation, mainly constituted by *Salicornia veneta*, *Limonium narbonense*, and *Sarcocornia fruticosa*, associated with *Spartina maritima*, *Juncus maritimus*, *Puccinellia palustris*, *Inula crithmoides*, *Suaeda maritima* and *Arthrocnemum macrostachyum* (Silvestri, 2000; Silvestri et al., 2005). In contrast, the Pagliaga salt marsh is located at the landward boundary of the lagoon, close to the estuary of the springwater Dese River which debouches into the Lagoon carrying an average freshwater discharge of about $6.5\,\mathrm{m}^3/\mathrm{s}$ and negligible sediment supply (Fig. 3.1). Freshwater inputs maintain a near-freshwater plant community dominated by *Phragmithes australis*, together with the halophytic species *Juncus maritimum*, *Salicornia veneta* and *Halimione portulacoides* (Silvestri, 2000). Similarly, the Campalto salt marsh is found along the lagoon-mainland boundary, though it was originated on continental grounds of the coastal plains that were reached and permeated by brackish waters (Bonometto, 2005). The Campalto marsh hosts halophytic species dominated by *Limonium narbonense*, associated with *Sarcocornia fruticosa*, *Spartina maritima*, *Salicornia veneta*, and scarce *Suaeda maritima*. Finally, the Fossei East and Fossei West salt marshes are in the southern part of the Venice Lagoon, about 7 km NW of the Chioggia inlet, within a wetland area originated from pre-existing brackish environments or salinized freshwaters arising from river diversions (Bonometto, 2005; Roner et al., 2021). These marshes were artificially established between 1994 and 1996 to limit the lateral erosion of wind-exposed natural marshes, and they have been colonized by the typical halophytic vegetation species mainly constituted by *Salicornia veneta*, *Limonium narbonense*, *Sarcocornia fruticosa*, *Suaeda maritima* and *Puccinellia palustris* (Cecconi et al., 1998).

3.4.2 Tea Bag Index

To estimate decomposition rates and organic matter stabilisation in salt marsh soils, the Tea Bag Index (TBI) protocol proposed by Keuskamp et al. (2013) was adopted. The protocol consists of a simplified litter-bag experiment carried out utilizing standard litter in the form of commercially available tea bags (Lipton, Uniliver). A simple approximation of the decomposition process can be obtained when grouping labile and recalcitrant compounds and separately estimating k values for those two groups (two pools) (Keuskamp et al., 2013; Wider and Lang, 1982):

$$W(t) = ae^{-k_1 t} + (1-a)e^{-k_2 t}, \tag{3.1}$$

where t denotes time and a and 1 a are the labile and the recalcitrant fraction of the substrate, respectively. The decomposition rate constants of the labile and recalcitrant fractions are described by k_1 and k_2, respectively. As during the first phase, the labile fraction is rapidly broken down and the weight loss of the litter is mainly determined by k_1, the Tea Bag Index approach assumes that the decomposition of recalcitrant materials is negligible for burial periods shorter than 3 months. As a consequence, k_2 equals zero, and a becomes the decomposable fraction. Specifically, the fractional weight, $W(t)$, of a buried bag content is assumed to change through time as a result of decomposition processes according to an exponential decay function with constant decomposition rate k:

$$W(t) = ae^{-kt} + (1-a). \tag{3.2}$$

During decomposition, parts of the labile compounds stabilise and become recalcitrant (Prescott, 2010), resulting in a deviation of the actual decomposed fraction a (i.e., limit value) from the hydrolysable fraction H (i.e., chemically labile). This deviation represents the stabilisation factor S, which, following Keuskamp et al. (2013), can be computed as:

$$S = 1 - \frac{a}{H}. \tag{3.3}$$

The calculation of both the decomposition rate (k) and the stabilisation factor (S) is carried following Keuskamp et al. (2013). By using two distinct tea types with contrasting decomposability, it is possible to estimate k and S using a single measurement in time. Keuskamp et al. (2013) assume that, after 3 months, the labile fraction of green tea, a_g, is almost completely decomposed. Hence, the labile fraction of green tea can be determined at the end of the incubation experiment. Using Eq. 3.3, and considering the green tea hydrolysable fraction H_g obtained from chemical analysis, the stabilisation factor S_g for green tea can be determined. The value of S is then assumed to be equal for both types of material used, being dependent only on environmental conditions (i.e., $S_g = S_r$). Consequently, the labile fraction a_r of rooibos tea can be estimated using Eq. 3.3 and decomposition constant rates k can be estimated using Eq. 3.2.

Two types of tea material were used: the green tea, with high cellulose content that is expected to undergo fast decomposition, and rooibos tea, characterized by high lignin content and expected to decompose slowly. Each tetrahedron-shaped synthetic tea bag contains about 2 g of tea and has a mesh size of 0.25 mm, allowing microorganisms and mesofauna to enter the bag and decompose the organic matter contained therein (Keuskamp et al., 2013).

Green and rooibos tea bags were buried pairwise in salt-marsh soils along linear transects and retrieved after about 90 days, with four transects having an incubation period $<$ 80 days (San Felice 1 and 2, Sant'Erasmo1 and 2 Jun 17 - Sept 2 2015) and one transect $>$ 100 days (San Felice - Tavolini Jun 24 - Oct 11 2016) (see Table 3.1). We buried 712 tea bags in total (356 green tea; 356 rooibos tea) along transects oriented perpendicularly to the marsh margin (Table 3.1). According to Keuskamp et al. (2013), the standard burial depth corresponds to 8 cm below the marsh surface. However, at some sites, tea bags were also placed at different depths, corresponding to 0, 16, 24, and 40 cm relative to the marsh surface (Table 3.1) to analyse the effects of burial depths on decomposition dynamics. The tea bags were deployed between April and October in 2015, 2016, and 2017. In some cases, experiments were repeated in different periods along the same transect (Table 3.1).

The initial weight of the tea bag content was determined by subtracting the mean weight of 10 empty bags (bag + string + label) from the weight of the intact tea bag prior to deployment (content + bag + string + label). Once retrieved, the content of tea bags was extracted, oven-dried for 48 h at 70 °C, and weighted. Then, as collected tea bags could be contaminated with soil, a Loss On Ignition procedure (LOI, by heating samples in a muffle oven at 550 °C for 3 h) was conducted to remove the OM and determine the inorganic fraction for each sample. The latter was corrected based on the percentage of non-labile material characterizing the two types of tea, determined by measuring the remaining material after the application of a LOI procedure to a group of 10 intact tea bags prior to deployment. The weight after incubation was determined by subtracting the inorganic fraction from the weight after drying. The results were finally used to estimate the Tea Bag Index according to the methodology proposed by Keuskamp et al. (2013).

We highlight that the Tea Bag Index approach describes only the behaviour of labile material in the first phase of the decomposition process and may provide incomplete information when considering longer time scales and the heterogeneity of soil organic matter. Indeed, recent models now deal with a number of pools with different decomposability to represent substrate heterogeneity and its variability through time (Sierra et al., 2011). However, the simplicity and cost-effectiveness of the method make it suitable for comparing decomposition rates between field experiments and analysing the effects of environmental variables.

	2015			**2016**				**2017**		
	Apr 29 - Jul 29 23.75 °C	Jun 11 - Sep 9 26.35 °C	Jun 17 - Sep 2 26.55 °C	Jun 24 - Sep 23 25.91 °C	Jun 24 - Oct 11 25.07 °C	Jun 30 - Sep 28 25.69 °C	Jul 13 - Oct 11 24.76 °C	Apr 12 - Jul 10 21.43 °C	Apr 12 - Jul 19 21.91 °C	Jul 10 - Oct 12 24.34 °C
S. Felice - Spaccotralo	−8 cm									
S. Felice - Spaccotralo 1			−8 cm					-8, −16 cm		0, -8, -16, −24 cm
S. Felice - Spaccotralo 2			−8 cm	−8 cm				-8, −16 cm		0, -8, -16, −24 cm
S. Felice - Tavolini	−8 cm				−8 cm					
Saline				−8 cm				-8, −16 cm		0, -8, -16, −40 cm
Sant'Erasmo 1			−8 cm							
Sant'Erasmo 2			−8 cm							
Scanello		−8 cm								
Pagliaga		−8 cm								
Campalto									-8, −16 cm	
Lazzaretto Nuovo							−8 cm			
Fossei E						−8 cm				
Fossei W						−8 cm				

Table 3.1: **Burial experiment design.** Incubation sites (Fig. 3.1) with relative incubation periods, mean water temperature during the incubation period, and burial depth.

3.4.3 Environmental parameters

In order to unravel the role of different environmental conditions on the decomposition rate and stabilisation factor, a number of environmental parameters were determined.

Mean water temperatures was determined for each incubation period by calculating the mean value of the water temperature measured every 10 minutes at Punta della Salute station by the CPSM - Centro Previsioni e Segnalazioni Maree of the Venice Municipality.

Elevation above Mean Sea Level (MSL) of each burial site was determined using two TOPCON GR-3 GPS receivers (dual frequency - L1/L2 - and dual constellation - NavStar/Glonass - with integrated Tx/Rx UHF radio). The real tea bag burial elevation (Z_β) was then calculated by subtracting the burial depth (ranging from 0 to 40 cm) to the elevation of the marsh surface.

The distance of each burial site from the edge of the nearest channel (ζ) was determined during field surveys. In order to collect information on flooding frequency and duration, based on the elevation of the burial sites, we calculated the percentage of the burial period during which each site was flooded by water (φ) (except for Fossei, Lazzaretto Nuovo and Campalto transects, where elevation data were not available), comparing local marsh elevations with tidal levels measured at 10-minute frequency by the nearest tidal gauge station of the CPSM - Centro Previsioni e Segnalazioni Maree monitoring network (Fig. 3.1). A replacement algorithm based on cross-correlation was used to complete the time series when tidal levels were missing.

3.4.4 Statistical analyses

To test for the effects of environmental parameters on k and S, the Kendall correlation coefficient (τ) (Kendall, 1938) was determined. The Kendall test is a non-parametric, rank-based method, aimed at determining whether there exists a monotonic relationship between two variables of interest. The value of the coefficient ranges from $+1$ to -1, indicating a positive or a negative association, respectively. Because of the large number of ties in our study, a modified equation that considers the number of ties was used (Soliani, 2019; Sprent and Smeeton, 2000).

In addition, we also employed the Wilcoxon signed-rank test to analyse the difference between decomposition metrics measured at different depths. The Wilcoxon signed-rank test is a non-parametric statistical hypothesis test used to compare two populations when the observations are paired, and it is appropriate for a repeated measure design where the same variables are evaluated under two different conditions.

3.5 Results and discussion

3.5.1 Tea Bag Index metrics for the Venice Lagoon

We first computed the decomposition metrics, namely the decomposition rate (k) and the stabilisation factor (S), for all the tea bag pair samples retrieved in the Venice lagoon, together with their frequency distributions (Fig. 3.2a, 3.2b). Decomposition rates vary between 0.003 and $0.027\,\mathrm{d}^{-1}$, with a median value of $0.012 \pm 0.003\,\mathrm{d}^{-1}$, whereas the stabilisation factors range between 0.016 and 0.544, their median value being equal to 0.15 ± 0.063.

A comparison between the values obtained for the Venice lagoon with those reported by Keuskamp et al. (2013) for different ecosystems is reported in Fig. 3.3, together with data derived for different salt-marsh ecosystems by Mueller et al. (2018) and Yousefi Lalimi et al. (2018). Our results confirm that salt marshes exhibit some of the lowest decomposition rates among different biomes, although that they are also characterized by reduced stabilisation factors (Keuskamp et al., 2013; Mueller et al., 2018; Yousefi Lalimi et al., 2018).

Assuming the labile OM fraction to decompose according to an exponential-decay model $W(t) = e^{-kt}$ (where W is the remaining fraction of the organic mass at time t and k is the decomposition rate), the computed value of $S = 0.012\,\mathrm{d}^{-1}$ for the Venice lagoon implies that 66% of the initial organic mass would decompose after 90 days. Conversely, a mean stabilisation factor of $S = 0.15$ leads, during an incubation timespan of 90 days, to the stabilization of about 15% of the labile material, the latter being therefore not affected by decomposition processes on the short term.

Following the above-recalled asymptotic model proposed by Keuskamp et al. (2013) described by Eq. 3.2, our results suggest that, in the short term, the remaining mass of organic matter strongly depends on the initial recalcitrant fraction $(1-a)$. Indeed, after the complete decomposition of the labile fraction, the remaining mass is equal to the recalcitrant fraction summed to the stabilised labile fraction.

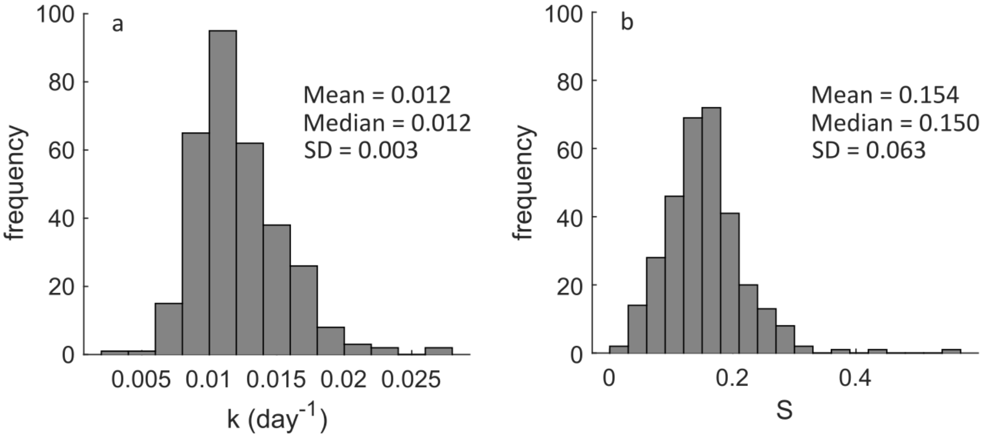

Figure 3.2: **The Tea Bag Index metrics for the analysed samples in the Venice Lagoon.** a) Frequency distribution of the decomposition rates (k); b) Frequency distribution of the stabilisation factors (S).

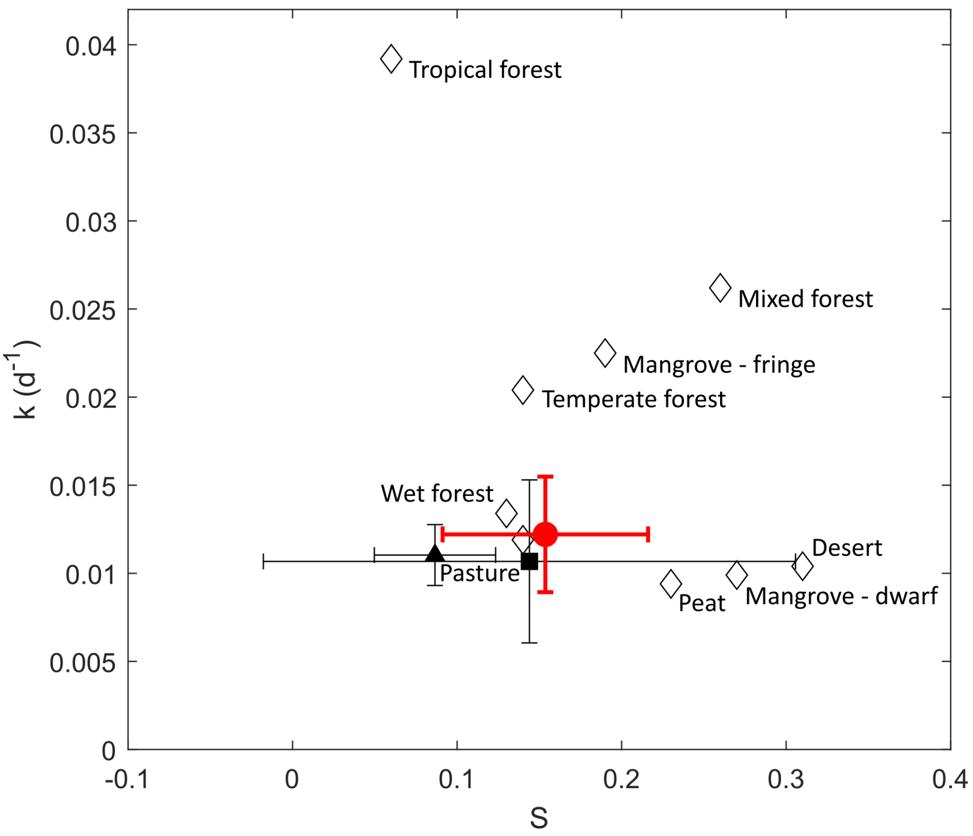

Figure 3.3: **Decomposition metrics in major biomes.** The mean values of the decomposition rate (k) and of the stabilisation factor (S) found in this study (red dot), compared with data from different ecosystems according to Keuskamp et al. (2013) (empty diamonds) and for different marshes around the world, based on data from Yousefi Lalimi et al. (2018) (solid triangle, from three transects in North Carolina (USA) marshes) and Mueller et al. (2018) (solid square, data from 30 tidal-wetland sites worldwide, most of which were salt marshes). Error bars indicate standard deviations.

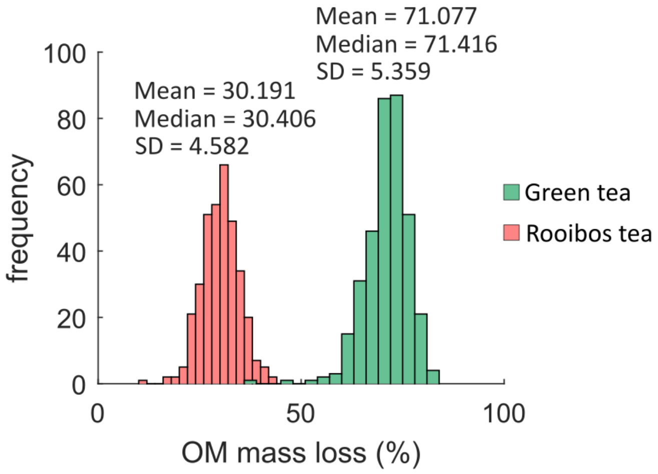

Figure 3.4: **Organic matter mass loss results.** Frequency distributions of the percent tea mass loss after 90 days of field incubation for the analysed samples of green tea (green) and rooibos tea (red).

As expected, mass loss after three months of field incubation (Fig. 3.4) was higher for green tea ($71.08 \pm 5.36\%$) than for rooibos tea ($30.19 \pm 4.58\%$).

Our results are overall consistent with findings by Kirwan et al. (2014) and Kirwan and Blum (2011), who measured the organic mass loss in decomposition experiments in the North American Atlantic coasts by computing the decay coefficient as $k^* = [-\ln(C_t/C_o)]/t$ where C_t and C_o are the mass of organic matter at the end and at the beginning of the experiment, respectively. Their approach, however, did not account for the proportion of recalcitrant and labile material. Calculating the decay coefficient k^* for our tea bag experiments, we obtained different values for the green tea ($0.014 \pm 0.002\,\mathrm{d}^{-1}$) and the rooibos tea ($0.004 \pm 0.001\,\mathrm{d}^{-1}$). As expected, this confirms that green tea is more labile, whereas rooibos is more recalcitrant (Fig. 3.4). Moreover, the decay coefficients k^* found by Kirwan and Blum (2011) for *Spartina alterniflora* stem and leaf material ($0.004 \div 0.016\,\mathrm{d}^{-1}$) and by Kirwan et al. (2014) for *Schoenoplectus americanus* root and rhizome material ($0.003 \div 0.007\,\mathrm{d}^{-1}$) were similar to our values for green tea and roiboos tea, respectively. In the case of salt-marsh vegetation, aboveground litter was observed to generally decompose faster than belowground litter (Scarton et al., 2002; Stagg et al., 2018). Therefore, green and rooibos tea showed consistent decay coefficients with respect to aboveground and belowground salt-marsh plant litter, respectively. Although the aim of Tea Bag Index analysis is to elucidate climate and environmental effects on decomposition processes, neglecting the influence of litter-quality, this comparison further confirms that tea material can be considered representative of organic matter in salt-marsh environments and further highlights the influence of litter quality on organic matter conservation.

3.5.2 Relationships between environmental parameters and decomposition processes

We analysed the effects of environmental variables such as temperature, elevation, distance from the marsh edge, and flooding period on both the decomposition coefficient (k) and on the stabilisation factor (S) (Fig. 3.5 and Fig. 3.6). By fitting linear regression models to our field data, we show that the average water temperature during the incubation period (T) holds the most statistically significant relationship with both k and S, thus suggesting a strong control of T on decomposition processes. Specifically, we found that the decomposition rate, k, increases with T, whereas the stabilisation factor, S, decreases as temperature increases (Kendall's tau test, p-value < 0.01). Notably, these relationships hold in spite of the relatively narrow range of temperature variability observed in our dataset, with $21\,^{\circ}\mathrm{C} < T < 27\,^{\circ}\mathrm{C}$ for all the experiments carried out in this study.

Such significant control of T on both S and k is consistent with previous findings highlighting the critical role of temperature on OM decay rates in tidal wetlands (Keuskamp et al., 2013; Kirwan et al., 2014; Kirwan and Blum, 2011; Montagna and Ruber, 1980; Mueller et al., 2018; White et al., 1978).

Being a chemical process mediated by microbial enzymes, the decomposition of SOM is generally agreed to be strongly affected by temperature (e.g., Davidson and Janssens, 2006; Moinet et al., 2020). Indeed, temperature can affect litter decomposition both directly, by regulating the activity of decomposers, and indirectly, through changes in other temperature-sensitive conditions influencing decomposition processes, such as soil moisture and oxygen diffusion. Oxygen diffusion from the atmosphere, plant aerenchyma, or aerated water, which increases with increasing temperature, affects oxygen availability for decomposition reactions. In saturated or partially saturated soils, oxygen availability represents a rate-limiting factor for decomposition processes (Kirwan et al., 2014). Indeed, flooding slows oxygen diffusion by suppressing microbial respiration and allowing only anaerobic decomposition, which includes fewer and generally slower degradative enzymatic pathways (Davidson and Janssens, 2006; Morris et al., 2016). Differences in flooding frequency along elevational gradients in tidal wetlands have proved to induce sharp gradients in oxygen availability and redox conditions (Kirwan et al., 2013; Morris et al., 2016). Therefore, the intrinsic spatial variability in salt-marsh topography is likely to influence microclimatic conditions affecting decomposition processes.

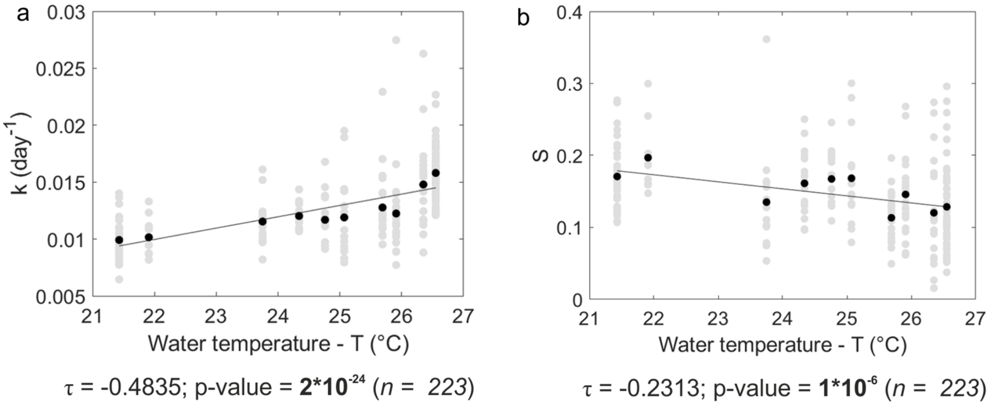

Figure 3.5: **Effect of temperature on decomposition metrics.** Decomposition rate (k) (a) and stabilisation factor (S) (b) as a function of the mean water temperature (T) measured during the incubation period. In the lower inset, results of the Kendall's tau test are also reported. **Bold text indicates p-values** lower than the chosen significance level ($p < 0.01$). The number of samples ($n = 223$) is also reported.

Indeed, we found a statistically-significant relationship between the decomposition rate (k) and both the burial elevation (Z_β) (Fig. 3.6a; Kendall's tau test, p-value = 0.0025; k increasing with elevation) and the distance from the closest marsh edge (ζ) (Fig. 3.6c; Kendall's tau test, p-value = 0.0010; k decreasing with increasing distance), the latter being a proxy for the distance to the nearest source of water and mineral sediments. Conversely, no significant relationship was found between the stabilisation factor (S) and either burial elevation (Z_β) or the distance from the marsh edge (ζ) (Fig. 3.6b, 3.6d). The stabilisation factor S is also negatively correlated to the duration of marsh flooding (φ) (Fig. 3.6f), whereas flooding (φ) displays no significant correlation with the decomposition rate k. (Fig. 3.6e).

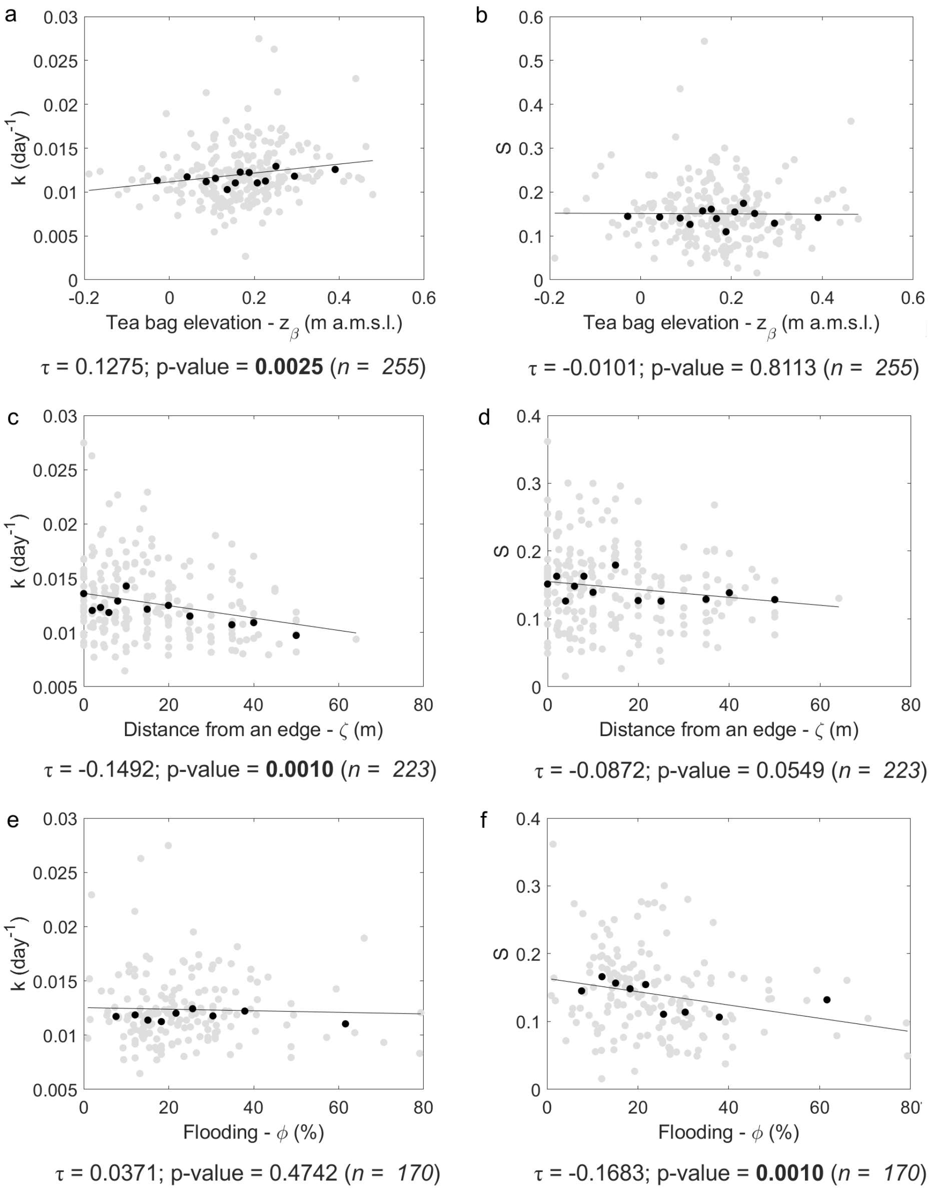

τ = 0.1275; p-value = **0.0025** (*n* = *255*)

τ = -0.0101; p-value = 0.8113 (*n* = *255*)

τ = -0.1492; p-value = **0.0010** (*n* = *223*)

τ = -0.0872; p-value = 0.0549 (*n* = *223*)

τ = 0.0371; p-value = 0.4742 (*n* = *170*)

τ = -0.1683; p-value = **0.0010** (*n* = *170*)

Figure 3.6: **Effects of environmental conditions on organic matter decomposition.** Decomposition rate (k) and stabilisation factor (S) as a function of *a,b)* burial elevation (Z_β) (all samples $n = 255$ considered); *c,d)* distance from the edge (ζ) (only samples buried at 8 cm depth considered, $n = 223$); *e,f)* salt-marsh flooding (φ), computed as the percentage of the burial period during which each site was submerged by water, (only samples buried at 8 cm depth considered, $n = 170$). In each panel, the results of the Kendall's tau test are reported in the lower inset, with **bold text indicating p-values** lower than the chosen significance level ($p < 0.01$).

The dependence of k on both Z_β and ζ is somehow expected in view of the typical concave-up morphology characterizing most of marsh ecosystems, where surface elevation decreases progressively moving away from the marsh edge towards the inner marsh. Clearly, marsh elevation also exerts a primary control on flooding frequency and duration (Chmura and Hung, 2004; D'Alpaos et al., 2007; Marani et al., 2006a). Thus, these interdependencies may suggest that larger oxygen availability in more elevated, which are less frequently flooded sites, promotes the decomposition of organic matter, enhancing microbial respiration. Other factors linked to these morphological features that could potentially influence decomposition processes are vegetation characteristics (i.e., above and belowground production, C-N ratio) and nutrient availability, which may affect microbial community (Kirwan et al., 2014; Mueller et al., 2018; Yarwood, 2018). However, the control of marsh flooding on OM decomposition is not as clear as those found for elevation and distance from the edge, with φ not being significantly correlated to k. Nevertheless, we should highlight that φ was derived indirectly by comparing site-specific measurements of marsh elevation with tide level data retrieved from nearby tidal gauge stations. Therefore, a degree of uncertainty is to be expected for φ, which might not be an optimal representation of the actual time during which the marsh soil is submerged, the latter process depending also on local marsh microtopography and on the characteristics of the extensive networks of tidal creeks that typically cut through the marsh platform.

Moreover, it is worthwile noting that soil aeration is affected also by plant evapotranspiration and water table dynamics. Groundwater flow and evapotranspiration are known to promote the formation of an aerated layer below the soil surface, thus allowing for a prolonged presence of oxygen for aerobic respiration even when the marsh is flooded (Boaga et al., 2014; Marani et al., 2004; Ursino et al., 2004). Ursino et al. (2004) and Marani et al. (2006b) showed that in the absence of evapotranspiration, and when water infiltration dominates over root uptake, more aerated soil conditions are found near the channels, whereas the inner marsh portions are more oxygenated when plant transpiration balances infiltration from the flooded surface. These inferences clearly highlight how soil and vegetation characteristics (e.g., hydraulic conductivity and vegetation density), which are in turn affected by local elevation and distance from the nearest marsh margin (e.g., Roner et al., 2016), might crucially affect soil aeration. Therefore, oxygen dynamics in marsh soil are quite complex and may cause difficulties in the detection and interpretation of the relationship between flooding conditions and decomposition processes.

These results highlight the need for further investigations on the relationship between decomposition processes and environmental parameters, including the use of non-linear multivariate approaches, which would allow one to account for the possible mutual relations between the analysed variables and their combined effect on decomposition.

When considering decomposition rate values, k, measured along single transects during different incubation periods, temperature showed to have the strongest influence on decomposition processes, as observed in the analyses presented above, whereas elevation and distance from the marsh edge did not significantly affect decomposition rates along single transects (Fig. 3.7).

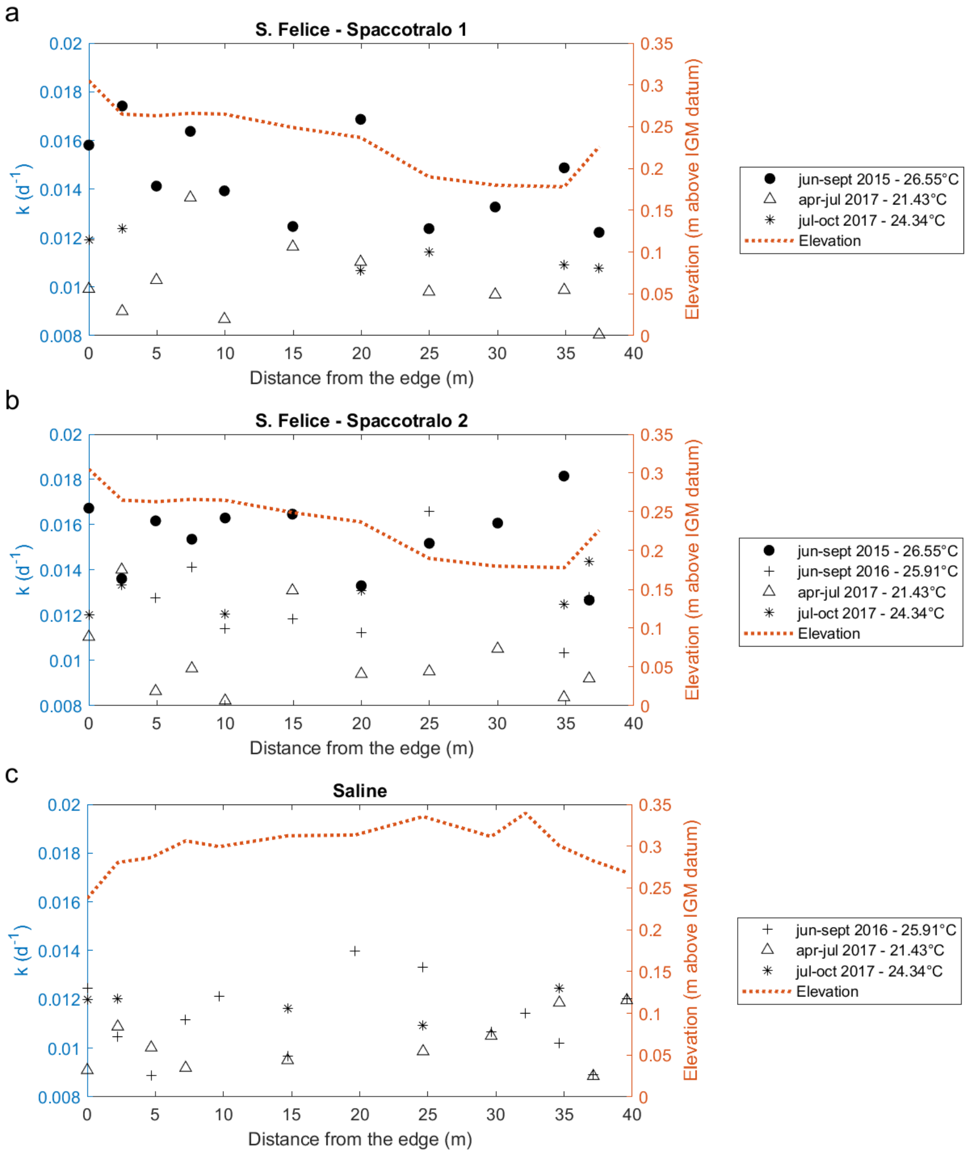

Figure 3.7: **Decomposition variability at the site scale.** Decomposition rates (k) for different periods with different mean water temperature along single transects, S. Felice – Spaccotralo 1 *(a)*, S. Felice – Spaccotralo 2 *(b)*, Saline *(c)*, with respect to marsh elevation.

3.5.3 Temperature sensitivity of SOM decomposition

Temperature sensitivity of SOM decomposition is usually described using Arrhenius' (1889) kinetic theory according to which, when substrates are abundant at enzymes reaction sites, decomposition rates increase exponentially with temperature (Davidson and Janssens, 2006; Moinet et al., 2020). In addition, the Arrhenius equation suggests that the sensitivity of the reaction rate on temperature increases with increasing availability of the recalcitrant fraction in the substrates (i.e., "intrinsic temperature sensitivity"). However, environmental constraints also influence the observed decomposition response to temperature (i.e., the "apparent temperature sensitivity"), affecting the accessibility to organic carbon substrates (Davidson and Janssens, 2006).

In order to examine the effects of temperature on decomposition processes, we considered the average values of k and S for every surveyed temperature value (Fig. 3.5). Our results suggest an exponential increase of SOM decomposition rates with temperature (Fig. 3.8a) ($k = ae^{bT}$), whereas the stabilisation factor, S, is shown to linearly decrease with temperature from about $S = 19\%$ at $21\,^{\circ}\mathrm{C}$ to approximately 12% at $27\,^{\circ}\mathrm{C}$.

In a complex system as a community of soil organisms, where the total decomposition activity is determined by the combined activity of a wide range of different organisms that presumably have different individual responses to temperature, the temperature-sensitivity indicator Q_{10} may represent a useful tool to summarize observed responses (Kirschbaum, 1995). Q_{10} is defined as the factor by which a reaction rate increases in response to a 10°C increase in temperature (Davidson and Janssens, 2006) (if $k = ae^{bT}$, $Q_{10} = e^{10b}$). According to the previously-recalled relation between k and temperature, a Q_{10} value of 2.22 ($Q_{10} = e^{10\times 0.08}$, see Fig. 3.8a for the value of $b = 0.08$) was computed based on our data (Langley et al., 2005), which is coherent with the typical values found for reaction rates in biological systems as well as for organic matter decomposition at ambient temperature (Davidson and Janssens, 2006; Kirschbaum, 1995; Singh and Gupta, 1977). The sensitivity of decomposition on temperature obtained in our analyses is lower than the sensitivity reported for litter bag experiments carried out directly on the soil surface in a rarely flooded salt marsh on the Virginia's coast ($Q_{10} = 3.44$, (Kirwan and Blum, 2011)). In addition, our Q_{10} value

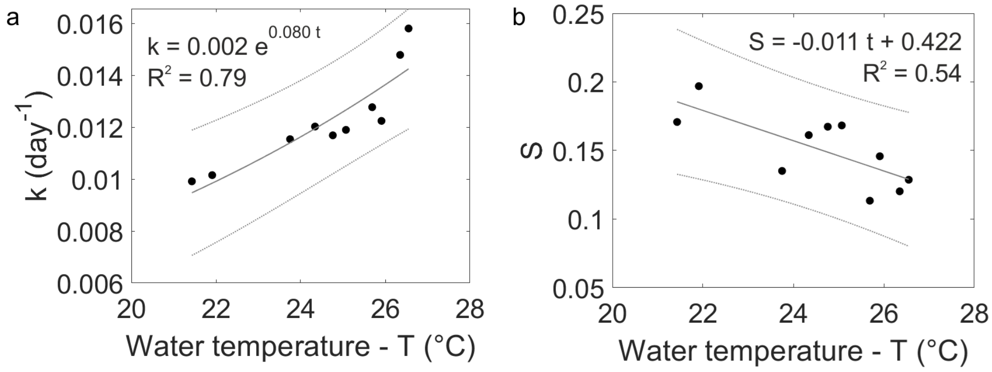

Figure 3.8: **Correlation between temperature and decomposition metrics.** Exponential regression of decomposition rate (k) (means of the values measured for each incubation period or temperature classes) as a function of the mean water temperature (Coefficients (with 95% confidence bounds): $a = 0.002$ $(0.0002, 0.003)$, $b = 0.08$ $(0.045, 0.115)$) *(a)*; and linear regression of the stabilisation factor (S) as a function of the mean water temperature (Coefficients (with 95% confidence bounds): $p1 = -0.011$ $(-0.02 - 0.003)$, $p2 = 0.422$ $(0.22, 0.63)$) *(b)*.

agrees with the estimated temperature sensitivities of CO_2 emissions from both freshwater wetland ($Q_{10} = 1.3$–2.5) (Inglett et al., 2012) and salt marsh soils ($Q_{10} = 1.5$–1.8) (Morris and Whiting, 1986), while appearing slightly larger than those reported by Kirwan et al. (2014) when estimating the range of temperature sensitivity of decomposition rate (k^*) ($Q_{10} = 1.3$–1.5), without accounting for the proportion of recalcitrant and labile material. Interestingly, when considering the Q_{10} values for the decomposition rates k^* of both green tea and rooibos in our tea bag experiments, we obtain $Q_{10} = 1.4$ and $Q_{10} = 1.9$ for green ($b = 0.033$) and rooibos tea ($b = 0.066$), respectively, that are closer to those reported by Kirwan et al. (2014). Our analysis on the decay coefficient k^* allowed us to observe a lower temperature sensitivity for more labile substrates (e.g., green tea in our TBI analysis) than for recalcitrant substrate (rooibos tea), consistently with the substrate-quality dependence of temperature sensitivity suggested by Arrhenius' (1889) kinetic theory (Davidson and Janssens, 2006). As to the stabilisation factor, S, we highlight that it declined by about 30% over the observed range of temperatures ($21\,°C < T < 27\,°C$). Therefore, our results show the dependency of decomposition processes on temperature and, consistently with recent analyses, further confirm the key role played by initial litter quality in terms of both chemical and physical composition in driving OM decomposition (Cornwell et al., 2008; Djukic et al., 2018).

3.5.4 SOM decomposition at different depths below the marsh surface

At some sites during the 2017 campaign some tea bags were buried at different depths, from the surface to a few tens of centimeters, to analyse depth-related decomposition variability. For 17 burial sites along three transects (S. Felice-Spaccotralo 1 and 2, and Saline) k and S values were measured at the same time on the marsh surface and at depths of 8, 16, 24, and 40 cm below the surface (Table 3.2).

The analysis of depth-related decomposition variability (Table 3.2) showed that decomposition rates measured on the marsh surface are in general significantly different from those measured belowground. As an example, the Wilcoxon matched pairs signed rank test revealed a significant difference in k between the surface and the 8-cm depth ($n = 17$, $Z = 2.0119$, $p = 0.0442 < 0.05$) and between the surface and the deepest tested layers (depths of 24 and 40 cm) ($n = 17$, $Z = -1.9645$, $p = 0.0495 < 0.05$), whereas no significant differences were observed between the surface and the 16-cm depth. The difference in decomposition rates, k, among different belowground layers (8, 16, 24, 40 cm depth), instead, proved not to be significant. Differences in stabilization factors, S, turned out to be significant only between the surface and the deepest layers tested (24 and 40 cm depth) ($n = 17$, $Z = -2.8166$, $p = 0.0049 < 0.05$).

Matched pairs	**n**	**Z value**	**p value**
k 0 / -8	17	2.0119	0.0442*
S 0 / -8	17	-1.8699	0.0615
k 0 / -16	17	1.0651	0.2868
S 0 / -16	17	-1.6805	0.0929
k 0 / max depth (-24 or -40)	17	1.9645	0.0495*
S 0 / max depth (-24 or -40)	17	-2.8166	0.0049*
k -8 / -16	17	-0.4971	0.6192
S -8 / -16	17	0.4971	0.6192
k -8 / max depth (-24 or -40)	17	0.3550	0.7226

Table 3.2: **Decomposition variations in matched paired samples at different depth.** Results of the Wilcoxon matched pairs signed rank test on the values of k and S measured at different depths. Asterisks indicate p values being less than the chosen significance level ($p < 0.05$).

For about 70% of burial sites along our study transects, deeper soil layers showed lower decomposition rates and higher stabilisation factors relative to the surface layer (Fig. 3.9a and 3.9b).

The differences between decomposition metrics measured at different depths are in any case limited and in most cases do not exceed 20% (Fig. 3.9c and 3.9d).

In agreement with Yousefi Lalimi et al. (2018), who found that decomposition rates and stabilisation factors of shallower soil layers (3-cm depth) and deeper layers (8-cm depth) were significantly different, our results suggest that there is a significant difference between the decomposition process on the marsh surface, probably consistent within the first few centimetres of soil, with respect to belowground conditions. Differences in k between different deeper layers within the soil are instead reduced, which may indicate either conditions becoming more uniform or a possible saturation of the effect of changing conditions. Lower decomposition rates and higher stabilisation factors (Fig. 3.9a and 3.9b) found in deeper soil layers are consistent with the reduced oxygen availability in those layers.

Despite our findings show that deeper soil layers are, on average, characterized by lower decomposition rates and higher stabilisation factors, this difference appears limited (Fig. 3.9c and 3.9d) and decomposition metrics from the study area indicate that the organic matter decay is rapid enough to consume all the labile material before it can be buried and stabilised.

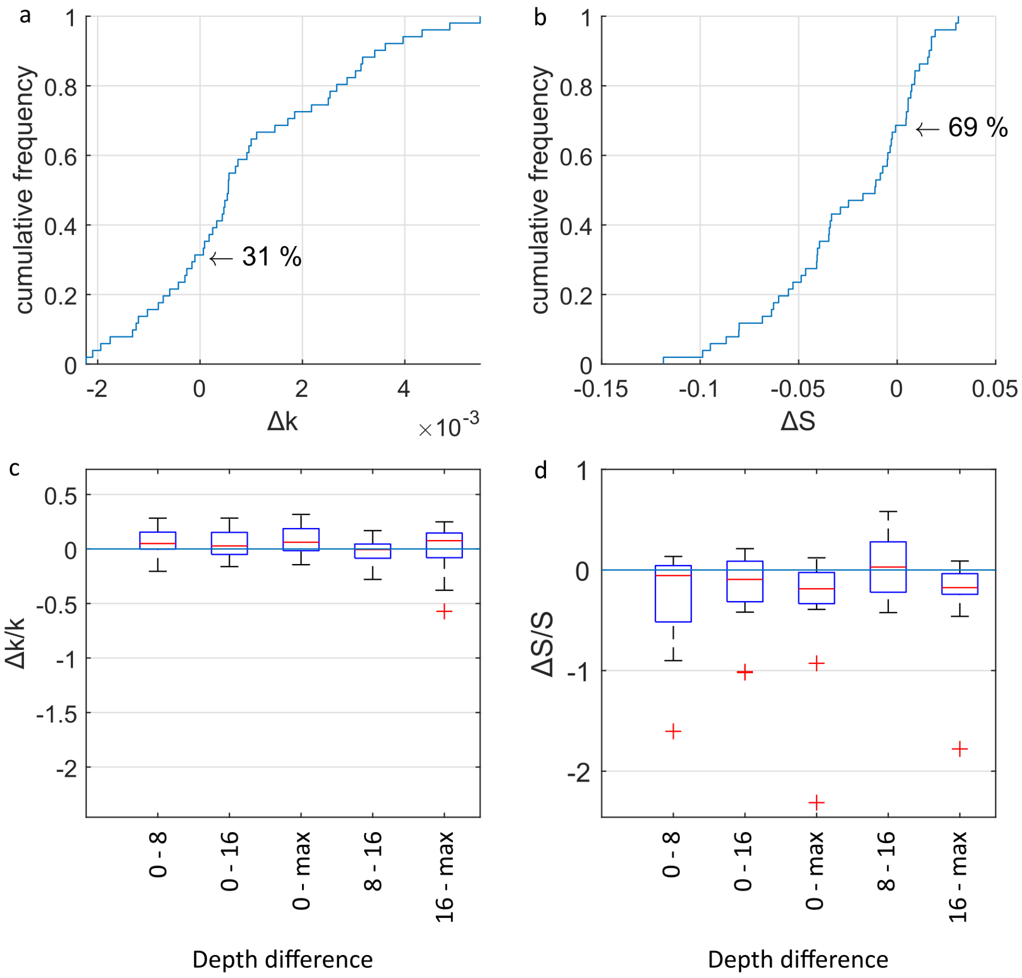

Figure 3.9: **Differences of decomposition metrics at different depth.** Cumulative distribution function of difference in k *(a)* and S *(b)* between the surface and all other deeper layers and box-plots representing the relative difference between k *(a)* and S *(b)* values at different depths. (The central mark indicates the median, and the bottom and top edges of the box indicate the 25th and 75th percentiles, respectively. Whiskers extend to the most extreme data points not considered outliers and the outliers are plotted individually using the '+' symbol).

3.6 Conclusions

To better understand the dynamics of organic matter which contributes to soil formation and carbon sequestration in salt marshes, we analysed decomposition processes in salt-marsh ecosystems found in the microtidal lagoon of Venice and investigated how they are influenced by environmental factors. We carried out a litterbag experiment using standardized organic material according to the Tea Bag Index protocol (Keuskamp et al., 2013), including only the initial phases of the decay (i.e., 3 months). Our results highlight that temperature plays a significant role in OM decomposition and that it is indeed responsible for an increase in the decomposition rate of about 8% per °C. Our results indicate a faster OM decay on the marsh edge and at higher elevations, supporting the idea of slower organic matter degradation towards inner and lower marsh portions (Roner et al., 2016). Moreover, our results suggest that oxygen availability importantly affects decomposition, even if the complexity of soil aeration dynamics prevented the detection of any clear trends in our dataset. We also suggest that the variability in decomposition metrics, namely the decomposition rate k and the stabilisation factor S, reflects site specific micro-scale variability of the environmental forcing affecting decomposition processes. Although actual values of S and k for salt-marsh organic matter may differ from those obtained using standard litter, the latter resulted to be comparable with the decay rates calculated using autochthonous plant litter (e.g., Yousefi Lalimi et al., 2018; Kirwan et al., 2014; Kirwan and Blum, 2011). Specifically, the decomposition rates measured during our study display a mean value of $0.012 \pm 0.003\,\mathrm{d}^{-1}$ (ranging between 0.003 and $0.027\,\mathrm{d}^{-1}$), which would lead to a loss of about two-thirds of the initial organic mass after 90 days. Nevertheless, salt-marsh decomposition rates are confirmed to be some of the lowest with respect to other biomes. As to the stabilization processes, our measurements highlight a high variability in stabilization factors: on average 15% of the organic matter was stabilised during the initial stage of decay, with values ranging between 2 and 54%. Within this scenario, in terms of future climate conditions, the initial litter quality appears to be a primary constraint for the amount of preserved organic matter contributing to carbon sequestration and marsh accretion, as also confirmed by the observed difference in mass loss between green and rooibos tea (mean mass loss of about 70% and 30% in 90 days, respectively). Faster initial decomposition of green tea was expected, and it is due to its higher fraction of water-soluble compounds in contrast to the low content of soluble or hydrolysable compounds in rooibos tea (Keuskamp et al., 2013). Numerous authors suggested that substrate quality, as a function of chemical and structural characteristics, is a primary control on organic litter decomposition rates, indicating C, N, P, lignin content and their ratios as good predictors for plant decomposability (Kazakou et al., 2009; Enríquez et al., 1993; Li et al., 2012; Prieto et al., 2016; Silver and Miya, 2001). This is confirmed also on a local scale and for costal marshes (Scarton et al., 2002; Stagg et al., 2018). Therefore, potential shifts in species relative abundance and primary production in the future caused by climate change and anthropogenic disturbances could have large effects on carbon cycle, affecting litter quality and consequently decomposition rates (Cornelissen et al., 2007; Cornwell et al., 2008; Djukic et al., 2018). This suggests the need to accounting for both direct and indirect effects of climate change as possibly affecting decomposition processes. Hence, we highlight the need for further analyses on autochthonous plant litter dynamics, also on longer time scales, considering their variability. However, the results of our short-term decomposition experiments cannot be extrapolated to predict long term behaviour of the decomposition processes, as Tea Bag Index protocol, by definition, describes early-stage decomposition. The mass loss of the organic litter during early stage decomposition may be more related to the leaching losses than to microbial mineralization of soil organic carbon and long term decomposition involves different litter components; consequently the drivers of decomposition are likely to vary over longer time scales (Djukic et al., 2018). Although caution is needed in the interpretation of the decomposition metric measured, our data provide additional insights to improve biogeomorphological model ability to describe marsh response to the effects of climate change and anthropogenic perturbation and further elucidate marsh importance within the global carbon cycle.

4

SPATIAL PATTERNS OF SOIL ORGANIC MATTER IN SALT MARSHES

This chapter is a manuscript ready to be submitted for publication under the title “Spatial patterns of Organic Matter content in the surface soil of the salt marshes of the Venice Lagoon (Italy)”. A.P., D.T., A.D. and M.M. designed the study. A.P., D.T., A.D. and M.M. developed the methodology. A.P. and D.T. collected the data and performed laboratory analyses. E.F. and N.R. provided the instrumentation and tools for grain-size analysis. A.P. and D.T. were responsible for data analysis and interpretation with the supervision of A.D., M.M. and M.G. All the authors discussed the data and agreed on their interpretation. A.P. wrote the original draft. D.T., A.D., M.G. and M.M. provided comments and suggestions to improve the original draft. All the co-authors contributed to the final polishing of the manuscript.

Spatial patterns of Organic Matter content in the surface soil of the salt marshes of the Venice Lagoon (Italy)

A. Puppin[1], D. Tognin[2], M. Ghinassi[1], E. Franceschinis[3], N. Realdon[3], M. Marani[2] and A. D'Alpaos[1].

[1]Department of Geosciences, University of Padua, Padua, Italy
[2]Department of Civil, Environmental and Architectural Engineering, University of Padua, Padua, Italy
[2]Department of Pharmaceutical and Pharmacological Sciences, University of Padova, Italy

4.1 Abstract

Salt marshes are crucial eco-geomorphic features of tidal environments as they provide numerous important ecological functions and deliver a wide range of ecosystem services that contribute to human well-being. Salt-marsh evolution is controlled by the interplay between hydrodynamics, geomorphology and vegetation, and they accrete vertically through the deposition of both organic matter (OM) and inorganic sediments. This allows marshes to keep pace with relative sea-level rise, and likewise capture and store carbon (C), making them valuable allies in climate mitigation strategies. Thus, Soil Organic Matter (SOM), i.e. the organic component of the soil, plays a key role within salt-marsh environments, directly contributing to soil formation and supporting C storage. This study aims at inspecting spatial patterns of SOM in surface salt-marsh soils, providing further insights into the physical and biological factors driving OM dynamics affecting salt-marsh survival and carbon sink potential. Our results reveal two scales of variations in sedimentary OM content in salt-marsh soils. At the marsh scale OM variability is influenced by the interplay between surface elevation and changes in sediment supply with the distance from tidal channels. At the system scale, OM content distribution is dominated by the gradient generated by marine and fluvial influence. Variations in autochthonous and allochthonous inputs, sediment grain size, and preservation conditions may explain the observed variability in SOM.

4.2 Introduction

Salt marshes may be defined as halophytic grasslands or dwarf brushwoods encroaching sediment platforms bordering saline tidal water bodies (Beeftink, 1977; Silvestri and Marani, 2004). Salt marshes lie at the upper margin of the intertidal environment and they are regularly flooded by the tides and occasionally by storm surges (Allen, 2000; Friedrichs and Perry, 2001; D'Alpaos and D'Alpaos, 2021). They occur worldwide, particularly in middle and high latitudes on low-energy coasts, both in microtidal and macrotidal regimes (Allen and Pye, 1992).

Coastal wetlands, situated at the interface between terrestrial and marine ecosystems, often lie in some of the World's most densely populated areas and deliver a wide range of ecosystem services that contribute to human well-being, being simultaneously some of the most economically relevant and vulnerable ecosystems on Earth (Costanza et al., 1997; D'Alpaos and D'Alpaos, 2021; de Groot et al., 2012). Salt marshes provide critical habitat for numerous species, protect coastal areas by buffering floods and wave action, improve water quality, support commercial fisheries, provide recreational opportunities and contribute to climate regulation by acting as carbon (C) sinks (e.g. Barbier et al., 2011; Boesch and Turner, 1984; Costanza et al., 1997; Lefeuvre et al., 2003; Temmerman et al., 2013).

However, salt-marsh ecosystems are exceptionally vulnerable to the effects of climate change and increasing human pressure such as accelerating relative sea-level rise, declining sediment supply, coastal land reclamation (D'Alpaos et al., 2011; Gedan et al., 2009; Kirwan et al., 2010; Marani et al., 2007; Morris et al., 2002; Mudd et al., 2004; Mudd, 2011; Temmerman et al., 2004; Silvestri et al., 2018), having lost between 25% and 50% of their global historical coverage (Mcowen et al., 2017).

Salt marshes are intrinsically dynamic environments and their evolution importantly depends on complex feedbacks between physical and biological components. The interplay between hydrodynamics, geomorphology and vegetation controls marsh vertical accretion, which has allowed marshes to keep pace with relative sea-level rise over thousands of years (Allen, 2000; D'Alpaos et al., 2007; Fagherazzi et al., 2012; Marani et al., 2007; Mudd et al., 2009, 2004). Vertical accretion in tidal marshes is driven by the deposition of both organic matter (OM) and inorganic sediments (Fagherazzi et al., 2012; Mudd et al., 2009; Neubauer, 2008; Nyman et al., 2006). Tides, wind waves, and storms are the main mechanisms for sediment transport, deposition or mobilisation on the marsh platform, shaping marsh morphology, which in turn influences water depth and flow velocity. Halophytic plants, spatially organized in characteristic patches related to soil elevation and hydroperiod (Bertness and Ellison, 1987; Pennings and Callaway, 1992; Silvestri et al., 2005; Silvestri and Marani, 2004), contribute considerably to marsh accretion, influencing the water flow, enhancing sediment settling, damping sediment resuspension and producing biomass, which results in OM accumulation (D'Alpaos et al., 2007; Marani et al., 2006a; Morris et al., 2002; Mudd et al., 2009). In some cases, OM contribution to tidal marsh volume and surface accretion can be much greater than that of mineral material (Allen et al., 2021; Ewers Lewis et al., 2020; Morris et al., 2016).

The organic material that helps to build marsh elevation is likely a combination of in situ production of belowground root tissue inserted into the sediments (Craft et al., 1993; Day et al., 1999) and autochthonous or allochthonous organic materials that are deposited in association with mineral sediment particles (Ewers Lewis et al., 2019; Mudd et al., 2009; Mueller et al., 2019; Nyman et al., 2006). Furthermore, tidal conditions and flooding inhibit microbial aerobic activity and slow down decomposition, fostering C accumulation in marsh soils (Keuskamp et al., 2013; Kirwan et al., 2014; Morris et al., 2016; Mueller et al., 2018). Thanks to these dynamics, the C captured through plant photosynthesis is buried and preserved as Soil Organic Carbon (SOC) and may be locked away from the atmosphere over centennial to millennial time scales (Duarte et al., 2005; Perillo et al., 2009).

The Carbon sink function of vegetated coastal ecosystems, including salt marshes, mangrove forests and seagrass meadows, has been increasingly recognised in recent years and the term "blue carbon" was coined to indicate the C sequestered in these ecosystems, with a potential role in climate change mitigation (Chmura et al., 2003; Duarte et al., 2005; Macreadie et al., 2019; McLeod et al., 2011; Nellemann et al., 2009).

Recent models of intertidal system dynamics predict marsh evolution incorporating both physical and ecological processes (e.g., D'Alpaos et al., 2007; Kirwan and Murray, 2007; Marani et al., 2007, 2013; Mudd et al., 2009; Morris et al., 2002;

Mudd et al., 2004). However, to refine current representations of SOM accumulation processes, a deeper understanding is needed of crucial biogeomorphological factors driving OM dynamics in tidal environments. Drivers of SOM variability in salt marshes are innately difficult to identify as SOM content is the result of many complex processes acting simultaneously.

The study of the interplay between these processes is complicated by the fact that they occur over a wide range of spatial scales (Ewers Lewis et al., 2020; Marani et al., 2006a). While at the global scale, climatic parameters appear to be important drivers for C sequestration and storage (Chmura et al., 2003), at the system scale, the position within the gradient generated by marine and fluvial influence was observed to be a key predictor of organic content, with the environmental conditions resulting from the interplay between physical and biological factors (Van De Broek et al., 2016; Kelleway et al., 2016). Geomorphological factors and vegetation characteristics appear to be important drivers of organic content variability when considering fine spatial scales (e.g. Chen et al., 2016; Leonard et al., 2002; Roner et al., 2016). For instance, elevation, hydroperiod and sediment supply affect sediment deposition and organic-matter trapping capacity (Chmura et al., 2003) other than microbial community and organic-matter preservation conditions (Kirwan et al., 2013; Marani et al., 2006a; Mudd et al., 2009; Yousefi Lalimi et al., 2018). The latter are influenced also by sediment type and grain size, which are additionally associated with different concentration of suspended particulate organic matter (Van De Broek et al., 2016; Kelleway et al., 2016; Saintilan et al., 2013). Therefore, sediment grain size was pointed as a key predictor of organic content by Ford et al. (2019) and Kelleway et al. (2016), whereas Van De Broek et al. (2016) reported variations in suspended sediment concentration and stable particulate OC as the main drivers of observed differences in organic storage. Considerable variability in sediment organic content has also been observed at different scales across vegetation types (Ewers Lewis et al., 2020; Saintilan et al., 2013), which determine above and belowground biomass production both quantitatively and qualitatively, in terms of decay resistance (Scarton et al., 2002; Stagg et al., 2018).

Here we aim at inspecting spatial patterns of Soil Organic Matter (SOM) in salt-marsh soils, providing further insights into the physical and biological factors driving OM dynamics, affecting salt-marsh survival and C sink potential. Toward these goals, we analysed soil organic content for the surface soil layer (0–20 cm) in 10 salt marshes of the Venice Lagoon from 60 sediment cores, together with different variables including soil, morphological and vegetation characteristics. By contributing to a better understanding of OM distribution and its controls in tidal marshes, our study has the potential to improve spatially explicit biomorphological models of salt-marsh evolution, allowing the evaluation of marsh resilience and associated C storage as an ecosystem service. Improved representation of SOM dynamics in biomorphodynamic models will provide critical information for management and conservation strategies, favouring the identification of optimal locations and actions where to direct protection and restoration efforts.

4.3 Material and methods

4.3.1 Study site

The Venice Lagoon is the largest brackish tidal basin of the Mediterranean Sea, located in the north-western Adriatic Sea, Italy. It is a shallow, microtidal, back-barrier system, characterized by a semidiurnal tidal regime with an average range of 1.0 m and a mean water depth over tidal flats of about 1.5 m, connected to the sea by three inlets (Lido, Malamocco, and Chioggia). The Venice Lagoon is also highly influenced by meteorological forcings, with the south-easterly Sirocco wind responsible for severe storm surges flooding the city of Venice, and the north-easterly Bora wind responsible for large wind waves (Tognin et al., 2021).

The present-day morphology of the Venice Lagoon is strongly affected by the intense human pressure occurred over the last centuries, going from the diversion of the main rivers, which are now debouching outside the Lagoon, to the more recent construction of jetties at the inlets and the excavation of large navigable channels, to the rash groundwater exploitation in the twentieth century. The above interventions have seriously modified sediment supply and dynamics, local hydrodynamics and morphology, together with rates of relative sea level rise, favouring sediment starvation and the deepening of the lagoon (Zecchin et al., 2009; Brambati et al., 2003). The recent activation of storm-surge barriers, designed to prevent flooding of the city of Venice, was proved to further alter the lagoon hydrodynamics (Mel et al., 2021) contributing to the deepening of the tidal flats and reducing salt-marsh sedimentation (Tognin et al., 2021, 2022). Salt-marsh areas of the Venice lagoon have dramatically shrunk in the last centuries, with a decrease in extension from about 180 km^2 in 1811 to about 43 km^2 in 2002 (Carniello et al., 2009; D'Alpaos, 2010; Tommasini et al., 2019).

The study sites are located in 10 salt marshes of the Venice lagoon, at variable distances from the inlets (Fig. 4.1). In the northern lagoon, Sant'Erasmo (SE), San Felice (SF) and Saline (SA) salt marshes border large tidal channels departing from the Lido inlet. These marshes host exclusively halophytic vegetation, mainly constituted by *Salicornia veneta*, *Limonium narbonense*, and *Sarcocornia fruticosa*, associated with *Spartina maritima*, *Juncus maritimus*, *Puccinellia palustris*, *Inula crithmoides*, *Suaeda maritima* and *Arthrocnemum macrostachyum* (Silvestri, 2000; Silvestri et al., 2005). In contrast, Pagliaga (PA) and Campalto (CA) sites are located at the lagoon-mainland boundary in the northern lagoon, with PA being close to the estuary of the springwater Dese River which debouches into the Lagoon carrying an average 65 $\mathrm{m}^3\,\mathrm{s}^{-1}$ freshwater discharge and negligible sediment supply. Freshwater inputs at PA site maintain a near-freshwater plant community dominated by *Phragmithes australis*, together with the halophytic species *Juncus maritimum*, *Salicornia veneta* and *Halimione portulacoides* (Silvestri, 2000). The CA marsh, whose main edge faces toward a shallow tidal flat exposed to Scirocco wind, hosts halophytic species dominated by *Limonium narbonense*, associated with *Sarcocornia fruticosa*, *Spartina maritima*, *Salicornia veneta*, and scarce *Suaeda maritima*, *Triglochin maritima* and *Juncus gerardii*. In the southern part of the Venice lagoon, Mira (MI) marsh is close to the landward boundary and it is characterized by the presence of *Phragmithes australis* on the marsh edge, together with the halophytic species *Juncus maritimum*, *Puccinellia palustris*, *Limonium narbonense*, and *Sarcocornia fruticosa*. Canale Virgilio (CV) and Fossei (FO) are located within the marsh belt in front of Malamocco and Chioggia inlets and host halophytic vegetation consisting mainly of *Limonium narbonense*, *Sarcocornia fruticosa*, *Puccinellia palustris*, together with *Juncus maritimum*, *Spartina maritima*, *Salicornia veneta* and *Suaeda maritima*. The Conche (CO) salt-marsh fringes the mainland and faces the wide subtidal flat that occupies the central-southern Venice Lagoon, being exposed to Bora wind. CO hosts halophytic species dominated by *Sarcocornia fruticosa*, *Suaeda maritima*, *Inula crithmoides*, and *Halimione portulacoides*. Finally, the Valle di Brenta (VB) salt marsh, at the southern end of the lagoon, is separated from the mainland by a channel and is characterized by the dominance of *Juncus maritimum*, *Sarcocornia fruticosa*, *Limonium narbonense* and *Puccinellia palustris*, with the presence of *Triglochin maritima*.

Figure 4.1: **Location of the study areas within the Venice Lagoon**. Insets show the position of the 30-m-long transects (orange lines) within each study area located perpendicularly to the main marsh edge: MI, CA, PA, SA, SF, SE, VB, CO, FO, CV (Map data: ©2022 Google-Landsat/Copernicus, Maxar Technologies).

Sediment cores were collected along linear transects from the marsh edge to the inner part of the 10 salt marshes, for a total of 60 cores. In most cases, transects start on an edge facing a channel, with the exception of CA and CO, as these marshes face a tidal flat. At each site, 6 cores were collected (0, 2.5, 5, 10, 20 and 30 m from the edge) so as to represent morphological and vegetation zonation. At each site where a core was collected, elevation above Mean Sea Level (MSL) and geographic location were measured using a GPS in RTK mode (Leica GS16) and vegetation characteristics were surveyed within a 1 ×1 m quadrat by the Braun-Blanquet method and registering species cover percentages (see Supporting Information, Tab. 4.1). For each quadrat, we estimated the aboveground biomass on the basis of species cover and live plant biomass as ash-free dry weight (AFDW) for each species from literature (see Supporting Information, Tab. 4.2). Shannon diversity index was used to measure the diversity of species in each sample community.

Surface soil samples were taken every 5 cm up to the depth of 20 cm (0, 5, 10, 15, 20 cm) from each core (Howard et al., 2014) and subsamples were oven dried at 60 °C for 48 h or to constant weight and prepared for different analyses, including OM and C content, soil density and grain size distribution. Percent OM of each sample was determined through a Loss On Ignition (LOI) procedure by combusting $\sim 2\,\mathrm{g}$ of ground sediment in a muffle furnace at 375 °C for 16 h of ground samples (Ball, 1964; Frangipane et al., 2009; Roner et al., 2016). The difference in weight between pre- and post-treatment provided the OM content as a weight percentage. Percent organic C was calculated from LOI using a local conversion equation built on a subsample analysed with an Elemental Analyser (see Chapter 6). Sediment Dry Bulk Density (DBD) was calculated from the water content, as the difference in weight between wet and dry samples, and organic and inorganic fractions, according to Kolker et al. (2009), by assuming water density $= 1.02\,\mathrm{g\,m^{-3}}$, and mineral and organic sediment density of $\rho_i = 2.6\,\mathrm{g\,m^{-3}}$ and $\rho_o = 1.2\,\mathrm{g\,m^{-3}}$, respectively, knowing the inorganic sediment and OM percentage from LOI analysis (Kolker et al., 2009). The product of percent OC and DBD determined soil carbon density (SCD). Soil carbon stocks in top 20 cm soil were calculated based on Howard et al. (2014) summing the C content in each soil interval along the core.

Inorganic particle size distribution analyses were performed, after the removal of the OM through a treatment with 35% hydrogen peroxide (H_2O_2) for 36 h, using laser granulometry (Mastersizer 2000 - Version 5.40, MALVERN INSTRUMENTS).

The reference layer for the analysis of OM content corresponds to the top 20 cm soil layer as we wanted to investigate the soil layer directly impacted by current vegetation and according to Trumbore (2009), in most vegetated ecosystems, the majority of underground plant biomass and microbial activity exists within the top 20 cm of soils. Conversely, in order to analyse sediment characteristics with reference to current hydromorphological dynamics, we limited the reference depth for grain-size analysis to 5 cm, considering the accreting behaviour of salt marshes.

Values of water salinity for each study area were calculated as the last-6-years mean of the quarterly measurements from the CTD multiparameter probes of the Veneto Region Environmental Protection Agency (ARPAV) (see Supporting Information, Tab. 4.3).

4.3.2 Statistical analysis

Statistical analyses were performed using MATLAB R2021a in order to investigate patterns, trends, and relationships among the data collected. Analyses included the use of the Kendall test, Kruskal-Wallis H test and post hoc median comparisons. The Kendall test is a non-parametric, rank-based method, and was used to determine whether there exists a monotonic relationship between soil characteristics, morphology and vegetation. The value of the coefficient ranges from $+1$ to -1, indicating a positive or a negative association, respectively. The Kruskal-Wallis test is a non-parametric version of classical one-way ANOVA using ranks of the data to compute the chi-square statistic and was used to compare the medians of the groups of data in different study sites and to determine if the samples come from the same population. When Kruskal-Wallis test showed a significant difference between groups, a multiple comparison test was used to determine which pairs of means were significantly different.

4.4 Results

4.4.1 Distribution of surface sediment variables along the transects

Fig. 4.2 and Fig. 4.3 show the distribution of the surface sediment variables analysed, namely OM content, DBD, grain size distribution, and the vegetation cover along the surface elevation profile of study transects in the northern and southern lagoon, respectively.

The topographic GPS field surveys show that marsh surface elevations along the transects range between about 0.20 and 0.60 m above MSL. CO is the highest site, with an average elevation on the transect of 0.55 m above MSL, while FO is the lowest site, with an average elevation of 0.24 m above MSL. Surface elevations are generally higher near the marsh edge, in presence of the channel levees, and they decrease toward the inner marsh. Some sites show a pronounced levee morphology (i.e. SF, SA and FO), while in other sites the latter is less distinct due to irregular (i.e. MI, CV, VB) or flattened profiles (i.e. PA, SE). CA and CO transects, which face a tidal flat and are exposed to wave energy, are characterized by higher surface elevation toward the inner marsh, with a convex shape profile (Tognin et al. (under review)). The vegetation cover is generally high (never below 50%), with no detectable trends along the transects.

OM content in surface soils (mean value in top 20 cm) ranges between 4% and 30% and shows important differences both within and among study areas. CA, FO, PA, VB, CV and MI show generally higher organic content, with average OM content value along the transects ranging between 15 and 21%, than CO, SF, SE and SA, with average OM content value along the transects ranging between 5 and 7%. OM content trend along the transects follows a more or less marked increase toward the inner marsh in most of the study sites (e.g. CA, PA, SF, SA, CV, CO, VB).

DBD in surface soil shows a distribution mirrored to that of OM content, with values ranging between 0.28 and $1.15\,\mathrm{g\,cm^{-3}}$, displaying a more or less marked decrease toward the inner marsh in most of the study sites. The highest values of DBD are found at CO, SE, SF and SA sites, with average values of 1.02, 0.81, 0.94 and $0.80\,\mathrm{g\,cm^{-3}}$, respectively.

Grain size of the surface inorganic sediment fraction ranges from clay to very fine sand, with a D50 (mean value in top 5 cm) ranging between 7 µm and 28 µm, with a mean value of 14 µm. Finer median grain size values are found at the PA site (average D50 value of 5 µm), which is characterized by higher percentages of clay. Whereas, coarser median grain size values are found in SF and CO sites (average D50 value of 19 and 20 µm, respectively), with the latter being characterized by some shell layers on the marsh surface. As to the distribution of the D50 along the transects, we observe coarser grains along the marsh edges (i.e. along the tidal channel levees) at SF, SA and VB, the latter displaying a sort of backward levee. CA and CO median grain size show a smooth trend with coarser particles in the central part of the transects. SE transect show slightly coarsening sediments toward the inner marsh, bordered by a tidal flat.

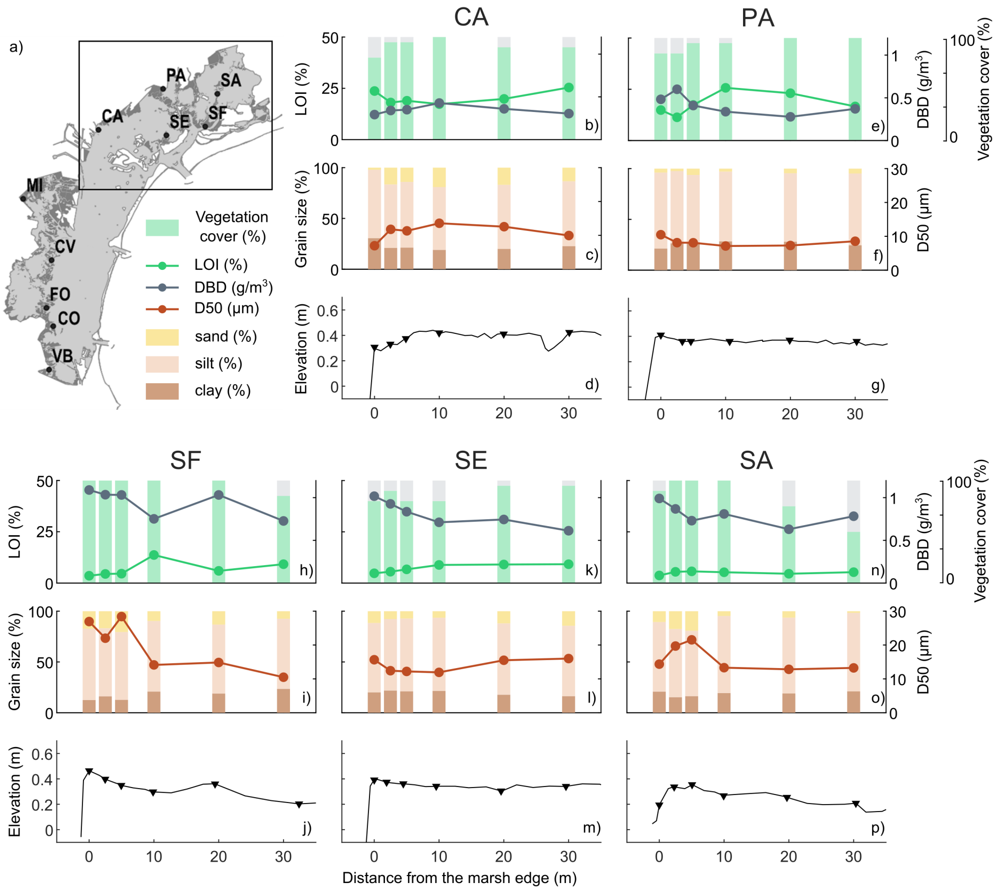

Figure 4.2: **Distribution of surface sediment variables analysed and surface elevation profile along the transects in northern lagoon**: organic matter content (LOI % - mean value in top 20 cm), Dry Bulk Density (g cm^{-3} - mean value in top 20 cm), vegetation cover (%), grain size distribution (D50 µm and sand-silt-clay percentage - mean value in top 5 cm) and surface elevation (m a.m.s.l.).

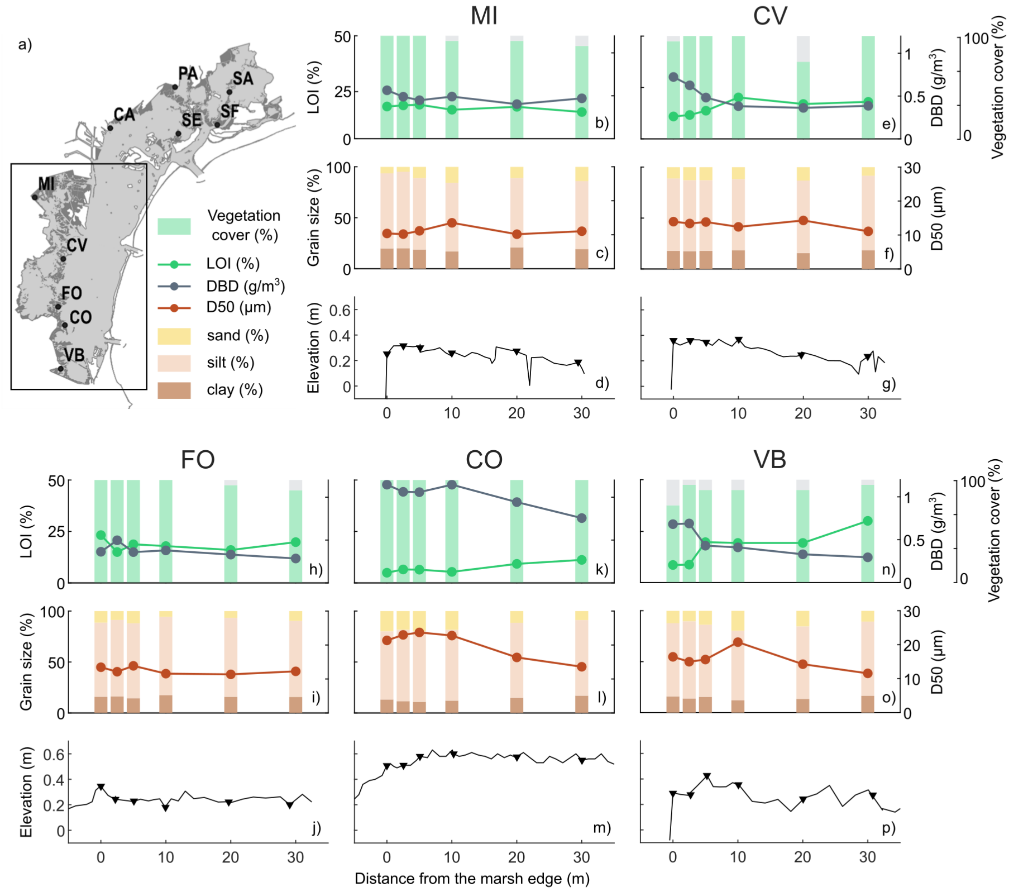

Figure 4.3: **Distribution of surface sediment variables analysed and surface elevation profile along the transects in southern lagoon**: organic matter content (LOI % - mean value in top 20 cm), Dry Bulk Density (g cm^{-3} - mean value in top 20 cm), vegetation cover (%), grain size distribution (D50 µm and sand-silt-clay percentage - mean value in top 5 cm) and surface elevation (m a.m.s.l.).

4.4.2 Dependence of sediment variables on the distance from the marsh edge

Considering the data from all our study areas, OM content in surface soils was significantly positively correlated with the distance from the marsh edge (Kendall's tau test, τ = 0.1532 p-value = 0.0002) (Fig. 4.4a), whereas DBD was significantly negatively correlated with the distance from the marsh edge (Kendall's tau test, τ = -0.2243 p-value = 6.3002×10^{-8}) (Fig. 4.4b). A significant negative correlation was found also between the median sediment grain size (D50) on the marsh surface and the distance from the marsh edge (Kendall's tau test, τ = -0.1509 p-value = 0.0222) (Fig. 4.4c). Distance from the marsh edge resulted to be negatively correlated to surface elevation in our study case (Kendall's tau test, τ = -0.1199 p-value = 0.0041), thus, as expected, DBD and D50 were positively correlated to marsh surface elevations (τ = 0.1387 and 0.1966 p-value = 0.0003 and 0.0015, respectively). Nevertheless, no significant relationship was found between the OM content and surface elevation.

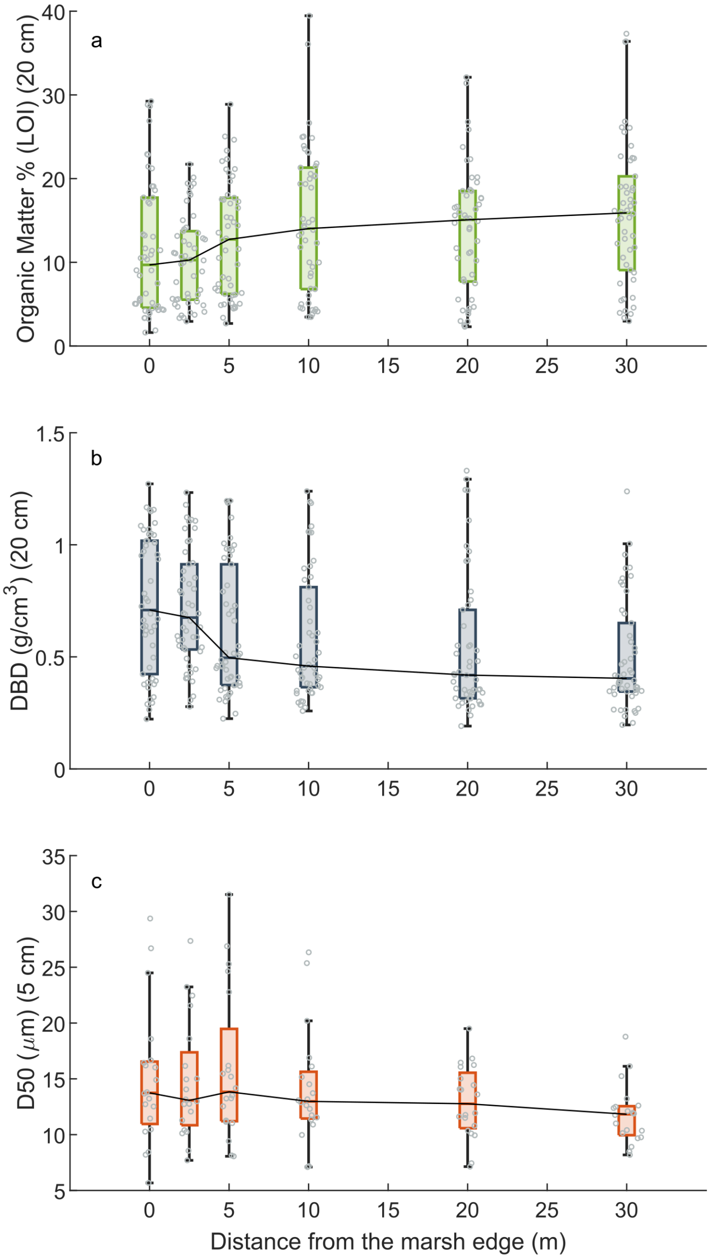

Figure 4.4: **Effects of the distance from the marsh edge on OM, DBD and grain size**: organic matter content (LOI % - mean value in top 20 cm) (a), Dry Bulk Density (g cm^{-3} - mean value in top 20 cm) (b), sediment median grain size distribution (D50 µm - mean value in top 5 cm) (c). Box plots show median and quartiles, swarm plots show single values.

4.4.3 Vegetation influence on SOM

Estimated aboveground biomass was highly variable in the analysed plots, ranging between about 200 and 1500 $\mathrm{g\,cm^{-2}}$ (AFDW) and showed no significant relationship with OM content in surface soils (Fig. 4.5a). When considering the dominant species, OM content of marsh surface soil displayed a wide variability (Fig. 4.5c). Higher mean organic content was observed in the presence of *Limonium narbonense* (Fig. 4.5e), *Phragmites australis* (Fig. 4.5d) and *Puccinellia palustris* as dominant species. Although highly variable, organic content showed a significant positive correlation with vegetation species diversity (Kendall's tau test for Shannon Diversity Index H and OC stock in top 20 cm: $\tau = 0.2011$ p-value $= 0.0239$, with mean SCD in top 20 cm $\tau = 0.1818$ p-value $= 0.0412$) (Fig. 4.5b).

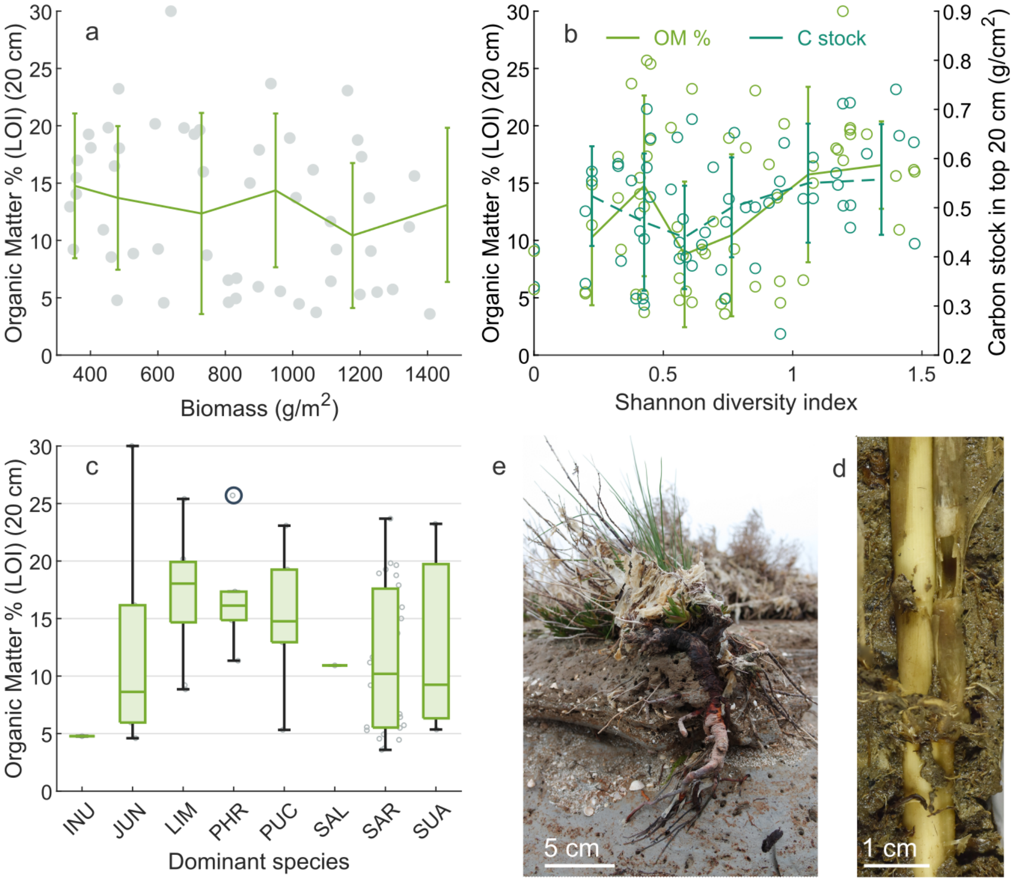

Figure 4.5: **Vegetation influence on SOM**. Organic matter content in marsh surface soils (LOI % - mean value in top 20 cm) as a function of biomass estimates (a) and dominant species (c) (INU = *Inula crithmoides*, JUN = *Juncus maritimus*, LIM = *Limonium narbonense*, PHR = *Phragmites australis*, PUC = *Puccinellia palustris*, SAL = *Salicornia veneta*, SAR = *Sarcocornia fruticosa*, SUA = *Suaeda maritima*). Organic matter content in marsh surface soils (LOI % - mean value in top 20 cm) and OC stock in top 20 cm as a function of Shannon Diversity Index H (b) in 1 ×1 m plot around core sites. *Limonium narbonense* roots exposed by marsh edge erosion at SE site (e) and *Phragmites australis* roots and stems within PA site soil (d).

4.4.4 Variability of sediment characteristics among study sites

As to the variability of marsh soil characteristics in different areas, Kruskal-Wallis analysis indicated that there was a significant difference between OM content in the 10 sites (p-value = 4.4928×10^{-34}) and post hoc test confirmed that CO, SA, SE and SF have significantly lower mean OM content in surface soil (Fig. 4.6a). Study sites were characterized by different mean water salinity ranging between 24.3 and 32.4 ‰, which revealed a significant negative relationship with OM content (Kendall's tau test, τ = -0.2574 p-value = 0.0061). CO, SA, SE and SF also show significantly higher values of DBD (Kruskal-Wallis, p-value = 2.3163×10^{-36}) (Fig. 4.6b). Mean SOC density in the top 20 cm (product of percent OC, which is function of OM, and DBD) ranged between 0.014 and 0.026 $\mathrm{g\,cm^{-3}}$ with lower values at SA, SF and SE (Fig. 4.6b). Carbon stock in top 20 cm ranged between 0.31 and 0.58 $\mathrm{g\,cm^{-2}}$ with lower values at SA, SF and SE (Fig. 4.6c). CO, which showed mean organic matter percentage similar to SA, SF and SE, displays, in contrast, higher values of SCD and C stock compared to SA, SF and SE, due to particularly high DBD values at this site. Median sediment grain size (D50) on marsh surface was not equal in different study sites (Kruskal-Wallis, p-value = 9.9686×10^{-11}), although not showing clear distribution patterns (Fig. 4.6d).

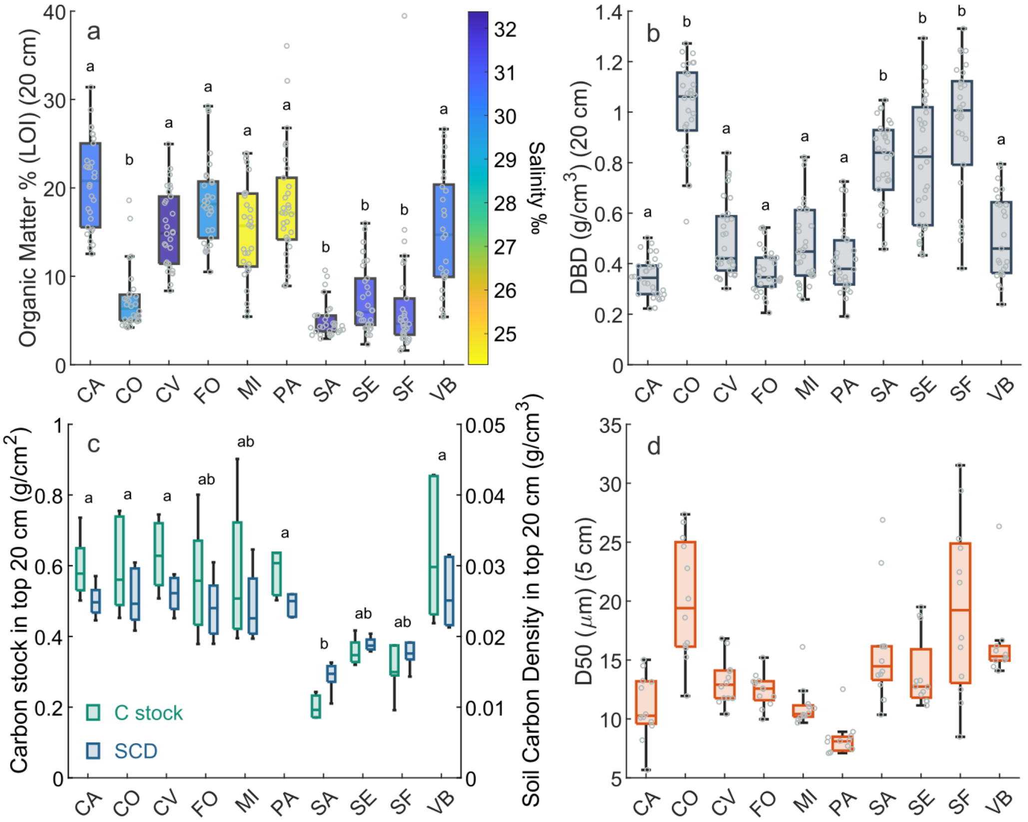

Figure 4.6: **Surface sediment variables at different study sites**: organic content (LOI % - mean value in top 20 cm) and water salinity at each study area (a), grain size distribution (D50 µg and sand-silt-clay percentage - mean value in top 5 cm) (b), Dry Bulk Density (g cm^{-3} - mean value in top 20 cm) (c), OC stock in top 20 cm (g cm^{-2}) and SOC Density (g cm^{-3} - mean value in top 20 cm) (d). Box plots show median and quartiles, swarm plots show single values. Different letters above the box plots indicate significant difference on the basis of Kruskal-Wallis test and post hoc multiple comparison test.

4.5 Discussion

4.5.1 Elevation profiles and grain size characteristics

Tidal currents deliver suspended sediments onto the marsh platform through inundation by apical flow at creek heads and by overbank flow along tidal channels (Torres and Styles, 2007). As soon as the flow reaches the vegetated marsh platform, current velocities and turbulent energy are rapidly decreased (D'Alpaos et al., 2007; Mudd et al., 2010), thus promoting the sedimentation of coarser suspended fraction in proximity of the channel edges (Christiansen et al., 2000; Roner et al., 2016). Indeed, elevation profiles and grain size characteristics observed along the transects reflect sediment supply dynamics, with the formation of levees along the tidal channels and the presence of coarser sediments on their top (Fig. 4.2 and Fig. 4.3), where tidal current flow is firstly slowed down favouring coarser particle settling. The increasing elevations and the grain size coarsening observed at the inner end of SE transect are likely due to the presence of a tidal flat at the inner border of the salt marsh, representing another source of sediment supply. The general pattern of sediment grain size is confirmed when considering all data together (Fig. 4.4b), as median sediment grain size (D50) on marsh surface was found to be significantly correlated to the distance from the marsh edge and to surface elevation. Interestingly, CA and CO transect, which are located on marsh edges adjacent to tidal flats and exposed to energetic wind-waves, displayed different surface morphology and sediment grain size patterns (Fig. 4.2 and Fig. 4.3) likely due to wave action pushing sediments and coarser particles further toward the inner marsh, as observed by Duvall et al., 2019 and Tognin, 2022.

At the lagoon scale, higher values of median grain size were observed at sites closer to the inlet (i.e., SF, SE) or adjacent to first order channel connected to them (SA) (Fig. 4.6d), whereas higher fractions of fine sediments were observed at the lagoon-mainland boundary, near to the Dese River mouth (PA) (Fig. 4.2). This pattern is consistent with the general grain-size gradient observed in the Venice lagoon, reflecting the typical pattern of decreasing hydrodynamic energy conditions from the inlets to the landward shore, with sandy sediment delivery from the sea and fine sediment from the mainland (Zonta et al., 2018). Accordingly, marsh edge levees seem to be more pronounced along the principal channels that depart from the inlets and hydrodynamically under their direct influence.

4.5.2 Organic content variability

The OM content in salt-marsh soils is likely a combination of in situ production of belowground biomass (root, rhizome and tuber tissue) inserted into the sediments (Craft et al., 1993; Rybczyk and Cahoon, 2002) and autochthonous or allochthonous organic materials that are deposited on the salt marsh (Nyman et al., 2006; Mudd et al., 2009; Ewers Lewis et al., 2019; Mueller et al., 2019). Spatial patterns in OM content are influenced by different conditions such as sediment supply, primary production and decomposition rates (Kirwan et al., 2013; Kolker et al., 2009; Morris et al., 2016; Mudd et al., 2009; Nyman et al., 2006; Turner et al., 2002). Overall, our data reveal two scales of variations in sedimentary OM content: one occurs on the order of meters to tens of meters along the transect, and another one is associated with the catchment scale.

The topographic and sedimentary structure of the salt marsh can influence a range of biological and physical processes and consequently affect the distribution of OM content (Chen et al., 2016), reflecting sediment supply dynamics along the distance from the tidal channel (i.e. sediment source) and salt marsh elevation, together with their dynamic feedbacks with primary productivity and vegetation characteristics (Perillo et al., 2009). Consistently with previous findings (e.g. Chen et al., 2016; Leonard et al., 2002; Roner et al., 2016) and despite a considerable variability, we found a significant correlation between OM content in surface soils and the distance from the marsh edge, with organic content generally increasing toward the inner marsh. The enriched OM content of inner marsh may be explained by the different sources of material available for salt marsh accretion across the platform (Miller et al., 2022). Due to the preferential deposition of the denser inorganic fraction of suspended sediments within tidal flow during the initial phase of inundation, inorganic sediment is mainly deposited near the marsh edge, whereas the inner marsh is supplied with more organic material due to the transport and deposition of less dense organic particles, in addition to in situ decaying vegetation (Leonard et al., 2002; Miller et al., 2022). Organic supply includes allochthonous particulate OM and organic debris and wrack deposited during storms (Miller et al., 2022), and autochthonous plant litter collected and moved above the marsh platform (Leonard et al., 2002).

Furthermore, inner, often lower, marsh areas are suggested to be characterized by better preservation conditions as anaerobic environments in frequently flooded sites reduce microbial respiration, slowing down organic matter decomposition (e.g. Halupa and Howes, 1995; Kirwan et al., 2013).

The observed pattern is consistent with the requirements for a steady state maintenance as suggested by field observation and numerical models (Roner et al., 2016; Mudd et al., 2004). Indeed, as inorganic accretion rates and the related platform elevations decrease with distance from the main channel, organic accretion should be expected to gradually increase as the distance from the main channel increases for the equilibrium assumption to hold.

As different species have different biomass productions and different resistance against decomposition, the type of vegetation populating the distinct marsh areas is another possible controlling factor for SOM content (e.g. Van De Broek et al., 2016; Ewers Lewis et al., 2020; Ford et al., 2019; Saintilan et al., 2013; Yuan et al., 2020). However, we observed no detectable trend of vegetation cover or plant biomass along the transect, nor a significant relationship between OM content and aboveground biomass estimates (Fig. 4.5a and c). In fact, a major influence was expected by belowground biomass, which inserting into the sediments directly contributes to SOM content (Craft et al., 1993; Rybczyk and Cahoon, 2002), and, unfortunately, lacks sufficient available estimates. Thus, our results suggest that aboveground species productivity is not a determinant in SOM at our study area. Furthermore, our aboveground biomass estimates neglect intraspecific biomass variability at the catchment scale, which could be represented only through direct measurements.

While our data do not allow for a full statistical analysis of the relationship between organic content and vegetation type, we observed higher mean OM content in presence of *Limonium narbonense*, *Phragmites australis* and *Puccinellia palustris*. We observed that *Phragmites australis* is characterized by a high belowground biomass, forming a dense and deep network of leathery stems, roots and rhizomes (Moore et al., 2012; Scarton et al., 2002) (Fig. 4.5e), *Limonium narbonense* produces massive woody roots (Fig. 4.5d) and *Puccinellia maritima* creates a dense root mat (Brooks et al., 2021), which can importantly contribute to SOM content quantitatively and qualitatively, as belowground litter decomposition was observed to decline with increasing lignin content (Stagg et al., 2018). In addition, OM content showed a significant positive correlation with vegetation species diversity (Fig. 4.5b), in agreement with Ford et al. (2019, 2016), who found that plant species richness was one of the most important explanatory variables of root biomass, and Xu et al. (2020), who suggested that species richness may increase biomass productivity due to multiple mechanisms including competition reduction, niche complementarity, selection effects, and biotic and abiotic facilitation.

At the catchment scale, the position within the gradient generated by marine and fluvial influence was previously observed to be a key predictor of organic content (e.g. Van De Broek et al., 2016; Ewers Lewis et al., 2020; Kelleway et al., 2016; Macreadie et al., 2017). Our results show lower mean OM content in surface soil in areas which are directly affected by marine influence, being closer to the inlets or along the main channels leading away from them (CO, SE, SF, SA) (Fig. 4.6a). Conversely, higher OM contents were observed in sites located closer to the mainland. In agreement with this result, a significant negative relationship was revealed between OM content and water salinity. This tendency is in agreement with observations in other studies (e.g. Van De Broek et al., 2016; Gorham et al., 2021; Hansen et al., 2017; Omengo et al., 2016) which attribute OM content increase toward the mainland to an increasing supply of already stabilized organic suspended particles from terrestrial sources and increasing macrophyte biomass. However, in the Venice lagoon, after historical river diversions, sediment supply from terrestrial sources was dramatically decreased. Freshwater inputs currently flow in the lagoon through twelve main tributaries distributed along the landward boundary of the lagoon, with a mean annual contribution of about $35\,\mathrm{m^3\,s^{-1}}$ and a peak discharge of $344\,\mathrm{m^3\,s^{-1}}$ (Zuliani et al., 2005). In addition, spatial and temporal variability in salinities in the Venice lagoon is influenced by groundwater inputs (Gieskes et al., 2013). Estimates of the volume of underground freshwaters entering the lagoon floor vary widely, from 15% of total freshwater flow to more than 100% (Zirino et al., 2014).

Another hypothesis is that at sites where inorganic sediment inputs are greater soil organic fraction is lower due to a dilution effect, reproduction of organogenic and minerogenic behaviour of salt marshes at different scales (Allen, 2000). Furthermore, considering the landward decreasing grain-size gradient observed within the lagoon, enhanced C preservation capacity of fine sediments (Kelleway et al., 2016) may have a role in the observed organic content pattern. However, as previous observations suggest an inverse relationship between soil salinity and decomposition (Hemminga et al., 1991; Wang et al., 2019), it is unlikely that salinity as such directly controls soil organic content, being this effect overcame by co-occurring effects of freshwater inputs.

As a consequence of organic content variability, SOC density and C stock show irregular values in different salt marshes, enhancing blue C assessment complexity. Based on our estimates of mean SOC density in top 20 cm and considering for salt marshes in equilibrium with RSLR an expected accretion rate of about $0.3\,\mathrm{cm\,yr^{-1}}$ (Day et al., 1998), the average C accumulation rate for the Venice lagoon salt marshes is estimated to be approximately equal to $69\,\mathrm{g\,C\,m^{-2}\,yr^{-1}}$. Our result is consistent with the mean C accumulation rate in the Australian tidal marshes of $54.52\,\mathrm{m^{-2}\,yr^{-1}}$ calculated by Macreadie et al. (2017) from 323 soil cores to the depth of 30 cm all around Australia and using a mean accretion rate of $0.21\,\mathrm{cm\,yr^{-1}}$. However, we observed that, under the same accretion rate, estimated SOC from our study may result in C accumulation rates varying up to 50% from one place to another.

4.5.3 Dry Bulk Density

Soil density is influenced both by OM content and grain size: various researchers found a strong and negative correlation between SOM and bulk density (e.g. Holmquist et al., 2018; Morris et al., 2016) and sand content showed a positive correlation with the soil bulk density (Tanveera et al., 2016). Our results highlight this relationship showing higher soil densities along marsh edge and at CO, SE, SF and SA sites, where organic content is generally lower and coarser sediments occurs.

4.6 Conclusions

Towards the goal of improving current understanding of salt-marsh biomorphodynamic evolution and carbon sink potential, we analyzed spatial patterns of SOM in salt-marsh soils, inspecting the physical and biological factors driving OM dynamics with respect to sediment, morphological and vegetation characteristics. Our observations on marsh morphology and grain size distribution further support previous field observations and modelling results emphasizing the interplay between hydrological, morphological, and biological dynamics. Elevation profiles and grain size characteristics observed along the transects reflect sediment supply dynamics, with the formation of levees along the tidal channels and median sediment grain size decreasing with increasing distance from the marsh edge and decreasing surface elevation. At the lagoon scale, sediment grain size distribution reflects the typical pattern of decreasing hydrodynamic energy conditions from the inlets to the landward portion of the tidal basin, with sandy sediment delivery from the sea and fine sediment from the mainland. OM content in surface soils (mean value in top 20 cm) ranges between 4% and 30% and shows important differences both within and among study areas.

Overall, our data reveal two scales of variations in sedimentary OM content in salt marsh soils. One occurs at the marsh scale and it is influenced by the interplay between surface elevation and sediment supply dynamics along the distance from the tidal channel. The other occurs at the catchment scale, and it is dominated by the gradient generated by marine and fluvial influence. Consistently with previous findings, our results show that OM content generally follows an inverse relationship with the distance from the marsh edge and broadly, higher OM contents were observed in sites located closer to the mainland, in salt marshes subjected to freshwater inputs and characterized by fine-grained sediments. Conversely, we found lower mean OM content in surface soils in areas which are directly affected by marine influence, being closer to the inlets or along the main channels departing from the inlets. In agreement with this result, a significant negative relationship was observed between OM content and water salinity. Although the interplay between physical and biological factors makes it difficult to unravel the direct cause-effect relationships, variations in allochthonous inputs, sediment grain size and/or preservation conditions may explain the observed variability in SOM.

As a consequence of organic content variability, SOC density and C stock show irregular trends in different salt marshes, enhancing blue C assessment complexity. Indeed, we observed that, under the same accretion rate, estimated SOC from our study may result in C accumulation rates varying up to 50% from one place to another.

Our data on local vegetation do not allow us to detect plant community characteristics controlling overall variations in SOM. Hence, we highlight the need for further analyses of quantitative and qualitative characteristics of different tidal marsh vegetation types. However, species diversity was observed to be an important factor influencing SOM content.

The observations on marsh morphology and grain size distribution further support previous field observations and modelling results emphasizing the interplay between hydrological, morphological and biological dynamics. Our data on the spatial distribution of SOM provide additional insights on organic matter dynamics in salt marshes and constrain model representations of SOM accumulation, improving the ability of biogeomorphological models to describe marsh response to the effects of climate change and anthropogenic perturbation and further elucidate marsh importance within the global C cycle. Furthermore, our findings may inform conservation strategies and restoration interventions giving directions on salt-marsh type prioritisation and providing information on conditions promoting OM storage and preservation, such as maintenance or recovery of freshwater inputs and finer sediment supply or enhancing vegetation diversity.

4.7 Supporting Information

	Inula crithmoides	**Aster tripolium**	**Limonium narbonense**	**Salicornia veneta**	**Sarcocornia fruticosa**	**Spartina maritima**	**Halimione portulacoides**	**Suaeda maritima**	**Pucinellia palustris**	**Juncus maritimus**	**Phragmites australis**	**Triglochin maritima**	**Suolo**
SF1			+		3		3						0
SF2			+		4					3			0
SF3					2					4			0
SF4					1					1			0
SF5			1		3					3			0
SF6			3	2									15
CO1	3		+		3								0
CO2	3	+	+		3			1					0
CO3					4		2	2					0
CO4							1	1					0
CO5		+			3			4	+				0
CO6					1		2	+					0
SE1	4				2								20
SE2			2		4				+				10
SE3			2		4								20
SE4			3		2								20
SE5					1								5
SE6			1		1								5
PA1		1									1		15
PA2		1									1		15
PA3		1									1		5
PA4		1									1		5
PA5		1								3	3		0
PA6		1					+			2	4		0
SA1			1		1	1							10
SA2					1				1				0
SA3					1								0
SA4			1		1				1				0
SA5			+	1	2				2				25
SA6			+	1					3				50
CV1	2		1	3				1	2				5
CV2			+		1	1			1				0
CV3			1		4	1			1				0
CV4			4		2	1			1				0
CV5			3	1		1		+		2			25
CV6			3		1				1	2			0
FO1					2			4					0
FO2				2	3			2	+				0
FO3					1	+		1	1				0
FO4			1		4	1		1	1				0
FO5			1	1	3	1			2	1			5
FO6			1	1	2				2				10
MI1			1		2		1			1	2		0
MI2		1	1		2		1			2	1		0
MI3		1	4	1	1					1	1		0
MI4		1	1						1				5
MI5		1	1						1				5
MI6		1	1						1				10
CA1			1		4								20
CA2			4		1	1						1	5
CA3			1		4				1				5
CA4					1				1				0
CA5			4		2								10
CA6			4						1				10
VB1		1	2		1				1	2			25
VB2					2					4			5
VB3			1		2				1	2		1	10
VB4			2		2				1	2			10
VB5		2	1						3	1			10
VB6			1		2				1	3			5

Table 4.1: **Vegetation survey**. Species composition at each studied site following Braun-Blanquet cover-abundance scale ($5 = 75 - 100\%$, $4 = 50 - 75\%$, $3 = 25 - 50\%$, $2 = 5 - 25\%$, $1 < 5\%$ numerous individuals, $+ < 5\%$ few individuals).

Species	**Live plant biomass** ($AFDW$ $\mathrm{g\,m^{-2}}$)	**Source**
Inula crithmoides	366	1
Aster tripolium	545	2
Limonium narbonense	276.3	3
Salicornia veneta	657.7	3
Sarcocornia fruticosa	1296.7	3
Spartina maritima	370.7	3
Halimione portulacoides	1540.7	3
Suaeda maritima	135,42	4
Pucinellia palustris	372.7	3
Juncus maritimus	601.3	3
Phragmites australis	1855	5
Triglochin maritima	500	6

Table 4.2: **Aboveground biomass**. Live plant biomass as ash-free dry weight (AFDW) for the species found in our study area. 1 = Zurayk and Baalbaki (1996) , 2 = Ingegnoli and Giglio (2004), 3 = Scarton (2006) , 4 = Mitra et al. (2005), 5 = Windham (2001), 6 = Kibby et al. (1980).

Study site	**ARPAV station**	**Mean salinity** (ppt)	**Standard deviation**
CA	PNC1_7B	30.45	2.94
CV	ENC1_4	32.38	2.02
FO	ENC1_VS/PC2_16B	29,81	3.8
MI	PC4_10B	24.6	5.45
PA	PC1_1B/PNC2_2	24.29	1.03
SA SF	EC_Ve8	32.16	2.3
SE	PNC2_SG	31.21	2.4
VB	PC3_VDB	30.57	2.57

Table 4.3: **Water salinity**. Values of water salinity for each study area as the last-6-years mean (2016-2022) of the quarterly measurements from the CTD multiparameter probes of the Veneto Region Environmental Protection Agency (ARPAV).

5

DEPTH DISTRIBUTION OF SOIL ORGANIC MATTER IN SALT MARSHES

This chapter is a manuscript ready to be submitted for publication under the title “Depth-distribution patterns of Soil Organic Matter in the tidal marshes of the Venice Lagoon (Italy): signatures of depositional and environmental conditions”. A.P., D.T., A.D. and M.M. designed the study. A.P., D.T., A.D. and M.M. developed the methodology. A.P. and D.T. collected the data and performed laboratory analyses. E.F. and N.R. provided the instrumentation and tools for grain-size analysis. A.P. and D.T. were responsible for data analysis and interpretation with the supervision of M.G., A.D. and M.M. All the authors discussed the data and agreed on their interpretation. A.P. wrote the original draft. D.T., A.D. and M.G. provided comments and suggestions to improve the original draft. All the co-authors contributed to the final polishing of the manuscript.

Depth-distribution patterns of Soil Organic Matter in the tidal marshes of the Venice Lagoon (Italy): signatures of depositional and environmental conditions.

A. Puppin[1], D. Tognin[2], M. Ghinassi[1], E. Franceschinis[3], N. Realdon[3], M. Marani[2] and A. D'Alpaos[1].

[1]Department of Geosciences, University of Padua, Padua, Italy
[2]Department of Civil, Environmental and Architectural Engineering, University of Padua, Padua, Italy
[2]Department of Pharmaceutical and Pharmacological Sciences, University of Padova, Italy

5.1 Abstract

Salt marshes are intertidal environments and their dynamic evolution is driven by complex feedbacks between hydrodynamic, morphological, and biological processes. They provide a diverse range of valuable ecosystem services and yet are exceptionally vulnerable to the effects of climate change and increasing human pressure. Soil Organic Matter (SOM) has a crucial role within salt-marsh environments, contributing to the build-up of marsh elevation and supporting a high carbon sink potential. Given the growing interest toward Organic Matter (OM) dynamics in salt-marsh environments, the aim of this work is to better understand variations in SOM distribution with depth within different geomorphic settings at the lagoon scale. We observe 2-fold higher median OM density in tidal marsh environments with respect to tidal flats and an increase in SOM content with increasing sediment grain size. In addition, we confirm the inverse relationship between organic content and soil density. Our results suggest that changes in the depositional environment are of primary importance in determining OM depth distribution and caution is needed in SOM prediction at unsampled soil depths through vertical distribution modelling. Current or past freshwater inputs, autochthonous and allochthonous organic inputs were observed to be importantly related to SOM variations. The outcomes of this study highlight the high po-

tential of salt marshes for carbon storage in intertidal environments and provide further insights into SOM dynamics and their drivers, to the benefits of coastal management strategies.

5.2 Introduction

Salt marshes are depositional landforms lying at the upper margin of the intertidal environment in saline tidal water bodies (Silvestri and Marani, 2004). They are characterized by the presence of vegetation mostly dominated by herbaceous halophytes adapted to regular inundation by saltwater (Perillo et al., 2009; Silvestri and Marani, 2004) and occur worldwide, particularly in middle and high latitudes on low-energy coasts, both in microtidal and macrotidal regimes (Adam, 1990; Allen and Pye, 1992; Mcowen et al., 2017). Salt marshes, situated at the interface between terrestrial and marine ecosystems, deliver a wide range of ecosystem services that contribute to human well-being, including carbon (C) storage, coastal protection and increase in biodiversity (e.g. Barbier et al., 2011; Boesch and Turner, 1984; Costanza et al., 1997; Lefeuvre et al., 2003; Temmerman et al., 2013). However, salt-marsh ecosystems are exceptionally vulnerable to the effects of climate change and increasing human pressure (e.g. accelerating relative sea-level rise, declining sediment supply, coastal land reclamation) (D'Alpaos et al., 2011; Fagherazzi et al., 2020; Gedan et al., 2009; Kirwan et al., 2010; Marani et al., 2007; Morris et al., 2002; Mudd, 2011; Silvestri et al., 2018; Temmerman et al., 2004), experiencing a steep global decline at rates four times faster than rain forests (Duarte, 2009). Being part of the complex intertidal system, including intertidal platforms and tidal channel networks, characterized by volatile boundary conditions (e.g. tidal range, sea level, sediment supply), salt marshes are intrinsically dynamic environments. Their evolution is driven by complex feedbacks between hydrodynamic, morphological, and biological processes, providing a great example of ecomorphodynamics (e.g. Marani et al., 2006a; D'Alpaos et al., 2007; Mudd et al., 2009; Marani et al., 2013). Salt-marsh landforms typically arise through the emergence of an elevated sedimentary platform (mudflats and sandflats), due to sediment deposition, above some critical elevation at which flow conditions become suitable for the settlement of pioneer vegetation (Perillo et al., 2009; Silvestri et al., 2005; Silvestri and Marani, 2004). Salt-marsh vegetation influences the water flow, favours sediment trapping and deposition and stabilizes the marsh platform (e.g., D'Alpaos et al., 2007; Marani et al., 2007, 2013; Kirwan and Murray, 2007; Mudd et al., 2009; Leonardi et al., 2018). Furthermore, in situ production of belowground biomass (root, rhizome and tuber tissue) inserted into the sediments (Craft et al., 1993; Rybczyk and Cahoon, 2002) and autochthonous or allochthonous organic materials, that are deposited on the salt marsh (Nyman et al., 2006; Mudd et al., 2009; Ewers Lewis et al., 2019; Mueller et al., 2019), directly contribute to soil formation. Thus, organic matter (OM) has a key role in salt-marsh dynamics as it strongly contributes to marsh surface accretion, furthermore feeding the high C sink potential of these environments. Although the OM content varies markedly between systems driven primarily by the accumulation of internally produced organic material and those characterized by the deposition of externally derived inorganic sediments (Perillo et al., 2009), soil organic matter (SOM), owing to its high porosity and low density, may contribute 1.5–3 times more toward vertical accretion than inorganic matter, having a key role in the persistence of coastal wetlands with low mineral sediment supply (Allen et al., 2021).

Vertical accretion and SOM accumulation dynamics give to salt-marsh environments a great potential for C storage and accumulation. In fact, the C captured through plant photosynthesis is buried and preserved in SOM over centennial to millennial time scales (Duarte et al., 2005; Perillo et al., 2009), also thanks to anaerobic tidal conditions slowing down OM decomposition (Keuskamp et al., 2013; Kirwan et al., 2014; Morris et al., 2016; Mueller et al., 2018). This provides the opportunity to include salt-marsh conservation and restoration among greenhouse-gas-offset activities in climate mitigation strategies, increasing the scientific and policy interest toward SOM dynamics in salt-marsh environments (e.g. Macreadie et al., 2017; McLeod et al., 2011; Saintilan et al., 2013).

Distribution patterns of SOM in salt marshes may vary in space and time across the range of tidal wetlands types and within individual wetlands depending on different conditions such as sediment supply and primary production (Kolker et al., 2009; Morris et al., 2016; Nyman et al., 2006; Turner et al., 2002). Numerous authors suggest geomorphic setting as the most important predictor of SOM content, with fluvially-influenced sites having twice the soil organic C (SOC) stock as seaward sites (e.g. Kelleway et al., 2016; Macreadie et al., 2017). SOM variations may be due to differences in vegetation types (Ewers Lewis et al., 2020; Saintilan et al., 2013), both in terms of biomass production and recalcitrant tissue variations (Scarton et al., 2002; Stagg et al., 2018), sediment and stable allochthonous OM supply (Van De Broek et al., 2016), sediment grain size (Ford et al., 2019; Kelleway et al., 2016).

In response to the increasing demand for the estimation and mapping of SOC storage at large spatial scales, in order to reduce sampling efforts, numerous studies are proposing predictive models for SOM in salt marshes (e.g. Bai et al., 2016; Ford et al., 2019; Wiese et al., 2016). The exponential depth model is the most widely accepted in SOM vertical distribution modelling (Bai et al., 2016; Wiese et al., 2016). Exponential depth models were broadly tested in terrestrial soils, where OM distribution is primarily controlled by biomass inputs from the surface and OM decomposition (Mueller et al., 2019; Murphy et al., 2019). However, in tidal environments, besides the effect of OC decay down-core, spatial and temporal variations in intertidal sediment accommodation and organic inputs, related to the ontogeny of salt-marsh environment, should be reflected in SOM distribution (Miller et al., 2022). Variations in organic content were reported for depositional environments forming intertidal deposits (Brevik and Homburg, 2004), thus the interpretation of stratigraphic patterns may be critical for the representation of SOM depth-distribution.

Although there is an increasing understanding of factors influencing SOM in coastal wetlands, further investigation is needed in order to improve model representation of SOM distribution patterns in heterogeneous and dynamic intertidal landscapes. SOM and SOC distribution representation and the identification of their drivers are important for accurate C assessment and planning of greenhouse-gas-offset activities.

The aim of our study is to better understand SOM depth distribution variations within different geomorphic settings at the lagoon scale and further comprehend SOM drivers affecting salt-marsh resilience and C sink potential. Toward these goals, we analysed soil organic content in 10 salt marshes of the microtidal sediment-starved Venice Lagoon from 60 sediment cores to the depth of 1 m, relating SOM spatial and vertical patterns to soil variables and depositional environment evolution testified by recent sedimentary successions. Our results may provide important insights in SOC depth distribution modelling to integrate environmental and depositional changes, enhancing their capability to predict carbon budgets in salt-marsh environments.

5.3 Material and methods

5.3.1 Study site

The Venice Lagoon is a back-barrier system located in the north-western Adriatic Sea, Italy, and connected to it by three inlets, namely Lido, Malamocco, and Chioggia (Fig. 5.1). It is a shallow lagoon (average depth of tidal flats and subtidal platforms of about 1.5 m), with a total extent of about 550 km^2, and a semi-diurnal micro-tidal regime with an average tidal range of 1.0 m.

The present-day morphology of the Venice Lagoon is the result of the combination of natural forcings and human interventions that occurred over the last centuries. To preserve channel and port functions, several hydraulic works have been carried out, which modified sediment supply, local hydrodynamics and the morphological setting, favouring sediment starvation and the deepening of the lagoon (Zecchin et al., 2009; Brambati et al., 2003; D'Alpaos, 2010). Between 1400 AD and 1600 AD the diversion of the major tributaries dramatically decreased the fluvial sediment input in the lagoon (Fig. 5.1) and since 1800 the excavation of new deep canals together with inlet modifications exacerbated sediment export towards the sea (Brambati et al., 2003; D'Alpaos, 2010; Finotello et al., 2022). Furthermore, intertidal areas were reclaimed to provide industrial and urban space, and between 1930 and 1970 intense groundwater exploitation for industrial purposes enhanced local subsidence (Brambati et al., 2003; Carbognin et al., 2004; Teatini et al., 1995). As a consequence, salt-marsh areas of the Venice lagoon have dramatically shrunk in the last centuries, with a decrease in extension from about 180 km^2 in 1811 to about 43 km^2 in 2002 (Carniello et al., 2009; D'Alpaos, 2010; Tommasini et al., 2019). In addition, recent activation of storm-surge barriers, designed to prevent flooding of the city of Venice, was proved to further alter the lagoon hydrodynamics (Mel et al., 2021) contributing to the deepening of the tidal flats and reducing salt-marsh sedimentation (Tognin et al., 2021). As external fluvial and marine sources of sediment are negligible, nowadays, the hydrodynamic processes, such as tidal currents, wind waves and storm surges, mainly rework and redistribute intra-lagoonal sediments (Tognin et al., 2021).

The study sites are located in 10 salt marshes of the Venice lagoon, at variable distances from the inlets (Fig. 5.1). In the northern lagoon, Sant'Erasmo (SE), San Felice (SF) and Saline (SA) salt marshes are located at the edges of large tidal channels departing from the Lido inlet. In contrast, Pagliaga (PA) and Campalto (CA) sites are found at the lagoon-mainland boundary in the northern lagoon. PA is located at the border of one of the few rivers still entering the lagoon, the springwater Dese River, whereas CA originated on continental ground (Bonometto, 2005). Salt marshes of the southern part of the Venice lagoon are known to be originating from pre-existing brackish environments or salinized freshwaters arising from river diversions (Bonometto, 2005), as this area was strongly influenced by fluvial inputs from the Brenta River, which was repeatedly diverted from and re-introduced into the Lagoon, as shown in Fig. 5.1 (e.g. Bondesan and Furlanetto, 2012; Roner et al., 2017). Mira (MI) and Valle di Brenta (BV) sites are located close to the landward boundary, whereas Canale Virgilio (CV) and Fossei (FO) are located within the marsh belt in front of Malamocco and Chioggia inlets. The Conche (CO) salt marsh edges the mainland and faces toward the wide subtidal flat that occupies the central-southern Venice Lagoon.

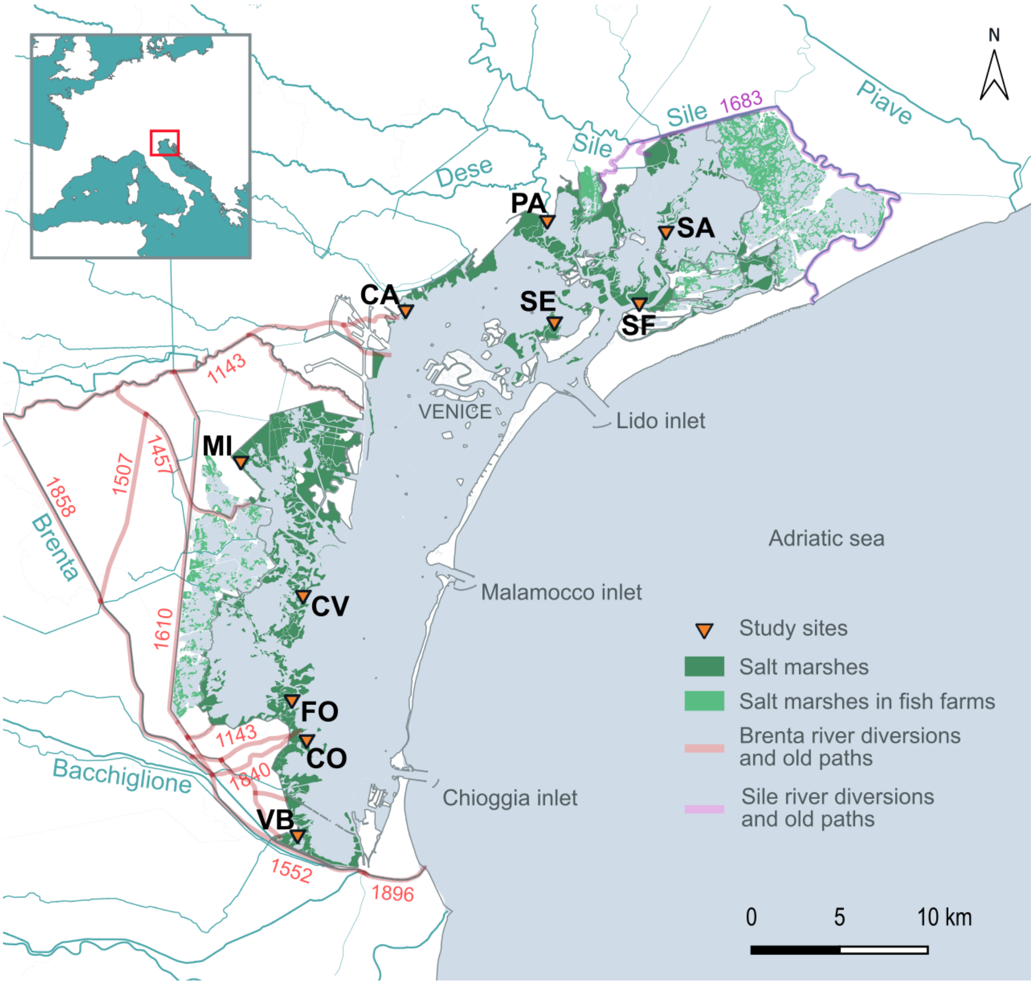

Figure 5.1: **Location of the study areas within the Venice Lagoon** (orange inverted triangles). Salt-marsh areas are in green. Red and purple signs represent Brenta and Sile river diversions and old paths, respectively.

5.3.2 Sediment sampling and sedimentological analyses

Sediment cores were collected along linear transects from the marsh edge to the inner part of the 10 salt marshes, for a total of 60 cores to the depth of 1 m. In most cases, transects start on an edge facing a channel, with the exception of CA and CO, as these marshes face a tidal flat. In each site, 6 cores were collected (0, 2.5, 5, 10, 20 and 30 m from the edge, respectively) so as to represent morphological and vegetation zonation. Core collection points were surveyed using a GPS in RTK mode (Leica GS16) and vegetation characteristics were recorded within a 1×1 m quadrat by the Braun-Blanquet method and registering species cover percentages.

Soil samples were taken at 12 depths (0, 5, 10, 15, 20, 25, 30, 35, 40, 45, 50, 75 cm) from each core (Howard et al., 2014) and subsamples were oven dried at 60 °C for 48 h or to constant weight and prepared for different analyses, including OM and C content, soil density and grain size distribution. Percent OM of each sample was determined through a Loss On Ignition (LOI) procedure by combusting $\sim$ 2 g of ground sediment in a muffle furnace at 375 °C for 16 h (Ball, 1964; Frangipane et al., 2009; Roner et al., 2016). The difference in weight between pre- and post-treatment provided the OM content as a weight percentage. Sediment Dry Bulk Density (DBD) was determined as the ratio between dry weight and estimated wet volume. The product of OM content (LOI) and DBD determined Organic Matter Density (OMD). Inorganic particle size distribution analyses were performed using laser granulometry (Mastersizer 2000 - Version 5.40, MALVERN INSTRUMENTS), after the removal of the OM through a treatment with 35% hydrogen peroxide (H_2O_2) for 36 h.

Sedimentological analyses were carried out on the study cores through the principles of modern facies analysis in order to link them with the corresponding sedimentary processes and depositional environments (Roner et al., 2017). Different types of deposits were differentiated on the basis of their distinctive features through the observation of their colour, grain size, texture, sedimentary structures and macroscopical biogenic content (e.g. shells, plant debris and vegetal remains). Differentiation of depositional environments within core stratigraphy allowed us to analyse the variability of soil characteristics in different types of deposits.

5.3.3 Statistical analysis

Statistical analyses were performed using MATLAB R2021a in order to investigate patterns and relationships of soil characteristics. The non-parametric rank-based Kendall test was used to determine whether there exists a monotonic relationship between SOM and sediment grain size. The value of the coefficient ranges from $+1$ to -1, indicating a positive or a negative association, respectively. The Kruskal-Wallis test, a non-parametric version of classical one-way ANOVA using ranks of the data to compute the chi-square statistic, was used to compare the medians of soil characteristics in different depositional environments to determine if the samples come from the same population. When Kruskal-Wallis test showed a significant difference between groups, a multiple comparison test was used to determined which pairs of means were significantly different.

As the exponential depth model is the most widely accepted in SOM vertical distribution modelling (Bai et al., 2016; Wiese et al., 2016), in order to test its viability for SOM prediction at different depths in our study case, we fitted our SOM data using an exponential function:

$$SOM = ae^{-bD} \tag{5.1}$$

where SOM is the percentage by weight of organic matter, D is the depth below the marsh surface (cm), and a and b are the parameters of the exponential function. Only SOM data from the current marsh deposits were considered in order to exclude major variations produced by a transition in depositional environment.

Exponential depth models were broadly tested in terrestrial soils, where SOM content primarily produced by belowground biomass growing in surface soils rapidly decline due to OC decomposition (Mueller et al., 2019; Murphy et al., 2019). However, tidal depositional environments are characterized by rapid vertical accretion through the accumulation of autochthonous and allochthonous organic material and inorganic sediments. Though SOM depth distribution is controlled by the effect of OM decay as well as spatial and temporal variations in intertidal sediment accommodation and organic inputs, which are in turn affected by numerous environmental variables (Miller et al., 2022). Indeed, simply accounting for an exponential decay of the OM currently present in the surface soil may underestimate the total amount of carbon in the case of higher organic inputs in the past.

5.4 Result and discussion

5.4.1 Depositional environment interpretation

Sedimentological analyses allowed us to differentiate four depositional environments (Fig. 5.2 , Fig. 5.3 , Fig. 5.4 , Fig. 5.5). Salt-marsh deposits formed by the accretion of current salt marsh environments were observed to be permeated by more or less abundant live roots and plant debris, sometimes concentrated in visible laminations. A so-called brackish marsh was distinguished on the basis of a reed-dominated plant community, whose dense and deep network of roots and stems or its remains are clearly recognisable in marsh soils. Marsh deposits currently dominated by *Phragmithes australis*, which is a near freshwater species, were sampled only at PA and MI sites. However, reed fragments were clearly visible in buried deposits at different sites, leading to the identification of buried brackish marshes, signature of past freshwater inputs or palustrine conditions. Tidal-flat deposits were defined by the absence of roots in life position, poor plant debris content, sandy laminations or massive coarser sediments. Lastly, as changing conditions usually lead to gradual evolution from a type of deposit to another, transition zones were differentiated. A transition zone generally occurs between salt-marsh deposits and tidal-flat deposits, being characterized by features from both depositional environments and mainly corresponding to tidal-flat deposits colonized by pioneer vegetation.

5.4.2 Sedimentological analyses and OM content along transects

At SA, SE and SF sites OM concentration rapidly decreases with depth and becomes stabilized roughly under 30 cm depth (Fig. 5.2). OMD depth-distribution follows OM patterns. Mean OM content in 1 m top soil is between 3 and 7%, reaching about 10% at SF when considering surface soil layer. SA site is characterized by a top layer 10-20 cm thick where current marsh plant roots (not very dense) are present and horizontal layering is hardly visible (Fig. 5.2 – insert f). Plant debris progressively decreases in salt-marsh deposits, grading downward into coarser massive deposits with some shell fragments (Fig. 5.2 – insert g). Sediments permeated by current salt-marsh plant roots are 20-30 cm thick at SE and 30-40 cm thick at SF sites, with plant debris progressively decreasing downward (Fig. 5.2 – insert d). Horizontal layering is clearly visible along the cores, being characterized by laminae rich in plant debris in surface sediments and sandy laminae downward (Fig. 5.2 – insert e). Yellowish oxidized areas (Fig. 5.2 – inserts d and e) are distributed along all depths and all cores, being evidence of periodic subaerial exposure, and a light pinkish layer of a few millimeters is visible at 20 cm depth at SE site (Fig. 5.2 – insert d) and between 40 and 10 cm depth (being deeper toward the marsh edge) at SF site. These deposits are characterized by an overall fining-upward grain size trend. Stratigraphic observations suggested the identification of salt-marsh deposits of different thickness (from 10-20 cm at SA to 20-50 cm at SF) grading downward into underlying tidal flat deposits. Sedimentation on the tidal flats bordering the channels and resulting elevation accretion likely allowed the encroachment of pioneer vegetation that boosted further sediment accumulation and, subsequently, allowed the establishment of a typical halophytic vegetation community. Reduced thickness of salt marsh deposits at SA may be explained by a reduction in the accommodation space, as moving away from the inlet, the tidal range decreases due to the dissipation induced by bottom friction.

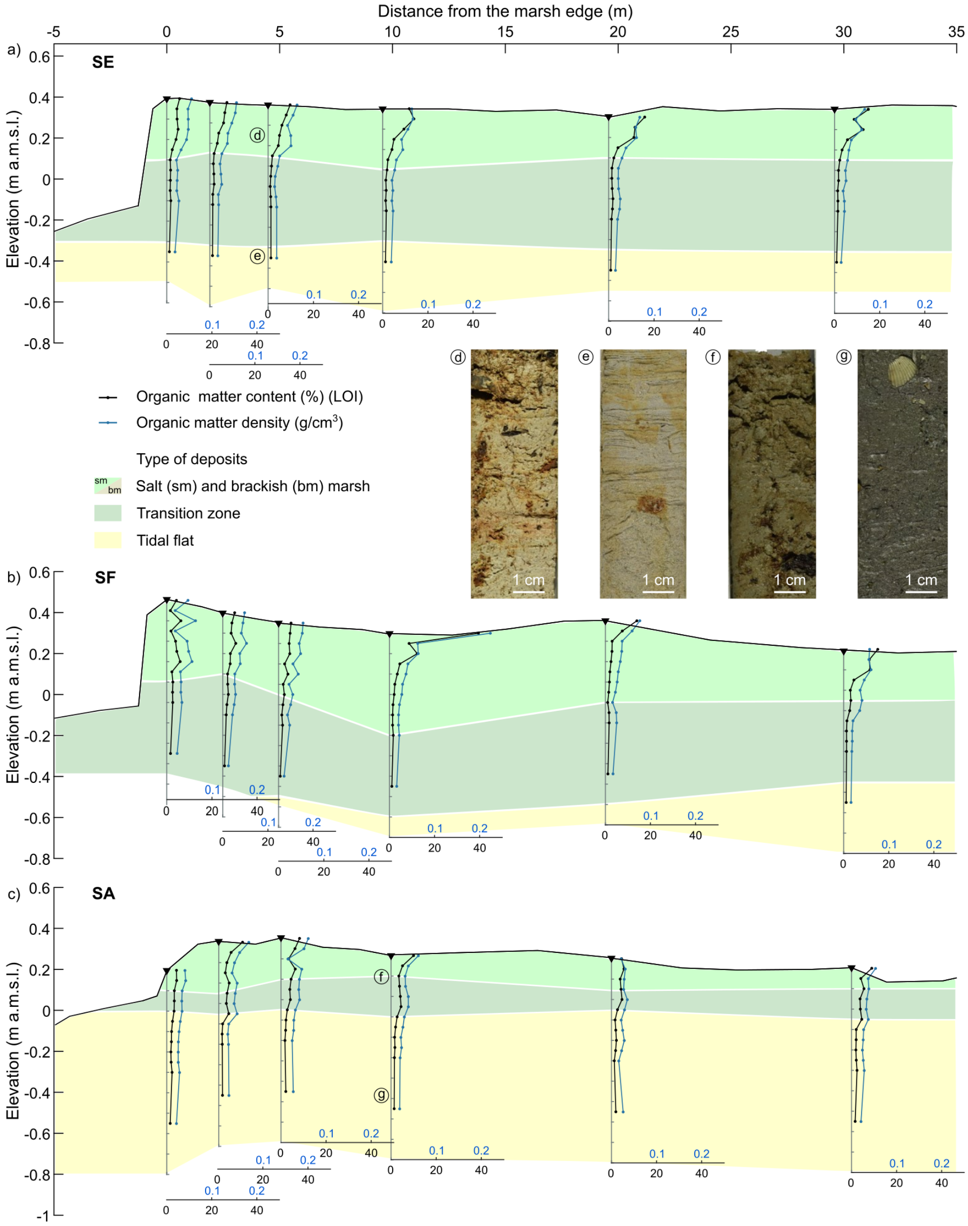

Figure 5.2: **Representation of transect vertical sections, OM content and sedimentological interpretation: SE, SF and SA**. Along the surface elevation profile, at each core site (from 1 to 6 respectively at 0, 2.5, 5, 10, 20 and 30 m from the marsh edge) depth-distribution of organic matter content (LOI - % weight – black scale from 0 to 50) and organic matter density ($\mathrm{g\,cm^{-3}}$ – blue scale from 0 to 0.25) are depicted. An interpretation of the study transect depositional environments is schematically illustrated by polygons of different colours on the basis of the sedimentological features and the spatial distribution of the different sedimentary deposits differentiated. Inserts (d-g) are pictures of core details and their position is indicated on transect section representations: d and f – roots and plant debris in salt-marsh deposits, e – sandy laminae in tidal flat deposits, g – shell fragments in sandy tidal flat deposits.

At PA site mean organic matter in 1 m top soil ranges between 14 and 26% (Fig. 5.3a). The depth profiles of OM concentration generally show some peaks around about 20 and 30 cm depth, with values higher than 40%. OM concentrations above and below the peaks are similar. On the contrary, OMD displays a much more constant trend without the presence of peaks, because OMD depends on both OM and DBD. Although OM increases, the presence of a peaty layer without a mineral component results in a low density value. Core deposits are permeated by the dense stem and root networks of the current vegetation community dominated by *Phragmites australis* at least down to 50 cm depth along the entire transect (Fig. 5.3 - insert d). The underlying layer is still rich in plant debris and clear rests of reeds (Fig. 5.3 - insert e). As no clear differentiation was observed, all the sampled deposits were attributed to a salt-marsh dominated by the near freshwater plant *Phragmites australis* (brackish marsh).

CA site shows quite irregular depth profiles of OM concentration, with mean values in 1 m top soil ranging between 15 and 22% (Fig. 5.3 b). A generally decreasing trend with depth can be observed, with some peaks (up to 40%) around 20-40 cm depth. OMD, instead, displays a much more constant trend without the presence of peaks, as OM increase is caused by OM rich layers with a low density. Surface deposits, down to 30-40 cm in depth, are characterized by the dense network of mainly fine roots of current vegetation, with discontinuous plant-debris-rich laminations (Fig. 5.3 - inset f). Below this layer, scattered, also large-sized, plant debris in life position are visible within a mud matrix. At the bottom of the cores, a peaty layer with reed fragments is present (Fig. 5.3 - insert h). Therefore, at CA site salt-marsh deposits overlay a buried palustrine environment/brackish marsh (dominated by *Phragmites australis*). At 10 m from the marsh edge, between 80 and 100 cm depth a subtle laminated layer is visible, with dark laminae rich in plant debris (Fig. 5.3 - insert g), which may be interpreted as the sign of a buried pond, as confirmed also by the presence of reed debris at higher elevation both at the margin and in the inner marsh. The transition from a brackish environment to a salt-marsh system marks a change in the salinity, probably driven by river diversion.

At MI site mean organic matter in 1 m top soil ranges between 10 and 20% (Fig. 5.3 c). The depth profiles of OM concentration generally show a decrease in the upper layer (30-40 cm) and then again, an increase in the deeper layer, reaching the highest values at 75 cm depth in the edge core, with 40% of organic matter. OM depth profiles are highly variable near the margin and more regular toward the inner marsh. OMD depth-distribution generally follows OM patterns. However, although OM shows very high value at 75 cm deep, the increase in OMD is much more reduced because of the lower DBD of the peaty deposit. Core 1 and 2, near the marsh edge, are entirely permeated by plant roots (Fig. 5.3 - insert i), with reed tissues becoming more evident below about 30 cm depth. Toward the inner marsh, surface layer characterized by the presence of fine roots of current salt-marsh plants progressively thins. Below salt-marsh deposits, light-coloured deposits can be defined, characterized by subtle horizontal layering, with laminae of darker colour and rich in plant debris (Fig. 5.3 - insert j). This laminated layer becomes thicker toward the inner marsh and overlies a dark shell-rich layer, that separates it from deposits rich in plant debris with reed fragments (Fig. 5.3 - insert k). Starting from about 3 m from the marsh edge, current marsh deposits are separated from the underling palustrine peat by a layer which we interpret as representative of a wide tidal depression (pan or pond) or a small tidal flat. A reed dieback (maybe due to a change in freshwater inputs and water salinity) might have caused a drowning of the platform starting from the inner marsh (likely richer in organic content and with smaller sediment supply). The latter was then covered by tidal flat muddy deposits ranging from massive to slightly laminated. The tidal flat or pond (still visible in the inner marsh in Fig. 5.3 - insert l) was later colonised by halophytic plants and reeds starting with a new expansion of the marsh deposits from the marsh edge to the inner part.

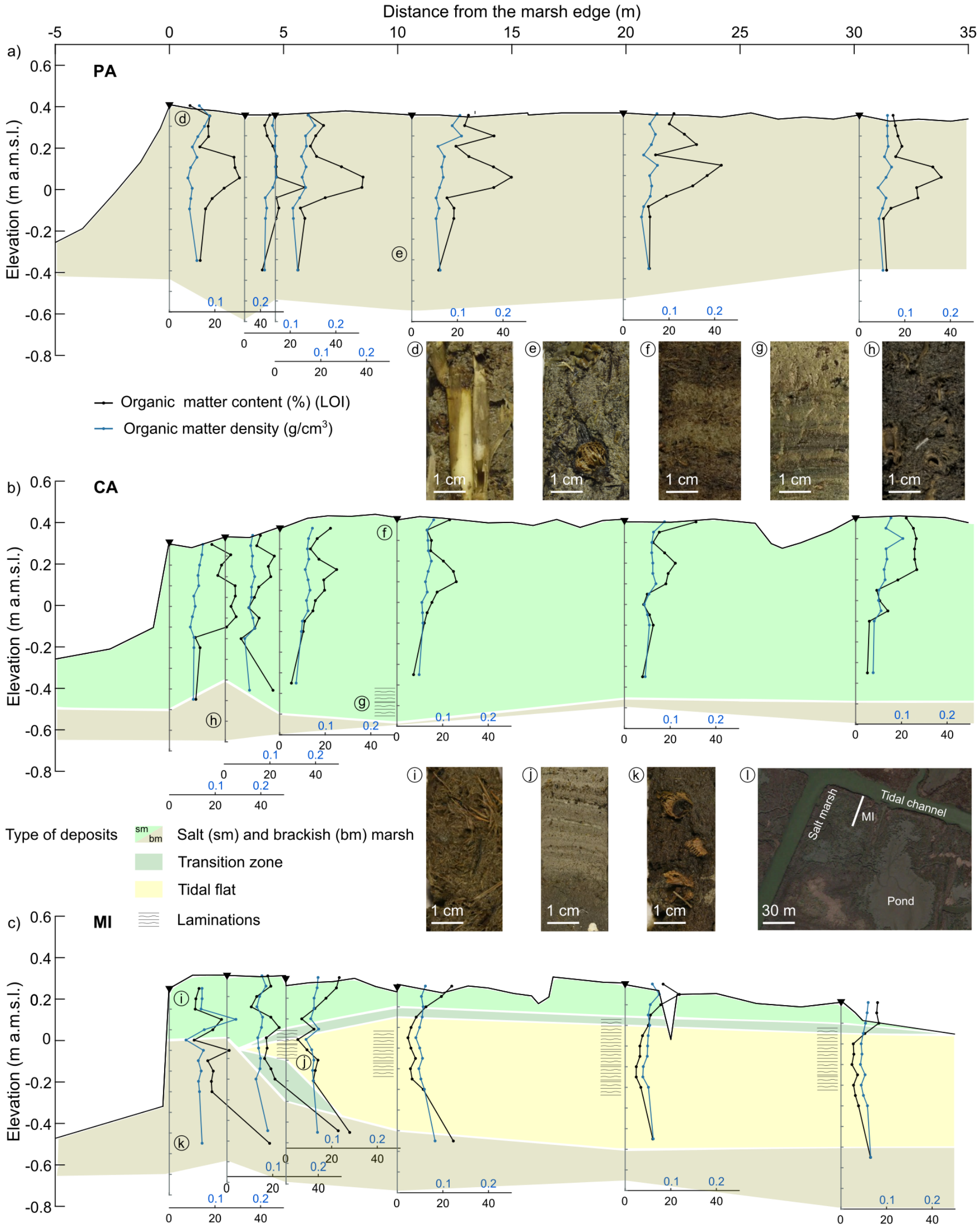

Figure 5.3: **Representation of transect vertical sections, OM content and sedimentological interpretation: PA, CA and MI**. Along the surface elevation profile, at each core site (from 1 to 6 respectively at 0, 2.5, 5, 10, 20 and 30 m from the marsh edge) depth-distribution of organic matter content (LOI - % weight – black scale from 0 to 50) and organic matter density ($\mathrm{g\,cm^{-3}}$ – blue scale from 0 to 0.25) are depicted. An interpretation of the study transect depositional environments is schematically illustrated by polygons of different colours on the basis of the sedimentological features and the spatial distribution of the different sedimentary deposits differentiated.

Figure 5.3: Inserts (d-l) are pictures of core details and their position is indicated on transect section representations: d – *Phragmites australis* aboveground tissues, e – reed fragments, f – plant-debris-rich laminations in salt-marsh deposits, g and j - plant-debris-rich laminae in pond deposits, h and k – reed fragments, i – roots and plant debris in salt-marsh deposits, l - a wide pond in the inner marsh at MI site (Map data: ©2022 Google-Landsat/Copernicus, Maxar Technologies).

At CV site the profiles of OM concentration with depth show no clear trend, with mean OM contents in 1 m top soil ranging between 10 and 17% (Fig. 5.4). They are approximately linear at the marsh edge, slightly decreasing in surface layer toward the inner marsh but with an increase at the core bottom. OMD distribution generally follows OM patterns. However OMD is reduced when low-density peaty deposits are encountered toward the inner marsh. Abundant roots and plant debris are visible along the entire profile in all the cores, with some dark laminae rich in organic debris (Fig. 5.4 - inserts 1 and 2). Toward the inner marsh, at the bottom of the cores a peaty layer with reed fragments is present (Fig. 5.4 - insert 3). Therefore, at CV site salt-marsh deposits are characterized by high thickness and in the inner marsh overlay a buried palustrine environment/brackish marsh (dominated by *Phragmites australis*).

At FO site the depth profiles of OM concentration show no clear trend, with mean OM contents in 1 m top soil ranging between 14 and 24%, and some peaks at different depths with values higher than 40% (Fig. 5.4). In contrast, OMD displays a much more constant trend without the presence of peaks, as OM increase is caused by low density layers. Roots and plant debris are generally abundant all along the profiles (Fig. 5.4 - insert 4). At the marsh edge plant fragments decreased downward degrading toward a layer where dark laminae rich in organic debris are visible (Fig. 5.4 - insert 5). Deeper deposits are characterized by a lighter colour, dark plant debris and wood fragments (Fig. 5.4 - inserts 6 and 7), overlaying in the inner marsh a brownish organic-rich layer. At the bottom of the innermost core, some reed fragments are visible overlaying a layer of millimetric, whitish, horizontal laminae (Fig. 5.4 - insert 8). Stratigraphic interpretation of FO observation suggests an articulated morphology resulting from dynamic evolution of micro environments ranging from intertidal and subtidal zones or ponds and pioneer salt marshes changing in space and time.

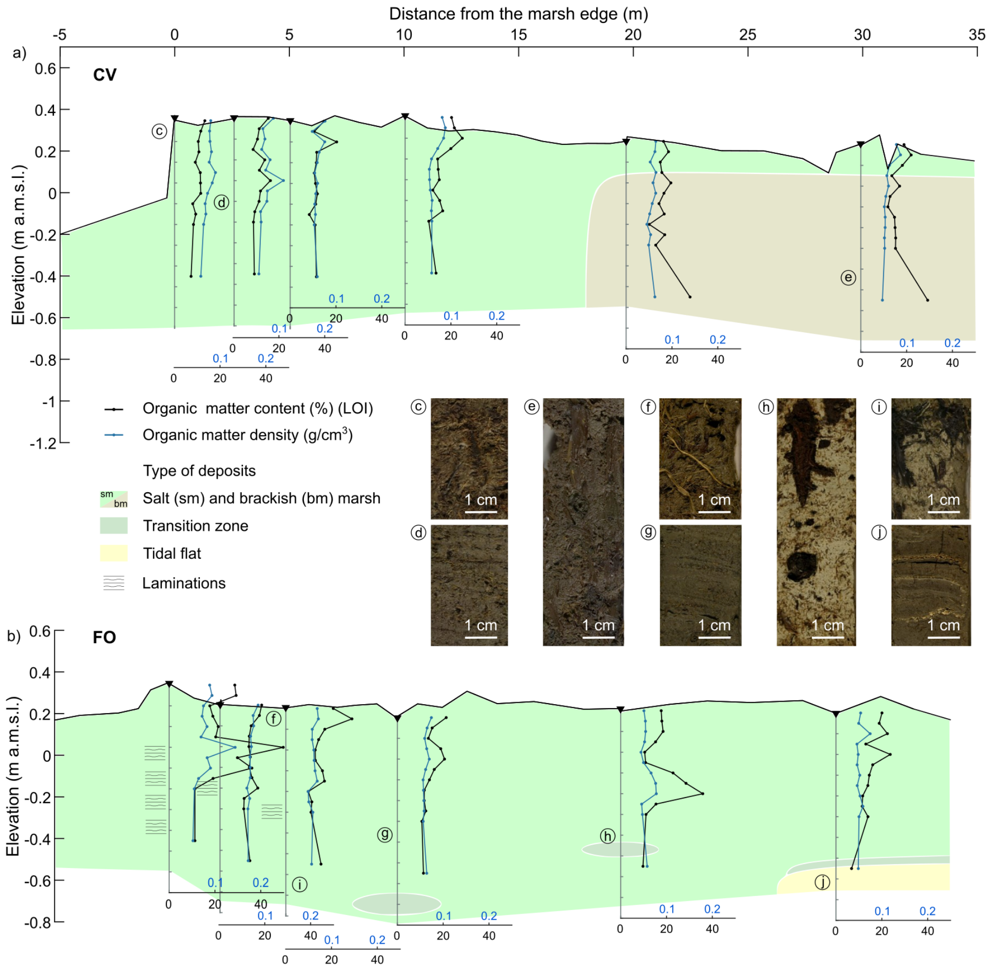

Figure 5.4: **Representation of transect vertical sections, OM content and sedimentological interpretation: CV and FO**. Along the surface elevation profile, at each core site (from 1 to 6 respectively at 0, 2.5, 5, 10, 20 and 30 m from the marsh edge) depth-distribution of organic matter content (LOI - % weight – black scale from 0 to 50) and organic matter density ($g\,cm^{-3}$ – blue scale from 0 to 0.25) are depicted. An interpretation of the study transect depositional environments is schematically illustrated by polygons of different colours on the basis of the sedimentological features and the spatial distribution of the different sedimentary deposits differentiated. Inserts (c-j) are pictures of core details and their position is indicated on transect section representations: c and d – plant debris and organic-rich laminae in salt-marsh deposits, e – reed fragments, f - roots and plant debris in salt-marsh deposits, g – plant-debris-rich laminae in pond deposits, h – *Limonium narbonense* root in life position, i – dark plant debris, j – millimetric, whitish, horizontal laminae.

At the CO site, mean organic matter in 1 m top soil ranges between 6 and 7% (Fig. 5.5). OM concentration generally shows a decrease with depth. The decrease is more pronounced toward the inner marsh, whereas the marsh edge displays quite irregular depth profiles with some peaks in OM concentration at the depth of 30 cm up to 25%. OMD distribution generally follows OM patterns. Top-20-cm deposits are characterized by sparse roots with rare laminations rich in plant debris. Furthermore, numerous shell fragments are present (Fig. 5.5 - insert 1). Between the depths of 30 and 40 cm along the entire transect, peculiar layers of plant debris which look like seagrass leaves alternate with sediment matrix (Fig. 5.5 - inserts 1 and 2). Their thickness varies between few millimeters and few centimeters and seagrass-leave remains sometimes appear regularly piled up and sometimes irregularly heaped up. Underlying deposits are characterized by abundant clear submillimetric to millimetric sandy laminations, often showing deformed structures (Fig. 5.5 - insert 4). The presence of an underlying thick sandy interval could explain the scarce penetration depth of the corer. Yellowish oxidized areas are distributed along all depths and all cores, being evidence of periodic subaerial exposure. The CO site is characterized by high energy phenomena, coherently with its exposure to energetic Bora wind-waves generated over the wide subtidal flat that occupies the central-southern Venice Lagoon. Localized shell concentrations in salt-marsh deposits are likely the result of sediment transport over the marsh platform during storm events. Furthermore, buried seagrass layers may be the remains of beach-cast seagrass wracks, abundant at this site, which are periodically deposited above tidal flat or pioneer salt marsh during storms and subsequently covered by sediment supplied. Organic-rich seagrass deposits suggest that in some cases allochthonous organic sources assume an important role in SOM distribution. Current marsh underlying layer represents tidal flat deposits bearing the marks of wind wave action, which promoted mud resuspension, thus causing the concentration of coarser deposits (i.e. sandy layers).

At the VB site observed mean organic matter in 1 m top soil displayed some variability ranging between 4% at the marsh edge and 17% in the inner marsh (Fig. 5.5). OM concentration, as well as OMD, generally shows a decrease with depth, following quite irregular depth profiles, although in some cases the 75-cm-depth sample displayed an increasing value. Surface deposits are permeated by dense root networks down to 30-40 cm depth. Plant debris (Fig. 5.5 - insert 5) progressively decrease downward, giving way to sandy laminated layers (Fig. 5.5 - insert 6). Underlying, darker deposits are visible with plant debris at different depths (Fig. 5.5 - insert 7) and reed fragments toward the margin cores (Fig. 5.5 - insert 8). Stratigraphic observations suggested the identification of 30-50 cm thick salt-marsh deposits grading downward into underlying tidal flat deposits, in turn overlying buried marsh deposits whose geometries were difficult to follow.

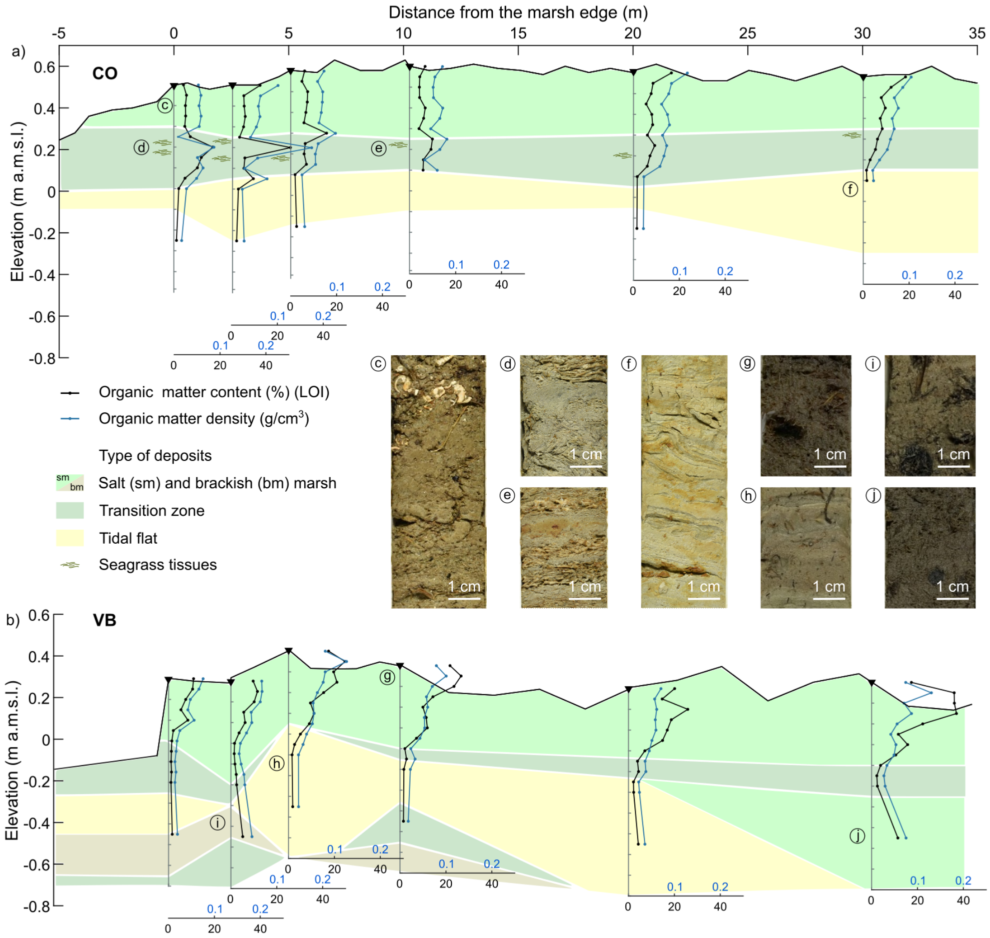

Figure 5.5: **Representation of transect vertical sections, OM content and sedimentological interpretation: CO and VB**. Along the surface elevation profile, at each core site (from 1 to 6 respectively at 0, 2.5, 5, 10, 20 and 30 m from the marsh edge) depth-distribution of organic matter content (LOI - % weight – black scale from 0 to 50) and organic matter density (g cm^{-3} – blue scale from 0 to 0.25) are depicted. An interpretation of the study transect depositional environments is schematically illustrated by polygons of different colours on the basis of the sedimentological features and the spatial distribution of the different sedimentary deposits differentiated. Inserts (c-j) are pictures of core details and their position is indicated on transect section representations: c– shell fragments and plant debris in surface salt-marsh deposits, d and e – seagrass leave layers, f – submillimetric to millimetric sandy laminations, with small scale load structures (flames structures), g – plant debris in salt-marsh deposits, h – sandy laminae in tidal flat deposits, i – dark plant debris, j – reed fragments.

5.4.3 Grain size distribution

Inorganic sediment fraction in 1 m marsh soils shows a median grain size (D50) ranging between 5 µm and 54 µm, with a mean value of 15 µm (Fig. 5.6). Finer median grain size values are found at sites located on the landward side of the lagoon (i.e. PA, CA and MI), which are characterized by higher percentages of clay (20-30%). Whereas, coarser median grain size values are found in SF, SA, SE, VB and CO sites (average D50 value between 17 and 20 µm). Furthermore, at SF, SA and SE sites a clear increase in grain size was observed below 30-40 cm depth with sand fraction reaching 20%. This pattern is consistent with the general grain-size gradient observed in the Venice lagoon, reflecting the decreasing hydrodynamic energy conditions from the inlets to the landward shore, with sandy sediment delivery from the sea and fine sediment from the mainland (Zonta et al., 2018). Furthermore, coarser sediments found below salt-marsh deposits at SE, SF and SA represent the legacy of past proximity of these sites to ancient sandy barriers, which knew a seaward migration during last about 1000 years due to the historical evolution of Lido inlet position and morphology (Bondesan and Meneghel, 2004; Favero and Serandrei-Barbero, 1981).

As to the variability within study areas, Chapter 4 describes the distribution of the D50 in surface soil layer along the transects. Coarser grains were observed along the marsh edges at SF, SA and VB, whereas at CA and CO coarser particles were observed in the central part of the transects. The SE transect shows slightly coarsening sediments toward the inner marsh, bordered by a tidal flat.

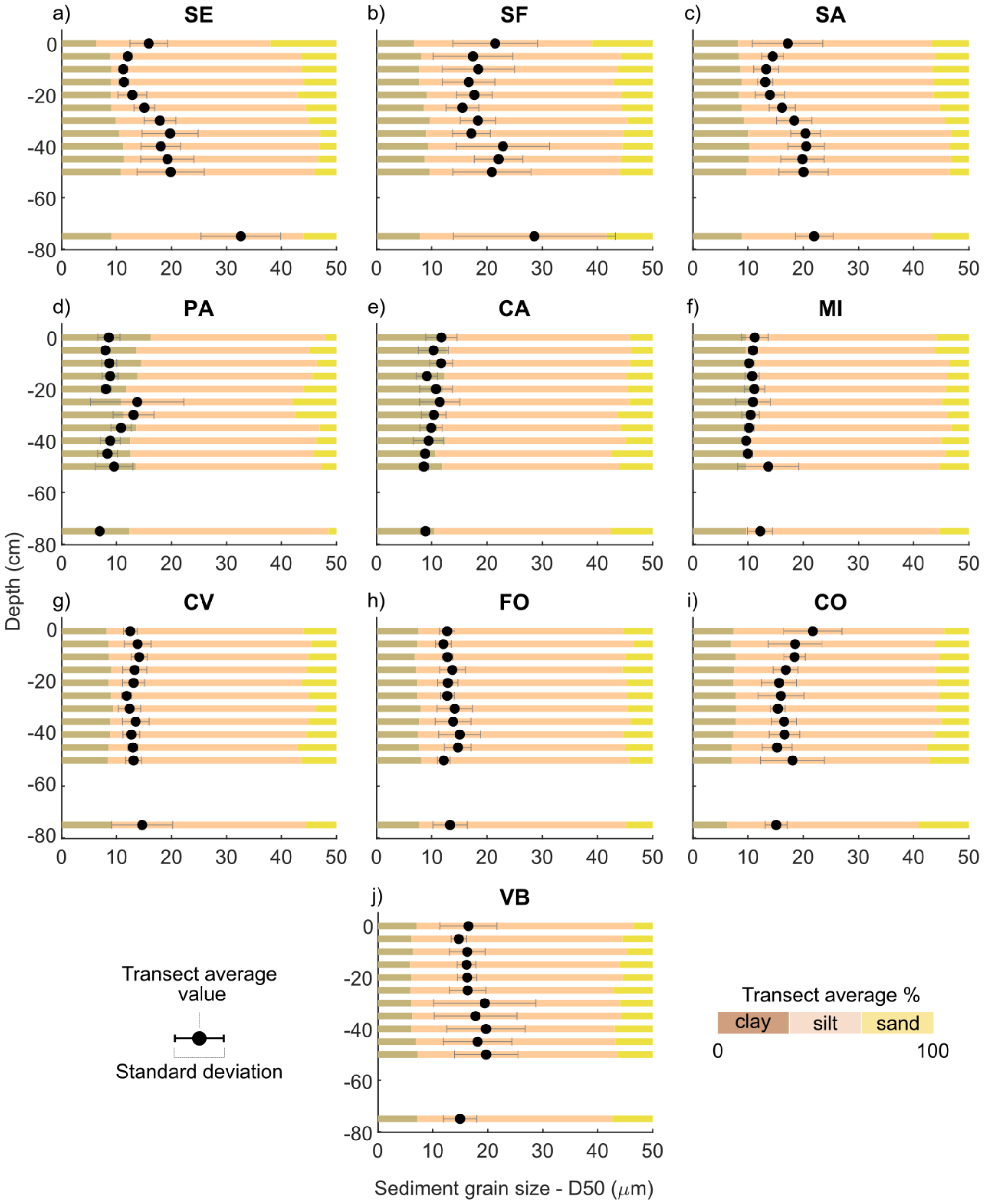

Figure 5.6: **Depth-distribution of sediment grain size**: average of median grain size (D50 - µm) with respective standard deviation and sand-silt-clay percentage at different depths at each of the 10 sites considered.

5.4.4 Soil characteristic variations in different depositional environments

As to the variability of marsh soil characteristics in different depositional environments, Kruskal-Wallis test indicated that there was a significant difference between OM content within the different types of deposits (p-value $= 4.6249 \times 10^{-65}$), with marsh deposits showing significantly higher OM content than tidal-flat and transitional deposits (Fig. 5.7a). Furthermore, brackish-marsh deposits revealed a significantly higher OM content than salt-marsh deposits. Dry Bulk Density was observed to be higher in tidal flat and transition zone deposits than in marsh deposits (Fig. 5.7b) (p-value $= 3.3731 \times 10^{-38}$). Despite this, OM density, resulting from the product of OM content and DBD, is still significantly higher in marsh deposits than in tidal-flat and transitional deposits (Fig. 5.7c) (p-value $= 3.4290 \times 10^{-47}$). For median grain size, the same behaviour of DBD was observed (p-value $= 3.8642 \times 10^{-35}$), with tidal-flat and transition zone deposits showing coarser sediments than marsh deposits, and brackish-marsh deposits being characterised by finer sediments with respect to salt-marsh deposits (Fig. 5.7d).

Our results attribute to tidal marsh environments higher C storage potential (directly depending on OM density) with respect to transition zones and tidal flats, with 2-fold higher median OM density. It is clearly impossible to recognise whether analysed tidal-flat deposits belong to vegetated tidal flats, however our outcomes are consistent with previous findings which report lower organic content for both bare tidal flats (Brevik and Homburg, 2004; Lee et al., 2021; Mao et al., 2021) and seagrasses (Duarte et al., 2013) with respect to salt marshes.

Furthermore, tidal marsh deposits proving to be influenced by freshwater inputs (i.e. classified as brackish marsh on the basis of *Phragmithes australis* dominance) showed higher OM content with respect to salt marshes, although OM density is not significantly different, likely due to the low density of most organic-rich deposits. However, previous findings suggest that fluvially-influenced tidal marshes display higher OC stocks (e.g. Kelleway et al., 2016; Macreadie et al., 2017; Saintilan et al., 2013). Low density of organic rich deposit may importantly influence C storage potential of wetland environments, nevertheless carbon accumulation rates strongly depends also on the time of development of different deposits. Therefore, we underline the importance of the availability of sediment accretion rate models to improve C accumulation rate assessments.

Grain size difference among type of deposits, with coarser sediments in tidal-flat and transition-zone deposits and finer sediments in brackish marsh deposits, are consistent with hydrodynamic properties expected for these depositional environments. In addition, our findings suggest 2-fold lower median DBD value for tidal marsh deposits with respect to tidal flat and transition zone deposits, consistently with OM content and grain size patterns, as soil density was observed to increase with increasing grain size and decrease with increasing OM content (Holmquist et al., 2018; Morris et al., 2016; Tanveera et al., 2016).

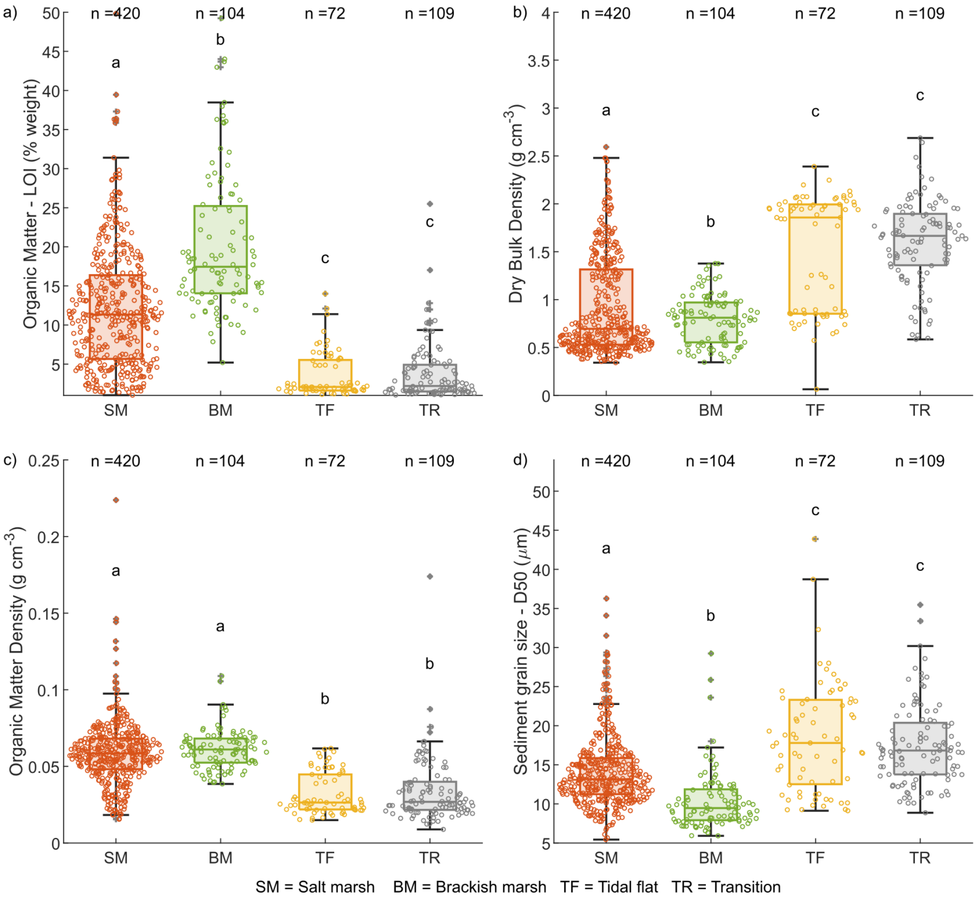

Figure 5.7: **Sediment characteristic variations in different depositional environments**: organic matter content (LOI - % weight) (a), Dry Bulk Density ($\mathrm{g\,cm^{-3}}$) (b), organic matter density ($\mathrm{g\,cm^{-3}}$) (c), grain size distribution (D50 - µm) (d). Box plots show median and quartiles, swarm plots show single values. Different letters above the box plots indicate significant difference on the basis of Kruskal-Wallis test and post hoc multiple comparison test.

5.4.5 Relationship between OM content and sediment grain size

Considering all our data, SOM content showed a significant relationship with sediment median grain size (D50) (Kendall's tau test, τ = -0.3843 p-value = 1.6998×10^{-53}), with organic content decreasing when sediments become coarser (Fig. 5.8). There are multiple mechanisms which may explain the negative relationship between SOM content and sediment grain size (Kelleway et al., 2016).

First, fine sediments have been recognised for their greater potential for protection of C through organic-mineral interaction and micro- or macro-aggregates due to their greater specific surface area than coarser sediments and cation exchange capacity of fine-grained minerals (Bader et al., 1960; Baldock and Skjemstad, 2000; De Gryze et al., 2006). Furthermore, enhanced C preservation would be expected in fine sediments through a reduced oxygen exchange due to lower porosity and drainage capacity, promoting anoxic conditions and consequently lower decomposition rates (Arnarson and Keil, 2007; Hartnett et al., 1998). Moreover, at the catchment scale, coarser sediments are more easily observed at the seaward boundary of the lagoon and finer sediments at the landward boundary, and at the same time higher organic content were observed at fluvially influenced sites with respect to marine influenced sites, likely due to the interplay between physical and biological factors (Van De Broek et al., 2016; Kelleway et al., 2016; Macreadie et al., 2017).

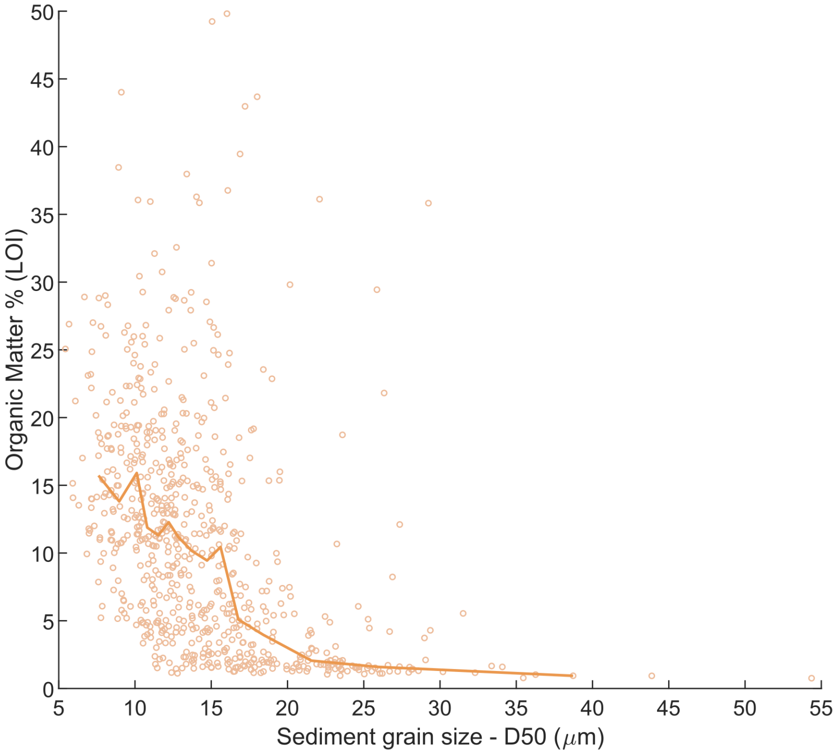

Figure 5.8: **Organic matter content as a function of median sediment grain size**: single values as orange circles and binned scatterplot (orange lines).

5.4.6 Relationship between OM content and DBD

As expected, a clear relationship was observed between SOM content and DBD, with soil density rapidly decreasing with increasing organic content (Fig. 5.9). We tested an ideal mixing model against our data, accordingly to Morris et al. (2016). The model assumes that bulk volume of a soil approximates to the summed self-packing volumes of the organic and mineral components, represented by the coefficients of the equation (Morris et al., 2016):

$$DBD = \frac{1}{\frac{LOI}{k_1} + \frac{(1-LOI)}{k_2}} \tag{5.2}$$

where DBD is the sediment Dry Bulk Density, LOI is the OM content resulting from LOI procedure, k_1 and k_2 are two coefficients. The fit over all our samples gave k_1 and k_2 coefficients of $0.014\,\mathrm{g\,cm^{-3}}$ and $2.28\,\mathrm{g\,cm^{-3}}$, respectively. Our results are consistent with those from Morris et al. (2016), also considering that our data do not cover the full spectrum of DBD and LOI values. In addition, we highlight that a non-negligible source of variability derives from the poor accuracy of wet sample volume estimates. For instance, we observed that PA samples evidently deviate from the fitting curve, likely due to the difficulties encountered when estimating the volume of irregular plant-debris-rich samples. Instead, sample depth appears not to influence the relationship between SOM content and DBD.

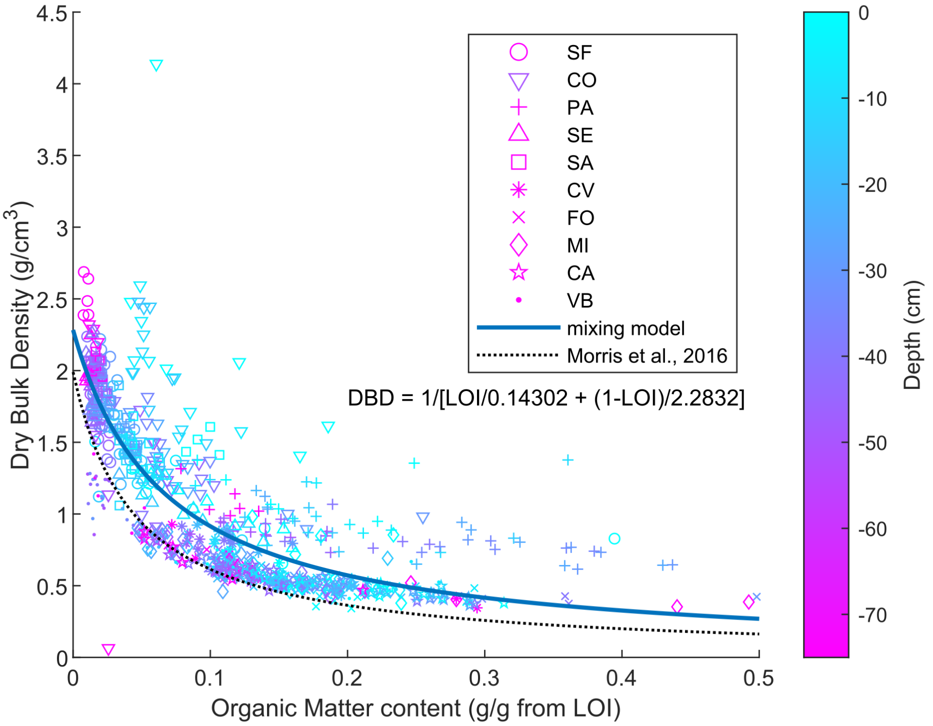

Figure 5.9: **Relationship between soil density and organic content**. The relationship between soil Dry Bulk Density, determined through the ratio between dry weight and estimated wet volume, and soil organic matter percentage measured through loss on ignition (LOI) in marsh soil samples (n = 706) and best fit of the ideal mixing model to our data following Morris et al. (2016).

5.4.7 Soil Organic Matter modelling with depth

Exponential function (Eq. 5.2) was fitted to SOM concentrations, in terms of percentage and density, of current salt-marsh deposits in each soil profile down to 1-m depth. The fitted exponential functions showed highly variable R^2 values ranging between 0.011 and 0.94 (Fig. 5.10 and Fig. 5.11). SE, VB and SF showed the highest mean R^2 values, 0.85, 0.81 and 0.75, respectively. With few exceptions, the exponential function poorly represents SOM depth-distribution in our study case, likely due to the presence of organic content peaks at different depths attributable to changing environmental conditions. Even excluding major changes producing a shift in depositional environment (we only considered current marsh deposits), drivers of OM accumulation (e.g. sediment supply, allochthonous organic inputs and vegetation characteristics) vary in a way that is difficult to predict. We argue that, besides decomposition processes, other mechanisms may affect OC content in salt-marsh deposits including changes in sedimentation rate during ecosystem development and variations in organic inputs (Mueller et al., 2019). Sedimentation rates can be higher during early ecosystem development and successively slow down, reflected in a decreasing dilution of autochthonous OC with mineral sediment up-ward in the core (Mueller et al., 2019). However, sedimentation rates may change differently due to varying fluvial discharge or subsidence rates, as it happened in the southern lagoon (Roner et al., 2017, 2021). Changes in organic inputs are attributable to shifts in plant species composition as well as allochthonous organic inputs, affecting both the amount of organic contribution and their resistance to decomposition. Indeed, Van de Broek et al., 2018 suggest that stabilized allochthonous OC is a main component of SOC that is effectively preserved in deeper sediments. This is likely the case, for instance, of the 30-cm-depth organic content peaks found at CO site, which we attribute to seagrass wracks deposition (Fig. 5.5).

Thus, our results suggest that caution is needed when using vertical distribution modelling for SOM prediction at unsampled soil depths, as unknown past conditions may lead to unreliable SOC stock estimates.

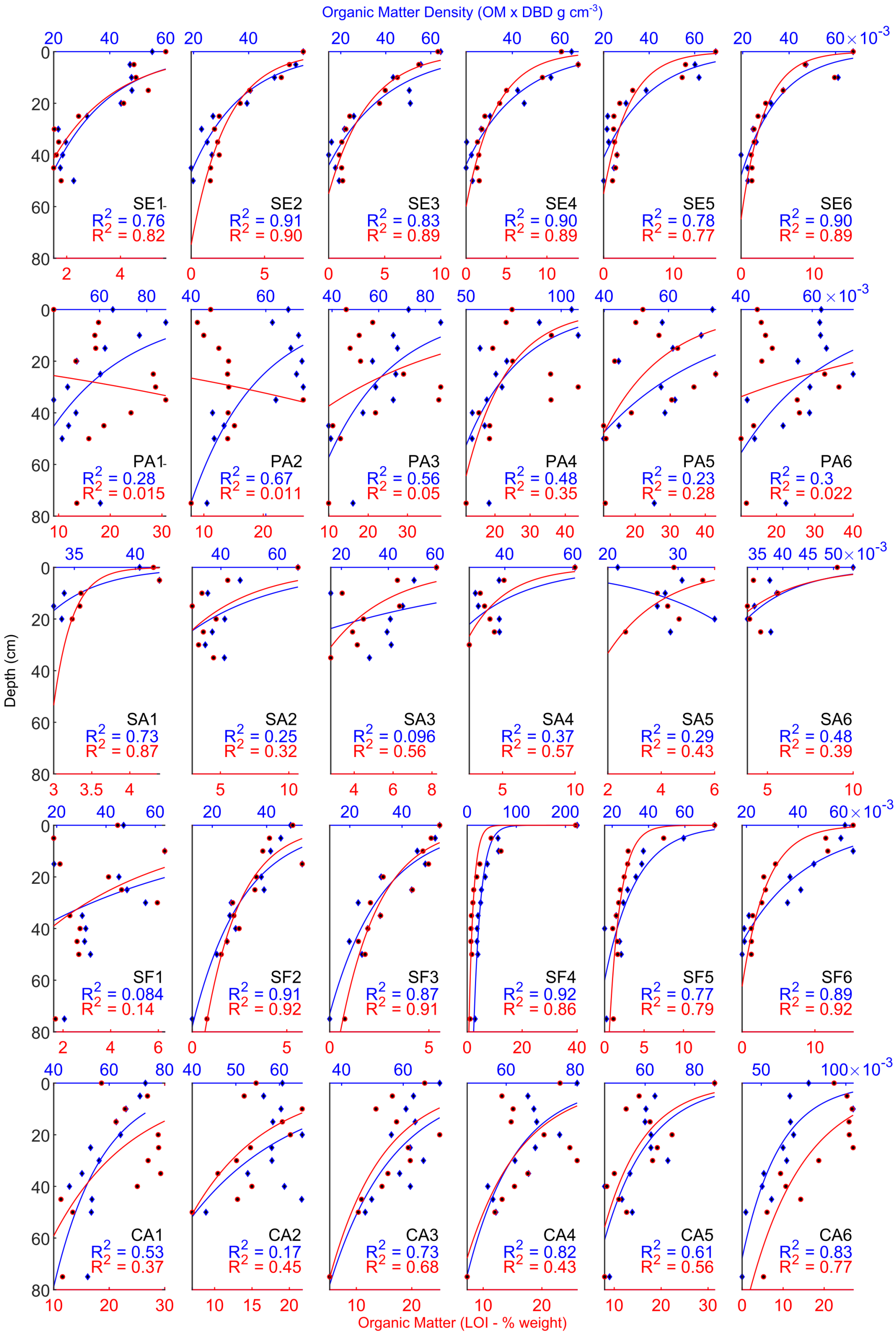

Figure 5.10: **Exponential fitting of OM depth-distribution (northern lagoon)**. Fitting curves of vertical distribution of organic matter content (LOI - % weight) (red) and organic matter density ($\mathrm{g\,cm^{-3}}$) (blue) in current salt marsh deposits using an exponential function (LOI = a exp (-bD)) at SE, SF, SA, PA, CA. Current marsh deposits were considered, including related transition zone, if present.

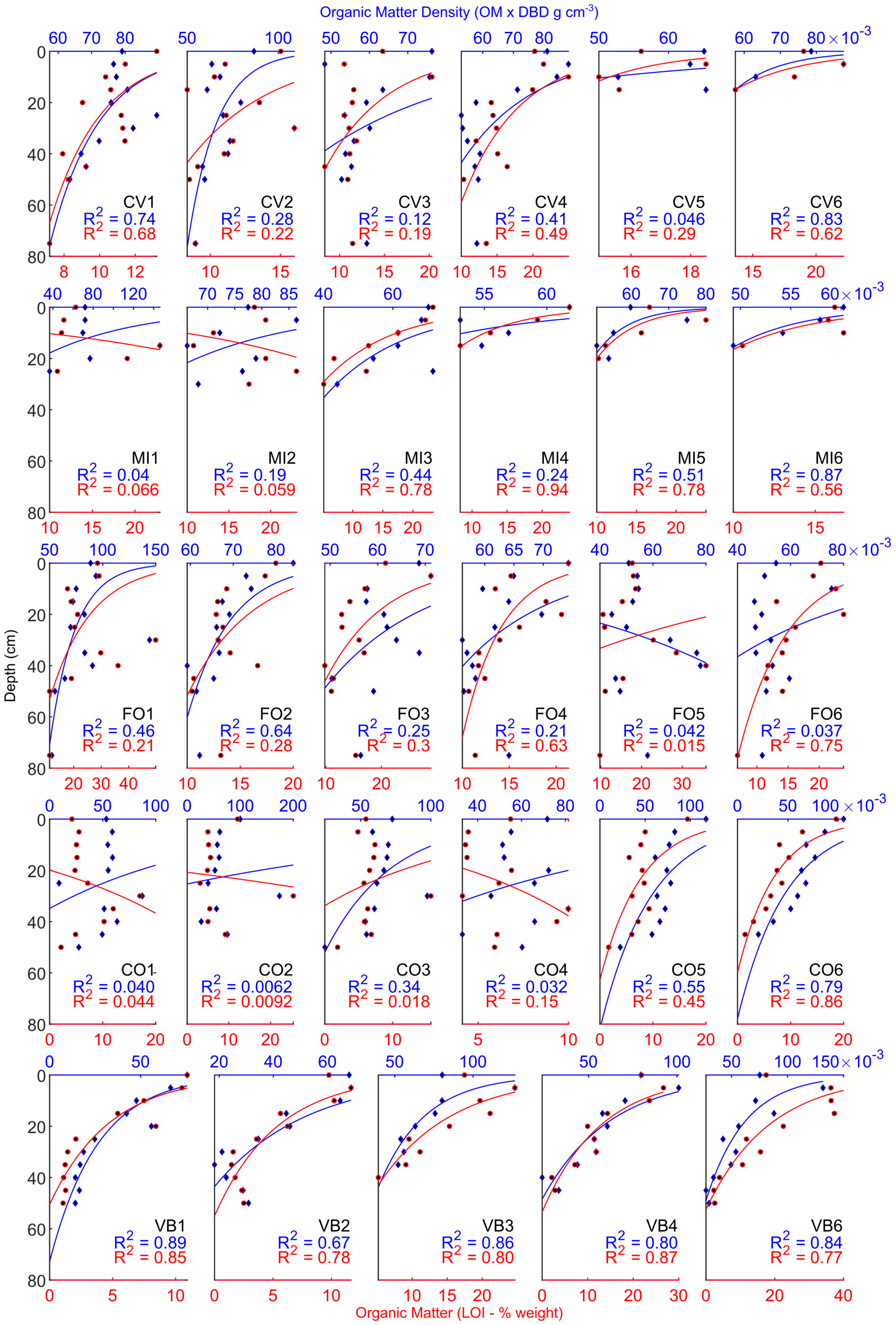

Figure 5.11: **Exponential fitting of OM depth-distribution (southern lagoon)**. Fitting curves of vertical distribution of organic matter content (LOI - % weight) (red) and organic matter density (g cm^{-3}) (blue) in current salt marsh deposits using an exponential function (LOI = a exp (-bD)) at MI, CV, FO, CO, VB, including related transition zone, if present.

5.5 Conclusions

We analysed OM spatial and vertical patterns in microtidal salt marsh soils with reference to environmental and depositional conditions as currently observed and testified by recent sedimentary successions. Higher OM contents were observed at sites located closer to the mainland and marsh deposits affected by current or past freshwater inputs. This outcome is in agreement with observations in other studies (e.g. Van De Broek et al., 2016; Gorham et al., 2021; Hansen et al., 2017; Omengo et al., 2016) which attribute OM content increase toward the mainland to the supply of already stabilized organic suspended particles from fluvial inputs and changing vegetation characteristics. In fact, higher OM contents were observed in current and past salt-marsh deposits dominated by *Phragmites australis*, a near freshwater plant which produces a high belowground biomass characterized by high resistance to decomposition (Moore et al., 2012; Scarton et al., 2002). Besides autochthonous biomass, allochthonous organic inputs, also linked to episodic events, proved to be in some cases a determinant factor affecting SOM distributions. Furthermore, sediment grain size is importantly related to SOM variations, as it is in turn correlated to geomorphic settings and has the potential to affect OM preservation conditions (Kelleway et al., 2016). We confirm previously observed relationships between SOM content and soil density, supporting OM role in salt-marsh vertical accretion. Our results suggest that changes in the depositional environment are of primary importance in determining OM depth distribution and caution is needed in SOM prediction at unsampled soil depths through vertical distribution modelling. We argue that models predicting carbon budget in wetland environments need to account for the variability of sediment supply, organic inputs and conservation conditions in their prediction scenarios, considering the effect of resulting soil density and irregular sedimentation rates. The outcomes of our study highlight the high as well as variable potential of salt marshes for C storage in intertidal environments and provide further insights into SOM dynamics and their drivers, to the benefits of coastal management strategies.

6

SALT-MARSH BLUE CARBON ASSESSMENT

This chapter is a manuscript ready to be submitted for publication under the title “Blue Carbon assessment in the salt marshes of the Venice lagoon (Italy): dimensions, variability and storm-surge barrier influence”. A.P., D.T., A.D. and M.M. designed the study. A.P., D.T., A.D. and M.M. developed the methodology. A.P. and D.T. collected the data and performed laboratory analyses. Z.M. and P.M. provided the instrumentation and tools for and P.M. performed the Elemental Analysis. A.P. and D.T. were responsible for data analysis and interpretation with the supervision of A.D., M.M. and M.G. All the authors discussed the data and agreed on their interpretation. A.P. wrote the original draft. A.D. and D.T. provided comments and suggestions to improve the original draft. All the co-authors contributed to the final polishing of the manuscript.

Blue Carbon assessment in the salt marshes of the Venice lagoon (Italy): dimensions, variability and storm-surge barrier influence

A. Puppin[1], D. Tognin[2], M. Paccagnella[3], M. Zancato[3], M. Ghinassi[1], M. Marani[2], D'Alpaos[1]

[1]Department of Geosciences, University of Padua, Padua, Italy
[2]Department of Civil, Environmental and Architectural Engineering, University of Padua, Padua, Italy
[3]Department of Pharmaceutical and Pharmacological Sciences, University of Padova, Italy

6.1 Abstract

Salt marshes are intertidal coastal ecosystems characterized by mostly herbaceous halophytic vegetation and shaped by complex feedbacks between hydrodynamic, morphological, and biological processes. These crucial yet endangered environments provide a diverse range of ecosystem services but are severely exposed to climate change and human pressure. The importance of salt marshes as 'blue carbon' (C) sinks, deriving from their primary production coupled with rapid surface accretion, has been increasingly recognized within the framework of climate mitigation strategies. However, large knowledge gaps and uncertainties remain in salt-marsh carbon (C) stock and sequestration estimation. In order to provide further knowledge in salt-marsh carbon assessment and investigate marsh C pool response to management actions under different scenarios, we analysed organic matter content in salt-marsh soils of the Venice Lagoon (Italy) from 60 sediment cores to the depth of 1 m and estimated carbon stock and accumulation rate in different areas. OC stocks in the surface 1 m were highly variable in different marshes averaging $17{,}108 \pm 5757$ ton OC km^{-2} (range $9800 - 24{,}700$ ton OC km^{-2}). Observed variations in carbon stock, determined by organic inputs and preservation conditions, are affected by vegetation characteristics as well as sedimentary conditions, with past and present fluvial inputs playing a crucial role. The es-

timated OC accumulation rate was $85 \pm 25\,\mathrm{ton\,OC\,km^{-2}\,yr^{-1}}$, confirming CO_2 sequestration potential of tidal environments, which, however, resulted to be crucially affected by marsh accretion rates and their human-induced variations.

6.2 Introduction

Vegetated coastal ecosystems, including salt marshes, mangrove forests and seagrass meadows, have been termed “Blue Carbon ecosystems” for their increasingly recognised carbon (C) sequestration and storage potential (Chmura et al., 2003; Duarte et al., 2005; Macreadie et al., 2019; McLeod et al., 2011; Nellemann et al., 2009). Researchers have estimated that the C burial rate per unit area in these ecosystems may be exceptionally high, exceeding that of terrestrial forests by 1–2 orders of magnitude (Chmura et al., 2003; Duarte et al., 2005; Macreadie et al., 2019; McLeod et al., 2011). In light of this, tidal wetlands may provide a considerable contribution to global long-term C sequestration, despite the limited areal extension (Chmura et al., 2003; Duarte et al., 2005; Macreadie et al., 2019; McLeod et al., 2011). Additionally, tidal wetlands support many other ecosystem services, whose high value is often difficult to estimate (Barbier et al., 2011; Costanza et al., 1997; D’Alpaos and D’Alpaos, 2021; de Groot et al., 2012). Tidal wetlands enhance biodiversity (Lefeuvre et al., 2003), protect coastal regions against erosion and storms (Allen, 2000; Möller et al., 2014; Temmerman et al., 2013), help maintaining commercial fisheries (Boesch and Turner, 1984), filter nutrients and pollutants (Costanza et al., 1997), support tourism and recreation activities (Barbier et al., 2011).

The intertidal landscape of low-energy temperate coasts is characterized by salt marshes, which are colonized by grass and shrub halophytic vegetation adapted to regular or occasional submersion (Adam, 1990; Allen and Pye, 1992; Perillo et al., 2009). Marshes are intrinsically dynamic environments and their evolution is affected by complex feedbacks between hydrodynamic, morphological, and biological processes, which have allowed them to build up balancing sea-level rise over thousands of years (Allen, 2000; D’Alpaos et al., 2007; Fagherazzi et al., 2012; Marani et al., 2007; Mudd et al., 2009). Beyond the CO_2 removed from the atmosphere through photosynthesis performed by marsh vegetation, soil stores 90% of carbon stock in salt marshes (Pendleton et al., 2012; Serrano et al., 2019). Plant tissues, litter and organic matter are buried into the soil by mineral sediment settling on the marsh, thus concurring also to building up balancing sea-level rise (Allen, 2000; D'Alpaos et al., 2007; Fagherazzi et al., 2012; Mudd et al., 2009). Moreover, by inhibiting microbial aerobic activity and slowing down decomposition (Keuskamp et al., 2013; Kirwan et al., 2014; Morris et al., 2016; Mueller et al., 2018; Yousefi Lalimi et al., 2018), tidal conditions further foster Soil Organic Carbon (SOC) preservation, thus locking away carbon from the atmosphere over centennial to millennial time scales (Duarte et al., 2005; Perillo et al., 2009).

However, climate change and anthropogenic disturbances dramatically alter salt-marsh biomorphodynamic equilibrium, jeopardizing their survival (Barbier et al., 2011; Duarte, 2009; Kirwan and Megonigal, 2013; McLeod et al., 2011; Valiela et al., 2001), therefore potentially affecting also marsh carbon sequestration potential and even shifting marshes from being net sinks to sources of carbon (McLeod et al., 2011; Pendleton et al., 2012). Global warming, increased carbon dioxide concentration and sea-level rise have the potential to alter biomass production, decomposition and surface accretion (Perillo et al., 2009; Reents et al., 2021). Human activities directly and indirectly interfere with marsh dynamics through land use changes and alterations of nutrient inputs, sediment dynamics and subsidence rates (Kirwan and Megonigal, 2013). Moreover, to reduce flooding risk, coastal communities are increasingly adopting coastal flooding protection infrastructures, which, however, may change sediment transport in coastal wetlands and reduce salt-marsh sediment supply, thus further questioning their future (Tognin et al., 2022). For example, the sediment supply on the salt marshes in the Venice Lagoon (Italy) was proved to be importantly reduced by the operation of the recently-activated storm-surge barrier, known as Mo.S.E. system, designed to protect the city of Venice from flooding (Tognin et al., 2021).

In light of the increasing interest to include blue C ecosystems as greenhouse-gas-offset activities in climate policy and considering the high uncertainty of existing blue C estimates (e.g., Chmura et al., 2003; Macreadie et al., 2017; Sifleet et al., 2011) there is a need to quantify the magnitude of C stocks and fluxes in salt-marsh ecosystems. In addition, it is crucial to estimate the potential spatial variability of C stocks and fluxes, especially in the sediments where the majority of the long-term C pool persists, and to understand how marshes will be affected by management actions under different scenarios.

Here we estimate the C storage and sequestration potential of the salt marshes of the Venice lagoon and the impact of flood regulation by means of the recently activated storm-surge barrier on C accumulation dynamics. Toward this goal, we analysed organic matter and organic carbon content in salt-marsh soils in 720 samples from 60 sediment cores to the depth of 1 m collected in different areas of the Venice lagoon, therefore estimating carbon stocks and carbon accumulation rates at the whole system scale, together with their spatial variability. Besides providing important knowledge for regional and national carbon assessments, which foster the inclusion of coastal wetland carbon sinks in greenhouse gases (GHG) inventories and climate mitigation strategies, our analyses allow us to estimate the possible reduction in salt-marsh carbon sequestration potential driven by anthropogenic disturbances, such as the reduction of sediment supply and accretion rates induced by flood-regulation strategies. Thus, the outcome of the present study, paired with the assessment of other ecosystem services, can inform territorial management decision makers, by enabling the identification of strategies for optimizing protection and restoration efforts. Furthermore, building interest in the recently-recognised value of tidal marshes in carbon offset markets and nature-based climate mitigation may be an opportunity to encourage their protection and restoration, at the same time contributing to the maintenance of a large number of naturally co-occurring ecosystem services.

6.3 Materials and methods

Six uncompacted cores were collected in each of the 10 selected salt marshes (Fig. 6.1a), for a total of 60 cores. Marshes were selected in the whole Venice Lagoon, in order to provide a spatially explicit assessment of C stock and sequestration rates. Core depth of 1 m was selected as generally agreed to provide an effective estimate of coastal soil carbon stock in temperate regions (Howard et al., 2014). For each core, soil samples were taken at 12 depths (0, 5, 10, 15, 20, 25, 30, 35, 40, 45, 50, 75 cm from the surface, see Howard et al. (2014)) and subsamples were prepared for different analyses, including soil density, organic matter and carbon content.

Samples were dried at 60 °C until a constant weight was achieved. The difference in weight between wet and dry samples was used to estimate the water content. Percent organic matter of each sample was determined through Loss On Ignition (LOI) of ground samples (375 °C for 16 h (Ball, 1964; Frangipane et al., 2009; Roner et al., 2016)). Water content and organic matter content were used to estimate the dry bulk density (DBD [ML^{-3}]) (Kolker et al., 2009).

Being a relatively cheap and rapid method, LOI has been widely used to measure organic matter content in marsh soil (Craft et al., 1991; Howard et al., 2014; Ouyang and Lee, 2020). However, LOI does not provide a direct measure of organic C. Empirical relationships between organic matter from LOI and organic C have been proposed for different wetland systems worldwide (Craft et al., 1991; Holmquist et al., 2018; Howard et al., 2014; Ouyang and Lee, 2020). Nevertheless, caution should be used in the application of these relationships to systems different from those for which they were calibrated. Site-specific relationship might provide a more accurate estimate of organic C content. For this reason, we selected a subset of 102 representative samples to directly determine C content using an Elemental Analyser (varioMicro Cube V4.0.10 Elementar Analysensysteme GmbH). In order to correct organic carbon measurements performed through elemental analysis for the inorganic carbon content, ashed subsamples (previously obtained from the LOI procedure) were also analysed. This procedure allowed us to determine the remaining inorganic carbon in each sample, which was then subtracted from the total carbon measurements. Directly determined C content data (from elemental analysis) were used to fit a regression equation and convert soil organic matter (from LOI) into organic C, following Craft et al. (1991) (Fig. 6.2).

Soil carbon stocks [ML^{-2}] in 1 m soil depth were calculated based on Howard et al., 2014 summing the carbon content in each soil interval along the core:

$$C_{\text{stock}} = \sum SCD_i \times l_i \tag{6.1}$$

$$SCD = OC_i \times DBD_i \tag{6.2}$$

where SCD_i is Soil Carbon Density [ML^{-3}], l_i is the soil thickness [L], OC_i is the organic carbon content and DBD_i is Dry Bulk Density [ML^{-3}] of the i-th interval. Carbon stocks within the cores collected in the same area were averaged and converted to ton OC km^{-2} to estimate total C stock down to 1 m depth for each location.

Carbon accumulation rates were estimated by multiplying the average soil carbon density in a reference interval of 5 cm (average value for each location) by salt-marsh accretion rates derived from direct measurements based on marker horizons and from literature (Day et al., 1999; Roner et al., 2017; Saintilan et al., 2013; Tognin et al., 2021) over a $2-20$ yr period (Section 6.5). Estimates of carbon accumulation rates were used to assess CO_2 sequestration by salt-marsh soils of the Venice lagoon, converting the mass of carbon into CO_2 equivalent (CO_2e) by multiplying by 44/12, i.e. by the ratio between the weight of carbon dioxide (44 atomic mass units) and the atomic weight of carbon (12 atomic mass units).

6.4 Results and discussion

6.4.1 OM content in the salt marshes of Venice lagoon

Organic matter content of marsh soils ranges between 1 and 50%, with remarkable variations both among and within study areas (Fig. 6.1a). Vertical trends of organic matter content showed variable patterns at different sites, as stratigraphy retains the signatures of past depositional and environmental conditions, which evolved differently in different areas of the lagoon, as shown in detail in Chapter 5.

At the SE, SF and SA salt marshes (Fig. 6.1b, 6.1c, 6.1d), which are adjacent to large tidal channels departing from the Lido inlet, organic carbon content rapidly decreased with depth, because of organic matter decomposition (Van De Broek et al., 2016; Zhou et al., 2006) and the shifting from salt-marsh to tidal-flat deposits in the deepest layers. Sites at the landward side of the lagoon and in the southern lagoon (e.g., PA, CA, MI, CV, CV, FO, VB, Fig. 6.1e-6.1k) showed irregular distributions of carbon content with depth, with organic-rich levels at different depths. The highest carbon contents were observed in the PA salt marsh (Fig. 6.1e), close to the estuary of the springwater Dese River, where the lower salinity allowed the encroachment of a near-freshwater plant community dominated by *Phragmites australis*, forming a dense and deep network of roots and rhizomes (Moore et al., 2012). Carbon-rich fragments of reeds and peat were also observed at the bottom of the cores in some sites at the lagoon-mainland boundary (CA) and in the southern lagoon (MI, CV, FO, VB), showing traces of pre-existing palustrine or brackish environments alternating through time (Bonometto, 2005; Favero and Seranderei Barbero, 1980; Roner et al., 2021).

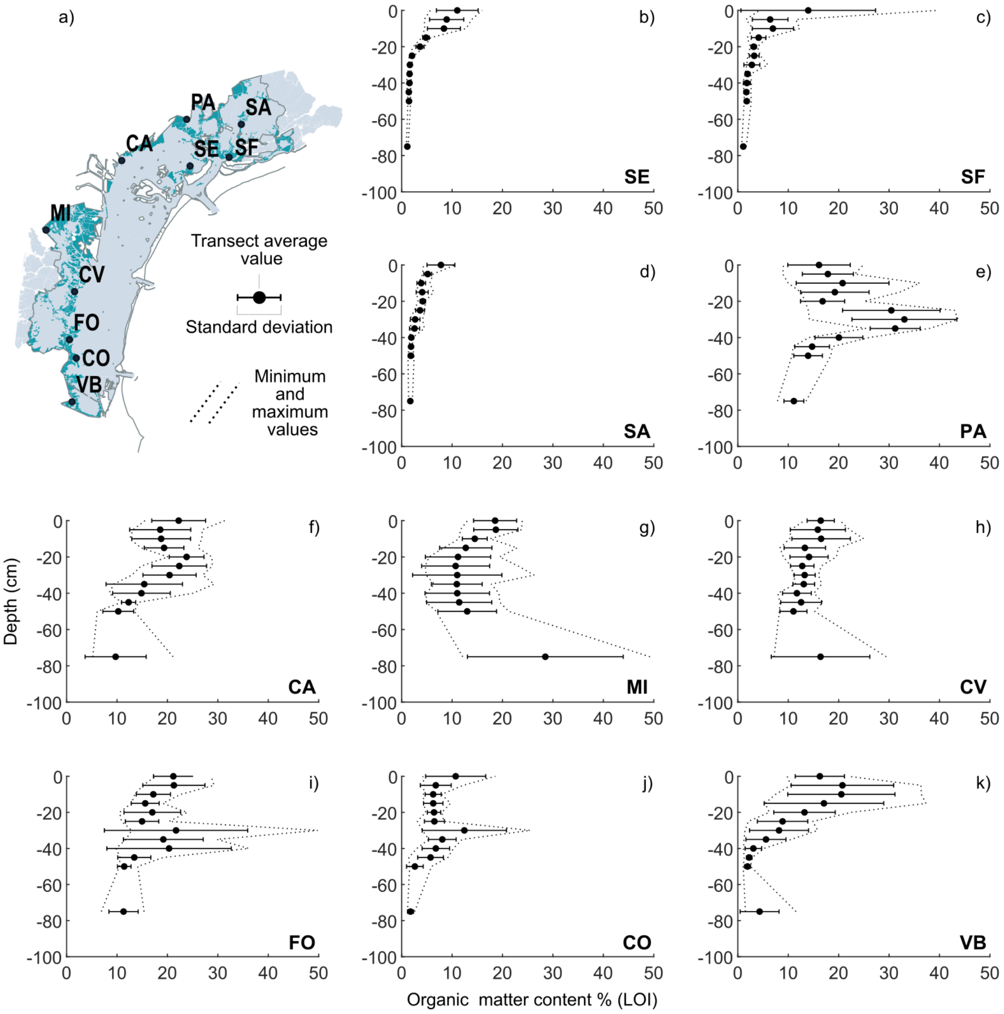

Figure 6.1: **Organic matter content variability.** Average of percent organic matter at different depths at each of the 10 sites considered with respective standard deviation, minimum and maximum. Names of the sites as follows: Sant'Erasmo (SE), San Felice (SF), Saline (SA), Pagliaga (PA), Mira (MI), Canale Virgilio (CV), Fossei (FO), Conche (CO), Valle di Brenta (VB). Organic matter content was estimated using the loss-on-ignition procedure by combusting ground soil samples in a muffle furnace at 375 °C for 16 h (Ball, 1964; Roner et al., 2016).

Hence, variations in organic carbon content, determined by organic inputs and preservation conditions, are affected by vegetation characteristics as well as sedimentary conditions, both highly variable in space and time, due to shifting ecosystem stages. Past and present fluvial inputs crucially affected organic carbon storage as they may influence hydrology, salinity, nutrient status, vegetation characteristics, sediment type, and supply (Ewers Lewis et al., 2020; Kelleway et al., 2016; Roner et al., 2021; Saintilan et al., 2013). Freshwater inputs affect salt-marsh vegetation fostering the growth of reeds (*Phragmites australis*), which are characterized by higher biomass and deeper roots (Moore et al., 2012; Scarton et al., 2002). In addition, fluvial inputs provide a greater contribution of terrestrial sediments, which may enhance accretion rates and carbon accumulation. Terrestrial sediments, indeed, are also usually characterized by smaller grain size, which can enhance C preservation by reducing sediment aeration compared to sandy sediments (Kelleway et al., 2016; Ward et al., 2021), and higher concentration of suspended particulate organic C (Van De Broek et al., 2016).

6.4.2 Relationship between OC and LOI

To estimate the C content in the soil of Venice marshes based on the LOI measurements, we evaluate the relationship between organic C determined through elemental analysis and organic matter measured through LOI on a representative set of subsamples (n = 102). Following Craft et al. (1991), we interpolated a quadratic relationship (Eq. 6.3) between OM and OC

$$OC = (0.37 \pm 0.01)LOI - (0.0024 \pm 0.0004)LOI \tag{6.3}$$

finding a very high correlation ($R^2 = 0.979$, $p \ll 0.0001$). Although the parameter values calibrated with our data are in close agreement with those obtained by Craft et al. (1991) by analysing 250 soil samples collected in the marshes in North Carolina, USA ($OC = (0.40 \pm 0.01)LOI + (0.0025 \pm 0.0003)LOI^2$), a site-specific relationship allows us to increase the accuracy of the estimate, especially for larger value of OM, where the difference between the relationships is slightly more pronounced.

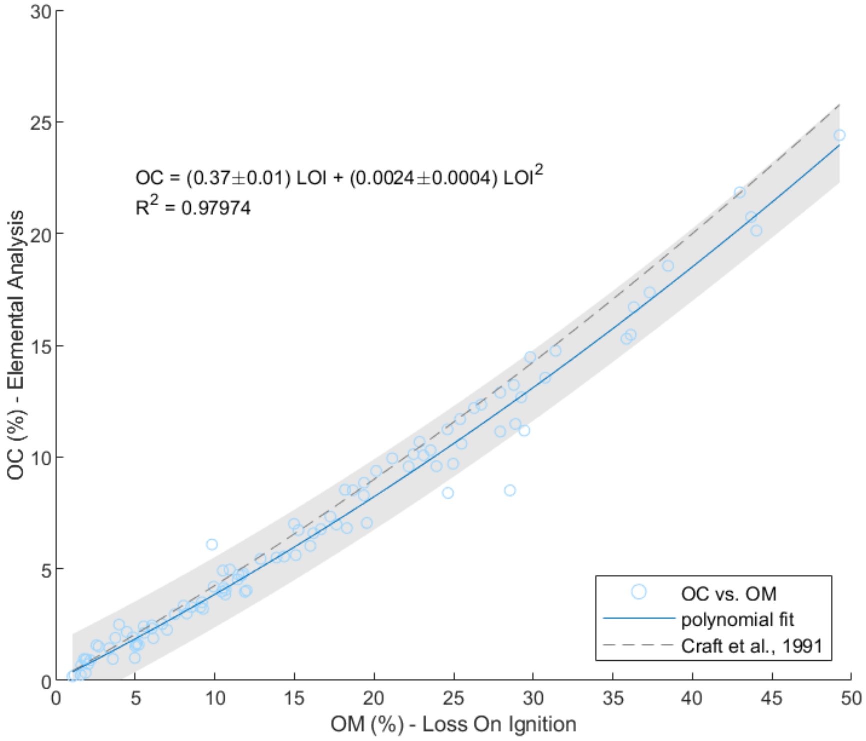

Figure 6.2: **Relation between Organic Carbon and Organic Matter.** The relationship between organic carbon percentage, directly determined through elemental analysis and organic matter percentage measured through loss on ignition (LOI) in marsh soils ($n = 102$).

6.4.3 Sediment carbon stock

Consistently with organic matter content variability, carbon stock estimates were highly variable in different marshes ranging between 9800 and 24,700 ton OC km^2(17,108±5757), with higher values generally occurring at the landward side of the lagoon boundaries (Fig. 6.3 and Fig. 6.2a). The average value from our study falls within previous global estimates of salt-marsh SOC stock (global estimates are reported by Duarte et al. (2013), with an average value of 16,200 ton OC km^{-2} and a maximum value of 25,900, by Pendleton et al. (2012) with an average value of 25,000 ton OC km^{-2}, by van Ardenne et al. (2018b) with 26,130 ton OC km^{-2} and by Macreadie et al. (2017) with 16,541 ton OC km^{-2}). Although some of the variability among global compilations may be due to methodological differences, our results suggest that the sedimentary history and the environmental conditions within a tidal system may generate variable and site-specific carbon accumulation patterns, enhancing blue carbon assessment complexity. Importantly, the values estimated in our study are comparable to carbon stock estimates attributed to temperate and tropical forests (24,300 and 15,300 ton $\mathrm{OC\,km^{-2}}$, respectively, (Watson et al., 2000)) and support salt-marsh importance as quite efficient carbon sinks. High content of organic carbon found deep in salt-marsh soils, with well-preserved plant debris dating back hundreds of years (Roner et al., 2017), further confirms salt-marsh potential to sequester carbon over long temporal scales and thus the eligibility of their carbon offsets for greenhouse gas markets. Furthermore, our results on near-surface carbon stock provide important information to estimate the amount of carbon which is mobilised and potentially lost after salt-marsh erosion, degradation or conversion. Even if further research is needed to quantitatively describe the fate of carbon after salt-marsh conversion or degradation, once sediment is destabilized or exposed to oxygen, the subsequent increased microbial activity may release large amounts of C to the atmosphere or water column (Kelleway et al., 2016; McTigue et al., 2021; Pendleton et al., 2012). In a carbon offset market, the potential value of the carbon stock locked in Venice salt marshes ($17{,}108 \pm 5757$ ton $\mathrm{OC\,km^{-2}}$, 1 m depth in 43 $\mathrm{km^2}$), when considered completely vulnerable to marsh loss or degradation, is estimated to be €16 million (mean EU auction price over the last year of about 80€ per ton of $\mathrm{CO_2}$e - European Energy Exchange AG).

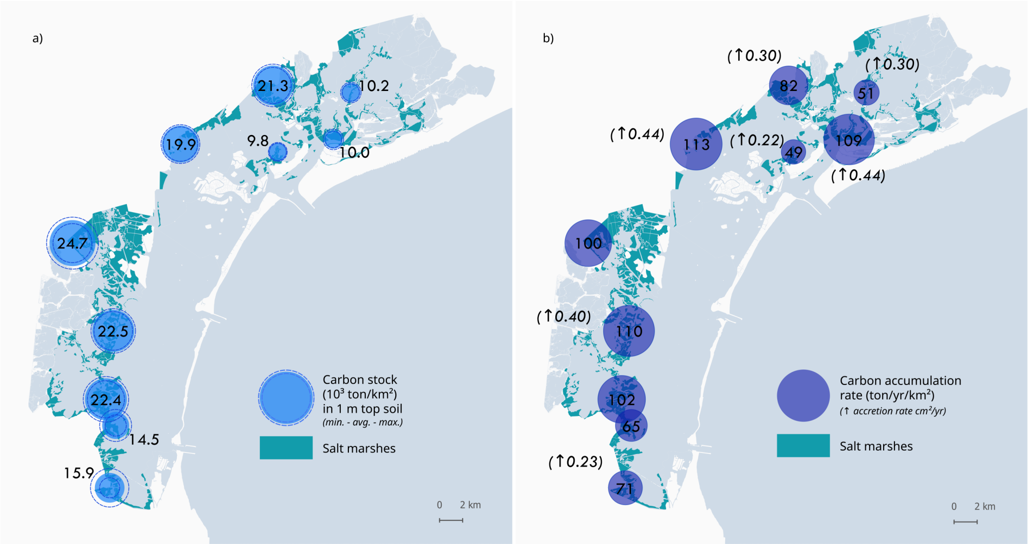

Figure 6.3: **Carbon storage and sequestration in the salt marshes of the Venice Lagoon.** Carbon stock in 1 m top soil (a) and carbon accumulation rate (b) estimates at each of the 10 salt-marsh sites analysed. Carbon stock is the sum of the organic carbon content in 1 m soil and carbon accumulation rate results from the product of carbon density in top 5-cm soil and vertical accretion rates derived from measurements from marker horizons (over a $2-20$ yr period).

6.4.4 Salt-marsh carbon accumulation rate

Carbon density within the top 5 cm soil displayed local mean values ranging between 0.017 and 0.031 $\mathrm{g\,cm^{-3}}$ (0.025 ± 0.004). Accretion rates measured at the study sites ranged between 0.22 and 0.44 $\mathrm{cm\,yr^{-1}}$ and they represented an important source of uncertainty for the calculation of carbon accumulation rates. As a result, estimates of carbon accumulation rates ranged from 49 to 113 $\mathrm{ton\,OC\,km^{-2}\,yr^{-1}}$ (85 ± 25) (Fig. 6.3b), and fall within the range of variability defined by previous estimates (between 27 and 273 $\mathrm{ton\,OC\,km^{-2}\,yr^{-1}}$ (Sifleet et al., 2011)). High uncertainty exists in estimating salt-marsh carbon sequestration potential and sources of variability are multiple, particularly due to methodological differences other than intrinsic diversity coming from both the terms of the calculation. Moreover, the temporal scale considered may importantly affect carbon sequestration estimates (DeLaune et al., 2018), involving differences in reference soil layer thickness and methods to determine accretion rates.

By multiplying the mean C accumulation rate in our study (85 ± 25 ton OC km^{-2} yr^{-1}) for the extent of salt-marsh area ($43\,km^2$, Carniello et al., 2009), we estimate that the salt marshes of the Venice lagoon may sequester about 13,436 tons of CO_2 per year, which is equal to about 20% of the annual emission from the waterborne navigation occurring in the city of Venice (66,000 ton CO_2e per year) and about 17% of the annual emission from the aviation system of the Venice Marco Polo Airport (77,000 ton CO_2e per year)(CIRIS - City Inventory Reporting and Information System - 2018). This confirms the great importance of salt-marsh ecosystems in contributing to mitigate GHG effects. In a carbon offset market, the financial value of the annual CO_2 sequestration from the salt marshes of the Venice lagoon (13,436 tons of CO_2 per year) may be estimated at about €1 million per year (mean EU auction price over the last year of about 80€ per ton of CO_2e - European Energy Exchange AG).

As the carbon accumulation rate is the product of carbon density and vertical accretion rate, changes in these factors directly affect carbon accumulation. Vertical accretion rate may be particularly low in sediment starved systems, such as the Venice Lagoon, which is nowadays characterized by negligible riverine and marine sediment inputs. Moreover, salt-marsh vertical accretion can be further reduced by the operation of the storm-surge barriers of the Mo.S.E. system reducing water levels within the lagoon during storm surges, which are fundamental suppliers of sediment to salt marshes (Tognin et al., 2021). As a consequence, Tognin et al. (2021) estimated an annual reduction in sediment accumulation on marsh platforms of more than 25%, which results in a vertical accretion reduction of 1.1 mm per year, regardless of the location. By recalculating carbon accumulation rates in the flood-regulated scenario, on the basis of decrease in the estimated accretion rate, we observe a reduction ranging between 25 and 50% (Fig. 6.4a). Because the decrease in the vertical accretion is constant, the relative reduction in carbon accumulation rates is larger at sites with lower accretion rates (e.g., SE).

Higher soil carbon density values would have the potential to mitigate the impact of accretion rate reduction on carbon accumulation rate, however, due to the different order of magnitude between accretion rates and carbon density, the variability of the latter was, in fact, not significant in the resulting carbon accumulation rate. We estimate that storm-surge-barrier operations may reduce the CO_2 sequestration potential of the salt marshes of the Venice lagoon by about

33% (Fig. 6.4b). This highlights the crucial role of the accretion rate for CO_2 sequestration potential of tidal environments, other than for the survival itself of salt marshes and the related ecosystem services. In terms of economic value, this reduction is equal to a loss of about 355,000€ per year.

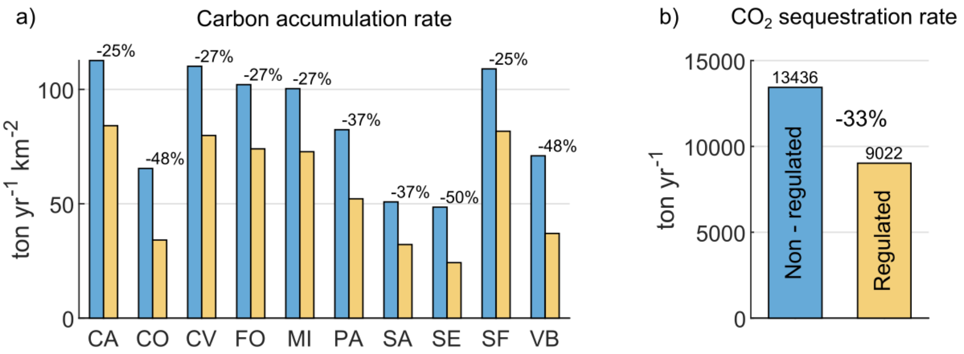

Figure 6.4: **Effect of storm surge barriers on the carbon sink potential of salt-marsh environment.** Comparison between non-regulated and regulated scenarios of carbon accumulation rate estimates in 10 salt-marsh study sites (a) and of total CO_2 sequestration potential of the salt marshes of the Venice lagoon (43 km^2) (b), considering a 1.1 mm per year reduction in salt marsh accretion rates due to barrier closures.

As a comprehensive strategy is needed to achieve emission reduction targets, our projection supports the usefulness of including blue C ecosystems in climate policies, starting from the local and regional scale. Moreover, our results highlight the potential impacts of storm-surge barriers on salt-marsh carbon storage and sequestration, revealing the need for integrated coastal management policies to enhance salt-marsh resilience and pursue the preservation of related ecosystem services.

In conclusion, our study sheds light on the significant role tidal marshes played in C sequestration in the past, through the development of OC stocks, and may play in the future, through C accumulation. Furthermore, these estimates give some indications of the magnitude of OC which may have been lost or may be at risk due to past and future marsh loss or degradation, highlighting the role of the integrated approach in maximising the outcomes of coastal management.

6.5 Supporting Information

6.5.1 Comparison with other tidal systems worldwide

Carbon accumulation estimates from our study are consistent with the results from Macreadie et al. (2017) who compiled all available data on soil organic carbon storage in Australia's tidal marshes (323 cores), reporting a mean carbon accumulation rate of $54.52 \pm 2.34\,\mathrm{ton\,OC\,km^{-2}\,yr^{-1}}$. Nevertheless, they are below the current global means (Nellemann et al., 2009; McLeod et al., 2011). However, our estimates fall within the wide range defined by previous estimates, between 27 and $273\,\mathrm{ton\,OC\,km^{-2}\,yr^{-1}}$ (Sifleet et al., 2011). As the product of soil carbon density and accretion rate, carbon accumulation estimates are affected by multiple sources of variability. Variations derive from methodological differences other than intrinsic diversity characterizing both the terms of the calculation (i.e. accretion rate and carbon density). Furthermore, comparisons between carbon accumulation rates in salt-marsh soils are complex due to variable temporal scale considered, differences in reference soil layer thickness and accretion rate calculation methods (Chmura et al., 2003; Sifleet et al., 2011).

Chmura et al. (2003) present data for a total of 154 sites from the western and eastern Atlantic and Pacific coasts, as well as the Indian Ocean, Mediterranean and Gulf of Mexico. They summarize information about organic carbon density and carbon accumulation rates within salt marsh (75%) and mangrove soils. In most cases, the soil carbon densities reported were derived from measurements of loss on ignition (LOI), but the Walkley Black and dichromate digestion methods were also used, as well as elemental analysis. LOI measurements were transformed through the relationship reported by Craft et al. (1991). Vertical soil accumulation rates represented averages over variable periods, from 1 to 100 years and were determined through ^{137}Cs and ^{210}Pb dating or marker horizons employment.

The average soil carbon density of salt marshes reported by Chmura et al. (2003) is $0.039 \pm 0.003\,\mathrm{g\,cm^{-3}}$ and is higher than the mean value measured in our study ($0.025 \pm 0.004\,\mathrm{g\,cm^{-3}}$). Larger values of soil carbon density were found in the Mississippi Delta by Bryant and Chabreck (1998) who measured values ranging between 0.093 and $0.19\,\mathrm{g\,C\,cm^{-3}}$. Apart from the Mississippi Delta data, soil carbon densities measured in our study are consistent with global data, as can be seen in Fig. 6.5a and 6.5c showing the frequency distribution of measured soil carbon density values. Thus, the higher mean global estimate of carbon accumulation rate reported by Chmura et al. (2003) for salt marshes ($218 \pm 24\,\text{ton OC}\,\text{km}^{-2}\,\text{yr}^{-1}$), with respect to our estimates, can be explained partially by the presence of local larger carbon density values, likely due to in situ differences in vegetation characteristics as well as allochthonous organic inputs.

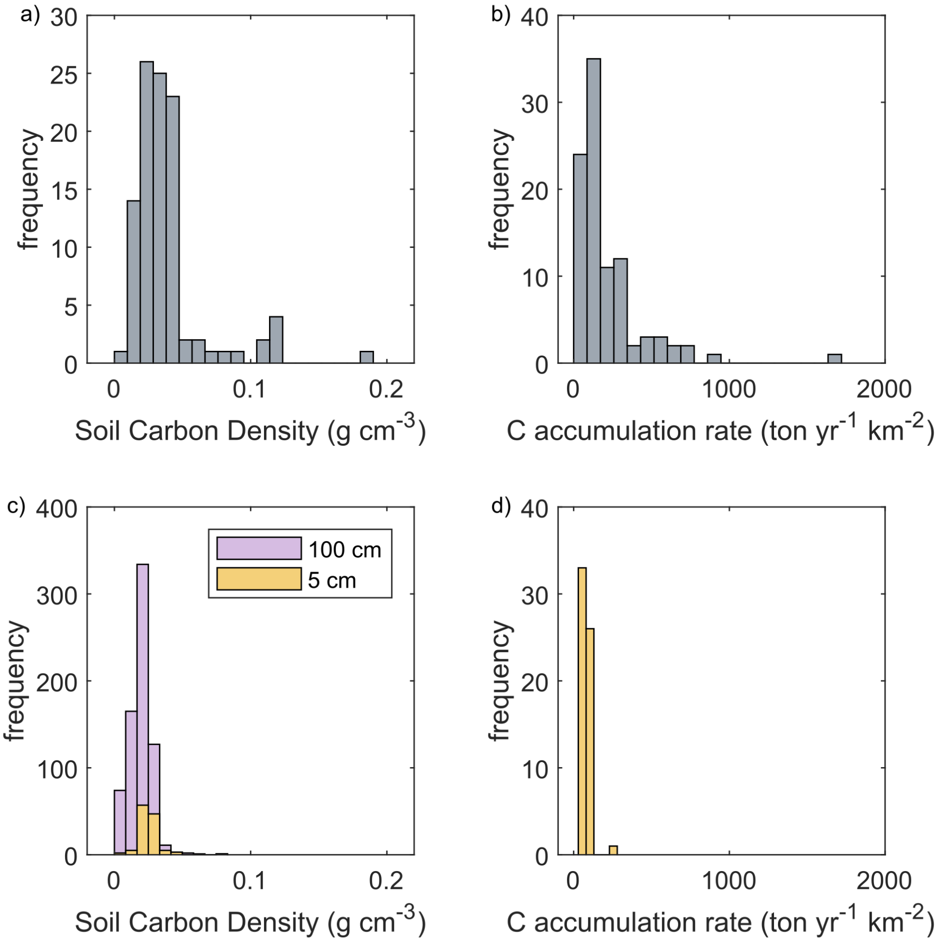

Figure 6.5: **Carbon density and accumulation results in relation to previous findings.** Comparison of the frequency distribution of Soil Carbon Density (c) and C accumulation rate (d) values found in the current study with literature data from Chmura et al. (2003) (a and b).

In addition, accretion rate variability strongly affects carbon accumulation rate estimates. Some of the highest values of carbon accumulation rate were reported by Oenema and DeLaune (1988) from the Eastern Scheldt, South-west Netherlands, where observed mean accretion rates varied between $0.4-0.9\,\mathrm{cm\,yr^{-1}}$ and $1.0-1.5\,\mathrm{cm\,yr^{-1}}$. Therefore, carbon accumulation estimates from our study can be considered in general consistent with previous findings (Fig. 6.5).

6.5.2 Accretion rates used for C accumulation rates estimations

Area	**Accretion rate** ($\mathrm{cm\,yr^{-1}}$)	**Reference**
SE	0.22	Tognin et al. (2021) - SE
SF	0.44	Tognin et al. (2021) – SF
SA	0.3	Saintilan et al. (2022)
PA	0.3	Tognin (2022)
CA	0.4	Day et al. (1999) - Tessera
CV	0.4	Saintilan et al. (2022)
MI	0.4	Saintilan et al. (2022)
FO	0.4	Saintilan et al. (2022)
CO	0.23	Tognin et al. (2021) - CO
VB	0.23	Tognin et al. (2021) - CO

Table 6.1: **References for accretion rate estimates in the study sites.** Vertical accretion rate assumed for C accumulation calculations in each area with relative reference. Accretion rates derived from measurements from marker horizons (over a $2-20\,\mathrm{yr}$ period).

6.5.3 C accumulation rate time scales

Carbon accumulation rate estimate importantly depends on time scale and reference interval considered (DeLaune et al., 2018), which leads to the risk of overestimation of C sequestration and OC stocks in blue C ecosystems due to frequently observed strong declines in OC density with soil depth (Mueller et al., 2019). For this reason, we inspected the difference between short-term and long-term estimates of carbon accumulation rate. Beside the short-term estimate, previously presented, a long-term estimate is provided on the basis of the average SCD in the top-1-m reference interval and accretion rates determined from ^{210}Pb profiles by Bellucci et al. (2007) (to the depth of 50-60 cm, back to about 100 years ago) (Tab. 6.2).

We observed that SCD is higher in the topsoil; however minor differences occur at sites at the landward side of the lagoon (e.g., PA, CA, MI, CV, FO) (Fig. 6.6), which showed irregular depth-distributions of carbon content, with organic-rich levels at deeper soil layers. Marsh accretion rate estimates show a contrasting behaviour in northern and southern lagoon sites, with higher short-term estimates in the northern lagoon and higher long-term estimates in the southern lagoon (Fig. 6.6). The latter may be attributable to accretion rate changes due to sediment supply variations during Brenta River repeated diversions into the southern Venice Lagoon (Roner et al., 2017). Consequently, the relationship between short-term and long-term carbon accumulation rate estimates at our study sites is variable. Short-term estimates are higher in the norther lagoon, where recent accretion rates are higher, whereas long-term estimates are generally slightly higher in the southern lagoon, where accretion rates decreased with respect to the past. This confirms time scale and reference interval as key factors in carbon accumulation rate estimates in wetland environment and highlight the need to take into consideration the historical evolution of the system object of study, in order to improve blue C assessments.

Area	**Accretion rate** ($\mathrm{cm\,yr^{-1}}$)	**Reference**
SE	0.13	Bellucci et al. (2007) - Treporti
SF	0.13	Bellucci et al. (2007) – Treporti
SA	0.28	Bellucci et al. (2007) - Ca' Zane
PA	0.24	Bellucci et al. (2007) - Cona
CA	0.24	Bellucci et al. (2007) - Cona
CV	0.45	Bellucci et al. (2007) - Canale Piovego
MI	0.45	Bellucci et al. (2007) - Canale Piovego
FO	0.47	Bellucci et al. (2007) - Punta Fossei
CO	0.47	Bellucci et al. (2007) - Punta Fossei
VB	0.47	Bellucci et al. (2007) - Punta Fossei

Table 6.2: **Long-term accretion rate estimates.** Salt-marsh accretion rates determined from ^{210}Pb profiles to the depth of 50-60 cm, back to about 100 years ago, by Bellucci et al., 2007.

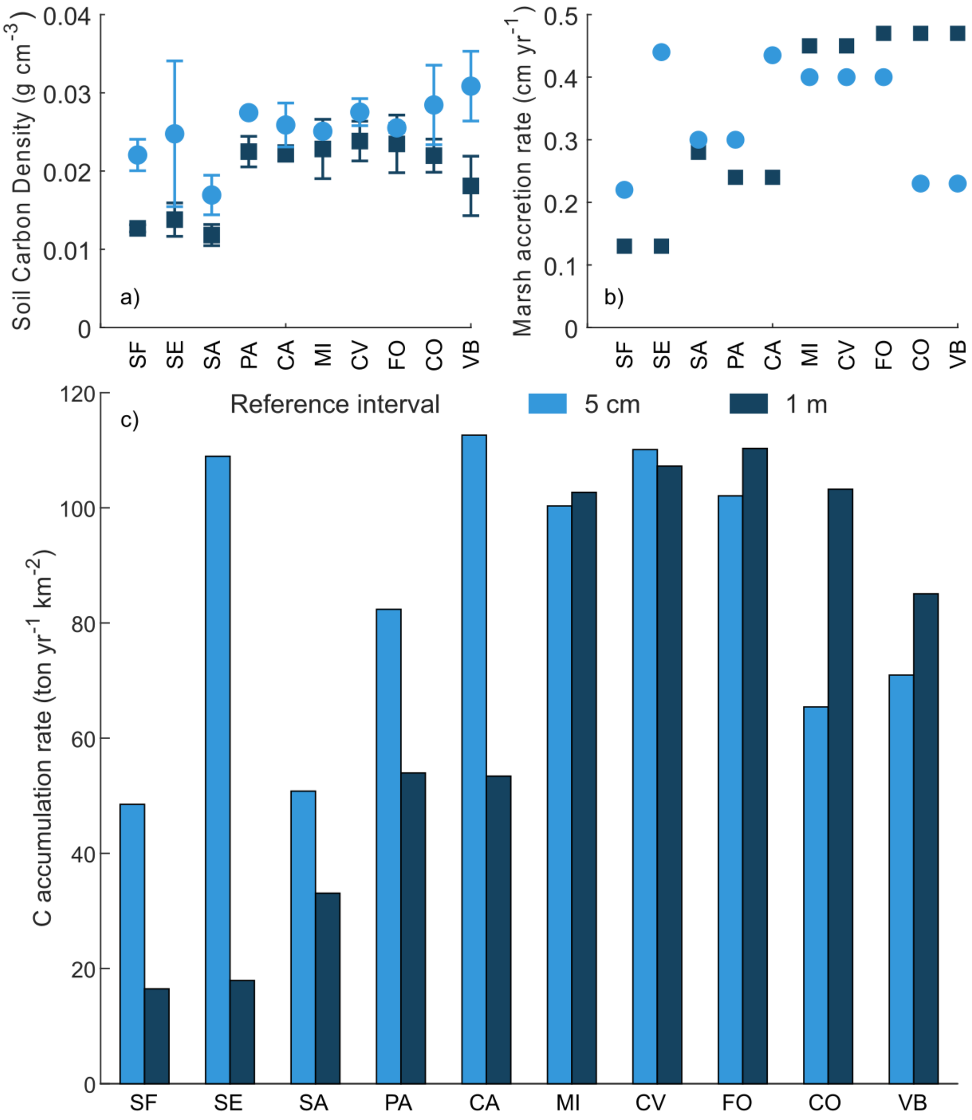

Figure 6.6: **Comparison between short-term and long-term carbon accumulation rate estimates.** Mean soil carbon density (a), marsh accretion rate estimate (b), and carbon accumulation rate estimate (c) in 10 salt-marsh study sites on a short-term (5-cm reference interval and marker-horizon accretion rate estimates) and long-term scale (1-m reference interval and ^{210}Pb-based dating methods).

7

CONCLUSIONS

Towards the goal of improving the current understanding of organic matter dynamics influencing coastal wetland resilience and its carbon sink potential, the present work inspects soil organic matter and carbon dynamics in microtidal salt marshes, under natural and anthropogenic forcing, by means of a multidisciplinary approach combining ecological and sedimentological evaluations through field observations, laboratory analyses, and statistical investigations. In particular, decomposition processes and relative forcing affecting organic matter fate in salt-marsh environments were analysed through a standard litter-bag experiment. Spatial and vertical patterns of soil organic matter in salt-marsh soils were investigated and their main drivers were explored combining the analysis of a large number of sediment samples to sedimentological, morphological and vegetational investigations. Finally, an assessment of carbon stock and carbon accumulation s in the salt marshes of the Venice Lagoon (Italy) was performed, emphasizing how natural and anthropogenic factors affect carbon sequestration potential in coastal wetlands. The main results of this research can be summarized as follows.

Our findings suggest that organic matter and carbon dynamics in salt-marsh soils are primarily determined by both organic inputs and outputs, affected by intertwined physical, hydromorphological and biological factors occurring at different scales. Indeed, organic matter contributions and their preservation in salt-marsh soils are importantly influenced by climate, vegetation characteristics, sediment properties, and geomorphological settings.

Our analysis on organic matter decomposition processes confirms that salt-marsh decomposition rates are some of the lowest with respect to other biomes. However, we also show that labile organic matter is subjected to quite rapid decay in surface salt-marsh soil. Decomposition processes are affected by site specific micro-scale variability of the environmental forcing, with anoxic conditions playing a key role in organic matter preservation, and, on a broader scale, they are importantly accelerated by warming temperature. Furthermore, the initial litter quality appears to be a primary constraint for the amount of preserved organic matter contributing to carbon sequestration and marsh accretion, as confirmed by the observed difference in mass loss between labile and recalcitrant material. Hence, we highlight the need for further analyses on autochthonous plant litter dynamics, also on longer time scales, considering their variability. Therefore, the effect of climate change and anthropogenic disturbances, including global warming and potential shifts in vegetation characteristics in the future, could have large effects on organic matter dynamics.

Our investigations on distribution patterns of soil organic matter in salt-marsh ecosystems suggest that soil organic matter variability is importantly affected by environmental and depositional conditions as currently observed and testified by recent sedimentary successions. Spatial patterns of soil organic matter in surface salt-marsh soils reveal two scales of variations in sedimentary organic matter content. The first occurs at the marsh scale and it is influenced by the interplay between surface elevation and sediment supply dynamics along the distance from the tidal channel, with organic content generally following an inverse relationship with the distance from the marsh edge. The other occurs at the catchment scale, dominated by the gradient generated by marine and fluvial influence, with highest organic matter content observed toward the mainland. Our results suggest that, besides organic matter decay, changes in the depositional environment during intertidal system development are of primary importance in determining soil organic matter depth distribution and caution is needed in soil organic matter prediction at unsampled soil depths through vertical distribution modelling. Marsh deposits showed significantly higher organic content with respect to tidal-flat and transition deposits. Thus, hydromorphological as well as biological factors show important influences on the observed variation in soil organic matter, although the interplay between them makes it difficult to unravel the direct cause-effect relationships. Despite the need for further analyses of quantitative and qualitative characteristics of different tidal marsh species, vegetation type and diversity were observed to affect soil organic matter content. For instance, some of the highest organic matter contents were observed in current and past salt-marsh deposits dominated by *Phragmites australis*, a near freshwater plant with high primary production and high resistance to decomposition. Besides autochthonous biomass, allochthonous, already stabilized organic inputs are relevant in soil organic matter distribution, as suggested by high organic content associated to fluvial discharge or episodic wrack deposits. Furthermore, sediment grain size is importantly related to soil organic matter variations, as it is in turn correlated to geomorphic settings and it has the potential to affect organic matter preservation conditions. Our assessment of Blue Carbon in the salt marshes of the Venice Lagoon supports salt-marsh importance as efficient carbon sinks, although emphasising its wide variability driven by aforementioned forcing. Mean carbon stock estimate amounts to 171 ± 57 Mg OC ha^{-1}, being comparable to carbon stock estimates attributed to temperate and tropical forests. High content of organic carbon found deep in salt-marsh soils, with well-preserved plant debris dating back hundreds of years, further confirms salt-marsh potential to sequester carbon over long temporal scales and thus the eligibility of their carbon offsets for greenhouse gas markets. Carbon accumulation rate evaluations, averaging $85 \pm 25\,\mathrm{ton\,OC\,km^{-2}\,yr^{-1}}$, indicate that the salt marshes of the Venice Lagoon may sequester every year about 20% of the annual CO_2 emission from the waterborne navigation occurring in the city of Venice. Nevertheless, caution is needed in the interpretation of CO_2 sequestration predictions, as they are affected by uncertainties due to estimate methodologies, time scales and reference intervals. However, we highlight the crucial role of surface accretion rate for CO_2 sequestration potential of tidal environments, other than for the survival itself of salt marshes and the related ecosystem services. In this regard, we estimated that the operation of the storm-surge barriers, reducing sediment supply to salt marshes and consequently their accretion, may reduce the CO_2 sequestration potential of the salt marshes of the Venice Lagoon by about 33%, with an economic loss of about 355,000€ per year. In conclusion, this work provides further understanding on the drivers of organic matter dynamics in microtidal salt-marshes offering additional insights to improve biogeomorphological model ability to describe marsh resilience to the effects of climate change and anthropogenic perturbation and further elucidate marsh importance within the global carbon cycle. Our research sheds light on the significant role tidal marshes played in carbon sequestration in the past and may play in the future, further giving some indications of the magnitude of organic carbon which may have been lost or may be at risk due to past and future marsh loss or degradation. Besides, it delivers important knowledge for regional and national carbon assessments, which foster the inclusion of coastal wetland carbon sinks in greenhouse gases inventories and climate mitigation strategies. Thus, the outcome of the present study, paired with the assessment of other ecosystem services, can inform territorial management decision makers, by enabling the identification of strategies for optimizing protection and restoration efforts. Furthermore, building interest in the recently-recognised value of tidal marshes in carbon offset markets and nature-based climate mitigation may be an opportunity to encourage their protection and restoration, at the same time contributing to the maintenance of a large number of naturally co-occurring ecosystem services. Insights from the present work improve current knowledge about organic matter dynamics in wetland environments, however, they claim for further investigations to be pursued in forthcoming studies, including further analyses of quantitative and qualitative characteristics of different tidal marsh species, in terms of aboveground and belowground primary production, and response to decomposition, refined description of carbon dynamics through sediment dating and carbon accumulation models, and lastly the investigation of soil organic matter sources through stable carbon and nitrogen isotope ratio analysis.

BIBLIOGRAPHY

P. Adam. *Saltmarsh Ecology.* Cambridge Studies in Ecology. Cambridge University Press, 1990. doi: 10.1017/CBO9780511565328.

P. Adam. Saltmarshes in a time of change. *Environmental Conservation*, 29: 39–61, 2002. doi: 10.1017/S0376892902000048.

J. R. Allen, J. C. Cornwell, and A. H. Baldwin. Contributions of organic and mineral matter to vertical accretion in tidal wetlands across a chesapeake bay subestuary. *Journal of Marine Science and Engineering*, 9(751), 2021. ISSN 20771312. doi: 10.3390/jmse9070751.

J. R. L. Allen. Morphodynamics of Holocene salt marshes: A review sketch from the Atlantic and Southern North sea coasts of Europe. *Quaternary Science Reviews*, 19:1255–1331, 2000. ISSN 02773791. doi: 10.1016/S0277-3791(00)00157-8.

J. R. L. Allen and K. Pye, editors. *Saltmarshes. Morphodynamics, Conservation and Engineering Significance.* Cambridge University Press, Cambridge, 1992.

T. S. Arnarson and R. G. Keil. Changes in organic matter–mineral interactions for marine sediments with varying oxygen exposure times. *Geochimica et Cosmochimica Acta*, 71(14):3545–3556, jul 2007. ISSN 0016-7037. doi: 10.1016/J.GCA.2007.04.027.

R. G. Bader, D. W. Hood, and J. B. Smith. Recovery of dissolved organic matter in sea-water and organic sorption by particulate material. *Geochimica et Cosmochimica Acta*, 19(4):236–243, aug 1960. ISSN 0016-7037. doi: 10.1016/0016-7037(60)90031-4.

J. Bai, G. Zhang, Q. Zhao, Q. Lu, J. Jia, B. Cui, and X. Liu. Depth-distribution patterns and control of soil organic carbon in coastal salt marshes with different plant covers. *Scientific Reports*, 6, 2016. doi: 10.1038/srep34835.

J. Baldock and P. Nelson. *Soil organic matter*, pages B25–B84. CRC Press, Boca Raton, FL, USA, 2000. doi: 10.1038/194324b0.

J. A. Baldock and J. O. Skjemstad. Role of the soil matrix and minerals in protecting natural organic materials against biological attack. *Organic Geochemistry*, 31(7):697–710, 2000. ISSN 0146-6380. doi: https://doi.org/10.1016/S0146-6380(00)00049-8.

D. F. Ball. Loss-on-ignition as an estimate of organic matter and organic carbon in non-calcareous soils. *Journal of Soil Science*, 15(1):84–92, 1964. doi: https://doi.org/10.1111/j.1365-2389.1964.tb00247.x.

E. Barbier, S. Hacker, C. Kennedy, E. Koch, A. Stier, and B. Silliman. The value of estuarine and coastal ecosystem services. *Ecological Monographs*, 81 (2):169–193, 2011. doi: 10.1890/10-1510.1.

A.-L. Barillé-Boyer, L. Barillé, H. Massé, D. Razet, and M. Héral. Correction for particulate organic matter as estimated by loss on ignition in estuarine ecosystems. *Estuarine Coastal and Shelf Science*, 58(1):147–153, 2003. doi: 10.1016/S0272-7714(03)00069-6.

W. Beeftink. The coastal salt marshes of western and northern Europe: an ecological and phytosociological approach. In V. J. Chapman, editor, *Ecosystems of the World 1: wet coastal ecosystems.* Elsevier, Amsterdam, v edition, 1977.

L. G. Bellucci, M. Frignani, J. K. Cochran, S. Albertazzi, L. Zaggia, G. Cecconi, and H. Hopkins. 210Pb and 137Cs as chronometers for salt marsh accretion in the Venice Lagoon - links to flooding frequency and climate change. *Journal of Environmental Radioactivity*, 97(2-3):85–102, 2007. ISSN 0265931X. doi: 10.1016/j.jenvrad.2007.03.005.

M. D. Bertness and A. M. Ellison. Determinants of Pattern in a New England Salt Marsh Plant Community. *Ecological Monographs*, 57(2):129–147, 1987. ISSN 00129615. doi: 10.2307/1942621.

S. Best, M. Van der Wegen, J. Dijkstra, P. W. Willemsen, B. W. Borsje, and D. J. Roelvink. Do salt marshes survive sea level rise? Modelling wave action, morphodynamics and vegetation dynamics. *Environmental Modelling & Software*, 109:152–166, nov 2018. ISSN 1364-8152. doi: 10.1016/J.ENVSOFT.2018.08.004.

A. Beudin, T. S. Kalra, N. K. Ganju, and J. C. Warner. Development of a coupled wave-flow-vegetation interaction model. *Computers & Geosciences*, 100:76–86, 2017. ISSN 0098-3004. doi: https://doi.org/10.1016/j.cageo.2016.12.010.

J. Boaga, A. D'Alpaos, G. Cassiani, M. Marani, and M. Putti. Plant-Soil interactions in salt marsh environments: Experimental evidence from electrical resistivity tomography in the Venice Lagoon. *Geophysical Research Letters*, 41 (17):6160–6166, 2014. doi: 10.1002/2014GL060983.

D. F. Boesch and R. E. Turner. Dependence of Fishery Species on Salt Marshes: The Role of Food and Refuge. *Estuaries*, 7(4):460–468, 1984. ISSN 01608347. doi: doi.org/10.2307/1351627.

A. Bondesan and P. Furlanetto. Artificial fluvial diversions in the mainland of the Lagoon of Venice during the 16th and 17th centuries inferred by historical cartography analysis. *Geomorphologie: Relief, Processus, Environnement*, 2: 175–200, 2012. ISSN 12665304. doi: 10.4000/geomorphologie.9815.

A. Bondesan and M. Meneghel. *Geomorfologia della provincia di Venezia. Note illustrative della carta geomorfologica della provincia di Venezia*. Esedra, Padova, 2004. ISBN 888641370X.

L. Bonometto. Functional characteristics of salt marshes (barene) in the Venice Lagoon, and environmental restoration scenarios. Workshop on Venice lagoon. In C. A. Fletcher and T. Spencer, editors, *Flooding and Environmental Challenges for Venice and its Lagoon: State of Knowledge*, chapter 52, pages 473–486. Cambridge University Press, New York, 2005.

T. J. Bouma, M. B. D. Vries, E. Low, G. Peralta, I. C. Tánczos, J. van de Koppel, and P. M. J. Herman. Trade-offs Related to Ecosystem Engineering: A Case Study on Stiffness of Emerging Macrophytes. *Ecology*, 86(8):2187–2199, 2005. ISSN 00129658, 19399170. doi: 10.1890/04-1588.

A. Brambati, L. Carbognin, T. Quaia, P. Teatini, and L. Tosi. The Lagoon of Venice: Geological setting, evolution and land subsidence. *Episodes*, 26(3): 264–265, 2003. ISSN 07053797. doi: 10.18814/epiiugs/2003/v26i3/020.

J. Braun-Blanquet. *Pflanzensoziologie. Grundzüge der Vegetationskunde.* Springer Vienna, Wien, 3 edition, 1964. ISBN 978-3-7091-8111-9. doi: https://doi.org/10.1007/978-3-7091-8110-2.

E. C. Brevik and J. A. Homburg. A 5000 year record of carbon sequestration from a coastal lagoon and wetland complex, Southern California, USA. *CATENA*, 57 (3):221–232, aug 2004. ISSN 0341-8162. doi: 10.1016/J.CATENA.2003.12.001.

S. D. Bridgham, P. Megonigal, J. K. Keller, N. B. Bliss, C. Trettin, J. P. Megonigal, J. K. Keller, N. B. Bliss, and C. Trettin. The Carbon Balance of North American Wetlands. *Wetlands*, 26(4):889–916, 2006. ISSN 02775212. doi: 10.1672/0277-5212(2006)26[889:TCBONA]2.0.CO;2.

H. Brooks, I. Möller, S. Carr, C. Chirol, E. Christie, B. Evans, K. L. Spencer, T. Spencer, and K. Royse. Resistance of salt marsh substrates to near-instantaneous hydrodynamic forcing. *Earth Surface Processes and Landforms*, 46(67-88), 2021. doi: https://doi.org/10.1002/esp.4912.

J. C. Bryant and R. H. Chabreck. Effects of Impoundment on Vertical Accretion of Coastal Marsh. *Estuaries*, 21(3):416–422, 1998.

D. R. Cahoon and G. R. Guntenspergen. Climate change, sea-level rise, and coastal wetlands. *National Wetlands Newsletter*, 32(1):8–12, 2010.

D. R. Cahoon and D. Reed. The relationship among marsh surface topography, hydroperiod, and soil accretion in a deteriorating Louisiana salt marsh. *Journal of Coastal Research*, 11:357–369, 1995.

L. Carbognin, P. Teatini, and L. Tosi. Eustacy and land subsidence in the Venice Lagoon at the beginning of the new millennium. *Journal of Marine Systems*, 51(1):345–353, 2004. ISSN 0924-7963. doi: https://doi.org/10.1016/j.jmarsys.2004.05.021.

L. Carniello, A. Defina, and L. D'Alpaos. Morphological evolution of the Venice lagoon: Evidence from the past and trend for the future. *Journal of Geophysical Research: Earth Surface*, 114(F4), 2009. doi: https://doi.org/10.1029/2008JF001157.

L. Carniello, A. Defina, and L. D'Alpaos. Modeling sand-mud transport induced by tidal currents and wind waves in shallow microtidal basins: Application to the Venice Lagoon (Italy). *Estuarine, Coastal and Shelf Science*, 102-103:105–115, 2012. ISSN 0272-7714. doi: https://doi.org/10.1016/j.ecss.2012.03.016.

G. Cecconi, F. Codato, P. Nascimbeni, and F. Mattarolo. Valore ambientale delle barene artificiali. *Quaderni Trimestrali Consorzio Venezia Nuova*, Anno IV(I): 27–49, 1998.

V. J. Chapman. *Coastal vegetation.* Pergamon, Oxford, 2nd edition, 1976.

V. J. Chapman. *Wet coastal ecosystems / edited by V. J. Chapman.* Ecosystems of the world ; 1. Elsevier Scientific Pub. Co. ; New York : distributors for the United States and Canada, Elsevier/North Holland, Amsterdam, 1977. ISBN 0444415602.

S. Chen, R. Torres, and M. A. Goñi. The Role of Salt Marsh Structure in the Distribution of Surface Sedimentary Organic Matter. *Estuaries and Coasts*, 39 (1):108–122, 2016. ISSN 1559-2731. doi: 10.1007/s12237-015-9957-z.

G. L. Chmura and G. A. Hung. Controls on salt marsh accretion: A test in salt marshes of Eastern Canada. *Estuaries*, 27(1):70–81, 2004. ISSN 0160-8347. doi: 10.1007/BF02803561.

G. L. Chmura, L. Helmer, C. Beecher, and E. Sunderland. Historical rates of salt marsh accretion on the outer Bay of Fundy. *Canadian Journal of Earth Sciences*, 38:1081–1092, 2001. doi: 10.1139/cjes-38-7-1081.

G. L. Chmura, S. C. Anisfeld, D. Cahoon, and J. Lynch. Global carbon sequestration in tidal, saline wetland soils. *Global Biogeochemical Cycles*, 17(4):22–1, 2003.

T. Christiansen, P. L. Wiberg, and T. G. Milligan. Flow and Sediment Transport on a Tidal Salt Marsh Surface. *Estuarine, Coastal and Shelf Science*, 50(3): 315–331, mar 2000. ISSN 0272-7714. doi: 10.1006/ECSS.2000.0548.

J. H. C. Cornelissen, P. M. Van Bodegom, R. Aerts, T. V. Callaghan, R. S. P. Van Logtestijn, J. Alatalo, F. Stuart Chapin, R. Gerdol, J. Gudmundsson, D. Gwynn-Jones, A. E. Hartley, D. S. Hik, A. Hofgaard, I. S. Jónsdóttir, S. Karlsson, J. A. Klein, J. Laundre, B. Magnusson, A. Michelsen, U. Molau, et al. Global negative vegetation feedback to climate warming responses of leaf litter decomposition rates in cold biomes. *Ecology Letters*, 10(7):619–627, 2007. doi: https://doi.org/10.1111/j.1461-0248.2007.01051.x.

W. K. Cornwell, J. H. C. Cornelissen, K. Amatangelo, E. Dorrepaal, V. T. Eviner, O. Godoy, S. E. Hobbie, B. Hoorens, H. Kurokawa, N. Pérez-Harguindeguy, H. M. Quested, L. S. Santiago, D. A. Wardle, I. J. Wright, R. Aerts, S. D. Allison, P. Van Bodegom, V. Brovkin, A. Chatain, T. V. Callaghan, et al. Plant species traits are the predominant control on litter decomposition rates within biomes worldwide. *Ecology Letters*, 11(10):1065–1071, 2008. ISSN 1461023X. doi: 10.1111/j.1461-0248.2008.01219.x.

R. Costanza, R. D'Arge, R. De Groot, S. Farber, M. Grasso, B. Hannon, K. Limburg, S. Naeem, R. V. O'Neill, J. Paruelo, R. G. Raskin, P. Sutton, and M. Van Den Belt. The value of the world's ecosystem services and natural capital. *Nature*, 387(6630):253–260, 1997. ISSN 00280836. doi: 10.1038/387253a0.

B. R. Couvillion, G. D. Steyer, H. Wang, H. J. Beck, and J. M. Rybczyk. Forecasting the effects of coastal protection and restoration projects on wetland morphology in coastal Louisiana under multiple environmental uncertainty scenarios. *Journal of Coastal Research*, 67(SPEC. ISSUE):29–50, 2013. ISSN 07490208. doi: 10.2112/SI_67_3.

C. B. Craft, E. D. Seneca, and S. W. Broome. Loss on ignition and kjeldahl digestion for estimating organic carbon and total nitrogen in estuarine marsh soils: Calibration with dry combustion. *Estuaries*, 14(2):175–179, 1991. ISSN 01608347. doi: 10.2307/1351691.

C. B. Craft, E. D. Seneca, and S. W. Broome. Vertical Accretion in Microtidal Regularly and Irregularly Flooded Estuarine Marshes. *Estuarine, Coastal and Shelf Science*, 37(4):371–386, 1993. ISSN 0272-7714. doi: https://doi.org/10.1006/ecss.1993.1062.

S. Crooks, D. Herr, J. Tamelander, D. Laffoley, and J. Vandever. *Mitigating Climate Change through Restoration and Management of Coastal Wetlands and Near-shore Marine Ecosystems : Challenges and Opportunities.* World Bank, Washington, DC, 2011.

A. D'Alpaos and M. Marani. Reading the signatures of biologic–geomorphic feedbacks in salt-marsh landscapes. *Advances in Water Resources*, 93:265–275, 2016. ISSN 0309-1708. doi: https://doi.org/10.1016/j.advwatres.2015.09.004.

A. D'Alpaos, S. Lanzoni, M. Marani, S. Fagherazzi, and A. Rinaldo. Tidal network ontogeny: Channel initiation and early development. *Journal of Geophysical Research: Earth Surface*, 110(2):1–14, 2005. doi: 10.1029/2004JF000182.

A. D'Alpaos, S. Lanzoni, M. Marani, and A. Rinaldo. Landscape evolution in tidal embayments: Modeling the interplay of erosion, sedimentation, and vegetation dynamics. *Journal of Geophysical Research: Earth Surface*, 112(F1), 2007. doi: 10.1029/2006JF000537.

A. D'Alpaos, S. M. Mudd, and L. Carniello. Dynamic response of marshes to perturbations in suspended sediment concentrations and rates of relative sea level rise. *Journal of Geophysical Research: Earth Surface*, 116(F4), 2011. doi: 10.1029/2011JF002093.

A. D'Alpaos, L. Carniello, and A. Rinaldo. Statistical mechanics of wind wave-induced erosion in shallow tidal basins: Inferences from the Venice Lagoon. *Geophysical Research Letters*, 40(13):3402–3407, 2013. doi: https://doi.org/10.1002/grl.50666.

C. D'Alpaos and A. D'Alpaos. The valuation of ecosystem services in the venice lagoon: A multicriteria approach. *Sustainability (Switzerland)*, 13(17), 2021. doi: 10.3390/su13179485.

L. D'Alpaos. Fatti e misfatti di idraulica lagunare. La laguna di Venezia dalla diversione dei fiumi alle nuove opere delle bocche di porto. *La laguna di Venezia dalla diversione dei fiumi alle nuove opere delle bocche di porto*, pages –329, 2010.

W. W. Daniel. *Applied Nonparametric Statistics*. Houghton Mifflin, Boston, 1978.

N. Dankers and R. Laane. A comparison of wet oxidation and loss on ignition of organic material in suspended matter. *Environmental Technology Letters*, 4(7): 283–290, 1983. doi: 10.1080/09593338309384208.

E. A. Davidson and I. A. Janssens. Temperature sensitivity of soil carbon decomposition and feedbacks to climate change. *Nature*, 440:165–173, 2006. ISSN 1476-4687. doi: 10.1038/nature04514.

A. J. Davy, J. P. Bakker, and M. E. Figueroa. *Human modification of European salt marshes*, pages 311–335. University of California Press, Berkeley CA, USA, 2009. ISBN 9780520258921.

J. W. Day, A. Rismondo, F. Scarton, D. Are, and G. Cecconi. Relative sea level rise and Venice lagoon wetlands. *Journal of Coastal Conservation*, 4(1):27–34, 1998. ISSN 14000350. doi: 10.1007/BF02806486.

J. W. Day, J. Rybczyk, F. Scarton, A. Rismondo, D. Are, and G. Cecconi. Soil accretionary dynamics, sea-level rise and the survival of wetlands in Venice Lagoon: A field and modelling approach. *Estuarine, Coastal and Shelf Science*, 49(5):607–628, 1999. ISSN 02727714. doi: 10.1006/ecss.1999.0522.

J. W. Day, L. D. Britsch, S. R. Hawes, G. P. Shaffer, D. J. Reed, and D. Cahoon. Pattern and process of land loss in the Mississippi Delta: a spatial and temporal analysis of wetland habitat change. *Estuaries*, 23(4):425–438, 2000.

R. de Groot, L. Brander, S. van der Ploeg, R. Costanza, F. Bernard, L. Braat, M. Christie, N. Crossman, A. Ghermandi, L. Hein, S. Hussain, P. Kumar, A. McVittie, R. Portela, L. C. Rodriguez, P. ten Brink, and P. van Beukering. Global estimates of the value of ecosystems and their services in monetary units. *Ecosystem Services*, 1(1):50–61, jul 2012. ISSN 2212-0416. doi: 10.1016/J.ECOSER.2012.07.005.

S. De Gryze, L. Jassogne, H. Bossuyt, J. Six, and R. Merckx. Water repellence and soil aggregate dynamics in a loamy grassland soil as affected by texture. *European Journal of Soil Science*, 57(2):235–246, 2006. doi: https://doi.org/10.1111/j.1365-2389.2005.00733.x.

D. J. de Jong, Z. de Jong, and J. P. M. Mulder. Changes in area, geomorphology and sediment nature of salt marshes in the Oosterschelde estuary (SW Netherlands) due to tidal changes. *Hydrobiologia*, 282(1):303–316, 1994. ISSN 1573-5117. doi: 10.1007/BF00024638.

R. D. DeLaune, J. R. White, T. Elsey-Quirk, H. H. Roberts, and D. Q. Wang. Differences in long-term vs short-term carbon and nitrogen sequestration in a coastal river delta wetland: Implications for global budgets. *Organic Geochemistry*, 123:67–73, 2018. ISSN 01466380. doi: 10.1016/j.orggeochem.2018.06.007.

I. Djukic, S. Kepfer-Rojas, I. K. Schmidt, K. S. Larsen, C. Beier, B. Berg, K. Verheyen, A. Caliman, A. Paquette, A. Gutiérrez-Girón, A. Humber, A. Valdecantos, A. Petraglia, H. Alexander, A. Augustaitis, A. Saillard, A. C. R. Fernández, A. I. Sousa, A. I. Lillebø, A. da Rocha Gripp, et al. Early stage litter decomposition across biomes. *Science of the Total Environment*, 628-629: 1369–1394, 2018. ISSN 18791026. doi: 10.1016/j.scitotenv.2018.01.012.

J. P. Doody. 'Coastal Squeeze': An Historical Perspective. *Journal of Coastal Conservation*, 10(1-2):129–138, 2004. ISSN 14000350, 18747841. doi: 10.1007/bf02818949.

J. Z. Drexler, M. J. Davis, I. Woo, and S. De La Cruz. Carbon Sources in the Sediments of a Restoring vs. Historically Unaltered Salt Marsh. *Estuaries and Coasts*, 43(6):1345–1360, 2020. ISSN 15592731. doi: 10.1007/s12237-020-00748-7.

C. M. Duarte. *Global Loss of Coastal Habitats Rates, Causes and Consequences.* Fundacion BBVA, Bilbao, 2009. ISBN 9788496515840.

C. M. Duarte, J. J. Middelburg, and N. Caraco. Major role of marine vegetation on the oceanic carbon cycle. *Biogeosciences*, 2(1):1–8, 2005. ISSN 17264170. doi: 10.5194/bg-2-1-2005.

C. M. Duarte, W. C. Dennison, R. J. W. Orth, and T. J. B. Carruthers. The Charisma of Coastal Ecosystems: Addressing the Imbalance. *Estuaries and Coasts*, 31:233–238, 2008. doi: 10.1007/s12237-008-9038-7.

C. M. Duarte, I. J. Losada, I. E. Hendriks, I. Mazarrasa, and N. Marbà. The role of coastal plant communities for climate change mitigation and adaptation. *Nature Climate Change*, 3(11):961–968, 2013. ISSN 1758678X. doi: 10.1038/nclimate1970.

M. S. Duvall, P. L. Wiberg, and M. L. Kirwan. Controls on Sediment Suspension, Flux, and Marsh Deposition near a Bay-Marsh Boundary. *Estuaries and Coasts*, 42(2):403–424, 2019. ISSN 15592731. doi: 10.1007/s12237-018-0478-4.

S. Enríquez, C. M. Duarte, and K. Sand-Jensen. Patterns in decomposition rates among photosynthetic organisms: the importance of detritus C:N:P content. *Oecologia*, 94(4):457–471, 1993. ISSN 00298549. doi: 10.1007/BF00566960.

G. Eshel, G. J. Levy, U. Mingelgrin, and M. J. Singer. Critical Evaluation of the Use of Laser Diffraction for Particle-Size Distribution Analysis. *Soil Science Society of America Journal*, 68(3):736–743, 2004. doi: https://doi.org/10.2136/sssaj2004.7360.

C. J. Ewers Lewis, J. A. Baldock, B. Hawke, P. S. Gadd, A. Zawadzki, H. Heijnis, G. E. Jacobsen, K. Rogers, and P. I. Macreadie. Impacts of land reclamation on tidal marsh 'blue carbon' stocks. *Science of the Total Environment*, 672: 427–437, 2019. ISSN 18791026. doi: 10.1016/j.scitotenv.2019.03.345.

C. J. Ewers Lewis, M. A. Young, D. Ierodiaconou, J. A. Baldock, B. Hawke, J. Sanderman, P. E. Carnell, and P. I. Macreadie. Drivers and modelling of blue carbon stock variability in sediments of southeastern Australia. *Biogeosciences*, 17(7):2041–2059, apr 2020. ISSN 17264189. doi: 10.5194/bg-17-2041-2020.

S. Fagherazzi, A. Bortoluzzi, W. E. Dietrich, A. Adami, S. Lanzoni, M. Marani, and A. Rinaldo. Tidal networks: 1. Automatic network extraction and preliminary scaling features from digital terrain maps. *Water Resources Research*, 35 (12):3891–3904, 1999. doi: https://doi.org/10.1029/1999WR900236.

S. Fagherazzi, M. L. Kirwan, S. M. Mudd, G. R. G. Guntenspergen, S. Temmerman, A. D'Alpaos, J. Van De Koppel, J. J. M. Rybczyk, E. Reyes, C. Craft, C. Craft, and J. Clough. Numerical models of salt marsh evolution: Ecological, geomorphic, and climatic factors. *Reviews of Geophysics*, 50(1), 2012. doi: https://doi.org/10.1029/2011RG000359.

S. Fagherazzi, G. Mariotti, P. L. Wiberg, and K. J. McGlathery. Marsh Collapse Does Not Require Sea Level Rise. *Oceanography*, 26(3):70–77, 2013. ISSN 10428275, 2377617X. doi: 10.5670/oceanog.2013.47.

S. Fagherazzi, G. Mariotti, N. Leonardi, A. Canestrelli, W. Nardin, and W. S. Kearney. Salt Marsh Dynamics in a Period of Accelerated Sea Level Rise. *Journal of Geophysical Research: Earth Surface*, 125(8):e2019JF005200, 2020. doi: https://doi.org/10.1029/2019JF005200.

M. Fan and R. C. Brown. Comparison of the loss-on-ignition and thermogravimetric analysis techniques in measuring unburned carbon in coal fly ash. *Energy & fuels*, 15(6):1414–1417, 2001.

V. Favero and R. Seranderei Barbero. Origine ed evoluzione della Laguna di Venezia - bacino meridionale. *Lavori - Società Veneziana di Scienze Naturali*, 5:49–71, 1980.

V. Favero and R. Serandrei-Barbero. Evoluzione paleoambientale della laguna di Venezia nell'area archeologica tra Burano e canale S. Felice. *Lavori - Società Veneziana di Scienze Naturali*, 6:119–134, 1981.

A. Finotello, D. Tognin, L. Carniello, M. Ghinassi, E. Bertuzzo, and A. D'Alpaos. Hydrodynamic feedbacks of salt-marsh loss in shallow microtidal back-barrier systems. *Earth and Space Science Open Archive*, page 32, 2022. doi: 10.1002/essoar.10511787.2.

D. FitzGerald and Z. Hughes, editors. *Salt Marshes: Function, Dynamics, and Stresses*. Cambridge University Press, Cambridge, 2021. doi: 10.1017/9781316888933.

H. Ford, A. Garbutt, C. Ladd, J. Malarkey, and M. W. Skov. Soil stabilization linked to plant diversity and environmental context in coastal wetlands. *Journal* *of Vegetation Science*, 27(2):259–268, 2016. doi: https://doi.org/10.1111/jvs.12367.

H. Ford, A. Garbutt, M. Duggan-Edwards, J. F. Pagès, R. Harvey, C. Ladd, and M. W. Skov. Large-scale predictions of salt-marsh carbon stock based on simple observations of plant community and soil type. *Biogeosciences*, 16(2):425–436, 2019. doi: 10.5194/bg-16-425-2019.

G. Frangipane, M. Pistolato, E. Molinaroli, S. Guerzoni, and D. Tagliapietra. Comparison of loss on ignition and thermal analysis stepwise methods for determination of sedimentary organic matter. *Aquatic Conservation: Marine and Freshwater Ecosystems*, 19(1):24–33, 2009. doi: https://doi.org/10.1002/aqc.970.

J. French. Tidal marsh sedimentation and resilience to environmental change: Exploratory modelling of tidal, sea-level and sediment supply forcing in predominantly allochthonous systems. *Marine Geology*, 235(1):119–136, 2006. ISSN 0025-3227. doi: https://doi.org/10.1016/j.margeo.2006.10.009.

J. R. French and T. Spencer. Dynamics of sedimentation in a tide-dominated backbarrier salt marsh, Norfolk, UK. *Marine Geology*, 110(3):315–331, 1993. ISSN 0025-3227. doi: https://doi.org/10.1016/0025-3227(93)90091-9.

G. T. Freschet, R. Aerts, and J. H. C. Cornelissen. A plant economics spectrum of litter decomposability. *Functional Ecology*, 26(1):56–65, 2012. ISSN 02698463. doi: 10.1111/j.1365-2435.2011.01913.x.

C. T. Friedrichs and O. S. Madsen. Nonlinear diffusion of the tidal signal in frictionally dominated embayments. *Journal of Geophysical Research: Oceans*, 97(C4):5637–5650, 1992. doi: https://doi.org/10.1029/92JC00354.

C. T. Friedrichs and J. E. Perry. Tidal Salt Marsh Morphodynamics: A Synthesis. *Journal of Coastal Research*, 27:7–37, 2001. ISSN 07490208, 15515036.

K. B. Gedan, B. Silliman, and M. Bertness. Centuries of Human-Driven Change in Salt Marsh Ecosystems. *Annual Review of Marine Science*, 1(117-41), 2009. ISSN 1941-1405. doi: 10.1146/annurev.marine.010908.163930.

L. Geng, A. D'Alpaos, A. Sgarabotto, Z. Gong, and S. Lanzoni. Intertwined Eco-Morphodynamic Evolution of Salt Marshes and Emerging Tidal Channel Networks. *Water Resources Research*, 57(11), 2021. doi: https://doi.org/10.1029/2021WR030840.

J. M. Gieskes, H. Elwany, L. Rasmussen, S. Han, A. Rathburn, and D. D. Deheyn. Salinity variations in the Venice Lagoon, Italy: Results from the SIOSED Project, May 2005–February 2007. *Marine Chemistry*, 154:77–86, aug 2013. ISSN 0304-4203. doi: 10.1016/J.MARCHEM.2013.05.011.

G. C. H. Goodwin and S. M. Mudd. Detecting the Morphology of Prograding and Retreating Marsh Margins—Example of a Mega-Tidal Bay. *Remote Sensing*, 12(1), 2020. ISSN 2072-4292. doi: 10.3390/rs12010013.

C. Gorham, P. Lavery, J. J. Kelleway, C. Salinas, and O. Serrano. Soil Carbon Stocks Vary Across Geomorphic Settings in Australian Temperate Tidal Marsh Ecosystems. *Ecosystems*, 24(2):319–334, mar 2021. ISSN 14350629. doi: 10.1007/S10021-020-00520-9.

R. Greenberg, J. Maldonado, S. Droege, and M. V. McDonald. Tidal marshes: A global perspective on the evolution and conservation of their terrestrial vertebrates. *BioScience*, 56(8):675–685, 2006. doi: 10.1641/0006-3568(2006)56[675:TMAGPO]2.0.CO;2.

J. Gu, M. Luo, X. Zhang, G. Christakos, S. Agusti, C. M. Duarte, and J. Wu. Losses of salt marsh in China: Trends, threats and management. *Estuarine, Coastal and Shelf Science*, 214:98–109, dec 2018. ISSN 0272-7714. doi: 10.1016/J.ECSS.2018.09.015.

P. J. Halupa and B. L. Howes. Effects of tidally mediated litter moisture content on decomposition of Spartina alterniflora and S. patens. *Marine Biology*, 123 (2):379–391, 1995. ISSN 1432-1793. doi: 10.1007/BF00353629.

K. Hansen, C. Butzeck, A. Eschenbach, A. Gröngröft, K. Jensen, and E.-M. Pfeiffer. Factors influencing the organic carbon pools in tidal marsh soils of the Elbe estuary (Germany). *Journal of Soils and Sediments*, 17:47–60, 2017. doi: 10.1007/s11368-016-1500-8.

H. Hartnett, R. Keil, J. Hedges, and A. Devol. Influence of oxygen exposure time on organic carbon preservation in continental margin sediments. *Nature*, 391: 572–574, 1998. doi: 10.1038/35351.

O. Heiri, A. F. Lotter, and G. Lemcke. Loss on ignition as a method for estimating organic and carbonate content in sediments: reproducibility and comparability of results. *Journal of Paleolimnology*, 25(1):101–110, 2001. doi: 10.1023/A: 1008119611481.

M. A. Hemminga, J. De Leeuw, W. De Munck, and B. P. Koutstaal. Decomposition in estuarine salt marshes: the effect of soil salinity and soil water content. *Vegetatio*, 94:25–33, 1991. doi: 10.1007/BF00044913.

F. Hjulstrom. Transportation of detritus by moving water. *Recent marine sediments*, pages 5–31, 1939.

J. R. Holmquist, L. Windham-Myers, N. Bliss, S. Crooks, J. T. Morris, J. P. Megonigal, T. Troxler, D. Weller, J. Callaway, J. Drexler, M. C. Ferner, M. E. Gonneea, K. D. Kroeger, L. Schile-Beers, I. Woo, K. Buffington, J. Breithaupt, B. M. Boyd, L. N. Brown, N. Dix, et al. Accuracy and precision of tidal wetland soil carbon mapping in the conterminous United States. *Scientific Reports*, 8 (9478), 2018. ISSN 20452322. doi: 10.1038/s41598-018-26948-7.

M. J. J. Hoogsteen, E. A. Lantinga, E. J. Bakker, J. C. J. Groot, and P. A. Tittonell. Estimating soil organic carbon through loss on ignition: effects of ignition conditions and structural water loss. *European Journal of Soil Science*, 66(2):320–328, 2015. doi: https://doi.org/10.1111/ejss.12224.

J. Howard, S. Hoyt, K. Isensee, M. Telszewski, and E. Pidgeon. *Coastal blue carbon: methods for assessing carbon stocks and emissions factors in mangroves, tidal salt marshes, and seagrasses.* Number Ci. Conservation International, Intergovernmental Oceanographic Commission of UNESCO, International Union for Conservation of Nature, Arlington, Virginia, USA, 2014.

J. Howard, A. Sutton-Grier, D. Herr, J. Kleypas, E. Landis, E. Mcleod, E. Pidgeon, and S. Simpson. Clarifying the role of coastal and marine systems in climate mitigation. *Frontiers in Ecology and the Environment*, 15(1):42–50, 2017. doi: https://doi.org/10.1002/fee.1451.

P. J. A. Howard and D. M. Howard. Use of organic carbon and loss-on-ignition to estimate soil organic matter in different soil types and horizons. *Biology and Fertility of Soils*, 9(4):306–310, 1990. ISSN 1432-0789. doi: 10.1007/BF00634106.

N. C. Howes, D. M. FitzGerald, Z. J. Hughes, I. Y. Georgiou, M. A. Kulp, M. D. Miner, J. M. Smith, and J. A. Barras. Hurricane-induced failure of low salinity wetlands. *Proceedings of the National Academy of Sciences*, 107(32):14014–14019, 2010. doi: 10.1073/pnas.0914582107.

R. Hughes and O. Paramor. On the loss of saltmarshes in south-east England and methods for their restoration. *Journal of Applied Ecology*, 41:440–448, 2004. doi: 10.1111/j.0021-8901.2004.00915.x.

V. Ingegnoli and E. Giglio. Proposal of a new method of ecological evaluation of vegetation: The case study of the vegetation of the Venice lagoon landscape and of its salt marshes. *Annali di Botanica*, 4:95–114, 2004.

K. Inglett, P. Inglett, K. Reddy, and T. Osborne. Temperature Sensitivity of Greenhouse Gas Production in Wetland Soils of Different Vegetation. *Biogeochemistry*, 108:77–90, 2012. doi: 10.1007/s10533-011-9573-3.

D. Ivajnšič, M. Kaligarič, E. Fantinato, S. Del Vecchio, and G. Buffa. The fate of coastal habitats in the Venice Lagoon from the sea level rise perspective. *Applied Geography*, 98:34–42, 2018. ISSN 01436228. doi: 10.1016/j.apgeog.2018.07.005.

R. B. Jackson, K. Lajtha, S. E. Crow, G. Hugelius, M. G. Kramer, and G. Piñeiro. The Ecology of Soil Carbon: Pools, Vulnerabilities, and Biotic and Abiotic Controls. *Annual Review of Ecology, Evolution, and Systematics*, 48:419–445, 2017. ISSN 15452069. doi: 10.1146/annurev-ecolsys-112414-054234.

J. L. Jensen, P. Schjønning, C. W. Watts, B. T. Christensen, and L. J. Munkholm. Soil texture analysis revisited: Removal of organic matter matters more than ever. *PLOS ONE*, 12(5):1–10, 2017. doi: 10.1371/journal.pone.0178039.

E. Kazakou, C. Violle, C. Roumet, C. Pintor, O. Gimenez, and E. Garnier. Litter quality and decomposability of species from a Mediterranean succession depend on leaf traits but not on nitrogen supply. *Annals of Botany*, 104(6):1151–1161, 2009. ISSN 03057364. doi: 10.1093/aob/mcp202.

J. J. Kelleway, N. Saintilan, P. I. Macreadie, and P. J. Ralph. Sedimentary Factors are Key Predictors of Carbon Storage in SE Australian Saltmarshes. *Ecosystems*, 19(5):865–880, 2016. ISSN 14329840. doi: 10.1007/s10021-016-9972-3.

A. C. Kemp, B. P. Horton, J. P. Donnelly, M. E. Mann, M. Vermeer, and S. Rahmstorf. Climate related sea-level variations over the past two millennia. *Proceedings of the National Academy of Sciences*, 108(27):11017–11022, 2011. doi: 10.1073/pnas.1015619108.

M. G. Kendall. A measure of rank correlation. *Biometrika*, 30(1-2):81–93, 1938. ISSN 0006-3444. doi: 10.1093/biomet/30.1-2.81.

J. A. Keuskamp, B. J. J. Dingemans, T. Lehtinen, J. M. Sarneel, and M. M. Hefting. Tea Bag Index: A novel approach to collect uniform decomposition data across ecosystems. *Methods in Ecology and Evolution*, 4(11):1070–1075, 2013. ISSN 2041210X. doi: 10.1111/2041-210X.12097.

H. V. Kibby, J. L. Gallagher, and W. D. Sanville. *Field guide to evaluate net primary production of wetlands.* Environmental Research Laboratory, Office of Research and Development, U.S. Environmental Protection Agency, Corvallis, Or, 1980.

M. U. F. Kirschbaum. The temperature dependence of soil organic matter decomposition, and the effect of global warming on soil organic C storage. *Soil Biology and Biochemistry*, 27(6):753–760, 1995. ISSN 0038-0717. doi: https://doi.org/10.1016/0038-0717(94)00242-S.

M. L. Kirwan and L. K. Blum. Enhanced decomposition offsets enhanced productivity and soil carbon accumulation in coastal wetlands responding to climate change. *Biogeosciences*, 8(4):987–993, 2011. ISSN 17264170. doi: 10.5194/bg-8-987-2011.

M. L. Kirwan and J. P. Megonigal. Tidal wetland stability in the face of human impacts and sea-level rise. *Nature*, 504(7478):53–60, 2013. ISSN 00280836. doi: 10.1038/nature12856.

M. L. Kirwan and S. M. Mudd. Response of salt-marsh carbon accumulation to climate change. *Nature*, 489(7417):550–553, 2012. ISSN 1476-4687. doi: 10.1038/nature11440.

M. L. Kirwan and A. B. Murray. A coupled geomorphic and ecological model of tidal marsh evolution. *Proceedings of the National Academy of Sciences*, 104 (15):6118–6122, apr 2007. ISSN 0027-8424. doi: 10.1073/PNAS.0700958104.

M. L. Kirwan, G. R. Guntenspergen, A. D'Alpaos, J. T. Morris, S. M. Mudd, and S. Temmerman. Limits on the adaptability of coastal marshes to rising sea level. *Geophysical Research Letters*, 37(23), 2010. doi: 10.1029/2010GL045489.

M. L. Kirwan, J. A. Langley, G. R. Guntenspergen, and J. P. Megonigal. The impact of sea-level rise on organic matter decay rates in Chesapeake Bay brackish tidal marshes. *Biogeosciences*, 10(3):1869–1876, 2013. ISSN 17264170. doi: 10.5194/bg-10-1869-2013.

M. L. Kirwan, G. R. Guntenspergen, and J. A. Langley. Temperature sensitivity of organic-matter decay in tidal marshes. *Biogeosciences*, 11(17):4801–4808, 2014. ISSN 17264170. doi: 10.5194/bg-11-4801-2014.

M. L. Kirwan, S. Temmerman, E. E. Skeehan, G. R. Guntenspergen, and S. Fagherazzi. Overestimation of marsh vulnerability to sea level rise. *Nature Climate Change*, 6(3):253–260, 2016. ISSN 1758-6798. doi: 10.1038/nclimate2909.

A. S. Kolker, S. L. Goodbred, S. Hameed, and J. K. Cochran. High-resolution records of the response of coastal wetland systems to long-term and short-term sea-level variability. *Estuarine, Coastal and Shelf Science*, 84(4):493–508, 2009. ISSN 02727714. doi: 10.1016/j.ecss.2009.06.030.

S. I. Lang, J. H. C. Cornelissen, T. Klahn, R. S. P. Van Logtestijn, R. Broekman, W. Schweikert, and R. Aerts. An experimental comparison of chemical traits and litter decomposition rates in a diverse range of subarctic bryophyte, lichen and vascular plant species. *Journal of Ecology*, 97(5):886–900, 2009. ISSN 00220477. doi: 10.1111/j.1365-2745.2009.01538.x.

J. A. Langley, N. C. Johnson, and G. W. Koch. Mycorrhizal Status Influences the

Rate but not the Temperature Sensitivity of Soil Respiration. *Plant and Soil*, 277(1):335–344, 2005. ISSN 1573-5036. doi: 10.1007/s11104-005-7932-3.

J. Lee, B. Kim, J. Noh, C. Lee, I. Kwon, B. O. Kwon, J. Ryu, J. Park, S. Hong, S. Lee, S. G. Kim, S. Son, H. J. Yoon, J. Yim, J. Nam, K. Choi, and J. S. Khim. The first national scale evaluation of organic carbon stocks and sequestration rates of coastal sediments along the West Sea, South Sea, and East Sea of South Korea. *Science of The Total Environment*, 793, nov 2021. ISSN 0048-9697. doi: 10.1016/J.SCITOTENV.2021.148568.

J.-C. Lefeuvre, V. Bouchard, E. Feunteun, S. Grare, P. Laffaille, and A. Radureau. European salt marshes diversity and functioning: The case study of the Mont Saint-Michel bay, France. *Wetlands Ecology and Management*, 8:147–161, 2000.

J.-C. Lefeuvre, P. Laffaille, E. Feunteun, V. Bouchard, and A. Radureau. Biodiversity in salt marshes: from patrimonial value to ecosystem functioning. The case study of the Mont-Saint-Michel bay. *Comptes Rendus Biologies*, 326:125–131, 2003. ISSN 1631-0691. doi: https://doi.org/10.1016/S1631-0691(03)00049-0.

L. A. Leonard. Controls of sediment transport and deposition in an incised mainland marsh basin, southeastern North Carolina. *Wetlands*, 17(2):263–274, 1997. ISSN 1943-6246. doi: 10.1007/BF03161414.

L. A. Leonard and M. E. Luther. Flow hydrodynamics in tidal marsh canopies. *Limnology and Oceanography*, 40(8):1474–1484, 1995. doi: https://doi.org/10.4319/lo.1995.40.8.1474.

L. A. Leonard, P. Wren, and R. Beavers. Flow dynamics and sedimentation in Spartina alterniflora and Phragmites australis marshes of the Chesapeake Bay. *Wetlands*, 22(2):415–424, 2002. doi: 10.1672/0277-5212(2002)022[0415:FDASIS]2.0.CO;2.

N. Leonardi, N. K. Ganju, and S. Fagherazzi. A linear relationship between wave power and erosion determines salt-marsh resilience to violent storms and hurricanes. *Proceedings of the National Academy of Sciences*, 113(1):64–68, 2016. doi: 10.1073/pnas.1510095112.

N. Leonardi, I. Carnacina, C. Donatelli, N. K. Ganju, A. J. Plater, M. Schuerch, and S. Temmerman. Dynamic interactions between coastal storms and salt marshes: A review. *Geomorphology*, 301:92 – 107, 2018. doi: 10.1016/j.geomorph.2017.11.001.

X. Li, B. Cui, Q. Yang, H. Tian, Y. Lan, T. Wang, and Z. Han. Detritus quality controls macrophyte decomposition under different nutrient concentrations in a eutrophic shallow lake, North China. *PLoS ONE*, 7(7), 2012. ISSN 19326203. doi: 10.1371/journal.pone.0042042.

C. E. Lovelock and C. M. Duarte. Dimensions of blue carbon and emerging perspectives. *Biology Letters*, 15, mar 2019. ISSN 1744957X. doi: 10.1098/rsbl.2018.0781.

R. A. MacKenzie and M. Dionne. Habitat heterogeneity: Importance of salt marsh pools and high marsh surfaces to fish production in two Gulf of Maine salt marshes. *Marine Ecology Progress Series*, 368:217–230, 2008. ISSN 01718630. doi: 10.3354/meps07560.

P. I. Macreadie, Q. R. Ollivier, J. J. Kelleway, O. Serrano, P. E. Carnell, C. J. Ewers Lewis, T. B. Atwood, J. Sanderman, J. Baldock, R. M. Connolly, C. M. Duarte, P. S. Lavery, A. Steven, and C. E. Lovelock. Carbon sequestration by Australian tidal marshes. *Scientific Reports*, 7(1):44071, mar 2017. ISSN 2045-2322. doi: 10.1038/srep44071.

P. I. Macreadie, A. Anton, J. Raven, N. Beaumont, R. M. R. Connolly, D. D. A. Friess, J. J. Kelleway, H. Kennedy, T. Kuwae, P. P. S. Lavery, C. E. Lovelock, D. A. Smale, E. T. Apostolaki, T. B. Atwood, J. Baldock, T. S. Bianchi, G. L. Chmura, B. D. Eyre, J. W. Fourqurean, J. M. Hall-Spencer, et al. The future of Blue Carbon science. *Nature Communications*, 10(1):1–13, 2019. ISSN 2041-1723. doi: 10.1038/s41467-019-11693-w.

Y. Mao, Q. Ma, J. Lin, Y. Chen, Q. Shu, and T. Spencer. Distribution and Sources of Organic Carbon in Surface Intertidal Sediments of the Rudong Coast, Jiangsu Province, China. *Journal of Marine Science and Engineering*, 9(992), 2021. ISSN 2077-1312. doi: 10.3390/jmse9090992.

M. Marani, S. Silvestri, E. Belluco, M. Camuffo, A. D'Alpaos, S. Lanzoni, A. Marani, and A. Rinaldo. Patterns in tidal environments: Salt-marsh channel networks and vegetation. In *International Geoscience and Remote Sensing Symposium (IGARSS)*, volume 5, pages 3269 – 3271, 2003.

M. Marani, S. Lanzoni, S. Silvestri, and A. Rinaldo. Tidal landforms , patterns of halophytic vegetation and the fate of the lagoon of Venice. *Journal of Marine Systems*, 51:191–210, 2004. doi: 10.1016/j.jmarsys.2004.05.012.

M. Marani, E. Belluco, S. Ferrari, S. Silvestri, A. D'Alpaos, S. Lanzoni, A. Feola, and A. Rinaldo. Analysis, synthesis and modelling of high-resolution observations of salt-marsh eco-geomorphological patterns in the Venice lagoon. *Estuarine, Coastal and Shelf Science*, 69(3-4):414–426, 2006a. ISSN 02727714. doi: 10.1016/j.ecss.2006.05.021.

M. Marani, S. Silvestri, E. Belluco, N. Ursino, A. Comerlati, O. Tosatto, and M. Putti. Spatial organization and ecohydrological interactions in oxygen-limited vegetation ecosystems. *Water Resources Research*, 42(6), 2006b. doi: https://doi.org/10.1029/2005WR004582.

M. Marani, A. D'Alpaos, S. Lanzoni, L. Carniello, and A. Rinaldo. Biologically-controlled multiple equilibria of tidal landforms and the fate of the Venice lagoon. *Geophysical Research Letters*, 34(11), 2007. doi: 10.1029/2007GL030178.

M. Marani, A. D'Alpaos, S. Lanzoni, L. Carniello, and A. Rinaldo. The importance of being coupled: Stable states and catastrophic shifts in tidal biomorphodynamics. *Journal of Geophysical Research: Earth Surface*, 115(F4), 2010. doi: https://doi.org/10.1029/2009JF001600.

M. Marani, A. D'Alpaos, S. Lanzoni, and M. Santalucia. Understanding and predicting wave erosion of marsh edges. *Geophysical Research Letters*, 38(21), 2011. doi: 10.1029/2011GL048995.

M. Marani, C. Da Lio, and A. D'Alpaos. Vegetation engineers marsh morphology through multiple competing stable states. *Proceedings of the National Academy of Sciences of the United States of America*, 110(9):3259–3263, 2013. ISSN 00278424. doi: 10.1073/pnas.1218327110.

G. Mariotti and S. Fagherazzi. Critical width of tidal flats triggers marsh collapse in the absence of sea-level rise. *Proceedings of the National Academy of Sciences*, 110(14):5353–5356, 2013. doi: 10.1073/pnas.1219600110.

K. L. McKee and W. H. Patrick. The Relationship of Smooth Cordgrass (Spartina alterniflora) to Tidal Datums: A Review. *Estuaries*, 11(3):143–151, 1988. ISSN 01608347. doi: 10.2307/1351966.

E. McLeod, G. L. Chmura, S. Bouillon, R. Salm, M. Björk, C. M. Duarte, C. E. Lovelock, W. H. Schlesinger, and B. R. Silliman. A blueprint for blue carbon: Toward an improved understanding of the role of vegetated coastal habitats in sequestering CO2. *Frontiers in Ecology and the Environment*, 9(10):552–560, 2011. ISSN 15409295. doi: 10.1890/110004.

C. J. Mcowen, L. V. Weatherdon, J.-W. Van Bochove, E. Sullivan, S. Blyth, C. Zockler, D. Stanwell-Smith, N. Kingston, C. S. Martin, M. Spalding, and S. Fletcher. A global map of saltmarshes. *Biodiversity Data Journal*, 5(1), 2017. ISSN 13142828. doi: 10.3897/BDJ.5.e11764.

N. D. McTigue, Q. A. Walker, and C. A. Currin. Refining Estimates of Greenhouse Gas Emissions From Salt Marsh “Blue Carbon” Erosion and Decomposition. *Frontiers in Marine Science*, 8, 2021. ISSN 2296-7745. doi: 10.3389/fmars.2021.661442.

R. A. Mel, D. P. Viero, L. Carniello, A. Defina, and L. D’Alpaos. The first operations of Mo.S.E. system to prevent the flooding of Venice: Insights on the hydrodynamics of a regulated lagoon. *Estuarine, Coastal and Shelf Science*, 261: 107547, 2021. ISSN 0272-7714. doi: https://doi.org/10.1016/j.ecss.2021.107547.

J. J. Middelburg, J. Nieuwenhuize, R. K. Lubberts, and O. Van De Plassche. Organic carbon isotope systematics of coastal marshes. *Estuarine, Coastal and Shelf Science*, 45(5):681–687, 1997. ISSN 02727714. doi: 10.1006/ecss.1997.0247.

C. B. Miller, A. B. Rodriguez, M. C. Bost, B. A. Mckee, and N. D. Mctigue. Carbon accumulation rates are highest at young and expanding salt marsh edges. *Communications Earth & Environment Environment*, 3, 2022. ISSN 2662-4435. doi: 10.1038/s43247-022-00501-x.

S. Mitra, R. Wassmann, and P. L. G. Vlek. An appraisal of global wetland area and its organic carbon stock. *Current Science*, 88(1):25–35, 2005. ISSN 00113891.

W. J. Mitsch and J. G. Gosselink. The value of wetlands: importance of scale and landscape setting. *Ecological Economics*, 35(1):25–33, 2000. ISSN 0921-8009. doi: https://doi.org/10.1016/S0921-8009(00)00165-8.

K. B. Moffett, S. M. Gorelick, R. G. McLaren, and E. A. Sudicky. Salt marsh ecohydrological zonation due to heterogeneous vegetation–groundwater–surface water interactions. *Water Resources Research*, 48(2), 2012. doi: https://doi.org/10.1029/2011WR010874.

G. Y. Moinet, M. Moinet, J. E. Hunt, C. Rumpel, A. Chabbi, and P. Millard. Temperature sensitivity of decomposition decreases with increasing soil organic matter stability. *Science of the Total Environment*, 704, 2020. ISSN 18791026. doi: 10.1016/j.scitotenv.2019.135460.

I. Möller, M. Kudella, F. Rupprecht, T. Spencer, M. Paul, B. Van Wesenbeeck, G. Wolters, K. Jensen, T. Bouma, M. Miranda-Lange, M. Miranda-Lange, and S. Schimmels. Wave attenuation over coastal salt marshes under storm surge conditions. *Nature Geoscience*, 7(10):727–731, 2014. doi: 10.1038/NGEO2251.

P. A. Montagna and E. Ruber. Decomposition ofSpartina alterniflora in different seasons and habitats of a Northern Massachusetts salt marsh, and a comparison with other Atlantic regions. *Estuaries*, 3(1):61–64, 1980. ISSN 0160-8347. doi: 10.2307/1351935.

D. C. Montgomery. *Design and analysis of experiments.* John Wiley and Sons, New York, 8th ed. edition, 2012.

D. H. Mook and C. M. Hoskin. Organic determinations by ignition: Caution advised. *Estuarine Coastal and Shelf Science*, 15:697–699, 1982.

G. E. Moore, D. M. Burdick, C. R. Peter, and D. R. Keirstead. Belowground Biomass of Phragmites australis in Coastal Marshes. *Northeastern Naturalist*, 19(4):611–626, 2012. ISSN 10926194, 19385307. doi: 10.1656/045.019.0406.

J. T. Morris and G. J. Whiting. Emission of gaseous carbon dioxide from salt-marsh sediments and its relation to other carbon losses. *Estuaries*, 9(1):9–19, 1986. ISSN 0160-8347. doi: 10.2307/1352188.

J. T. Morris, P. V. Sundareshwar, C. T. Nietch, B. Kjerfve, and D. R. Cahoon. Responses of coastal wetlands to rising sea level. *Ecology*, 83(10):2869–2877, 2002. ISSN 00129658. doi: 10.1890/0012-9658(2002)083[2869:ROCWTR]2.0.CO;2.

J. T. Morris, D. C. Barber, J. C. Callaway, R. Chambers, S. C. Hagen, C. S. Hopkinson, B. J. Johnson, P. Megonigal, S. C. Neubauer, T. Troxler, and C. Wigand. Contributions of organic and inorganic matter to sediment volume and accretion in tidal wetlands at steady state. *Earth's Future*, 4(4):110–121, 2016. ISSN 23284277. doi: 10.1002/2015EF000334.

S. M. Mudd. The life and death of salt marshes in response to anthropogenic disturbance of sediment supply. *Geology*, 39(5):511–512, 2011. ISSN 0091-7613. doi: 10.1130/focus052011.1.

S. M. Mudd, S. Fagherazzi, J. T. Morris, and D. J. Furbish. *Flow, Sedimentation, and Biomass Production on a Vegetated Salt Marsh in South Carolina: Toward a Predictive Model of Marsh Morphologic and Ecologic Evolution*, chapter 9, pages 165–188. American Geophysical Union (AGU), 2004. ISBN 9781118665114. doi: https://doi.org/10.1029/CE059p0165.

S. M. Mudd, S. M. Howell, and J. T. Morris. Impact of dynamic feedbacks between sedimentation, sea-level rise, and biomass production on near-surface marsh stratigraphy and carbon accumulation. *Estuarine, Coastal and Shelf Science*, 82(3):377–389, 2009. ISSN 0272-7714. doi: https://doi.org/10.1016/j.ecss.2009.01.028.

S. M. Mudd, A. D'Alpaos, and J. T. Morris. How does vegetation affect sedimentation on tidal marshes? Investigating particle capture and hydrodynamic controls on biologically mediated sedimentation. *Journal of Geophysical Research: Earth Surface*, 115(F3), 2010. doi: https://doi.org/10.1029/2009JF001566.

P. Mueller, L. M. Schile-Beers, T. J. Mozdzer, G. L. Chmura, T. Dinter, Y. Kuzyakov, A. V. De Groot, P. Esselink, C. Smit, A. D'Alpaos, C. Ibáñez,

M. Lazarus, U. Neumeier, B. J. Johnson, A. H. Baldwin, S. A. Yarwood, D. I. Montemayor, Z. Yang, J. Wu, K. Jensen, and S. Nolte. Global-change effects on early-stage decomposition processes in tidal wetlands-implications from a global survey using standardized litter. *Biogeosciences*, 15(10):3189–3202, 2018. ISSN 17264189. doi: 10.5194/bg-15-3189-2018.

P. Mueller, N. Ladiges, A. Jack, G. Schmiedl, L. Kutzbach, K. Jensen, and S. Nolte. Assessing the long-term carbon-sequestration potential of the semi-natural salt marshes in the European Wadden Sea. *Ecosphere*, 10(1), 2019. ISSN 21508925. doi: 10.1002/ecs2.2556.

P. J. Mumby. Statistical power of non-parametric tests: a quick guide for designing sampling strategies. *Marine pollution bulletin*, 44(1):85–87, 2002. ISSN 0025-326X. doi: 10.1016/s0025-326x(01)00097-2.

B. W. Murphy, B. R. Wilson, and T. Koen. Mathematical Functions to Model the Depth Distribution of Soil Organic Carbon in a Range of Soils from New South Wales, Australia under Different Land Uses. *Soil Systems*, 3(3), 2019. doi: 10.3390/soilsystems3030046.

C. Nellemann, E. Corcoran, C. M. Duarte, L. Valdés, C. De Young, L. Fonseca, and G. Grimsditch. *Blue carbon: A Rapid Response Assessment.* UN Environment, GRID-Arendal, 2009. ISBN 9788277010601.

S. C. Neubauer. Contributions of mineral and organic components to tidal freshwater marsh accretion. *Estuarine, Coastal and Shelf Science*, 78(1):78–88, 2008. ISSN 0272-7714. doi: https://doi.org/10.1016/j.ecss.2007.11.011.

B. Neumann, A. T. Vafeidis, J. Zimmermann, and R. J. Nicholls. Future Coastal Population Growth and Exposure to Sea-Level Rise and Coastal Flooding - A Global Assessment. *PLOS ONE*, 10(3):1–34, 2015. doi: 10.1371/journal.pone.0118571.

T. Nguyen, H. Hoang, B. Thi, and K. Anh. The removal of heavy metals by iron mine drainage sludge and Phragmites australis. *Environmental Research Letters*, 10, 2015. doi: 10.1088/1748-9326/10/11/115006.

J. A. Nyman, R. J. Walters, R. D. Delaune, and W. H. Patrick. Marsh vertical accretion via vegetative growth. *Estuarine, Coastal and Shelf Science*, 69(3-4): 370–380, 2006. ISSN 02727714. doi: 10.1016/j.ecss.2006.05.041.

O. Oenema and R. D. DeLaune. Accretion rates in salt marshes in the Eastern Scheldt, South-west Netherlands. *Estuarine, Coastal and Shelf Science*, 26(4): 379–394, apr 1988. ISSN 0272-7714. doi: 10.1016/0272-7714(88)90019-4.

F. O. Omengo, N. Geeraert, S. Bouillon, and G. Govers. Deposition and fate of organic carbon in floodplains along a tropical semiarid lowland river (Tana River, Kenya). *Journal of Geophysical Research Biogeosciences*, 121:1131 –1143, 2016. doi: 10.1002/2015JG003288.

M. J. Osland, C. A. Gabler, J. B. Grace, R. H. Day, M. L. McCoy, J. L. McLeod, A. S. From, N. M. Enwright, L. C. Feher, C. L. Stagg, and S. B. Hartley. Climate and plant controls on soil organic matter in coastal wetlands. *Global Change Biology*, 24(11):5361–5379, 2018. ISSN 13541013. doi: 10.1111/gcb.14376.

X. Ouyang and S. Y. Lee. Improved estimates on global carbon stock and carbon pools in tidal wetlands. *Nature Communications*, 11(1):1–7, 2020. ISSN 20411723. doi: 10.1038/s41467-019-14120-2.

M. A. Pavao-Zuckerman. Soil Ecology. In S. Jørgensen and B. D. Fath, editors, *Encyclopedia of Ecology*, pages 3277–3283. Elsevier Inc., 2008. ISBN 9780080914565; 9780080454054. doi: 10.1016/B978-008045405-4.00850-8.

L. Pendleton, D. C. Donato, B. C. Murray, S. Crooks, W. A. Jenkins, S. Sifleet, C. Craft, J. W. Fourqurean, J. B. Kauffman, N. Marbà, P. Megonigal, E. Pidgeon, D. Herr, D. Gordon, and A. Baldera. Estimating Global "Blue Carbon" Emissions from Conversion and Degradation of Vegetated Coastal Ecosystems. *PLoS ONE*, 7(9), 2012. ISSN 19326203. doi: 10.1371/journal.pone.0043542.

S. C. Pennings and R. M. Callaway. Salt Marsh Plant Zonation: The Relative Importance of Competition and Physical Factors. *Ecology*, 73(2):681–690, 1992. doi: https://doi.org/10.2307/1940774.

G. M. E. Perillo, E. Wolanski, D. R. Cahoon, and C. S. Hopkinson. *Coastal wetlands: an integrated ecosystem approach*. Elsevier, ii edition, 2009.

J. S. Pethick. Long-term accretion rates on tidal salt marshes. *Journal of Sedimentary Research*, 51(2):571–577, 1981. ISSN 1527-1404. doi: 10.1306/212F7CDE-2B24-11D7-8648000102C1865D.

C. E. Prescott. Litter decomposition: what controls it and how can we alter it to sequester more carbon in forest soils? *Biogeochemistry*, 101(1):133–149, 2010. ISSN 1573-515X. doi: 10.1007/s10533-010-9439-0.

I. Prieto, A. Stokes, and C. Roumet. Root functional parameters predict fine root decomposability at the community level. *Journal of Ecology*, 104(3):725–733, 2016. ISSN 00220477. doi: 10.1111/1365-2745.12537.

K. M. Ratliff, A. E. Braswell, and M. Marani. Spatial response of coastal marshes to increased atmospheric CO2. *Proceedings of the National Academy of Sciences*, 112(51):15580–15584, 2015. doi: 10.1073/pnas.1516286112.

D. J. Reed. The impact of sea-level rise on coastal salt marshes. *Progress in Physical Geography: Earth and Environment*, 14(4):465–481, 1990. doi: 10.1177/030913339001400403.

S. Reents, P. Mueller, H. Tang, K. Jensen, and S. Nolte. Plant genotype determines biomass response to flooding frequency in tidal wetlands. *Biogeosciences*, 18(2):403–411, jan 2021. ISSN 1726-4189. doi: 10.5194/bg-18-403-2021.

M. Riaz, T. Mahmood, and M. Arslan. Non-parametric versus parametric methods in environmental sciences. *Bulletin of environmental studies (BES)*, 1: 28–30, 2016.

K. Rogers, J. J. Kelleway, N. Saintilan, J. P. Megonigal, J. B. Adams, J. R. Holmquist, M. Lu, L. Schile-Beers, A. Zawadzki, D. Mazumder, and C. D. Woodroffe. Wetland carbon storage controlled by millennial-scale variation in relative sea-level rise. *Nature*, 567(7746):91–95, mar 2019. ISSN 14764687. doi: 10.1038/s41586-019-0951-7.

M. Roner, A. D'Alpaos, M. Ghinassi, M. Marani, S. Silvestri, E. Franceschinis, and N. Realdon. Spatial variation of salt-marsh organic and inorganic deposition and organic carbon accumulation: Inferences from the Venice lagoon, Italy.

Advances in Water Resources, 93:276–287, 2016. ISSN 03091708. doi: 10.1016/j.advwatres.2015.11.011.

M. Roner, M. Ghinassi, M. Fedi, L. Liccioli, L. G. Bellucci, L. Brivio, and A. D'Alpaos. Latest Holocene depositional history of the southern Venice Lagoon, Italy. *The Holocene*, 27(11):1731–1744, 2017. doi: 10.1177/0959683617708450.

M. Roner, M. Ghinassi, A. Finotello, A. Bertini, N. Combourieu-nebout, S. Donnici, A. Gilli, M. Vannacci, L. Vigliotti, L. G. Bellucci, M. Fedi, L. Liccioli, L. Tommasini, and A. D'Alpaos. Detecting the Delayed Signatures of Changing Sediment Supply in Salt-Marsh Landscapes: The Case of the Venice Lagoon (Italy). 8, 2021. doi: 10.3389/fmars.2021.742603.

J. M. Rybczyk and D. R. Cahoon. Estimating the potential for submergence for two wetlands in the Mississippi River delta. *Estuaries*, 25(5):985–998, 2002. ISSN 01608347. doi: 10.1007/BF02691346.

N. Saintilan, K. Rogers, D. Mazumder, and C. Woodroffe. Allochthonous and autochthonous contributions to carbon accumulation and carbon store in southeastern Australian coastal wetlands. *Estuarine, Coastal and Shelf Science*, 128: 84–92, 2013. ISSN 0272-7714. doi: https://doi.org/10.1016/j.ecss.2013.05.010.

N. Saintilan, K. E. Kovalenko, G. Guntenspergen, K. Rogers, J. C. Lynch, D. R. Cahoon, C. E. Lovelock, D. A. Friess, E. Ashe, K. W. Krauss, N. Cormier, T. Spencer, J. Adams, J. Raw, C. Ibanez, F. Scarton, S. Temmerman, P. Meire, T. Maris, K. Thorne, J. Brazner, G. L. Chmura, T. Bowron, V. P. Gamage, K. Cressman, C. Endris, C. Marconi, P. Marcum, K. S. Laurent, W. Reay, K. B. Raposa, J. A. Garwood, and N. Khan. Constraints on the adjustment of tidal marshes to accelerating sea level rise. *Science*, 377(6605):523–527, 2022. doi: 10.1126/science.abo7872.

J. Sanderman and R. Amundson. Biogeochemistry of Decomposition and Detrital Processing. In H. D. Holland and K. K. Turekian, editors, *Treatise on Geochemistry: Second Edition*, volume 10, pages 217–272. Elsevier Inc., 2013. ISBN 9780080983004. doi: 10.1016/B978-0-08-095975-7.00807-X.

J. I. Santisteban Navarro, R. M. Mediavilla López, E. López Pamo, C. J. Dabrio, M. B. Ruiz Zapata, M. J. Gil García, S. Castaño Castaño, and P. E. Martínez Alfaro. Loss on ignition: a qualitative or quantitative method for organic matter and carbonate mineral content in sediments? *Journal of paleolimnology*, 32(3): 287–299, 2004. doi: 10.1023/B:JOPL.0000042999.30131.5b.

M. Sarika and A. Zikos. Coastal Salt Marshes. In M. Grigore, editor, *Handbook of Halophytes*, number September, pages 199–273. Springer, Cham, 2021. ISBN 9783030178543. doi: 10.1007/978-3-030-57635-6_7.

F. Scarton. Produttività primaria epigea di sette alofite in laguna di Venezia. *Bollettino del Museo civico di storia naturale di Venezia*, 57:53–71, 2006.

F. Scarton, J. W. Day, and A. Rismondo. Primary production and decomposition of Sarcocornia fruticosa (L.) scott and Phragmites australis Trin. Ex Steudel in the Po Delta, Italy. *Estuaries*, 25(3):325–336, 2002. ISSN 0160-8347. doi: 10.1007/BF02695977.

W. H. Schlesinger. Evidence from chronosequence studies for a low carbon-storage potential of soils. *Nature*, 348(6298):232–234, 1990. ISSN 00280836. doi: 10.1038/348232a0.

M. Schuerch, T. Spencer, and B. Evans. Coupling between tidal mudflats and salt marshes affects marsh morphology. *Marine Geology*, 412:95–106, 2019. ISSN 0025-3227. doi: https://doi.org/10.1016/j.margeo.2019.03.008.

O. Serrano, C. E. Lovelock, T. B. Atwood, P. I. Macreadie, R. Canto, S. Phinn, A. Arias-Ortiz, L. Bai, J. Baldock, C. Bedulli, P. Carnell, R. M. Connolly, P. Donaldson, A. Esteban, C. J. Ewers Lewis, B. D. Eyre, M. A. Hayes, P. Horwitz, L. B. Hutley, C. R. Kavazos, et al. Australian vegetated coastal ecosystems as global hotspots for climate change mitigation. *Nature Communications*, 10 (1), dec 2019. ISSN 20411723. doi: 10.1038/s41467-019-12176-8.

D. J. Sheskin. *Handbook of Parametric and Nonparametric Statistical Procedures, Fifth Edition.* Chapman and Hall/CRC, New York, 5th ed. edition, 2011. doi: 10.1201/9780429186196.

C. A. Sierra, M. E. Harmon, and S. S. Perakis. Decomposition of heterogeneous organic matter and its long-term stabilization in soils. *Ecological Monographs*, 81(4):619–634, 2011. doi: https://doi.org/10.1890/11-0811.1.

S. Sifleet, L. Pendleton, and B. C. Murray. State of the Science on Coastal Blue Carbon A Summary for Policy Makers. Technical Report May 2011, Nicholas Institute for Environmental Policy Solutions, Duke University, mar 2011.

W. L. Silver and R. K. Miya. Global patterns in root decomposition: Comparisons of climate and litter quality effects. *Oecologia*, 129(3):407–419, 2001. ISSN 00298549. doi: 10.1007/s004420100740.

S. Silvestri. *La vegetazione alofila quale indicatore morfologico negli ambienti a marea.* Phd thesis, University of Padova, 2000.

S. Silvestri and M. Marani. Salt-Marsh Vegetation and Morphology: Basic Physiology, Modelling and Remote Sensing Observations. *The Ecogeomorphology of Tidal Marshes, Coastal Estuarine Stud*, 59:5–25, 2004. doi: 10.1029/ce059p0005.

S. Silvestri, A. Defina, and M. Marani. Tidal regime, salinity and salt marsh plant zonation. *Estuarine, Coastal and Shelf Science*, 62(1-2):119–130, 2005. ISSN 02727714. doi: 10.1016/j.ecss.2004.08.010.

S. Silvestri, A. D'Alpaos, G. Nordio, and L. Carniello. Anthropogenic Modifications Can Significantly Influence the Local Mean Sea Level and Affect the Survival of Salt Marshes in Shallow Tidal Systems. *Journal of Geophysical Research: Earth Surface*, 123(5):996–1012, 2018. doi: https://doi.org/10.1029/2017JF004503.

J. S. Singh and S. R. Gupta. Plant decomposition and soil respiration in terrestrial ecosystems. *The Botanical Review*, 43(4):449–528, 1977. ISSN 1874-9372. doi: 10.1007/BF02860844.

J. Six, R. T. Conant, E. A. Paul, and K. Paustian. Stabilization mechanisms of soil organic matter: Implications for C-saturation of soils. *Plant and Soil*, 241: 155–176, 2002. doi: 10.1023/A:1016125726789.

L. Soliani. *Statistica non parametrica classica e moderna.* Piccin Nuova Libraria S.p.A, Padova, 2019. ISBN 978-88-299-3033-3.

P. Sprent and N. C. Smeeton. *Applied Nonparametric Statistical Methods.* Chapman and Hall/CRC, New York, 3rd editio edition, 2000.

C. L. Stagg, M. M. Baustian, C. L. Perry, T. J. B. Carruthers, and C. T. Hall. Direct and indirect controls on organic matter decomposition in four coastal wetland communities along a landscape salinity gradient. *Journal of Ecology*, 106(2):655–670, 2018. ISSN 00220477. doi: 10.1111/1365-2745.12901.

J. C. Stevenson, L. G. Ward, and M. S. Kearney. Vertical accretion in marshes with varying rates of sea level rise. In D. A. Wolfe, editor, *Estuarine variability*, pages 241–259. Academic Press, New York, 1986. ISBN 978-0-12-761890-6. doi: 10.1016/B978-0-12-761890-6.50020-4.

R. A. Sutherland. Loss-on-ignition estimates of organic matter and relationships to organic carbon in fluvial bed sediments. *Hydrobiologia*, 389(1):153–167, 1998. doi: 10.1023/A:1003570219018.

A. Tanveera, T. A. Kanth, P. A. Tali, and M. Naikoo. Relation of soil bulk density with texture, total organic matter content and porosity in the soils of Kandi Area of Kashmir valley, India. *International Journal of Earth Sciences*, 4(1): 1–6, 2016.

P. Teatini, G. Gambolati, and L. Tosi. New three-dimensional nonlinear model of the subsidence at Venice. In *IAHS-AISH Publication*, number 234, pages [d]353–361, 1995.

A. Teixeira, B. Duarte, and I. Caçador. *Salt Marshes and Biodiversity*, pages 283–298. Springer Netherlands, Dordrecht, 2014. ISBN 978-94-007-7411-7. doi: 10.1007/978-94-007-7411-7_20.

S. Temmerman, G. Govers, S. Wartel, and P. Meire. Spatial and temporal factors controlling short-term sedimentation in a salt and freshwater tidal marsh, Scheldt estuary, Belgium, SW Netherlands. *Earth Surface Processes and Landforms*, 28(7):739–755, 2003. doi: https://doi.org/10.1002/esp.495.

S. Temmerman, G. Govers, S. Wartel, and P. Meire. Modelling estuarine variations in tidal marsh sedimentation: response to changing sea level and suspended sediment concentrations. *Marine Geology*, 212(1):1–19, 2004. ISSN 0025-3227. doi: https://doi.org/10.1016/j.margeo.2004.10.021.

S. Temmerman, T. J. Bouma, G. Govers, Z. B. Wang, M. B. De Vries, and P. M. J. Herman. Impact of vegetation on flow routing and sedimentation patterns: Three-dimensional modeling for a tidal marsh. *Journal of Geophysical Research: Earth Surface*, 110(F4), 2005. doi: https://doi.org/10.1029/2005JF000301.

S. Temmerman, T. J. Bouma, J. de Koppel, D. der Wal, M. B. De Vries, and P. M. J. Herman. Vegetation causes channel erosion in a tidal landscape. *Geology*, 35(7):631 – 634, 2007. doi: 10.1130/G23502A.1.

S. Temmerman, P. Meire, T. Bouma, P. Herman, T. Ysebaert, and H. De Vriend. Ecosystem-based coastal defence in the face of global change. *Nature*, 504(7478): 79–83, 2013. doi: 10.1038/nature12859.

D. Tognin. *Natural and anthropogenic drivers of erosional and depositional dynamics in shallow tidal systems.* PhD thesis, University of Padova, 2022.

D. Tognin, A. D'Alpaos, M. Marani, and L. Carniello. Marsh resilience to sea-level rise reduced by storm-surge barriers in the Venice Lagoon. *Nature Geoscience*, 14(12):906–911, 2021. doi: 10.1038/s41561-021-00853-7.

D. Tognin, A. Finotello, A. D'Alpaos, D. P. Viero, M. Pivato, R. A. Mel, A. Defina, E. Bertuzzo, M. Marani, and L. Carniello. Loss of geomorphic diversity in shallow tidal embayments promoted by storm-surge barriers. *Science Advances*, 8(13), 2022. doi: 10.1126/sciadv.abm8446.

D. Tognin, L. Carniello, L. D'Alpaos, A. Rinaldo, and A. D'Alpaos. Sediment transport dynamics in the Venice Lagoon: a statistical characterization over four centuries. *Geology*, under review.

L. Tommasini, L. Carniello, M. Ghinassi, M. Roner, and A. D'Alpaos. Changes in the wind-wave field and related salt-marsh lateral erosion: inferences from the evolution of the Venice Lagoon in the last four centuries. *Earth Surface*

Processes and Landforms, 44(8):1633–1646, 2019. ISSN 10969837. doi: 10.1002/esp.4599.

R. Torres and R. Styles. Effects of topographic structure on salt marsh currents. *Journal of Geophysical Research: Earth Surface*, 112(F2), 2007. doi: https://doi.org/10.1029/2006JF000508.

S. Trumbore. Radiocarbon and Soil Carbon Dynamics. *Annual Review of Earth and Planetary Sciences*, 37(1):47–66, 2009. doi: 10.1146/annurev.earth.36.031207.124300.

R. Turner, E. Swenson, and C. Milan. *Organic and Inorganic Contributions to Vertical Accretion in Salt Marsh Sediments*, pages 583–595. Springer Netherlands, Dordrecht, 2002. ISBN 0-7923-6019-2. doi: 10.1007/0-306-47534-0_27.

N. Ursino, S. Silvestri, and M. Marani. Subsurface flow and vegetation patterns in tidal environments. *Water Resources Research*, 40(5), 2004. doi: https://doi.org/10.1029/2003WR002702.

I. Valiela, J. L. Bowen, and J. K. York. Mangrove forests: One of the world's threatened major tropical environments. *BioScience*, 51(10):807–815, 2001. ISSN 00063568. doi: 10.1641/0006-3568(2001)051[0807:MFOOTW]2.0.CO;2.

I. Valiela, J. Lloret, T. Bowyer, S. Miner, D. Remsen, E. Elmstrom, C. Cogswell, and E. Robert Thieler. Transient coastal landscapes: Rising sea level threatens salt marshes. *Science of The Total Environment*, 640-641:1148–1156, 2018. ISSN 0048-9697. doi: https://doi.org/10.1016/j.scitotenv.2018.05.235.

L. van Ardenne, S. Jolicoeur, D. Bérubé, D. Burdick, and G. L. Chmura. High resolution carbon stock and soil data for three salt marshes along the northeastern coast of North America. *Data in Brief*, 19:2438–2441, 2018a. doi: 10.1016/j.dib.2018.07.037.

L. B. van Ardenne, S. Jolicouer, D. Bérubé, D. Burdick, and G. L. Chmura. The importance of geomorphic context for estimating the carbon stock of salt marshes. *Geoderma*, 330:264–275, nov 2018b. ISSN 00167061. doi: 10.1016/j.geoderma.2018.06.003.

M. Van De Broek, S. Temmerman, R. Merckx, and G. Govers. Controls on soil organic carbon stocks in tidal marshes along an estuarine salinity gradient. *Biogeosciences*, 13(24):6611–6624, 2016. ISSN 17264189. doi: 10.5194/bg-13-6611-2016.

M. Van de Broek, C. Vandendriessche, D. Poppelmonde, R. Merckx, S. Temmerman, and G. Govers. Long-term organic carbon sequestration in tidal marsh sediments is dominated by old-aged allochthonous inputs in a macrotidal estuary. *Global Change Biology*, 24(6):2498–2512, jun 2018. ISSN 13652486. doi: 10.1111/gcb.14089.

F. Wang, K. D. Kroeger, M. E. Gonneea, J. W. Pohlman, and J. Tang. Water salinity and inundation control soil carbon decomposition during salt marsh restoration: An incubation experiment. *Ecology and Evolution*, 9(4):1911–1921, 2019. ISSN 20457758. doi: 10.1002/ece3.4884.

H. Wang, S. C. Piazza, L. A. Sharp, C. L. Stagg, B. R. Couvillion, G. D. Steyer, and T. E. McGinnis. Determining the Spatial Variability of Wetland Soil Bulk Density, Organic Matter, and the Conversion Factor between Organic Matter and Organic Carbon across Coastal Louisiana, U.S.A. *Journal of Coastal Research*, 33(3):507–517, 2017. doi: 10.2112/JCOASTRES-D-16-00014.1.

M. A. Ward, T. M. Hill, C. Souza, T. Filipczyk, A. M. Ricart, S. Merolla, L. R. Capece, B. C. O'Donnell, K. Elsmore, W. C. Oechel, and K. M. Beheshti. Blue carbon stocks and exchanges along the California coast. *Biogeosciences*, 18(16): 4717–4732, 2021. doi: 10.5194/bg-18-4717-2021.

E. B. Watson. Changing Elevation, Accretion, and Tidal Marsh Plant Assemblages in a South San Francisco Bay Tidal Marsh. *Estuaries*, 27(4):684–698, 2004. ISSN 01608347.

R. Watson, I. Noble, B. Bolin, N. Ravindranath, D. Verardo, and D. Dokken. Land Use, Land-Use Change, and Forestry. Technical report, IPCC, 2000.

K. Weliky, E. Suess, C. A. Ungerer, P. J. Muller, and K. Fischer. Problems with accurate carbon measurements in marine sediments and particulate matter in seawater: A new approach1. *Limnology and Oceanography*, 28(6):1252–1259, 1983. doi: https://doi.org/10.4319/lo.1983.28.6.1252.

D. A. White, T. E. Weiss, J. M. Trapani, and L. B. Thien. Productivity and Decomposition of the Dominant Salt Marsh Plants in Louisiana. *Ecology*, 59 (4):751–759, 1978. doi: 10.2307/1938779.

R. K. Wider and G. E. Lang. A critique of the analytical methods used in examining decomposition data obtained from litter bags. *Ecology*, 63(6):1636–1642, 1982. ISSN 00129658, 19399170.

L. Wiese, I. Ros, A. Rozanov, A. Boshoff, W. de Clercq, and T. Seifert. An approach to soil carbon accounting and mapping using vertical distribution functions for known soil types. *Geoderma*, 263:264–273, feb 2016. ISSN 0016-7061. doi: 10.1016/J.GEODERMA.2015.07.012.

L. Windham. Comparison of biomass production and decomposition between Phragmites australis (common reed) and spartina patens (salt hay grass) in brackish tidal marshes of New Jersey, USA. *Wetlands*, 21(2):179–188, 2001. ISSN 02775212. doi: 10.1672/0277-5212(2001)021[0179:COBPAD]2.0.CO;2.

C. D. Woodroffe. *Coasts: form, process and evolution.* Cambridge University Press, Cambridge, 2003.

P. Xin, T. Zhou, C. Lu, C. Shen, C. Zhang, A. D'Alpaos, and L. Li. Combined effects of tides, evaporation and rainfall on the soil conditions in an intertidal creek-marsh system. *Advances in Water Resources*, 103:1–15, 2017. ISSN 0309-1708. doi: https://doi.org/10.1016/j.advwatres.2017.02.014.

S. Xu, N. Eisenhauer, O. Ferlian, J. Zhang, G. Zhou, X. Lu, C. Liu, and D. Zhang. Evidence synthesis Species richness promotes ecosystem carbon storage: evidence from biodiversity-ecosystem functioning experiments. *Proceedings of the Royal Society B*, 287(1939):1–14, 2020. doi: 10.1098/rspb.2020.2063.

S. A. Yarwood. The role of wetland microorganisms in plant-litter decomposition and soil organic matter formation: A critical review. *FEMS Microbiology Ecology*, 94(11):1–17, 2018. ISSN 15746941. doi: 10.1093/femsec/fiy175.

F. Yousefi Lalimi, S. Silvestri, A. D'Alpaos, M. Roner, and M. Marani. The Spatial Variability of Organic Matter and Decomposition Processes at the Marsh

Scale. *Journal of Geophysical Research: Biogeosciences*, 123(12):3713–3727, 2018. ISSN 21698961. doi: 10.1029/2017JG004211.

Y. Yuan, X. Li, J. Jiang, L. Xue, and C. B. Craft. Distribution of organic carbon storage in different salt-marsh plant communities: A case study at the Yangtze Estuary. *Estuarine, Coastal and Shelf Science*, 243, 2020. ISSN 02727714. doi: 10.1016/j.ecss.2020.106900.

S. Yue, P. Pilon, B. Phinney, and G. Cavadias. The influence of autocorrelation on the ability to detect trend in hydrological series. *Hydrological Processes*, 16 (9):1807–1829, 2002. doi: https://doi.org/10.1002/hyp.1095.

M. Zecchin, G. Brancolini, L. Tosi, F. Rizzetto, M. Caffau, and L. Baradello. Anatomy of the Holocene succession of the southern Venice lagoon revealed by very high-resolution seismic data. *Continental Shelf Research*, 29(10):1343–1359, may 2009. ISSN 0278-4343. doi: 10.1016/J.CSR.2009.03.006.

J. Zhou, Y. Wu, J. Zhang, Q. Kang, and Z. Liu. Carbon and nitrogen composition and stable isotope as potential indicators of source and fate of organic matter in the salt marsh of the Changjiang Estuary, China. *Chemosphere*, 65(2):310–317, 2006. ISSN 00456535. doi: 10.1016/j.chemosphere.2006.02.026.

A. Zirino, H. Elwany, C. Neira, F. Maicu, G. Mendoza, and L. A. Levin. Salinity and its variability in the Lagoon of Venice, 2000–2009. *Advances in Oceanography and Limnology*, 5(1):41–59, 2014. doi: 10.1080/19475721.2014.900113.

R. Zonta, M. Botter, D. Cassin, L. G. Bellucci, R. Pini, and J. Dominik. Sediment texture and metal contamination in the Venice Lagoon (Italy): A snapshot before the installation of the MOSE system. *Estuarine, Coastal and Shelf Science*, 205:131–151, 2018. ISSN 02727714. doi: 10.1016/j.ecss.2018.03.007.

A. Zuliani, L. Zaggia, F. Collavini, and R. Zonta. Freshwater discharge from the drainage basin to the Venice Lagoon (Italy). *Environment International*, 31(7): 929–938, sep 2005. ISSN 0160-4120. doi: 10.1016/J.ENVINT.2005.05.004.

R. A. Zurayk and R. Baalbaki. Inula crithmoides: A candidate plant for saline agriculture. *Arid Soil Research and Rehabilitation*, 10(3):213–223, 1996. ISSN 08903069. doi: 10.1080/15324989609381436.